Book of Abstracts

EGAS
CONFERENCE
KRAKÓW

9-13
July
2018

Jagiellonian University
Kraków / Poland

Book of abstracts of the 50th Anniversary EGAS conference

DTP Krzysztof Magda

Published in 2018

Published by
Faculty of Physics, Astronomy and Applied Computer Science
Jagiellonian Uniwersity
Address: prof. Stanisława Łojasiewicza 11 30-348 Kraków, Poland

Printed in Poland

ISBN: 978-83-945937-5-9

Faculty of Physics, Astronomy
and Applied Computer Science

PRECOPTIC Co.

Local Organizing Committee

Szymon Pustelny (Chair)
pustelny@uj.edu.pl

Krzysztof Dzierżęga (Co-chair)
krzysztof.dzierzega@uj.edu.pl

Tomasz Kawalec (Secretary/Webmaster)
tomasz.kawalec@uj.edu.pl

Jarosław Koperski (Co-chair)
jaroslaw.koperski@uj.edu.pl

Tomasz Urbańczyk
tomek.urbanczyk@uj.edu.pl

Adam Wojciechowski (Secretary)
a.wojciechowski@uj.edu.pl

Witold Zawadzki
witold.zawadzki@uj.edu.pl

Honorary Committee

Prof. Katarzyna Chałasińska-Macukow
University of Warsaw

Prof. Karol Musioł
Jagiellonian University in Kraków

Prof. Ewa Gudowska-Nowak
Jagiellonian University in Kraków

Prof. Marek Stankiewicz
National Synchrotron Radiation Centre SOLARIS, Kraków

Prof. Stanisław Kistryn
Jagiellonian University in Kraków

Prof. Józef Szudy
Nicolaus Copernicus University in Toruń

Prof. Maciej Kolwas
Polish Academy of Sciences, Warszawa

Prof. Mariusz Zubek
Gdańsk University of Technology

Conference Programme

Monday, 9 July (AUDITORIUM MAXIMUM)

17:00-19:00 REGISTRATION and EGAS Board Meeting

19:00-21:00 WELCOME RECEPTION

Tuesday, 10 July (AUDITORIUM MAXIMUM)

10:30-11:00 Coffee break

Session A

Session B

Session A

Session B

17:15-19:15 POSTER SESSION A

Wednesday, 11 July (AUDITORIUM MAXIMUM)

10:30-11:00 Coffee break

Session A

Session B

11:00-11:30 *Invited talk*
L. Fallani
Synthetic quantum systems with ultracold two-electron fermions 36

11:30-11:50 *Contributed talk*
M. Witkowski
Photoassociation and photoionization in a two-species Rb-Hg MOT 37

11:50-12:10 *Contributed talk*
H. L. Bethlem
A Molecular Fountain 38

12:10-12:30 *Contributed talk*
H. J. Williams
Producing, trapping and controlling ultracold molecules 39

12:30-14:00 LUNCH

14:00-19:00 EXCURSIONS: Kraków City Tour and Wieliczka Salt Mine

Thursday, 12 July (AUDITORIUM MAXIMUM)

9:00-9:45 *Plenary talk*
U. Keller
Attosecond ionization time delays from atoms, molecules to solid surfaces 42

9:45-10:15 EGAS General Assembly

10:15-10:30 CONFERENCE PHOTO

10:30-11:00 Coffee break

Session A

11:00-11:30 *Invited talk*
A. Weis
Characterizing and Imaging Magnetic Nanoparticles by Optical Magnetometry 43

11:30-11:50 *Contributed talk*
V. Lebedev
Magnetic Susceptometry Imaging with Robust Atomic Magnetometers 44

11:50-12:10 *Contributed talk*
A. Akulshin
Continuous-wave mirrorless lasing for directional laser guide stars and remote magnetometry 45

Session B

12:30-14:00 LUNCH and EGAS Board meeting

14:00-15:45 POSTER SESSION B

15:45-18:00 Transfer to the Benedictine Abbey in Tyniec, ABBEY TOUR and CONCERTO

18:00-21:00 CONFERENCE DINNER at the Benedictine Abbey

Friday, 13 July – Prof. Gawlik 70th birthday Symposium (UNIVERSITY CAMPUS)

8:45-9:00 Opening

Table of contents

Table of contents

Table of contents

Table of contents

Table of contents

Table of contents

Table of contents

Dear Participants of the 50th Jubilee EGAS Conference,

For 50 years, representatives of the atomic, molecular and optical physics have been meeting at conferences organized by the European Group on Atomic Systems (formerly known as European Group on Atomic Spectroscopy) – EGAS. Participants have changed, research topics have changed, and tools for their implementation have changed but high quality of the Conference, as well as its kind and friendly character remained untouched. It is here that many PhD students and postdocs kicked off their careers, later becoming leaders in their fields. It is also here where acquaintances, later turned into life-lasting friendships and collaborations, were formed.

Ahead of us is the 50th EGAS Conference, which returns to Kraków after 41 years. In 1977, the iron curtain was still dividing Europe into two hostile blocks and communism in Poland was held firmly. Regardless, that conference is still remembered as a unique event that opened the doors to great Science for scholars of Central and Eastern Europe.

Nowadays, Poland is a completely different country. We are a member of the European Union. We can trade and travel the world freely. Poland is an open country and Kraków is regularly selected for the TOP10 touristic wonders of the world.

The program of this year's EGAS Conference is again interesting and impressive. In addition to the plenary talks of the most renowned experts in the field, such as prof. Theodor Hänsch, many of the young but already recognized scientists will deliver their invited talks. Twenty six carefully selected contributed presentations will be given and nearly 150 posters will be presented. Apart from the scientific program, various social events will be organized, including a Kraków city tour and a visit to the nearby salt mine in Wieliczka. A conference dinner will be held at the 1,000 years old Benedictine abbey in Tyniec. We hope that all these features, in conjunction with the customary Polish hospitality and the magic of Kraków, will provide plenty of opportunities for creative exchanges, but also socializing, soon resulting in new research projects and, ultimately, breakthroughs.

On behalf of the Local Organizing Committee, we would like to warmly welcome you at the 50th Jubilee EGAS Conference in Kraków and wish you many fruitful debates and a successful and exciting stay in Kraków.

Kraków – a truly extraordinary place

In addition to its historic charm, Kraków has a truly magical power of attracting people from the most remote corners of the world. This is a royal city, which prosperity was provided by merchants and craftsmen, while artists and scientists contributed to the development of culture and science. Kraków is a city full of treasures, a coronation city of Polish kings, a royal necropolis, a city of old churches and synagogues. Kraków is also the home for famous writers and poets, musician and painters, actors and performers. Finally, it is a scientific and political center of the region strongly contributing to Polish politics.

The beginnings

Archaeological excavations reveal that men lived in the present-day Krakow already in the prehistoric era (about 200,000 BC). During the Lusatian culture (around 1,300 BC) agricultural settlements were already present in the area. Nonetheless, the first stories about the city mention a legendary Slav ruler – prince Krak, who founded his stronghold on a rocky hill (Wawel hill), rising above the Vistula River. In 965, Ibrahim-Ibn-Jakub, an Arab merchant travelling across Europe, wrote that Kraków was a rich city located at the crossing of main trade routes. Those times are commemorated by two earth mounds erected by the Krakowians in the 19th century in honor of prince Krak and his daughter Wanda.

The Middle Ages

In the 10th century, prince Mieszko I (Mieszko I of Poland) the first ruler of Poland, incorporated Kraków into the newly formed Polish state. The city became the capital of Poland in 1038, during the reign of Kazimierz Odnowiciel (Casimir I the Restorer), who made Wawel castle his seat. In the 13th century, the city was rebuilt and chartered under the Magdeburg rights. At the time, a large market square was built, and a chessboard layout of the city was formed. In 1320, after nearly 200 years of regional fragmentation of Poland, Władysław Łokietek (Vladislaus the Elbow-high) was crowned the king of Poland in Wawel Castle cathedral. Since then, for over 400 years, the cathedral was the coronation place for Polish kings. Its crypts also became the burial place for them and their families.

Die Reisebilder Pfalzgraf Ottheinrichs aus den Jahren 1536/37

Another important date in the history of Kraków is May 12, 1364. Just then, the son of Łokietek, Kazimierz Wielki (Casimir the Great), great patron of art and protector of science, established Studium Generale, one of the first universities in Europe. Soon after, Studium became one of the most renowned universities in medieval Europe.

Long and peaceful ruling of Kazimierz Wielki enabled him to completely reform the country. The king, who according to a Polish proverb, found Poland wooden and left made of stone, also transformed his capital. He expanded the medieval market halls, built a cloth hall and several beautiful Gothic temples (including St. Mary's Church). He also expanded the royal castle on Wawel hill, modernized the city's fortifications, ordered the streets to be paved, and founded waterworks.

In 1384, Jadwiga (Hedwig of Anjou) the daughter of Ludwik Węgierski (Louis I of Hungary) and the king(!) of Poland, married the Grand Duke of Lithuania, Władysław Jagiełło (Jogaila). Jagiełło, crowned king of Poland in 1386, started the greatest Polish dynasty that ruled the country for the next 200 years. In her last will, Jadwiga donated all her private fortune to the University (some items can still be found in university museum). Thanks to Jagiełło's efforts, a medieval university modelled after the Paris Sorbone with faculties of theology, law, medicine and philosophy, was created in Kraków. In 1818, the university was named the Jagiellonian University to emphasize the contribution of the Jagiellonians to its renewal.

Since the 15th century, the university was attracting many students from all over Europe. It was especially famous for its law, mathematics and astronomy. In 1491, Nicolaus Copernicus enrolled into the university later becoming one of its most famous alumni.

A peak of Kraków's prosperity was 15th and 16th centuries. During the renaissance Kraków was a city of culture and science. It attracted the greatest artists, whose works such as the altar in St. Mary's Church made by Wit Stwosz (Veit Stoss), arcades in Wawel designed by Bartolomeo Berrecci, and beautiful tapestries designed by Michał Coxie, commissioned by King Zygmunt August, can be still admired. Also the largest Polish bell „Zygmunt" was hung in the tower of the cathedral.

The 17th and 18th centuries

After the "golden age", the power of Poland started to wane at the beginning of the 17th century. In 1609, king Zygmunt III Waza (Sigmund III Vasa) moved the capital to Warsaw. From that time, Kraków lost its importance, keeping only the representative role of the city of royal coronations and funerals. The capture of the city during Potop Szwedzki (Swedish Deluge) in the mid-17th century resulted in significant damages, and many priceless works of art were looted by the invaders. At the time, population of the city also suffered due to the flood of the Vistula River and black pox epidemic. The greatest blows for the city were however the partitions of Poland in 1772 and 1793.

During the time, the reform of the Kraków Academy, conducted by Hugo Kołłątaj, brought a new era to the University. Particularly, faculties of science were formed and first medical clinic, astronomical observatory and botanical garden were also established.

In 1794, Tadeusz Kosciuszko, the great Polish patriot, pledged all Poles a fight for Polish independence on Kraków's Market Square. Unfortunately, the Insurekcja Kościuszkowska (Kosciuszko Insurrection) ended in defeat and the final partition of Poland occurred in 1795 wiping Poland out of the map for the next 123 years.

The 19th century

After the Congress of Vienna in 1815, Kraków along with its district constituted the Republic of Kraków under the joint supervision of all partitioners: Austria, Prussia and Russia. Subsequent uprisings did not bring the desired freedom to the Polish nation.

In the second half of the 19th century, Kraków found itself in the borders of Galicja (Galicia), which enjoyed great autonomy. This was a significantly better time for the city. Since Galicja had its own administration, education and judiciary, the University was also rapidly developing.

The 20th century

The imminent war with Russia inevitably intensified the independence movements in Poland. On August 6, 1914, Pierwsza Kadrowa (First Cadre Company) set off from Kraków's Oleandrów. Kraków was one of the first Polish cities to regain freedom after World War I. It happened on October 31, 1918. During a whole interwar period Kraków was the leading center of culture, art and science in Poland. Simultaneously, the industry was rapidly growing.

On September 6, 1939, 6 days after the beginning of the World War II, German troops entered Kraków. Schools and universities, museums and theaters were closed. November 6, 1939 marks one of the saddest day in the history of the Jagiellonian University. On that day, 183 people, professors of the Jagiellonian University and the Kraków University of Technology were invited to University Collegium Novum for a doctor B. Muller's lecture. Instead of listening of the

lecture and discussing reopening of the universities, however, the professors were imprisoned and sent to the concentration camp in Sachsenhausen, where many of them died.

In 1939 Hitler established Kraków as the capital of the General Government, and appointed Hans Frank as its governor. Frank took Wawel castle as his residence. Poles were displaced from many districts, and public executions were often carried out in the city streets. Jews were persecuted. In particular, in March 1941, the German occupant closed down about 60,000 Jews in the Kraków Ghetto. People recognized as Jews were murdered during the liquidation action in March 1943, as well as in the concentration camps in Płaszów, Bełżec, and Auschwitz.

Throughout the war, underground organizations were active in Kraków. A great role was played by a conspiratorial cultural and educational life. Young people gathered in secret theaters and schools. One of them was Karol Wojtyła, the future pope John Paul II.

Kraków was liberated from German occupation on January 18, 1945. Admittedly, unlike other Polish cities, Kraków was not destroyed during the war. Yet, the privileged role of the city has changed. A new communist government, under Soviet auspices, wanted to have a decisive influence on shaping the new socialist society. An expression of these efforts was the construction of Nowa Huta (New Ironworks), a model socialist city, without the intelligentsia and religion. To accomplish the task the government orchestrated a huge population influx from underdeveloped parts of Poland who found employment in a newly built Metallurgical Combine of Nowa Huta. However, contrary to the assumptions of the communist authorities, this plan did not work out and the communistic government failed to create frictions between the intellectual Kraków and proletarian Nowa Huta, nor to keep the religion out of the city. Particularly, during the Polish

Martial law (13.12.1981-22.07.1983) Nowa Huta has witnessed the largest manifestation to defend the outlawed „Solidarity" movement. Today, the „old" Nowa Huta has been registered as a monument and is an example of socialist realism urban planning in Poland.**Present day**

Present day Kraków is a large European city, which strives to become a real leader in entrepreneurship, attracting large high-tech companies as well as start-ups. Kraków other focuses are the development of tourism and contemporary art. The city is one of the leading scientific and didactic centers in Poland, with competitive staff and modern scientific-research and laboratory infrastructure. There are 33 higher education institutions in the city (including 19 non-public ones), with over 200,000 students. The prestige and centuries-old tradition draw people from all over the world.

At the modern University

At the Jagiellonian University, which combines the medieval tradition with the state-of-the-art science, there are currently almost 50,000 students, studying at 16 faculties (including three medical faculties). In addition to students from European Union countries, the University teaches a large group of students from Eastern European, particularly Ukraine and Belarus, and slowly also from Asia and Africa. Among the faculties, the Faculty of Physics, Astronomy and Applied Computer Science, the co-organizers of the conference, is one of the largest. The Faculty trains over 1,000 students in physics, biophysics, advanced materials and nanotechnology, astronomy, and computer science. Its newly commissioned building hosts one of the most advanced laboratories in Poland, where cutting edge experiments in various fields of physics are performed. The Faculty also operates the first Polish synchrotron "Solaris", located just 500 meters from the Faculty buildings.

Maria Pawłowska (translation Szymon Pustelny)

Tuesday

Precision frontier in laser spectroscopy

T. W. Hänsch[1,2]
1. Faculty of Physics, Ludwig-Maximilian-University, Munich, Germany
2. Max-Planck-Institute of Quantum Optics, Garching, Germany

Precision laser spectroscopy of the simple hydrogen atom has long provided an intriguing path to fundamental physics research at low energies. Since the first Doppler-free saturation spectroscopy of the Hydrogen Balmer-alpha line in 1972, the accuracy of laser spectroscopic measurements in atomic hydrogen has advanced by 8 orders of magnitude, approaching the limit set by the definition of the unit of time. The challenges encountered along this path have motivated a number of inventions, including laser cooling of atomic gases and the laser frequency comb technique. Laser combs are now the most precise tool for precision measurements. They provide the long-missing clockwork for optical atomic clocks, and they are enabling powerful new approaches to broadband and precise atomic and molecular spectroscopy. Spectroscopic measurements of hydrogen resonances permit tests of quantum electrodynamic theory, they yield values of the Rydberg constant and the proton charge radius, and they provide a reference for laser spectroscopy of antihydrogen and of other hydrogen-like exotic atoms, notably muonic hydrogen and muonic deuterium. The root mean square proton charge radius, as derived from laser measurements of the 2s - 2p Lamb shift in muonic hydrogen some years ago, is about 4% smaller than that obtained from hydrogen spectroscopy or electron scattering experiments. This “proton size puzzle” has not yet been resolved. Current experiments in our laboratory aim to confirm or resolve this puzzle. They include fluorescence spectroscopy of 2s - np transitions in a cold collimated atomic beam, and direct Doppler-free frequency comb spectroscopy of the 1s - 3s, 3d two-photon transition in a cold atomic sample. Future precision spectroscopy of hydrogen-like cold, trapped He^+ ions, using a high harmonic generation frequency comb source near 60 nm, will permit even more sensitive searches for possible new physics. These experiments will be augmented by measurements of the helium nuclear charge radius via the 2s - 2p Lamb shift in hydrogen-like muonic helium ions.

Extreme light for molecules at the extremes

S. Bartalini[1], S. Borri[1,2], F. Cappelli[1], L. Consolino[1], I. Galli[1], P. Maddaloni[3], D. Mazzotti[1], G. Santambrogio[4], P. De Natale[*1,2]

1. CNR-INO, Istituto Nazionale di Ottica, Largo E. Fermi 6, 50125 Firenze, and LENS, via N. Carrara 1, 50019 Sesto Fiorentino, Italy
2. INFN, Istituto Nazionale di Fisica Nucleare, Sez. di Firenze, via G. Sansone 1, 50019 Sesto Fiorentino, Italy
3. CNR-INO, Istituto Nazionale di Ottica, Via Campi Flegrei 34, 80078 Pozzuoli, and INFN, Istituto Nazionale di Fisica Nucleare, Sez. di Napoli, Complesso Universitario di M.S. Angelo, Via Cintia, 80126 Napoli, Italy
4. INRIM, Istituto Nazionale di Ricerca Metrologica, Strada delle Cacce 91, 10135, Torino, Italy

Interrogation and manipulation of molecules is a challenging task, when sensitivities beyond parts per trillion or accuracies for frequency measurements approaching the uncertainty of primary frequency standards are requested. It indeed requires an overall rethinking of radiation sources, spectroscopic techniques and molecular samples preparation. Compared to atoms, difficulties are increased by the weaker absorption line-strengths, as well as by the need to cover the huge 2-1000 micron wavelength interval, where fundamental ro-vibrational bands of molecules are found, by appropriate photonic tools and spectroscopic techniques. To make matters worse, cryogenic cooling is often required to suppress the strong background radiation noise from which this spectral range suffers. However, a tremendous progress in photonics and spectroscopy, as well as in molecular sample preparation, is revolutionizing the scenario [1]. In the last twenty years, the main game changers on the photonics side have been frequency comb synthesizers [2-3], quantum cascade lasers [4-5] and quasi-phase-matching schemes for nonlinear generation of coherent radiation [6]. For spectroscopy, extension to the infrared and THz range of precision frequency measurements, beyond 10^{-11}, and the achievement of sensitivities better than 1 part-per-trillion are providing novel, powerful physical probes and new areas of application for sensing [7]. On the side of molecular samples, a key role is played by the emerging technologies for the production of cold and ultra-cold stable molecules, including buffer-gas cooling and magneto-optical trapping [8-11].

Several examples showing significant, often ground-breaking, results in the areas cited above will be discussed, together with perspectives in these areas.

References

[1] P. Maddaloni, M. Bellini, and P. De Natale, *Laser-based Measurements for Time and Frequency Domain Applications. A Handbook*, Series in Optics and Optoelectronics, Taylor&Francis Group 2013.
[2] T. Udem, R. Holzwarth, and T. W. Hänsch, Nature **416,** 233 (2002).
[3] S. Bartalini, L. Consolino, P. Cancio, P. De Natale, P. Bartolini, A. Taschin, M. De Pas, H. Beere, D. Ritchie, M. S. Vitiello, and R. Torre, Phys. Rev. X **4**, 021006 (2014).
[4] J. Faist, *Quantum Cascade Lasers*, Oxford University Press 2013.
[5] F. Cappelli, G. Campo, I. Galli, G. Giusfredi, S. Bartalini, D. Mazzotti, P. Cancio, S. Borri, B. Hinkov, J. Faist, and P. De Natale, Laser Photon. Rev. **10**, 623 (2016).
[6] G. Insero, C. Clivati, D. D'Ambrosio, P. De Natale, G. Santambrogio, P. G. Schunemann, J.-J. Zondy, and S. Borri, Opt. Lett. **41**, 5114 (2016).
[7] I. Galli, S. Bartalini, R. Ballerini, M. Barucci, P. Cancio, M. De Pas, G. Giusfredi, D. Mazzotti, N. Akikusa, and P. De Natale, Optica **3**, 385 (2016).
[8] L. Santamaria, V. Di Sarno, P. De Natale, M. De Rosa, M. Inguscio, S. Mosca, I. Ricciardi, D. Calonico, F. Levi, and P. Maddaloni, Phys. Chem. Chem. Phys. **18**, 16715 (2016).
[9] G. Insero, S. Borri, D. Calonico, P. Cancio Pastor, C. Clivati, D. D'Ambrosio, P. De Natale, M. Inguscio, F. Levi, and G. Santambrogio, Sci. Rep. **7**, 12780 (2017).
[10] S. Truppe, H. J. Williams, M. Hambach, L. Caldwell, N. J. Fitch, E. A. Hinds, B. E. Sauer, and M. R. Tarbutt, Nature Phys. **13**, 1173 (2017).
[11] L. Anderegg, B. L. Augenbraun, E. Chae, B. Hemmerling, N. R. Hutzler, A. Ravi, A. Collopy, J. Ye, W. Ketterle, and J. M. Doyle, Phys. Rev. Lett. **119**, 103201 (2017).

[*]Corresponding author: paolo.denatale@ino.cnr.it

Spectroscopy of hydrogen 1S-3S transition with a cw-laser at 205 nm

H. Fleurbaey[1], S. Galtier[1], S. Thomas[1], M. Bonnaud[1], M. Abgrall[2], J.Guéna[2], L. Julien[1], F. Biraben[1], F. Nez*[1].

1. Laboratoire Kastler Brossel, Sorbonne Université, CNRS, ENS-Université PSL, Collège de France, 4 place Jussieu, Case 74,75252 Paris Cedex 05, France

2. LNE-SYRTE, Observatoire de Paris, ENS-Université PSL, CNRS, Sorbonne Université, 61 avenue de l'Observatoire, 75014 Paris, France

High resolution spectroscopy of simplest atomic systems provides access to fundamental quantities of physics such as the Rydberg constant and the proton charge radius (r_p) as these systems are calculable. In 2010, the spectroscopy of muonic hydrogen (made of a proton and a muon) yielded a value of r_p an order of magnitude more precise, but about 4% smaller, than the CODATA-recommended value [2]. This discrepancy has become known as the proton radius puzzle [3].

A recent measurement of the hydrogen $2S-4P$ [4] transition frequency in Garching has brought a new dimension to this conundrum, as it agrees with the smaller muonic value of the proton charge radius, in disagreement with other spectroscopic measurements in electronic hydrogen.

Recently we have improved the spectroscopy of hydrogen $1S-3S$ transition [5] [6] with a cw-laser at 205 nm [7]. It is now realized with a relative uncertainty of 9×10^{-13} [8]. It yields a value of the proton charge radius that appears to support the CODATA-recommended value (see Fig. 1). We will present our experiment and our current efforts to improve it.

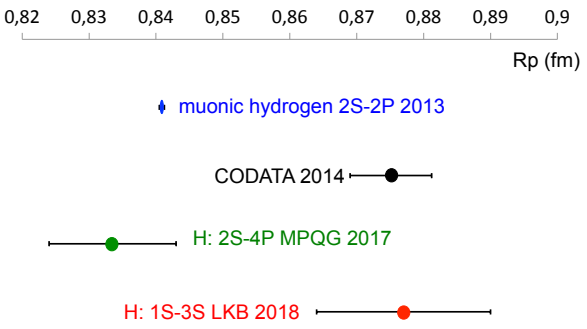

Fig. 1: Recent determinations of the proton charge radius.

Acknowledgement: This work is supported by the French National Research Agency (ANR) through the cluster of excellence FIRST-TF (ANR-10-LABX-48), the PROCADIS project (ANR-2010-BLANC:04510) and the Equipex REFIMEVE+ (ANR-11-EQPX-0039) and by the CNRS. The authors are indebted to O. Acef for the loan of various devices.

References

[1] A. Antognini, F. Nez, K . Schuhmann et al, Science **339** (2013) 417.
[2] [2] P. Mohr, D. Newell, B. Taylor, Rev. Mod. Phys. **88** (2016) 035009.
[3] C. E. Carlson, Prog. Part. Nucl. Phys. **82**, 59 (2015).
[4] A. Beyer, L. Maisenbacher, A. Matveev et al, Science **358** (2017) 79-85.
[5] O. Arnoult, F. Nez, L. Julien, and F. Biraben, Eur. Phys. J. D **60**, 243 (2010).
[6] D.C. Yost, A. Matveev, A. Grinin et al, Phys. Rev. A **93**, 042509 (2016)
[7] S. Galtier, F. Nez, L. Julien, and F. Biraben, Opt. Commun. 324, 34 (2014).
[8] H. Fleurbaey, S. Galtier, S. Thomas et al, Phys. Rev. Lett. accepted for publication.

*Corresponding author: francois.nez@lkb.upmc.fr

High-Precision Measurement of the Proton's Atomic Mass

G. Werth*[1], F. Heiße[2,3], S. Rau [2] F. Köhler-Langes [2], J. Hou[2], S. Junck[1], A. Kracke [1], A. Mooser[4], W. Quint[3], S. Ulmer[4], K. Blaum[2], S. Sturm[2]

1. Institut für Physik, Johannes Gutenberg-Universität Mainz, D-55099 Mainz, Germany
2. Max-Planck-Institut für Kernphysik, Saupfercheckweg 1, D-69117 Heidelberg, Germany
3. GSI Helmholtzzentrum für Schwerionenforschung, D-64291 Darmstadt, Germany
4. RIKEN, Ulmer Fundamental Symmetries Laboratory, Wako, Saitama 351-0198, Japan

The electron, the proton and the neutron are the basic building blocks of the visible universe. The precise knowledge of their properties is of great interest for tests of fundamental physics and metrology.

To measure the proton's mass in atomic mass units, a new cryogenic fivefold Penning-trap setup was constructed, which is termed LIONTRAP (Light ION TRAP). It is the successor experiment of the former *g*-factor experiment for highly charged ions, which provided the most stringent tests of bound-state QED [1],[2],[3].

The measurement principle is based on a phase-sensitive comparison of the proton's cyclotron frequency to that of a carbon nucleus ($^{12}C^{6+}$) as reference. To accomplish high precision a purpose-built doubly compensated Penning trap was set up, consisting of seven cylindrical electrodes. These electrodes serve to produce an extremely harmonic quadrupole trapping field by canceling out higher order electric field contributions using properly chosen voltages (Fig. 1).

We achieved a fractional uncertainty of 32 parts per trillion. This is a factor of 3 smaller than presently listed in the CODATA tables of fundamental constants [4]. Our value deviates, however, by about 3 standard deviations to the listed value (Fig. 2) [5]. At this conference, the new LIONTRAP setup as well as the latest results on the proton's atomic mass and the next major upgrades are presented.

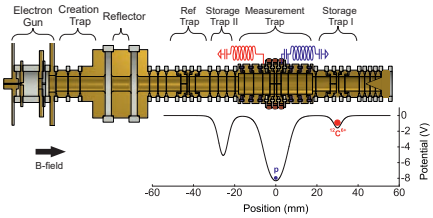

Fig. 1: Triple Penning trap for single particle mass spectrometry. The stored ions can be shifted between the different potential minima and their cyclotron frequencies are alternatively determined in the Measurement Trap.

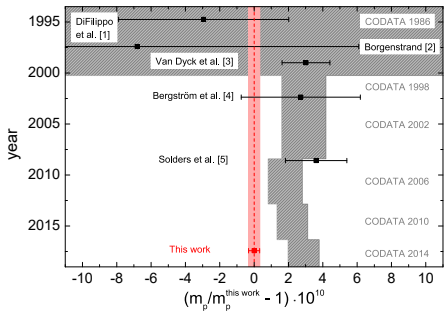

Fig. 2: Comparison of our proton mass value with previously obtained results.

References

[1] S. Sturm *et al.*, Phys. Rev. Lett. **107**, 023002 (2011).
[2] A. Wagner *et al.*, Phys. Rev. Lett. **110**, 033003 (2013).
[3] F. Köhler-Langes *et al.*, Nat. Commun. **7**, 10246 (2016).
[4] P. J. Mohr, D. B. Newell and B. N. Taylor, Rev. Mod. Phys. **88**, 035009 (2016).
[5] F. Heiße *et al.*, Phys. Rev. Lett. **119**, 033001 (2017).

*Corresponding author: werth@uni-mainz.de

Dark matter searches within the intercontinental optical atomic clock network

P. Wcisło[1], P. Ablewski[1], K. Beloy[2], S. Bilicki[1,3], M. Bober[*1], R. Brown[2], R. Fasano[2], R. Ciuryło[2], H. Hachisu[4], T. Ido[4], J. Lodewyck[3], A. Ludlow[2], W. McGrew[2], P. Morzyński[1,4], D. Nicolodi[2], M. Schioppo[2,5], M. Sekido[4], R. Le Targat[3], P. Wolf[3], X. Zhang[2], B. Zjawin[1], and M. Zawada[†1],

1. Institute of Physics, Faculty of Physics, Astronomy and Informatics, Nicolaus Copernicus University, Grudziadzka 5, 87-100 Torun, Poland
2. National Institute of Standards and Technology, 325 Broadway, Boulder, CO 80305, USA
3. LNE-SYRTE, Observatoire de Paris, Université PSL, CNRS, Sorbonne Université, 61 avenue de l'Observatoire 75014 Paris, France
4. National Institute of Information and Communications Technology 4-2-1 Nukuikitamachi, Koganei, 184-8795 Tokyo, Japan
5. National Physical Laboratory (NPL), Teddington, TW11 0LW, United Kingdom

We report preliminary results of dark mater searches within the worldwide network made of our laboratories. We demonstrate that data routinely collected by our currently operating optical atomic clocks without any further developments of the experimental set-ups may be used to run a global program aimed on searches of dark matter.

Optical atomic clocks are the most precise scientific instruments available to humanity. Their accuracy and stability reach eighteen significant digits. Therefore, optical atomic clocks are one of those experiments that push the boundaries of knowledge and metrology. The cost of their construction and maintenance, however, is many times lower and the needed research team is smaller in comparison to other great experiments that enlarge our knowledge on structure and history of our Universe, and as a consequence, bring new emerging technologies into our lives. The unique properties of these sensors are direct consequences of a typical optical atomic clock set-up. A standard optical atomic clock consists of two state-of-the-art components: an ultra-stable high-Q optical cavity which transfers stability of the length into stability of the frequency, and an atomic sample which transfers accuracy of the energy of the ultra-precise atomic clock transition into accuracy of the frequency. These two components have different susceptibilities to the external perturbations such as electric and magnetic fields, and to the possible changes of fundamental physical constants.

In this paper, we use this property to derive new constraints for oscillating massive scalar fields [1] and topological defects in the scalar fields [2] couplings to standard matter exceeding previously reported limits [3] by several orders of magnitude. These constraints were obtained by tracking the imprint of these effects in the frequency difference between cavities and atoms of several clocks distributed worldwide and running simultaneously. In this network of clocks, the technical noises (thermal noise, drift of cavities) is uncorrelated, while the effects we probe would yield correlations in remote measurements. As a consequence the optical clocks within our network do not have to be linked via phase-noise-compensated optical fibre links but only via a standard internet connection.

References

[1] A. Arvanitaki, J. Huang, K. Van Tilburg, Phys. Rev. D, **91**, 015015 (2015).
[2] A. Derevianko, M. Pospelov, Nat. Phys., **10**, 933 (2014).
[3] P. Wcisło, et al., Nat. Astron., **1**, 0009 (2016).

[*]Corresponding author: bober@fizyka.umk.pl
[†]Corresponding author: zawada@fizyka.umk.pl

Long Baseline Molecular Interferometry

Y. Y. Fein*[1], S. Gerlich[1], P. Geyer[1], L. Mairhofer[1], F. Kialka[1,2], B. A. Stickler[2], K. Hornberger[2], M. Arndt[1]
1. Faculty of Physics, University of Vienna, Boltzmanngasse 5, A-1090 Vienna, Austria
2. Faculty of Physics, University of Duisburg-Essen, Lotharstraße 1, 47048 Duisburg, Germany

High-mass matter-wave interferometry is of interest due to the uniquely macroscopic nature of the quantum wavefunctions produced as well as the range of sensitive sensing applications for which it is well suited. On the fundamental side, matter-wave interferometry enables new tests of the equivalence principle [1] and spontaneous collapse models [2], and is potentially even sensitive to a certain class of dark matter particles [3]. On the more applied side, interference with molecules allows for sensitive measurements of molecular properties in free flight. By measuring the deflection or reduction of the interference fringes due to electric, magnetic or optical fields, the associated molecular properties can be measured with a high level of precision [4].

We report on the development and first results of the Long Baseline Universal Matter-wave Interferometer (LUMI) in Vienna. LUMI is a near-field, Kapitza-Dirac-Talbot-Lau type interferometer [5] with a baseline of two meters. The order of magnitude increase in length over previous molecular interferometers should allow the experiment to demonstrate interference of particles beyond 100,000 amu. The connection between mass and length in Talbot-Lau type interferometers arises due to the Talbot condition, $L_T = d^2/\lambda$, where λ is the de Broglie wavelength. The interferometer length also makes LUMI more sensitive for metrological applications.

LUMI has recently shown its first high contrast interference signal with C60 and C70 fullerenes beyond the 40th Talbot order. This has allowed for the fine-alignment of the interferometer and preliminary metrology experiments which already indicate an improvement in resolution and accuracy. The strong fullerene signal also provides a testbed for the development of techniques required for reaching interference of molecules and clusters of up to 100,000 amu, such as compensation of the Coriolis effect.

References

[1] J. Rodewald, A. Grimalsi, P. Geyer, L. Felix, M. Mayor, A. Shayegi, and M. Arndt, N. J. Phys. 20, 033016 (2018)
[2] A. Bassi, K. Lochan, S. Satin, T. Singh, and H. Ulbricht, Rev. Mod. Phys. 85, 471 (2013)
[3] C. J. Riedel and I. Yavin, Physical Review D 96 (2017)
[4] L. Mairhofer, S. Eibenberger, J. P. Cotter, M. Romirer, A. Shayeghi, and M. Arndt, Angew. Chem. Int. Ed. 56, 10947 (2017).
[5] S. Gerlich, L. Hackermüller, K. Hornberger, A. Stibor, H. Ulbricht, M. Gring, F. Goldfarb, T. Savas, M. Müri, M. Mayor, and M. Arndt, Nature Phys. 3, 711 (2007).

*Corresponding author: yaakov.fein@univie.ac.at

Electron and Nuclear Dynamics in the Hard X-ray Domain

M.N. Piancastelli[*1,2]

1. Department of Physics and Astronomy, Uppsala University, PO BOX 516, 75120 Uppsala, Sweden
2. Sorbonne Université, CNRS, Laboratoire de Chimie Physique-Matière et Rayonnement, F-75005 Paris, France

The 'tender' x-ray domain, from 2 to 13 keV, has recently become available for atomic and molecular studies at the French synchrotron SOLEIL on the GALAXIES beam line with state-of-the-art photon and electron energy resolution. The GALAXIES beamline is dedicated to inelastic x-ray scattering (IXS) and high-energy x-ray photoemission (HAXPES) in the hard x-ray range. The beamline is designed to provide a monochromatic and microfocused beam with the highest flux possible in the 2.3-13 keV spectral range and an adaptable energy bandwidth between 50 meV and 1 eV.

We have investigated there a wealth of new phenomena by means of photoelectron and Auger spectroscopy. The list includes recoil due to the photoelectron's momentum [1,2], ultrafast nuclear motion on the femto- and sub-femtosecond time scale [3], double-core-hole studies [4-8], novel interference phenomena [9-12], ultrafast photodissociation in the Auger cascade following deep-core ionization [13,14], direct derivation of potential energy surfaces [15] (see also [16] for a recent review).

Another key experiment has been performed at SPring-8, Japan, where even higher photon energy is available, which has allowed us to measure for the first time the Xe 1s photoelectron spectrum [17].

We demonstrate that the newly accessible extended photon energy range does not simply allow studying more systems with deeper core edges, but opens a totally new horizon in what concerns electron and nuclear dynamics of deep-core-excited and core-ionized isolated species.

References

[1] M. Simon *et al*, Nat. Commun. **5**, 4069 (2014)
[2] E.Kukk *et al*, Phys.Rev.A **95,** 042509 (2017)
[3] M.N. Piancastelli et al, J. Phys. B: At. Mol. Opt. Phys. **47,** 124031 (2014)
[4] R. Püttner *et al*, Phys.Rev.Lett. **114**, 093001 (2015)
[5] S. Carniato *et al*, Phys.Rev. A **94**, 013416 (2016)
[6] G. Goldsztejn *et al*, Phys.Rev.Lett. **117**, 133001 (2016)
[7] R. Feifel *et al*, Sci.Rep. **7**, (2017) 13317
[8] D. Koulentianos *et al*, Phys.Chem.Chem.Phys. **20**, (2018) 2724
[9] D.Céolin *et al*, Phys.Rev.A **91**, 022502 (2015)
[10] R.K.Kushawaha *et al*, Phys.Rev.A **92**, 013427 (2015)
[11] G. Goldsztejn *et al*, Phys.Rev.A **95**, 012509 (2017)
[12] G. Goldsztejn *et al*, Phys.Chem.Chem.Phys. **18**, 15133 (2016)
[13] O.Travnikova *et al*, Phys.Rev.Lett. **116**, 213001 (2016)
[14] O.Travnikova *et al,* Phys.Rev.Lett. **118**, 213001 (2017)
[15] T.Marchenko *et al*, Phys.Rev.Lett. **119**, 133001 (2017)
[16] M.N.Piancastelli *et al*, J.Phys.B: At. Mol. Opt. Phys. **50,** 042001 (2017)
[17] M.N.Piancastelli *et al*, Phys.Rev.A **95**, 061402(R) (2017)

[*]Corresponding author: mailto:maria-novella.piancastelli@physics.uu.se

Probing electronic wavefunctions by all-optical attosecond interferometry

M. Krüger[*1], **D. Azoury**[1], **O. Kneller**[1], **G. Orenstein**[1], **S. Rozen**[1], **A. Clergerie**[2], **B. Fabre**[2], **B. Pons**[2], **Y. Mairesse**[2], **B.D. Bruner**[1], **N. Dudovich**[1]

1. Department of Physics of Complex Systems, Weizmann Institute of Science, Rehovot 76100, Israel

2. Université de Bordeaux - CNRS - CEA, CELIA, UMR5107, F-33405 Talence, France

Attosecond spectroscopy enables real-time observations of electron dynamics on their natural time scale (1 as = 10^{-18} s) [1]. It is based on steering electron motion by the electric field waveform of strong laser pulses. High-harmonic generation (HHG), the mechanism underlying the production of attosecond pulses in the extreme ultraviolet (XUV) provides an built-in spectroscopic pump-probe measurement with extremely high spatial and temporal accuracy. Here, under the influence of a strong laser field an electron is liberated from an atom by tunneling ionization, propagates in the laser field and is driven back to the parent ion. Recollision and recombination of the electron with the ion leads to the emission of photons in the extreme ultraviolet (XUV) regime. The amplitude and phase of the emitted XUV radiation encodes all parts of the light-matter interaction in the recollision process, enabling attosecond self-probing spectroscopy.

Here we present two applications of attosecond self-probing spectroscopy. In the first study [2], we initiate HHG with an XUV pulse instead of tunneling ionization, enabling us to measure and control the XUV photo-ionization dynamics in the presence of a strong infrared (IR) field in amplitude and phase. The existence of multiple quantum paths leading to the same final state within XUV-initated HHG naturally leads to quantum interference; this *in-situ* interferometer is controlled by the temporal delay between the IR field and the XUV pulse, enabling us to fully reconstruct the ionization process in the dressed atomic system. Our scheme opens the door to measurements of inner-shell multielectron dynamics by the self-probing scheme.

In the our study [3], we implement an *ex-situ* XUV interferometer in order to establish a powerful alternative to photoelectron spectroscopy. In the latter, the ionized electron wavefunction carries information on the structure of the bound orbital, the ionic potential as well as the photo-ionization dynamics itself. While photoelectron spectroscopy resolves the absolute amplitude of the wavefunction, retrieving the spectral phase information has been a long-standing challenge. Here, we transfer the electron phase retrieval problem into an optical one by measuring the time-reversed process of photoionization – photorecombination – in HHG (Fig. 1ab).

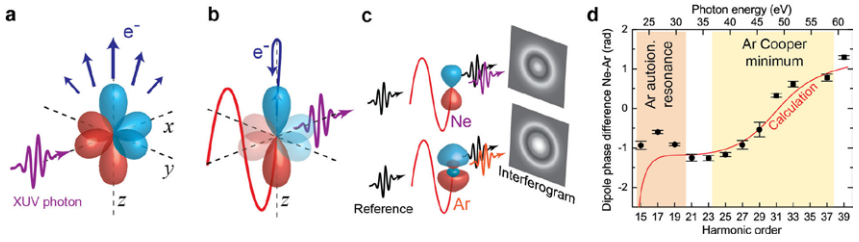

Fig. 1: a, Photoelectron spectroscopy. The emitted electron wavefunction carries the full spectroscopic information, but integrates over all angles and initial orbitals. **b**, Self-probing spectroscopy. IR-driven tunneling ionization selects one initial orbital; the returning electron is recombining through a single scattering angle and transfers its phase to an XUV photon. **c**, *Ex-situ* XUV interferometer. Interfering a reference XUV field (black) with XUV fields from either Ar or Ne leads to an interferogram, revealing their relative phases. **d**, Recombination phase difference of Ne and Ar with phase signatures of an autoionizing resonance and the Cooper minimum.

Here, we demonstrate all-optical interferometry of two independent phase-locked attosecond light sources and measure the difference in the recombination phase of different atomic species (Fig. 1c). Our scheme enables us to directly determine the scattering phase shift in simple quantum systems such as helium and neon, over a large energy range (Fig. 1d). In addition, the strong-field nature of attosecond pulse generation resolves the dipole phase around the Cooper minimum in argon through a single scattering angle, along with phase signatures of multielectron effects. Our study bears the prospect of probing complex orbital phases in molecular systems as well as electron correlations through resonances subject to strong laser fields, and also enables studies of chiral phenomena in the XUV, such as circular dichroism [4].

References

[1] F. Calegari et al., *J. Phys. B: At. Mol. Opt. Phys.* **49**, 062001 (2016).
[2] D. Azoury, M. Krüger, G. Orenstein, H.R. Larsson, S. Bauch, B.D. Bruner and N. Dudovich, *Nat. Comm.* **8**, 1453 (2017).
[3] D. Azoury et al., "Probing electronic wavefunctions by all-optical attosecond interferometry", submitted to *Nat. Phot.*
[4] D. Azoury et al., "Interferometric attosecond lock-in measurement of extreme ultraviolet circular dichroism", submitted to *Nat. Phot.*

[*]Corresponding author: michael.krueger@weizmann.ac.il

Calculations of Positron Binding to Polyatomic Molecules

A. R. Swann[*1], **G. F. Gribakin**[†1]
1. School of Mathematics and Physics, Queen's University Belfast, Belfast BT7 1NN, UK

Our work provides the first quantitative explanation for positron binding to nonpolar molecules (alkanes, C_nH_{2n+2}), including the near-linear dependence on the size of the molecule and emergence of the 2nd bound state at $n = 12$.

Positron-molecule binding energies have been measured for over 70 molecules [1]. The majority (about 60) are nonpolar or weakly polar species, for which binding is made possible by polarisation of the electron cloud. In contrast, almost all existing calculations of positron-molecule binding deal with strongly polar species (see, e.g., Ref. [2]), using approaches such as configuration interaction and diffusion Monte Carlo. For these molecules, binding occurs even at the lowest (Hartree-Fock) level of the theory, but is greatly enhanced by electron-positron correlations, e.g., polarisation [3]. Only 6 molecules have been studied both experimentally and theoretically, and the best agreement for the binding energy is only at the level of 25% for acetonitrile [4].

We have developed a model-potential approach to calculating positron-molecule binding energies. We write the positron-molecule interaction potential as $V(\mathbf{r}) = V_{\rm st}(\mathbf{r}) + V_{\rm cor}(\mathbf{r})$, where $V_{\rm st}(\mathbf{r})$ is the electrostatic potential of the ground-state molecule (described at the Hartree-Fock level), and $V_{\rm cor}(\mathbf{r})$ is a model correlation potential, viz., $V_{\rm cor}(\mathbf{r}) = -\frac{1}{2}\sum_A \alpha_A |\mathbf{r} - \mathbf{r}_A|^{-4} g_A(\mathbf{r})$, where the sum is over the molecule's constituent atoms A (whose nucleus is at position $\mathbf{r}_A$), α_A is the hybrid polarisability of atom A [5], and $g_A(\mathbf{r}) = 1 - \exp[(|\mathbf{r} - \mathbf{r}_A|/\rho_A)^6]$ is a cutoff function that prevents $V_{\rm cor}(\mathbf{r})$ from diverging near an atomic nucleus, with ρ_A a free parameter. In practice, a standard quantum-chemistry package [6] is used to compute $V_{\rm st}(\mathbf{r})$ and has been modified to include $V_{\rm cor}(\mathbf{r})$ for the positron. The figures below shows the results of the simplest calculation for several n-alkanes, taking $\rho_A = 2.2$ or 2.25 a.u. for all atoms, along with experimental data [7]. Our calculations correctly predict the existence of a second bound state for dodecane ($C_{12}H_{26}$) and larger alkanes.

Future work will entail adjusting values of ρ_C and ρ_H to obtain binding energies in closer agreement with experiment for the alkanes. We will also study aromatic hydrocarbons, alcohols, aldehydes, ketones, formates, acetates, nitriles and halogenated hydrocarbons. These calculations will provide insight into most of the molecules for which binding energies have been measured. The positron bound-state wavefunctions will be used to compute the electron-positron contact densities, positron annihilation rates and annihilation γ-ray spectra.

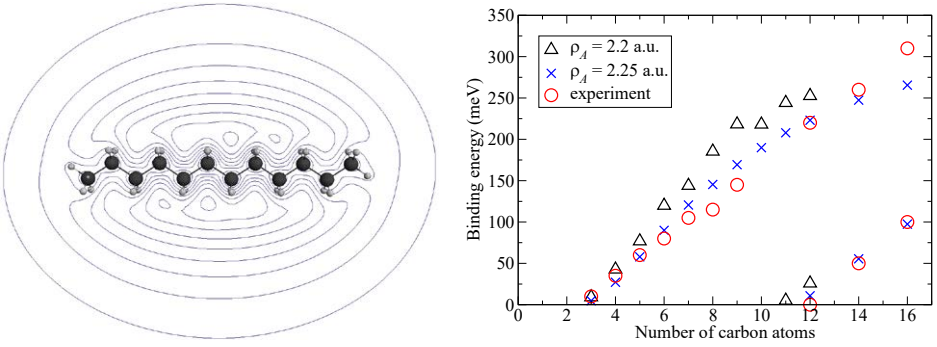

Fig. 1: Left: the positron bound state wavefunction in dodecane ($C_{12}H_{26}$) for $\rho = 2.25$ a.u. Right: comparison of the measured binding energies for n-alkanes C_nH_{2n+2} (circles) [7] with the calculated values that use the cutoff radius $\rho = 2.2$ a.u. and $\alpha_{\rm mol}$ from [8] (triangles), or $\rho = 2.25$ a.u., with $\alpha_C = 7.096$ and $\alpha_H = 2.650$ a.u. obtained from a linear fit of the molecular polarisabilities from Ref. [5] (crosses).

References

[1] J. R. Danielson, J. A. Young and C. M. Surko, J. Phys. B **85**, 022709 (2012); J. R. Danielson, J. J. Gosselin, and C. M. Surko, Phys. Rev. Lett. **104**, 233201 (2010); J. R. Danielson, A. C. L. Jones, J. J. Gosselin, M. R. Natisin, and C. M. Surko, Phys. Rev. A **85**, 022709 (2012).
[2] G. F. Gribakin, J. A. Young, and C. M. Surko, Rev. Mod. Phys. **82**, 2557 (2010).
[3] G. F. Gribakin and A. R. Swann, J. Phys. B **48**, 215101 (2015).
[4] M. Tachikawa, J. Phys. Conf. Ser. **488**, 012053 (2014).
[5] K. J. Miller, J. Am. Chem. Soc. **112**, 8533 (1990).
[6] M. W. Schmidt et al., J. Comput. Chem. **14**, 1347 (1993); P. E. Adamson *et al.*, J. Phys. Chem. A **112**, 1346 (2008).
[7] J. A. Young and C. M. Surko, Phys. Rev. A **77**, 052704 (2008).
[8] *CRC Handbook of Chemistry and Physics*, 89th edition, Ed. D. R. Lide (Boca Raton, CRC Press, 2008–2009).

*Corresponding author: a.swann@qub.ac.uk
†Corresponding author: g.gribakin@qub.ac.uk

Squeezing on Momentum States for Atom Interferometry

L. Salvi[*1],
N. Poli[1,2], **V. Vuletić**[3], **G. M. Tino**[1]
1. Dipartimento di Fisica e Astronomia and LENS — Università di Firenze, INFN — Sezione di Firenze, Via Sansone 1, 50019 Sesto Fiorentino, Italy
2. Consiglio Nazionale delle Ricerche, Istituto Nazionale di Ottica (INO), Largo E. Fermi 6, 50125 Firenze, Italy
3. Department of Physics, Research Laboratory of Electronics, Massachusetts Institute of Technology, Cambridge, Massachusetts 02139, USA

Atom interferometers for accurate gravity measurements can now be operated at the Standard Quantum Limit (SQL) of phase estimation [1]. More complex, entangled atomic states need to be implemented in an atom interferometer in order to overcome this limit. Many successful attempts to operate atomic clocks beyond the SQL have relied on the generation of squeezed states of the internal atomic motion, through high-finesse optical resonators.

In this talk I will describe a method that allows for the production of squeezed states of the atomic center-of-mass motion that can be injected into an atom interferometer [2]. The scheme employs dispersive probing in a ring resonator on a narrow atomic transition in order to provide a collective measurement of the relative population of two momentum states, see Fig. 1. It will be shown that this strategy is applicable to a Bragg diffraction-based strontium atom interferometer with large diffraction orders. Moreover, this technique can be extended to small diffraction orders and large atom numbers N by inducing atomic transparency at the frequency of the probe field, reaching an interferometer phase resolution scaling $\Delta\phi \sim N^{-3/4}$. Remarkably, a 20 dB gain in interferometer phase estimation compared to the SQL can be reached for realistic experimental parameters. The method can be extended to a number of other atomic species where atomic transparency close to a bare absorption resonance can be induced.

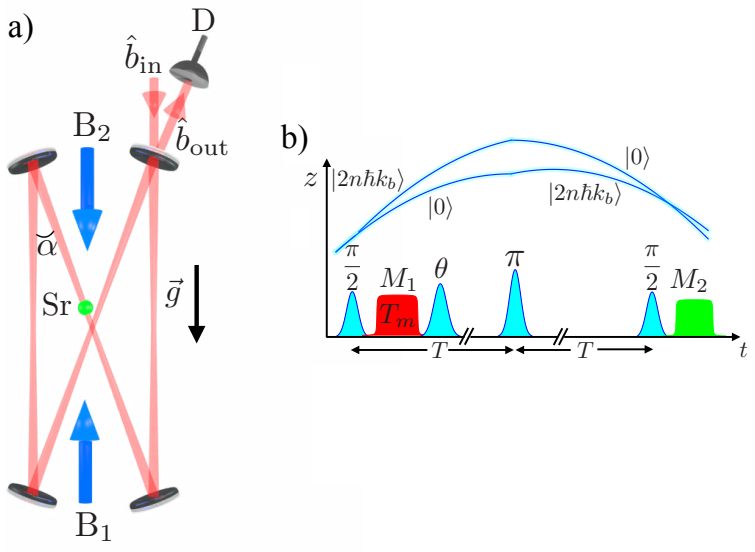

Fig. 1: Scheme of the proposal for squeezing on momentum states. a) Setup for dispersive probing of the population difference between momentum states. B_1 and B_2 are the laser beams that induce Bragg diffraction and the output field $\hat{b}_{\rm out}$ is measured through the detector D. b) Atomic trajectories in a Mach-Zehnder $\pi/2-\pi-\pi/2$ interferometer. Squeezing is induced by the measurement M_1, after which the state is transformed into a phase-sensitive state for the interferometer by the pulse θ.

References

[1] G. Rosi, F. Sorrentino, L. Cacciapuoti, M. Prevedelli and G. M. Tino, *Nature* **510**, 518-521 (2014)
[2] L. Salvi, N. Poli, V. Vuletić and G. M. Tino, *Phys. Rev. Lett.* **120**, 033601 (2018)

*Corresponding author: leonardo.salvi@unifi.it

Towards the control of delocalized states of interacting emitters

B. Lounis[*1,2]
1. Univ Bordeaux, LP2N, F-33405 Talence, France
2. Institut d'Optique & CNRS, LP2N, F-33405 Talence, France

Optical resolution of solid-state single quantum emitters at the nanometer scale is a challenging step towards the control of delocalized states formed by strongly and coherently interacting emitters, and for efficient and deterministic coupling of emitters to photonic or plasmonic nanostructures.

I will describe a simple super-resolution optical nanoscopy method operating at cryogenic temperatures, which is based on optical saturation of the excited state of single fluorescent molecules with laser-shaped beams. Sub-5 nm resolution in the transverse plane and 20 nm resolution in the longitudinal direction have been achieved. Combining this approach with single molecule super-localization techniques, we could perform the study of coherent interactions between single emitters and manipulate their degree of entanglement.

The second part of my talk is dedicated to the hybridization of quantum emitters and plasmonic nanostructures in order to achieve long-range qubit entanglement. Recent theoretical studies suggest that the plasmonic field mainly acts as a communication bus allowing for intense cross-talking between emitters, and leading to the formation of collective states known as superradiant states. In such regime the synchronized dipoles radiate at an increased rate which scales with the number of emitters, as in the case of the Dicke superradiance. Yet, experimental evidence of plasmonic superradiance is still lacking mainly because of difficulties to engineer systems with precise control of the number and positions of emitters around a metallic nanostructure.

I will present our experimental investigations of plasmonic superradiance in nanohybrids constituted of a gold core capped with a silica shell grafted with fluorescent dyes. Single particle studies revealed that the average decay rate scales with the number of grafted emitters, in agreement with theoretical predictions. Observation of plasmonic superradiance at room temperature opens questions about the robustness of collective states against decoherence processes in the condensed matter.

[*]Corresponding author: brahim.lounis@u-bordeaux.fr

Hybrid human-machine learning in quantum physics and beyond

J. Sherson[*1]
1. Department of Physic and Astronomy, Aarhus University, Ny Munkegade 120, 8000 Århus C, Denmark

Despite enabling impressive advances, the big-data driven deep learning paradigm has been challenged by AI scholars for not holding the potential to reach human scale intelligence. Instead, they propose studies of the human ability to reach heuristic solutions from little data as a basis for hybrid human-machine intelligence. An open question for the future of research is therefore how to design interfaces that allow for an optimal interaction between human intuition, complex machinery, and increasingly powerful ML.

In the www.scienceathome.org project, we have developed gamified interfaces allowing so far 250,000 players to contribute to research by providing insightful seeds for quantum optimization algorithms and remote access to our ultra-cold atoms experiment for amateur scientists, students, and researchers. Finally, I will discuss our effort to provide efficient, game-based heuristics for NP-hard computational problems related to spin glasses and ongoing efforts to demonstrate quantum supremacy using quantum annealing.

[*]Corresponding author: sherson@phys.au.dk

Evaporative cooling of atomic and molecular ions by autoresonance in an electrostatic ion beam trap

Oded Heber*[1], Reetesh Kumar Gangwar#[1], Koushik Saha[1], Michael Rappaport[2], Daniel Zajfman[1]
1. Department of Particle Physics and Astrophysics, Weizmann Institute of Science, Rehovot 7610010, Israel
2. Department of Physics Core Facilities, Weizmann Institute of Science, Rehovot 7610010, Israel

Translational cooling of atomic and molecular ions is a requisite in several research areas. An Electrostatic Ion Beam Trap (EIBT) can trap any ion with any mass or charge using the same tuning conditions; therefore, it is an ideal ion trap for ion beam cooling. An external chirp sinusoidal electric field is applied on one of the EIBT mirror electrodes. In this procedure, called autoresononace (AR), a bunch of ions is accelerated out of the rest of the ion beam population. Depending upon the chirped field intensity and rate, one can cool such a bunch of ions. A cooling process has been demonstrated in the EIBT that, by using an autoresonance procedure, reduced the temperature of ions from an initial value of ~40 K down to about 0.15 K in 80 ms and with ion-ion interaction [1]. Figure 1 shows the calculated bunch internal temperature as a function of the AR voltage using the measured ion bunch velocity distributions. The AR threshold field for an ion bunch acceleration is about 0.052 V. The arrow in the figure indicates the initial temperature of the ions in the trap before the AR process.

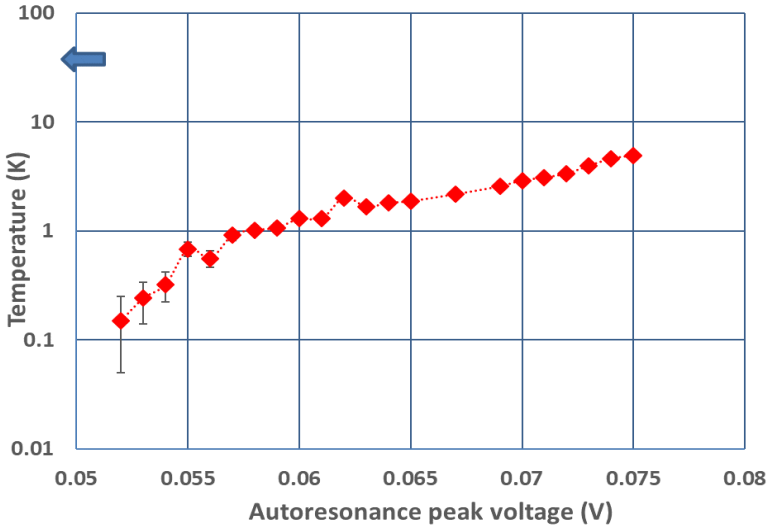

Fig 1: The temperature of the ion bunch after the autoresonance dragging process. The arrow represents the intial temerature of the ions in the EIBT

During the process, it has been shown[1] that the ion-ion collisions transfer kinetic energy from the cold population to the hotter population, which in turn is evaporated from the ion bunch, hence reducing the temperature and increasing the phase-space density. Further experiments and theoretical models are ongoing to improve the cooling efficiency and to achieve lower temperatures.

References

[1] R. K. Gangwar, K. Saha, O. Heber, M. L. Rappaport, and D. Zajfman, Phys. Rev. Lett. 119, 103202 (2017).

* Corresponding author: oded.heber@weizmann.ac.il
# present address : Department of Physics, Visvesvaraya National Institute of Technology, South Ambazari Road, Nagpur 440010, India

Cooling of atoms using an optical frequency comb

N. Šantić[1], A. Cipriš[2], D. Buhin[1], D. Kovačić[1], I. Krešić[1], D. Aumiler[1], T. Ban*[1]
1. Institute of Physics, Bijenička cesta 46, 10000 Zagreb, Croatia
2. Université Côte d'Azur, CNRS, Institut de Physique de Nice, Valbonne F-06560, France

Laser cooling and trapping brings atomic and molecular physics to one of the most exciting frontiers in science, with applications ranging from atom interferometry and optical frequency standards to high precision spectroscopy and ultracold chemistry. Regardless of such a great importance, laser cooling techniques are still limited to atoms with simple energy level structure and closed transitions accessible by current continuous wave (CW) laser technology. Laser cooling of more complex atomic species and molecules, or even simple atoms with strong cycling transitions in the vacuum ultraviolet (VUV) where generation of CW laser light is demanding, still remains an experimental challenge.

The aforementioned problems can be approached by using mode-locked femtosecond (fs) or picosecond (ps) lasers with high pulse repetition rates which produce stabilized optical frequency combs (FCs). FCs simultaneously provide high peak powers needed for the efficient frequency conversion, and the long coherence of CW lasers needed for the efficient cooling [1], [2].

I will present our recent results on sub-Doppler cooling of rubidium atoms on a dipole-allowed transition at 780 nm by using a frequency comb (FC) [3]. Temperatures as low as 55 μK were measured in a one-dimensional FC cooling geometry using time-of-flight spectroscopy. We attribute the sub-Doppler temperatures observed in FC cooling to the same mechanisms that produce sub-Doppler temperatures when cooling with continuous-wave lasers. Laser cooling with FCs could enable achieving sub-Doppler temperatures for the atoms with dipole-allowed transitions in the vacuum ultraviolet. This can significantly improve the precision of optical frequency standards, enable measurements of fundamental constants with unprecedented accuracy, and open up the possibility to reach quantum degeneracy with atoms that have optical transitions unreachable by continuous wave lasers such as hydrogen, deuterium and antihydrogen.

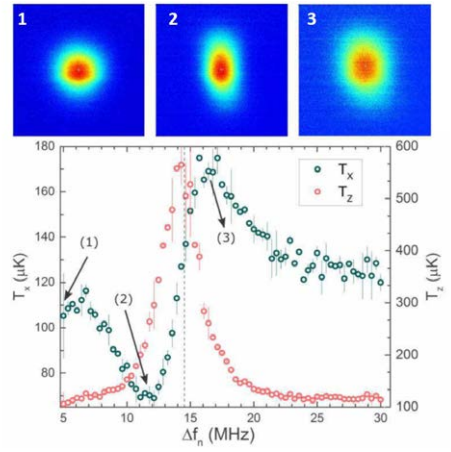

Fig. 1: Temperature obtained by TOF spectroscopy after 1D FC cooling as a function of FC detuning

References

[1] J. Davila-Rodriguez, A. Ozawa, T. W. Hänsch, and T. Udem, PRL 116, 043002 (2016) .
[2] A. M. Jayich, X. Long, and W. C. Campbell,Phys Rev X 6, 041004 (2016) .
[3] N. Šantić, A. Cipriš, D. Buhin, D. Kovačić, I. Krešić, D. Aumiler, and T. Ban, in preparation .

*Corresponding author: ticijana@ifs.hr

Menagerie of MOTs

K. N. Jarvis*[1], B. E. Sauer, M. R. Tarbutt
1. Centre for Cold Matter, Blackett Laboratory, Imperial College London, Prince Consort Road, London SW7 2AZ, UK

Ever since the first demonstration of the magneto-optical trap (MOT), made over three decades ago, examples have existed of 'type-II' MOTs [1]. In contrast to a normal atomic MOT, where the hyperfine quantum number of the excited state F' is related to that of the ground state F by $F' = F + 1$, type-II MOTs have $F' \leq F$. The presence of dark ground-state sublevels in type-II systems leads to the unfavorable characteristics of high temperature and poor confinement, and so these MOTs have not been studied much. In recent years, however, the diatomic molecules SrF [2] and CaF [3],[4] have been successfully laser cooled and trapped in a MOT using type-II transitions. Despite this impressive progress, the inherently low phase-space densities are likely to hamper some of the most exciting proposed applications of laser-cooled molecules from being realized. Using ^{87}Rb we demonstrate that the properties of type-II MOTs can be dramatically improved by using a novel approach where the light is blue-detuned from the transition [5], and present a detailed characterization of the blue-detuned MOT. The phase-space density is increased by almost a factor of one million over comparable red-detuned MOTs. Additionally, we demonstrate the existence of at least eight stable magneto-optical trapping configurations, in addition to the type-I MOT, and present an overview of the properties of these new MOTs. Our findings could be used in the study of cold and ultracold collisions between atoms.

References

[1] E. L. Raab, M. Prentiss, A. Cable, S. Chu, and D. E. Pritchard. Trapping of neutral sodium atoms with radiation pressure, Physical Review Letters, 59(23):2631-2634, 1987.
[2] J. F. Barry, D. J. McCarron, E. B. Norrgard, M. H. Steinecker, and D. DeMille. Magneto-optical trapping of a diatomic moleucle. Nature, 512:286-289, 2014
[3] S. Truppe, H. J. Williams, M. Hambach, L. Caldwell, N. J. Fitch, E. A. Hinds, B. E. Sauer, and M. R. Tarbutt. Molecules cooled below the Doppler limit. Nature Physics, 13(12):1173-1176, 2017.
[4] L. Anderegg, B. L. Augenbraun, E. Chae, B. Hemmerling, N. R. Hutzler, A. Ravi, A. Collopy, J. Ye, W. Ketterle, and J. Doyle. Radio frequency magneto-optical trapping of CaF with high density. Physical Review Letters 119(10):103201, 2017.
[5] K. N. Jarvis, J. A. Devlin, T. E. Wall, B. E. Sauer, and M. R. Tarbutt. Blue-detuned magneto-optical trap, Physical Review Letters, 120(8):083201, 2018.

*Corresponding author: k.jarvis14@imperial.ac.uk

Trapping Rydberg helium atoms above a 44-electrode chip device

V. Zhelyazkova[1], M. Žeško[1], J. A. Agner[1], H. Schmutz[1], and F. Merkt*[1]
1. Laboratory of Physical Chemistry, ETH Zurich, Vladimir-Prelog-Weg 2, 8093 Zurich, Switzerland

Atoms and molecules excited to Rydberg-Stark states can possess very large electric dipole moments μ_e (e.g., for $n = 27$ the maximal electric dipole moment $\mu_e^{max} \approx 2700$ D) and are thus amenable to translational manipulation with inhomogenous time-dependent electric fields. In particular, deceleration and trapping of H, D, H_2 and He samples generated in supersonic-beam sources and excited to Rydberg-Stark states in the vicinity of $n = 30$ has been demonstrated in experiments using 3D electrode structures [1],[2], as well as chip-based printed-circuit-board devices [3].

We present the results of experiments in which Rydberg helium atoms produced in a supersonic beam are decelerated and trapped above the surface of a 44-electrode chip kept at a cryogenic temperature. A fraction of the atomic population survives as long as 0.5 ms in the trap, an order of magnitude longer than in previous studies [3]. The helium atoms are first excited to the metastable 1s2s $^3S_1$ state in an electric discharge located at the exit of a pulsed valve. After passing through a skimmer, the atoms are excited in the presence of an electric field to a low-field-seeking Rydberg-Stark states of the $n = 27$ manifold (typically $|n,k,m_l\rangle = |27,+19,1\rangle$, where k is the label of the Rydberg-Stark state) in a one-photon excitation scheme. After excitation, the atoms fly over the 44-electrode chip, kept at 4.7 K, where they are captured in a moving quadrupole trap and brought to rest from a typical initial velocity of 880 m/s in approximately 112 μs and deceleration distance of 36 mm. After being held in the trap for a variable trapping time, the Rydberg atoms are re-accelerated to 400 m/s towards the detection region where they are detected by pulsed field ionization.

After approximately 75 μs of trapping time, during which the atoms fill up the available phase-space, we measure a trap life-time of approximately 180 μs, significantly longer than the fluorescence lifetime of the $|27,+19,1\rangle$ state of ~ 48 μs. This prolonged trap lifetime could be attributed to $m-$changing collisions of the atoms inside the trap, as described in Ref. [2], which populate high-m states. These high-m states are not accessible in direct laser excitation and are characterized by increased lifetimes, as a consequence of the reduced number of lower states to which they can decay. We further investigate the $n-$dependence and temperature dependence of the trap lifetime, as well as the collisional and radiative processes at play inside the trap.

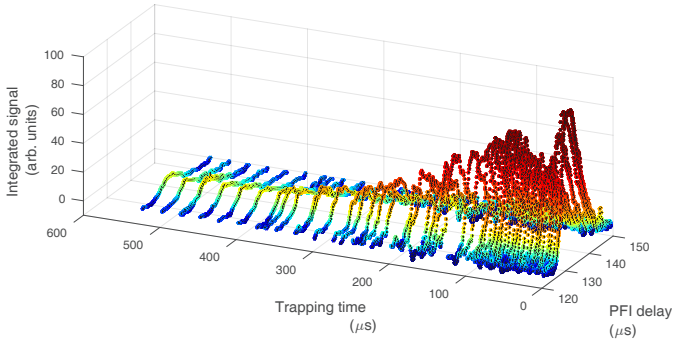

Fig. 1: Integrated atom Rydberg signal generated by pulsed-field ionization of atoms trapped for variable periods before being accelerated towards the detection region.

References

[1] Ch. Seiler, S. D. Hogan, and F. Merkt, Chimia **66**(4), 208-211 (2012) .
[2] Ch. Seiler, J. A. Agner, P. Pillet, and F. Merkt, J. Phys. B: At. Mol. Opt. Phys. **49**(9), 094006 (2016).
[3] P. Allmendinger, J. A. Agner, H. Schmutz, and F. Merkt, Phys. Rev. A **88**(4), 043433 (2013).

*Corresponding author: merkt@xuv.phys.chem.ethz.ch

The single ion heat engine — towards a sensitive quantum probe for non-classical baths

K. Singer[*1]
1. Universität Kassel, Heinrich-Plett-Straße 40, 34132 Kassel, Germany

Thermodynamic machines can be reduced to the ultimate atomic limit [1], using a single ion as a working agent. The confinement in a linear Paul trap with tapered geometry allows for coupling axial and radial modes of oscillation. The heat-engine is driven thermally by coupling it alternately to hot and cold reservoirs, using the output power of the engine to drive a harmonic oscillation [2]. From direct measurements of the ion dynamics, the thermodynamic cycles for various temperature differences of the reservoirs can be determined [3] and the efficiency compared with analytical estimates. I will describe how the engine principle can be exploited to implement a differential probe for non-classical baths.

References

[1] J. Rossnagel et al., Science **352**, 325 (2016).
[2] O. Abah et al., Phys. Rev. Lett. **109**, 203006 (2012).
[3] J. Rossnagel et al., New J. Phys. **17**, 045004 (2015).

[*]Corresponding author: ks@uni-kassel.de

Sensing buckyball spin qubits using color centers in diamond

D. Pinto[*1,2], **D. Paone**[1,2], **L. Schlipf**[1], **B. Kern**[1], **R. Wieczorek**[4], **W. Harneit**[4], **J. Wrachtrup**[1,2] **& K. Kern**[1,3]

1. Max Planck Institute for Solid State Research, 70569 Stuttgart, Germany
2. Institute of Physics, SCoPE and IQST, University of Stuttgart, 70569 Stuttgart, Germany
3. Institut de Physique, École Polytechnique Fédérale de Lausanne, 1015 Lausanne, Switzerland
4. Quantum Spintronics Research Group, University of Osnabrück, D-49074 Osnabrück, Germany

Molecular spin qubits show great promise for quantum technologies. An interesting case is that of the endofullerene N@C_{60}, which consists of a single nitrogen atom encapsulated in a C_{60} cage. N@C_{60} has some fascinating properties as an atomic spin qubit– the high-symmetry of the buckyball cage results in a long coherence time, it is thermally stable at room temperature, and the inherent scalability of fullerene networks allows for construction of complex nanoscale devices [1]. However, there is a problem – until now, the spin state readout of *single* endofullerene qubits has proven to be very difficult.

Our approach to single endofullerene qubit readout mechanism utilizes single nitrogen-vacancy (NV) color centers in diamond [2]. We use the magnetic dipolar coupling between single NV centers and N@C_{60} spins in a low-temperature (4.2 K) and ultra-high vacuum (10^{-10} mbar) experimental setup capable of performing confocal microscopy, $g^{(2)}$ autocorrelation and pulsed EPR measurements.

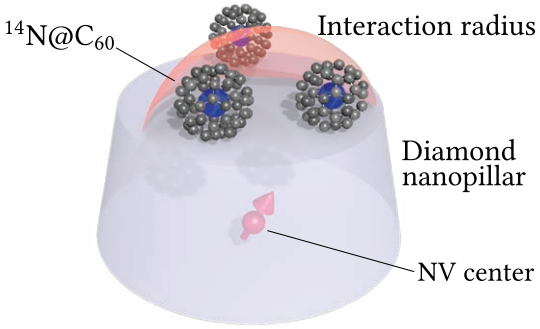

Fig. 1: Schematic of a diamond nanopillar ($r \sim 100$ nm) containing a single nitrogen-vacancy color center which is coupled to few N@C_{60} spin qubits on the surface (image not to scale).

Utilzing this readout mechanism we performed double electron resonance spectroscopy (DEER) between the NV center and the N@C_{60} spins. This allowed us to observe the hyperfine interaction of encapsulated nitrogen. Additionally, we also implemented simple quantum gate operations by driving spin state transitions of ^{14}N. These results are possibly the first steps towards realizing endofullerene based quantum registers [3], and even alternative quantum processors such as the quantum cellular automaton [4].

References

[1] Benjamin, S. C. *et al. J. Phys-Condens. Mat.* **18,** S867 (2006).
[2] Jelezko, F. and Wrachtrup, J. *Phys. Status Solidi A*, **203**: 3207-3225 (2006).
[3] Harneit, W. *Phys. Rev. A* **65**, 032322 (2002)
[4] Twamley, J. *Phys. Rev. A* **67**, 052318 (2003)

*Corresponding author: d.pinto@fkf.mpg.de

Spatially distributed genuine multipartite entanglement enables Einstein-Podolsky-Rosen steering of atomic clouds

Philipp Kunkel*[1], Maximilian Prüfer [1], Helmut Strobel [1], Daniel Linnemann [1], Anika Frölian [1], Thomas Gasenzer [1], Martin Gärttner [1], and Markus K. Oberthaler [1]

1. Kirchhoff-Institut für Physik, Universität Heidelberg, Im Neuenheimer Feld 227, 69120 Heidelberg, Germany

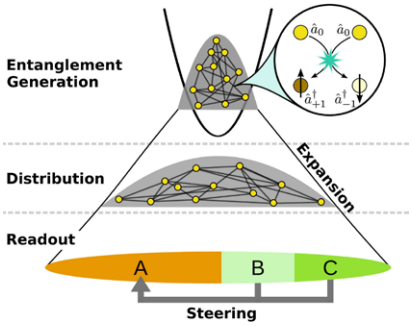

Figure 1: Experimental scheme to distribute entanglement in space [1].

Heisenberg's uncertainty relation poses a fundamental limit on the simultaneous knowledge of two noncommuting observables. Yet, quantum mechanics allows for nonlocal correlations between two systems such that a measurement in one system enables predicting the outcome in the other one with a precision beating the local uncertainty limit which is known as Einstein-Podolsky-Rosen (EPR) steering [2]. These nonclocal correlations are one of the key resources for quantum technologies. Here, we experimentally show that entanglement, which is produced in a Bose-Einstein condensate (BEC) by local contact interactions in a single spatial mode, can be spatially distributed to yield nonlocal correlations which we verify by demonstrating EPR steering ([1], see Fig. 1). Our experiment illustrates that entanglement of indistinguishable particles can be mapped to individually addressable subsystems, which has been proposed recently [3][4]. This kind of entanglement is therefore as useful, in the sense of the LOCC (local operation and classical communication) paradigm, as entanglement between distinguishable particles.

We start our experiment with a ^{87}Rb BEC held in a crossed optical dipole trap. The atoms are prepared in the magnetic substate $m_F = 0$ of the $F = 1$ hyperfine manifold. We use spin mixing to coherently populate the states $m_F = +1$ and $m_F = -1$ with atom pairs which is equivalent to spin nematic squeezing [5]. Since the atoms of the BEC are in principle indistinguishable, the correlations are shared among all atoms in the atomic cloud. By switching off the longitudinal confinement, the BEC expands in the remaining wave-guide potential and the entanglement is distributed in space. After expansion, we read out the relevant spin observable by applying a resonant rf-pulse followed by state selective absorption imaging. The high optical resolution of our imaging system enables the definition of distinct systems by partitioning the absorption signal. We measure two noncommuting spin observables and find in each partition that the fluctuations well exceed the local uncertainty constraint. Yet, we show that the measurement outcome in one subsystem of the atomic cloud can be used to infer the result in the remaining part better than allowed by the fundamental local Heisenberg uncertainty, which verifies that these parts are EPR entangled. Moreover, by partitioning the absorption signal into three parts of equal length, we demonstrate that each part is steered by the remaining ones. This confirms threeway steering.

To further elucidate the multipartite character of the generated entanglement, we construct a witness which connects the inference value of bipartite EPR steering to genuine multipartite entanglement. With this witness we reveal up to genuine five-partite entanglement.

References

[1] P. Kunkel, M. Prüfer, H. Strobel, D. Linnemann, A. Frölian, T. Gasenzer, M. Gärttner, M. K. Oberthaler, Science **360**, 413-416 (2018).
[2] M. D. Reid et al., Rev. Mod. Phys. **81**, 1727-1751 (2009).
[3] P. Hyllus, L. Pezzé, A. Smerzi, G. Tóth, Phys. Rev. A **86**, 012337 (2012).
[4] N. Killoran, M. Cramer, M. Plenio, Phys. Rev. Lett. **112**, 150501 (2014).
[5] C. D. Hamley, C. S. Gerving, T. M. Hoang, E. M. Bookjans, M. S. Chapman, Nat. Phys. **11**, 167-172 (2015)

*Corresponding author: steering@matterwave.de

Towards Cavity-Based Entanglement of an Atomic Register Under a Microscope

Francesco Ferri[1], Mohamed Baghdad[1], Arthur La Rooij[1], Sylvain Schwartz[1], Jakob Reichel[1], Romain Long*[1]

1. Laboratoire Kastler Brossel, ENS–Université PSL, CNRS, Sorbonne Université, Collège de France, 24 rue Lhomond, 75005 Paris, France

We present a new experimental platform combining optical cavity quantum electrodynamics (CQED) with a single-atom resolution microscope. Our experiment is aimed at extending the generation of multiparticle entanglement to a 1D register of up to a 100 neutral atoms, while detecting and controlling the state of each individual atom.

To achieve this goal, we have developped a new generation of dual-wavelength high-finesse fiber Fabry-Perot cavity [1]. Rubidium atoms are trapped in a one-dimensional optical lattice (at 1560 nm) along the axis of the cavity. An effective long range interaction between the atoms is provided by their coupling with a cavity mode resonant at the Rb atomic transition (780 nm). By optimizing the overlap between the two intracavity standing waves, every trapped atoms is strongly and identically coupled with the entangling mode at 780 nm. As shown on Figure 1, the microcavity has been placed under a high-resolution microscope, which we plan to use for single-site detection and addressing.

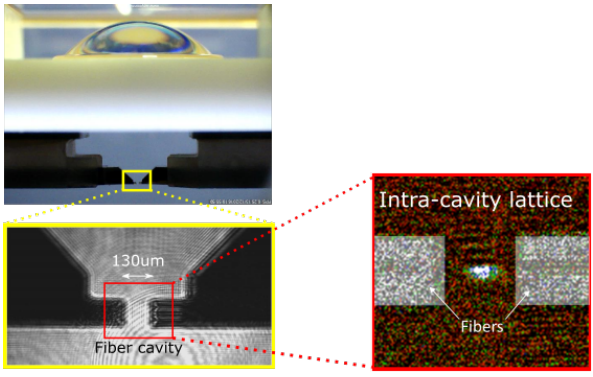

Fig. 1: Optical image of the heart of the all-in-vacuum experiment. The fiber Fabry-Perot cavity (first inset) is placed at the focus of a high-numerical aperture lens. The second inset shows an absorption image of 2000 trapped atoms in the cavity lattice.

Starting from a magneto-optical trap about 1 cm below the resonator, we load up to 2000 atoms in the cavity mode by transporting them in an "atom elevator". It is based on a moving crossed dipole trap, where one of the laser beam is displaced by an acousto-optical deflector. We will present the first signature of strong coupling between the atoms and the resonant cavity mode, which is the observation of large collective Rabi coupling of 3 GHz for 2000 atoms. We will also show the latest results of our effort to detect trapped atoms with single-site resolution in the intracavity lattice. The implementation of a moving laser beam through the microscope for single-site addressing will also be discussed.

This new experimental platform will provide an ideal test-bed to investigate multi-particle entanglement generation in many different contexts, such as in Quantum Zeno Dynamics schemes [2], at the critical point of an effective Dicke model [3], as well as reservoir-engineering techniques [4] .

References

[1] S. Garcia *et al.*, arXiv:1805.04089.
[2] G. Barontini *et al.*, Science **349**, 6254 (2015).
[3] F. Dimer *et al.*, Phys. Rev. A **75**, 013804 (2015); Z. Zhiqiang *et al.*, Optica **4**, 424 (2017).
[4] E. G. Dalla Torre *et al.*, Phys. Rev. Lett. **110**, 120402 (2013).

*Corresponding author: long@lkb.ens.fr

Experimental many-body physics using arrays of individual Rydberg atoms

S. de Léséleuc[*1], **V. Lienhard**[1], **P. Scholl**[1], **D. Barredo**[1], **T. Lahaye**[1], **A. Browaeys**[1]
1. Laboratoire Charles Fabry, Institut d'Optique Graduate School, CNRS, Université Paris-Saclay, 91127 Palaiseau Cedex, France

I will present our efforts to control the dipole-dipole interaction between single Rydberg atoms to implement various spin Hamiltonians such as the Ising model or the Su-Schrieffer-Heeger (SSH) model.

Our platform is based on single atoms trapped in an array of optical tweezers generated by holography. With our atom assembler technique [1] (see also [2]), we overcome the random loading of the traps by active sorting to prepare fully loaded arrays of single atoms. We recently extended this technique to three dimensions using fast tunable lenses and prepared structures of up to 70 single atoms spanning several planes [3].

By exciting the ground-state atoms to Rydberg states, we induce strong dipole-dipole interactions in our system. Using the van der Waals regime of this interaction, we implement the Ising model with a transverse field and study its magnetic properties [4]. I will describe the evolution of the system after a sudden quench of the Hamiltonian, or contrarily after an adiabatic change of the parameters, where we observed the build-up of anti-ferromagnetic correlations between the effective spins [5] (see also [6]).

Using the resonant dipole-dipole regime between Rydberg states of different parities now gives rise to a spin-exchange (or XY) Hamiltonian [7]. I will show how it allows us to explore the physics of the SSH chain, a basic example of topological problems in 1D.

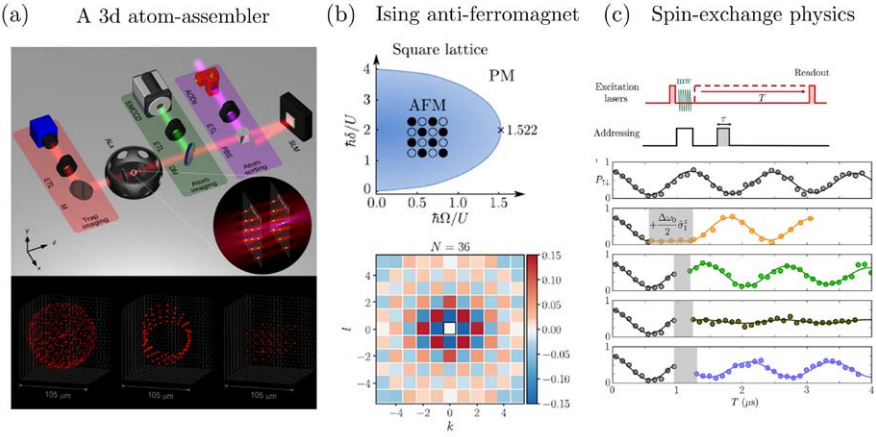

Fig. 1: (a) Atom-assembler setup using electrically tunable lenses (ETLs) and a selection of 3d structures of optical tweezers. (b) Phase diagram of the Ising model showing paramagnetic (PM) and anti-ferromagnetic (AFM) phases. Lower part: An experimental correlation map obtained by tuning the system through the quantum phase transition and ending in the AFM phase. (c) Control of the spin exchange dynamics using an addressing laser. The spin-exchange dynamics between two atoms (1st curve) can be stopped by switching on the addressing beam (2nd curve). If the system is in a superposition of two states, a relative dynamical phase can be imprinted (0, $\pi/2$ and π for the 3rd, 4th and 5th curves).

References

[1] D. Barredo *et al.*, *An atom-by-atom assembler of defect-free arbitrary 2d atomic arrays*, Science **354**, 1021 (2016)
[2] M. Endres *et al.*, *Atom-by-atom assembly of defect-free one-dimensional cold atom arrays*, Science **354**, 1024 (2016)
[3] D. Barredo *et al.*, *Synthetic three-dimensional atomic structures assembled atom by atom*, arXiv:1712.02727
[4] S. de Léséleuc *et al.*, *Accurate mapping of multilevel Rydberg atoms on interacting spin-1/2 particles for the quantum simulation of Ising models*, Phys. Rev. Lett. **120**, 113602 (2018)
[5] V. Lienhard *et al.*, *Observing the space- and time-dependent growth of correlations in dynamically tuned synthetic Ising antiferromagnets*, Phys. Rev. X (in press), arXiv:1711.01185
[6] E. Guardado-Sanchez *et al.*, *Probing quench dynamics across a quantum phase transition into a 2D Ising antiferromagnet*, Phys. Rev. X (in press), arXiv:1711.00887
[7] S. de Léséleuc *et al.*, *Local optical control of the resonant dipole-dipole interaction between Rydberg atoms*, Phys. Rev. Lett. **119**, 053202 (2017)

*Corresponding author: sylvain.leseleuc@institutoptique.fr

Wednesday

Building quantum systems from scratch

T. Esslinger[*1]
1. Institute for Quantum Electronics, ETH Zurich, Otto-Stern-Weg-1, 8093 Zurich, Switzerland

Cooling and manipulating atomic gases have opened up new avenues to explore fundamental concepts in quantum many-body physics. Synthetically created potentials and control of atom-atom interactions have made it possible to tailor the properties of experimental systems at a microscopic level. This led to the concept of quantum simulation – here a system capable of reproducing the physics of many-body Hamiltonians. One of the goals of this approach is to provide answers to open questions in the context of condensed matter physics. An equally important frontier is the construction of novel systems, which may at present not be realisable in solid-state or other systems. This path leads to new questions and surprises.

[*]Corresponding author: esslinger@phys.ethz.ch

Quantum Simulation with Cold Atoms and Ions

P. Zoller[*1,2]

1. Institute for Theoretical Physics, University of Innsbruck
2. Institute for Quantum Optics and Quantum Information, Austrian Academy of Sciences, Innsbruck

We give an overview of the field of quantum simulation with cold atoms and ions from the theory perspective, with particular focus on recent developments and future prospects. Quantum simulation with atoms aims at engineering controlled quantum many-body systems to study synthetic quantum matter, building on experimental progress in obtaining complete quantum control and measurement on the level of single atoms and quanta. While we will review briefly the traditional approaches of 'digital' and 'analog' quantum simulators, as implemented e.g. with trapped ions and atoms in optical lattices, and more recently with Rydberg atoms in optical tweezer arrays, we will discuss also on some recent developments as 'hybrid classical – quantum simulation', which we apply to condensed matter and high energy physics problems. Here a feedback loop between a classical and quantum computer optimizes a (highly entangled) ground state wave function a programmable quantum simulator. We will present results from an ongoing theory-experiment collaboration with the trapped ion group in Innsbruck for quantum electrodynamics as a lattice gauge theory. As a second topic, we discuss first theoretically measurement protocols enabled by the present generation of quantum simulators with single particle control. The example to be discussed is Renyi entropies as a witness of entanglement in quantum simulators, and in particular recent work on Renyi entropies from 'random measurements', including trapped ion experimental results. We conclude with a brief outlook how ideas and concepts of generating entangled many-atom states in atomic quantum simulation can provide novel tools and approaches in atomic spectroscopy, illustrated with the example of Ramsey interferometry with entangled states.

[*]Corresponding author: Peter.Zoller@uibk.ac.at

Quantum liquid droplets in a mixture of Bose-Einstein condensates

L. Tarruell[*1]
1. ICFO-The institute of Photonic Sciences, Castelldefels (Barcelona), Spain

Dilute quantum droplets are clusters of ultra-cold atoms self-trapped by attractive mean-field forces, and stabilized against collapse by the repulsive effect of quantum fluctuations. Despite not falling into the standard van der Waals paradigm, their properties are those of a liquid and reveal beyond mean-field effects in a weakly interacting system. In my talk I will describe our recent observation of quantum droplets in a mixture of Bose-Einstein condensates and the experimental study of the corresponding liquid-to-gas phase transition [1]. I will also discuss the difference existing between bright solitons and quantum droplets, which from a non-linear optics perspective can be understood as high-dimensional solitons stabilized by a higher order non-linearity due to quantum fluctuations [2].

References

[1] C. R. Cabrera, L. Tanzi, J. Sanz, B. Naylor, P. Thomas, P. Cheiney, and L. Tarruell, Science 359, 301 (2018).
[2] P. Cheiney, C. R. Cabrera, J. Sanz, B. Naylor, L. Tanzi, and L. Tarruell, Phys. Rev. Lett. 120, 135301 (2018).

[*]Corresponding author: leticia.tarruell@icfo.eu

Many-body localization of bosons in optical lattices

Piotr Sierant[*1], **Jakub Zakrzewski**[1,2]
1. Instytut Fizyki imienia Mariana Smoluchowskiego, Uniwersytet Jagielloński, ulica Łojasiewicza 11, PL-30-348 Kraków, Poland
2. Mark Kac Complex Systems Research Center, Uniwersytet Jagielloński, Kraków, Poland

This contribution is based mainly on [1]. Many-body localization for a system of bosons trapped in a one dimensional lattice is discussed. Two models that may be realized for cold atoms in optical lattices are considered. The first one is Bose–Hubbard model with a random on–site potential

$$H = -J\sum_{\langle i,j\rangle}\hat{a}_i^{\dagger}\hat{a}_j + \frac{U}{2}\sum_i \hat{n}_i(\hat{n}_i-1) + \sum_i \mu_i\hat{n}_i \tag{1}$$

where $a_i^{\dagger}$ and a_i are operators creating and annihilating boson at site i of the lattice, J and U are respectively tunneling amplitude and interaction strength and μ_i is a random on–site potential distributed uniformly in interval $[-W,W]$. The model (1) is compared with random interactions model [2-3]

$$H = -J\sum_{\langle i,j\rangle}\hat{a}_i^{\dagger}\hat{a}_j + \frac{1}{2}\sum_i U_i\hat{n}_i(\hat{n}_i-1) \tag{2}$$

where $U_i \in [0,U]$ is random interaction strength. While the origin and character of the disorder in both systems is different they show interesting similar properties. In particular, many-body localization appears for a sufficiently large disorder strengths W and U as verified by a time evolution of initial density wave states as well as using statistical properties of energy levels for small system sizes. Starting with different initial states, we observe that the localization properties are energy-dependent which reveals an inverted many-body localization edge in both systems – that finding is also verified by statistical analysis of energy spectrum – see Fig. 1. Moreover, we consider computationally challenging regime of transition between many body localized and extended phases where we observe a characteristic algebraic decay of density correlations which may be attributed to subdiffusion (and Griffiths-like regions) in the studied systems. Ergodicity breaking in the disordered Bose-Hubbard models is compared with the slowing-down of the time evolution of the clean system at large interactions.

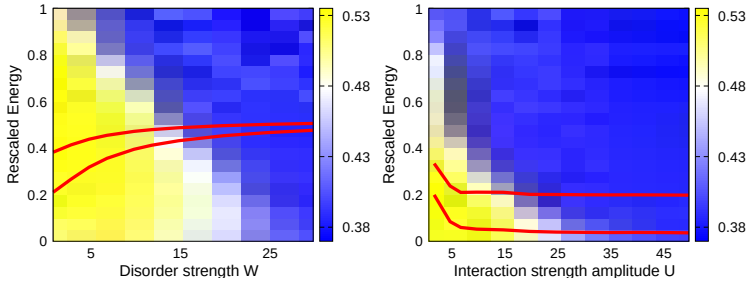

Fig. 1: The mean gap ratio $\bar{r}$ in the plane of disorder strength (W or U depending on the model) and the relative position in the spectrum of the system ε with $N = 12$ bosons on $L = 8$ sites. Left panel – random chemical potential for $U = 1$; right panel – the random interactions case. Yellow color corresponds to $\bar{r} \approx 0.53$ and to the ergodic regime, whereas the blue color denotes $\bar{r}$ characteristic for localized states. Red curves indicate energies of the density wave states $|2121...\rangle$ and $|3030...\rangle$ which are studied in the context of their localization properties. Observe that both systems are characterized by an inverted mobility edge – a feature characteristic for bosonic systems.

References

[1] P. Sierant and J. Zakrzewski, *Many-body localization of bosons in optical lattices*, New J. Phys. **20** 043032 (2018)

[2] Piotr Sierant, Dominique Delande, and Jakub Zakrzewski, *Many-body localization due to random interactions*, Phys. Rev. A **95**, 021601 (2017)

[3] Piotr Sierant, Dominique Delande, Jakub Zakrzewski, *Many-body localization for randomly interacting bosons*, Acta Physica Polonica A **132**, 1707 (2017)

*Corresponding author: sierant.piotr@gmail.com

Four-dimensional quantum walks on an optical quasicrystal

Edward Carter[*1], **Konrad Viebahn**[1], **Matteo Sbroscia**[1], **Jr-Chiun Yu**[1], **and Ulrich Schneider**[1]
1. Cavendish Laboratory, AMOP group, JJ Thomson Avenue, Cambridge CB3 0HE, UK

Ultracold atoms in optical lattices (OLs) are a powerful tool for simulating a variety of condensed-matter systems, allowing us to create designer potentials via the light shift by interfering off-resonant laser beams. Our group has constructed the first-ever such experiment to simulate a two-dimensional quasicrystal, a state of matter with long-range order but no translational symmetry. We achieve this by superimposing four mutually incoherent one-dimensional OLs at 45° angles, creating a pattern with eightfold rotational symmetry that by the crystallographic restriction theorem cannot be periodic. By exposing a BEC of ^{87}Rb to brief pulses of lattice light lasting a few µs and imaging in time of flight, we can observe this lattice in momentum space (see Fig. 1).

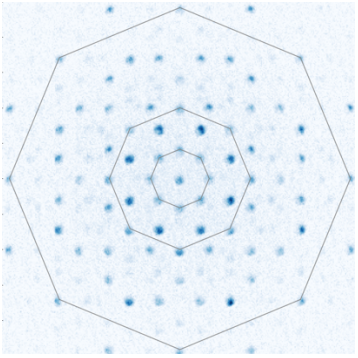

Fig. 1: Raw time-of-flight image of a BEC exposed to a 6 µs pulse of the quasicrystal lattice. This eightfold-symmetric pattern corresponds to the structure factor of the lattice. By varying the pulse duration we can observe the BEC spreading in momentum space, which simulates a quantum random walk in four dimensions. The octagons illustrate the self-similarity of the quasicrystal, which repeats itself infinitely on ever-larger lengthscales.

The irrational value of sin(45°) results in two lengthscales along each axis: 1 and $\frac{\sqrt{2}}{2}$. This requires each point to be indexed with a total of four integers, corresponding to the number of momentum kicks along each of the four lattice beams, and this in turn means that the pattern simulates a four-dimensional simple-cubic crystal. This provides a powerful and flexible experimental platform, as the dimensionality reduces by one for each laser we switch off: we can repeat the same experiments in one, two, three and four dimensions.

So far we have worked in momentum space to see how our BEC spreads out to new diffraction peaks with increasing pulse length, simulating a quantum random walk (equivalent to classical ballistic expansion). We plan to upgrade our experiment to work with ^{39}K (bosonic) in the near future and ^{40}K (fermionic) after that, allowing us to repeat these measurements without interactions by taking advantage of Feshbach resonances.

In addition we are interested in the real-space physics of the quasicrystal, especially relating to transport. By altering the power in two of the four lattice beams we can tune continuously between the periodic and quasiperiodic limits, which will allow us to chart a two-dimensional phase diagram in interaction energy U and quasidisorder Δ (as has been done by D'Errico et al for a one-dimensional quasicrystal [1]). We expect to observe Bose glass and Mott insulating phases, and many-body localisation at higher energies.

References

[1] C D'Errico et al, Phys. Rev. Lett. 113, 095301, August 2014

*Corresponding author: eac65@cam.ac.uk

Interplay between atoms and optical vortices through a Raman transition

Aurélien Chopinaud[1], Marion Jacquey[1], Bruno Viaris de Lesegno[1] and Laurence Pruvost[*1]

[1]Laboratoire Aimé Cotton, CNRS, Université Paris-Sud, ENS Paris-Saclay, Université Paris-Saclay, bat 505, 91405 Orsay, France

The orbital angular momentum of light (OAM) is a quantized variable, which is explored for quantum technology, its key strength being a wide set of values offering a large basis for encoding, entanglement, etc. In this context we study the interplay between vortices and atoms to realize quantum memories, vortex-pairs, OAM-conversion or OAM mathematical operations.

Using a Raman two-photon transition experienced in a rubidium vapour, namely the $5S_{1/2}$-$5D_{5/2}$ one (see Fig.1), we have studied the vortex conversion from a red input vortex (at 776 nm) to a blue output one (at 420 nm) for large OAMs (ℓ from -30 to 30) and we have examined the efficiency and the selection rules associated to the orbital angular momentum exchange [1].

The atomic vapour is excited by two co-propagating input lasers (780 and 776 nm) which produce a photon pair (5.23 µm and 420 nm) via the decay of the 5D level. In this four-wave mixing process we analyse the blue output wave (its shape, OAM and power) when the input laser at 776 nm is an optical vortex with ℓ varying from -30 to 30. We show that the output blue vortex respects the azimuthal phase matching, has a size determined by the product of the input beam intensities, a power decreasing with ℓ in agreement with their overlap. Finally the propagation indicates that the generated blue wave is a nearly pure mode. In addition, we explain why the input OAM is mainly transferred to the blue wave, with at large OAM input the possibility of sharing the OAM between the IR and blue wave: it relies on a combined azimuthal and Gouy phase matching conditions.

This work opens to new interplays between atoms and optical vortices, for example involving many input vortices [2], or processes for OAM storage [3] or schemes with more excited levels.

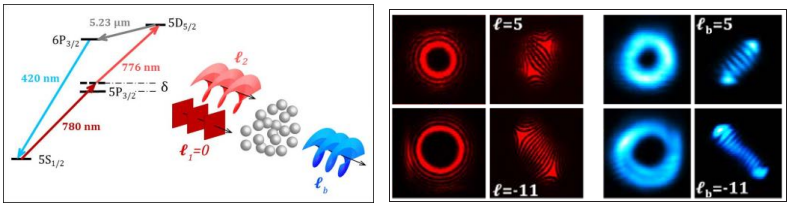

Fig. 1: on the left : principle of vortex conversion based on the two-photon Raman transition in rubidium. On the right : input red vortices and corresponding output blue vortices for ℓ=5 and ℓ=-11. The rings are the intensity profiles, the fringes pattern are the OAM characterisation.

References

[1] A. Chopinaud, M. Jacquey, B. Viaris de Lesegno and L. Pruvost, *High Helicity Vortex Conversion in a Rubidium Vapor*, Phys Rev A 2018, to appear

[2] see G. Walker, A. S. Arnold, and S. Franke-Arnold, Phys. Rev. Lett. **108**, 243601 (2012). A. M. Akulshin, et al., Opt. Lett. **40**, 1109 (2015). And references therein.

[3] see A. Nicolas et al, Nat. photonics **8**, 234 (2014). A. J. F. de Almeida et al. Opt. Lett. **40**, 2545 (2015). And references therein.

*Corresponding author: laurence.pruvost@u-psud.fr

Synthetic quantum systems with ultracold two-electron fermions

L. Fallani[*1]
1. Università degli Studi di Firenze, Italy

Ultracold gases of neutral atoms are a powerful resource for engineering synthetic many-body quantum systems. In a "quantum simulation" perspective, it is possible to control the atomic state to provide almost exact experimental realizations of fundamental theoretical models and to achieve new "extreme" states of matter.

I will report on recent experiments performed at University of Florence with degenerate gases of ultracold ^{173}Yb fermions. These two-electron atoms exhibit a rich internal structure, with distinct degrees of freedom – nuclear spin and electronic state – that can be both manipulated with high levels of quantum control. For instance, coherent coupling between nuclear spin states allowed the implementation of synthetic magnetic fields for effectively charged atoms, where the nuclear spin can be mapped onto an effective synthetic dimension [1]. Recently, we have implemented synthetic flux ladders using single-photon transitions between long-lived electronic states, which allowed us to measure chiral edge currents as a function of a fully tunable synthetic magnetic flux [2], also opening new directions for the study of spin-orbit-coupled ultracold Fermi gases with tunable interactions [3] for the realization of topological states of matter.

References

[1] M. Mancini et al., Science **349**, 1510 (2015).
[2] L. F. Livi et al., Phys. Rev. Lett. **117**, 220401 (2016).
[3] G. Pagano et al., Phys. Rev. Lett. **115**, 265301 (2015).

[*]Corresponding author: fallani@lens.unifi.it

Photoassociation and photoionization in a two-species Rb-Hg MOT

M. Witkowski[*1,2], **R. Muñoz-Rodriguez**[1], **M. Borkowski** [1], **P. S. Żuchowski** [1], **R. Ciuryło** [1], **M. Zawada** [1]
1. Institute of Physics, Faculty of Physics, Astronomy and Informatics, Nicolaus Copernicus University in Toruń, Grudziadzka 5, 87-100 Toruń, Poland
2. Institute of Physics, University of Opole, Oleska 48, PL-45-052 Opole, Poland

We present the detection of near-threshold bound states of excited heteronuclear Rb*Hg molecules through photoassociation spectroscopy [1] near the 795 nm Rb D1 line. The necessary ultracold mixture of Rb and Hg atomic gases was produced using a two-species magneto-optical trap (MOT) [2]. The interaction properties of the RbHg system as well as the prospects for photoassociation near Rb resonance lines and the production of RbHg molecules in their rovibrational ground state were recently analysed *ab initio* [3]. These theoretical predictions helped find and identify the photoassociation resonances.

Ground state molecules composed of an alkali-metal and a closed-shell atom, like RbYb [4] or RbHg, offer both permanent magnetic-dipole and electric-dipole moments thanks to their unpaired valence electron. Recently, magnetic Feshbach resonances were observed in such systems [5] providing a valuable tool for efficient control of atomic collisions. On the other hand, Hg is applicable in fundamental research with optical atomic clocks [6]. Dimers containing Hg were also proposed as good candidate species in the search for the electron electric dipole moment [7].

We also measure photoionization cross sections of the $5S_{1/2}$ and $5P_{3/2}$ states of ^{87}Rb in the Rb-Hg MOT using the Hg cooling laser operating at 254 nm. Since the 254 nm laser ionizes both the $5S_{1/2}$ and $5P_{3/2}$ states, we calibrate the latter state fraction by measuring the photoionization rate induced by an additional 401.5 nm laser. The photoionization cross section for the Rb $5P_{3/2}$ state at 401.5 nm agrees quantitatively with previous determinations [8].

References

[1] K. M. Jones, E. Tiesinga, P. D. Lett, and P. S. Julienne, Rev. Mod. Phys. **78** 483 (2006).
[2] M. Witkowski, B. Nagórny, R. Muñoz-Rodriguez, R. Ciuryło, P. S. Żuchowski, S. Bilicki, M. Piotrowski, P. Morzyński, and M. Zawada, Opt. Express **91** 879 (2017).
[3] M. Borkowski, R. Muñoz-Rodriguez, M. B. Kosicki, R. Ciuryło, and P. S. Żuchowski, Phys. Rev. A **96** 063411 (2017).
[4] N. Nemitz, F. Baumer, F. Münchow, S. Tassy, and A. Görlitz, Phys. Rev. A **79** 061403(R) (2009).
[5] V. Barbe, A. Ciamei, B. Pasquiou, L. Reichsollner, F. Schreck, P. S. Żuchowski, and J. M. Hutson, Nat. Phys. (2017) (in press) arXiv:1710.03093.
[6] K. Yamanaka, N. Ohmae, I. Ushijima, M. Takamoto, and H. Katori, Phys. Rev. Lett. **114** 230801 (2015).
[7] E. R. Meyer, J. L. Bohn Phys. Rev. A **80** 042508 (2009).
[8] T. P. Dinneen, C. D. Wallace, K.-Y. N. Tan, and P. L. Gould Opt. Lett. **17** 1706 (1992).

*Corresponding author: mwitkowski@uni.opole.pl

A Molecular Fountain

Cunfeng Cheng[1], **Aernout P.P. van der Poel**[1], **Wim Ubachs**[1], **Hendrick L. Bethlem**[*1]
1. LaserLaB, Department of Physics and Astronomy, Vrije Universiteit, De Boelelaan 1081, 1081 HV Amsterdam, The Netherlands

The resolution of any spectroscopic or interferometric experiment is ultimately limited by the total time a particle is interrogated. Here we present the first molecular fountain, a development which permits hitherto unattainably long interrogation times with molecules. In our experiments, ammonia molecules are decelerated and cooled using electric fields, launched upwards with a velocity between 1.4 and 1.9m/s and observed as they fall back under gravity. A combination of quadrupole lenses and bunching elements is used to shape the beam such that it has a large position spread and a small velocity spread (corresponding to a transverse temperature below 10μK and a longitudinal temperature below 1μK) when the molecules are in free fall, while being strongly focused at the detection region. The molecules are in free fall for up to 266ms, making it possible, in principle, to perform sub-Hz measurements in molecular systems and paving the way for stringent tests of fundamental physics theories [1].

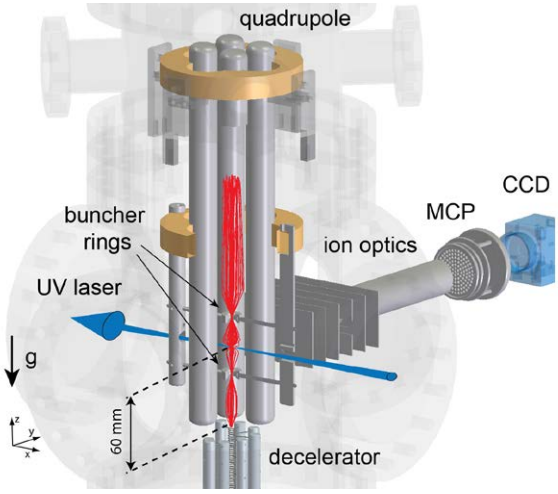

Fig. 1: Schematic view of the top part of the setup with simulated trajectories.

References

[1] C. Cheng, A.P.P. van der Poel, P. Jansen, M. Quintero-Pérez, T.E. Wall, W. Ubachs, and H.L. Bethlem, Phys. Rev. Lett. **117**, 253201 (2016).

*Corresponding author: H.L.Bethlem@vu.nl

Producing, trapping and controlling ultracold molecules

H. J. Williams*[1], L. Caldwell, N. J. Fitch,S. Truppe, J. Rodewald, E. A. Hinds, B. E. Sauer & M. R. Tarbutt
1. Department of Physics, Imperial College London, London, SW7 2BW, UK

Ultracold molecules promise to be important in the future of many experimental research areas; from quantum simulation, to collisions and cold chemistry, to precision measurement. The complicated internal structure of even the simplest of molecules makes them difficult to cool. However, recently a handful of diatomic molecules have been directly cooled and trapped. I will present recent work on the production, trapping and controlling of ultracold calcium monofluoride molecules. Using frequency-chirped laser slowing, molecules are decelerated toa low velocity, and then loaded into a magneto-optical trap [1][2]. The molecules are then cooled to 50 μK, well below the Doppler limit, in a blue-detuned optical molasses [3]. This temperature is achieved via polarisation gradient cooling.

Whilst in the molasses the molecules aren't trapped and they are distributed amongst 24 Zeeman sub-levels. We use optical pumping to transfer most of the molecules into a single level. From here we use microwave pulses to coherently transfer the population between different rotational levels demonstrating quantum state control over the molecules [4],[5].These quantum-state-selected molecules are loaded into a magnetic trap, where they have a lifetime of 4.5 s, limited by black-body radiation.

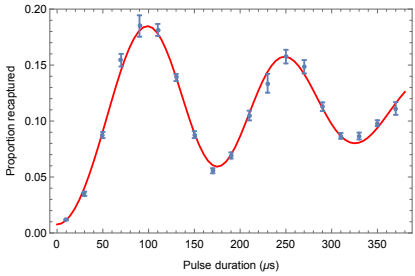

Fig. 1: Rabi oscillations between two rotational states of a CaF molecule driven by microwaves.

References

[1] An intense, cold, velocity-controlled molecular beam by frequency-chirped laser slowing. S. Truppe, H. J. Williams, N. J. Fitch, M. Hambach, T. E. Wall, E. A. Hinds, B. E. Sauer & M. R. Tarbutt. New Journal of Physics **19** 022001 (2017)
[2] Characteristics of a magneto-optical trap of molecules. H. J. Williams, S. Truppe, M. Hambach, L. Caldwell, N. J. Fitch, E. A. Hinds, B. E. Sauer & M. R. Tarbutt. New Journal of Physics **19**, 113035 (2017)
[3] Molecules cooled below the Doppler limit. S. Truppe, H. J. Williams, M. Hambach, L. Caldwell, N. J. Fitch, E. A. Hinds, B. E. Sauer & M. R. Tarbutt. Nature Physics **13**, 1173 (2017)
[4] Magnetic trapping and coherent control of laser-cooled molecules. H. J. Williams, L. Caldwell, N. J. Fitch, S. Truppe, J. Rodewald, E. A. Hinds, B. E. Sauer & M. R. Tarbutt. Physical Review Letters, **120**, 163201 (2018)
[5] Ultracold molecules: a platform for quantum simulation. J. A. Blackmore, L. Caldwell, P. D. Gregory, E. M. Bridge, R. Sawant, J. Aldegunde, J. Mur-Petit, D. Jaksch, J. M. Hutson, B. E. Sauer, M. R. Tarbutt & S. L. Cornish arXiv:1804.02372 (2018)

*Corresponding author: hjw10@imperial.ac.uk

Thursday

Attosecond ionization time delays from atoms, molecules to solid surfaces

U. Keller[*1]
1. ETH Zurich, Physics Department, Switzerland

Attosecond photo ionization delays have been first measured in my group in the multi-photon / strong field regime in 2008. Since then it has been a strong research effort and we have extensively studied the dynamics of ionization/photoemission from atoms, molecules and solids in regimes ranging from tunnel-ionization to single-photon ionization. In the simplest case, when the electron is promoted into a flat (non-resonant) continuum by direct laser-assisted single photon ionization, the measured delay after absorbing a single XUV photon is related to the group delay of the departing electron wave packet induced by the ionic potential and laser field, respectively. This delay is also referred to as the Wigner delay. This is however not the case for tunnel ionization. More recently our work in the gas phase revolved around fundamental aspects of ionization in the vicinity of autoionizing states. We could demonstrate in collaboration with Anne L'Huillier that not only the phase of the photoelectron wave packet is significantly distorted in the presence of resonances, but that this distortion depends on the electron emission angle. In H_2, on the other hand, we obtained the first experimental evidence for the importance of the coupled electron-nuclear motion for the attosecond ionization dynamics confirmed by a complete *ab initio* theoretical study with the group of Fernando Martín. Further studies on CO with an asymmetric Coulomb potential revealed that the accumulated phase of the escaping electron wave packet is not only energy- and molecular orientation dependent, but can give insight into the mean position of the ionization within the CO molecular potential. This dependence is unique to the molecular photoionization process and has been supported by two different theoretical models by S. Patchkovskii's and A. Landsman's groups. And finally our experiments on attosecond photoemission dynamics from a Cu(111) surface showed that the effective mass is a valid concept within our temporal resolution of 350 as and travel distances of only 5-7 Å.

[*]Corresponding author: keller@phys.ethz.ch

Characterizing and Imaging Magnetic Nanoparticles by Optical Magnetometry

A. Weis[*1], **S. Colombo** [1], **V. Dolgovskiy** [1], **Z. D. Grujić** [1], **S. Pengue** [1], **V. Lebedev** [1]
1. Department of Physics, University of Fribourg, Chemin du Musée 3, 1700 Fribourg, Switzerland

Biomedical applications of magnetic nanoparticles (MNP) witness a rapid development over the past decade. The targeted drug delivery by functionalized MNPs demands fast, sensitive and reliable techniques for characterizing the size distribution and other physical MNP sample parameters. In the past 4 years we have deployed atomic magnetometers (AM) for various MNP studies, viz., (•) the precision measurement of blocked MNP size distributions, their saturation magnetization, anisotropy constant, and iron content using AM-detected magneto-relaxation (MRX) [1], (•) the imaging of the magnetic field pattern from magnetized MNP by an AM-based "Magnetic Source Imaging Camera" (MSIC) [2], and more recently, source reconstruction from the field images as well as (•) the recording of $M(H)$ magnetization curves [3] and magnetic AC-suceptibilities $\chi_{AC} = dM(H)/dH$ [4] of liquid suspended MNPs by an AM. I will briefly review these studies and then focus on our recent (unpublished) demonstration of AM-based 1D and 2D MPI (Magnetic Particle Imaging) scanners based on atomic magnetometry, which closely follows the method proposed in Ref. [5].

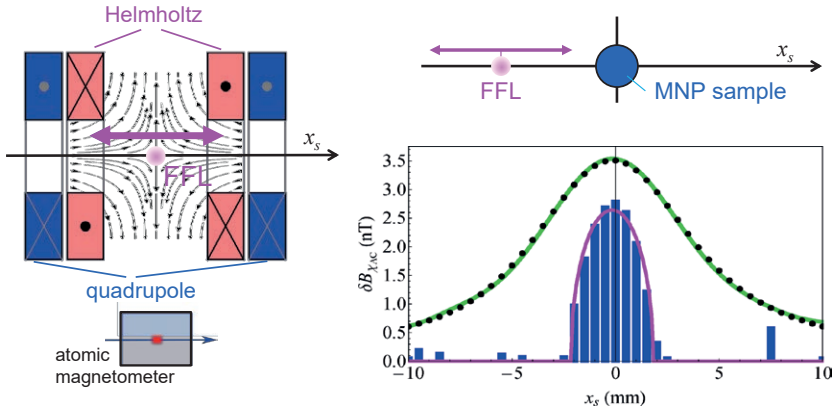

Fig. 1: Left: Principle of 1D-MPI scanner with gradient and homogenous field coils producing a field-free line (FFL), whose position can be moved along the x_s axis by scanning the the Helmholtz coil current (compensation coils [5] not shown). Right: Raw magnetometer signal (green line) from a cylindrical 4 mm diameter MNP sample, and inferred 1D MNP density distribution (blue histogram) and reconstructed signal (black dots).

Details of the MPI scanner are shown in Fig. 1. A cylindrical quadrupole field with a field-free line (FFL) is produced by 4 straight conductors. A homogeneous field produced by a second set of straight conductors is superposed on the quadrupole field, thus allowing to displace the FFL along the x_s direction. Right, top: An MNP sample (4 mm inner diameter capillary filled with ∼50 μl of Ferrotec© EMG707 ferrofluid, oriented parallel to the FFL) is located at the center of the coil system. A nearby atomic magnetometer measures the field produced by the magnetized MNPs. A field modulation technique with lock-in demodulation is used to detect a signal only when the FFL is in the vicinity of the MNP sample. Raw magnetometer data are shown as green line on the lower right. Deconvolution of the raw data with the known system point-spread function allows us to infer the MNP density distribution (blue histogram), which reproduces well the known density distribution (magenta line). The black dots represent the reconstruction of the experimental signal from the inferred density distribution.

I refer to the poster by V. Lebedev et al. for details of the method and its extension to two dimensions.

References

[1] V. Dolgovskiy, V. Lebedev, S. Colombo, A. Weis, B. Michen, L. Ackermann-Hirschi, and A. Petri-Fink, J. Magn. Magn. Mater. **379**, 137 (2015).
[2] V. Dolgovskiy, I. Fescenko, N. Sekiguchi, S. Colombo, V. Lebedev, J. Zhang, and A. Weis, Appl. Phys. Lett. **109**, 023505 (2016).
[3] S. Colombo, V. Lebedev, Z. D. Grujić, V. Dolgovskiy, and A Weis, Int. J. Mag. Part. Imag. **2**, 604001 (2016).
[4] S. Colombo, V. Lebedev, Z. D. Grujić, V. Dolgovskiy, and A Weis, Int. J. Mag. Part. Imag. **2**, 606002, (2016).
[5] S. Colombo, V. Lebedev, A. Tonyushkin, Z. Grujić, V. Dolgovskiy, and A Weis, Int. J. Mag. Part. Imag. **3**, 703006 (2017).

*Corresponding author: antoine.weis@unifr.ch

Magnetic Susceptometry Imaging with Robust Atomic Magnetometers

V. Lebedev[*1], **S. Colombo**[1], **V. Dolgovskiy**[1], **A. Tonyushkin**[2], **Z. D. Grujić**[1], **T. Scholtes**[1], **A. Weis**[1]
1. Department of Physics, University of Fribourg, Chemin du Musée 3, Fribourg, CH-1700, Switzerland
2. University of Massachusetts Boston, Physics Department, Boston, MA 02125-3393, USA

Atomic magnetometers (AM) are compact magnetic field sensors based on the optical detection of spin precession in a magnetized atomic gas. AMs perform best in highly homogeneous fields and in a magnetically silent environment. An unshielded environment, or the presence of field gradients in excess of a few nT/mm rapidly degrade the magnetometer performance (sensitivity). For this reason, the deployment of conventional AMs in biomedical imaging techniques that rely on rapidly varying strong magnetic field gradients is quite challenging. In applications based on magnetic nanoparticles (MNP) [1], such as Magnetic Particle Imaging (MPI) [2] and Magnetorelaxometry (MRX)[3], MNPs have to be magnetized by fields of a few ten mT in order to produce detectable nonlinear induction. Moreover, in scanning imaging modalities the MNPs are exposed additionally to gradients of a few T/m.

We have investigated and implemented ways to overcome those limitations and have demonstrated a coil system and an AM design allowing MNP imaging by MPI. This dedicated magnetometry system – of suitable size for small animal applications – features a high bandwidth and a high sensitivity based on feedback operation of a pump-probe variant of the M_x scheme in Cs. We have designed a compact self-shielding magnetic system, suppressing – at the nearby AM position – by three orders of magnitude the stray components of the fields and gradients needed to magnetize the MNPs and to encode their spatial distribution (Fig. 1, left). We deployed a heated, diffusion-limited Cs buffer gas cell with a mm^3-scale sensing volume that minimizes the inhomogeneous broadening of the magnetic resonance line by the fringe fields. We have optimized the resonance amplitude by varying the atomic density, light power, and deploying a repumping laser beam to compensate for hyperfine losses of pumped state population, thus keeping the sensitivity in the few pT range (Fig. 1, right top) in presence of the nearby mT field and T/m gradient sources.

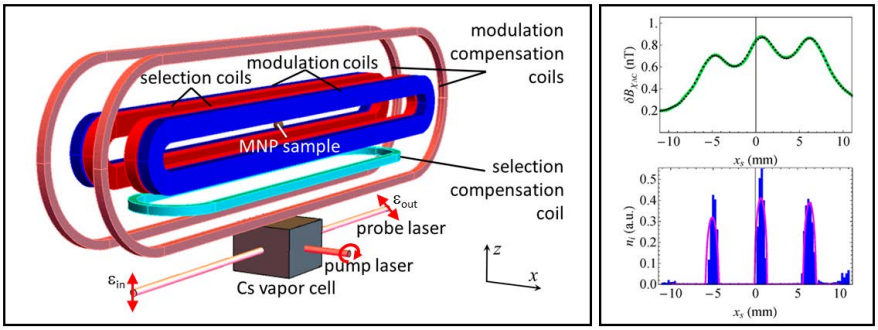

Fig. 1: Left: Sketch of the experimental set-up for performing MPI measurements on MNPs with a Cs AM. Right: Example of a 1D MPI scan of a structured MNP sample (top) and deconvoluted MNP density distribution (bottom).

In order to extract the spatial distribution of the MNPs (Fig. 1, right bottom) from the signal patterns recorded by the AM (Fig. 1, right top), we have developed efficient (off-line) data analysis routines deploying simulated annealing techniques. With the presented system we have recorded 1D mechanical (Fig. 1, right), 1D magnetic, and hybrid 2D magneto-mechanical scanned images of MNP distributions in up to a 20×40 mm^2 phantom, using the standard Resovist MNP agent.

References

[1] S. Colombo, V. Lebedev, Z. D. Grujić, V. Dolgovskiy, and A. Weis, Int. J. Magn. Part. Imag. **2**, 1604001 (2016).
[2] S. Colombo, V. Lebedev, A. Tonyushkin, Z. D. Grujić, V. Dolgovskiy, and A. Weis, Int. J. Magn. Part. Imag. **3**, 1703006 (2017).
[3] V. Dolgovskiy, V. Lebedev, S. Colombo, A. Weis, B. Michen, L. Ackermann-Hirschi, A. Petri-Fink, J. Magn. Magn. Mat. **379**, 137 (2015).

*Corresponding author: victor.lebedev@unifr.ch

Continuous-wave mirrorless lasing for directional laser guide stars and remote magnetometry

A. Akulshin[*1,2], **F. Pedreros Bustos**[†2], **N. Rahaman**[1], **R. McLean**[1], **D. Budker**[2,3]
1. Centre for Quantum and Optical Science, Swinburne University of Technology, Melbourne, Australia
2. Helmholtz-Institute, Johannes Gutenberg University, Mainz, Germany
3. Department of Physics, University of California, Berkeley, USA

The commonly used laser guide star (LGS) method developed for image correction in optical astronomy is based on the detection of near-isotropic fluorescence from the mesospheric sodium layer [1]. Even with the great recent progress in the LGS techniques, there is a widely recognized need for stronger return signals that could make image correction faster and more accurate. Low-divergence downward-directed emission generated in the sodium layer could constitute a solution to the problem. Backward cooperative emission from dense Na vapours in a cell was demonstrated using an femtosecond laser [2]; however, here we suggest an alternative approach based on continuous-wave (cw) mirrorless lasing in mesospheric Na atoms.

We report on a study of the spectral and spatial characteristics of directional emission from alkali vapours two-photon excited with cw resonant laser light in the sub-100 mW power range. In atomic media excited by cw resonant light, new optical fields can be generated by nonlinear processes such as parametric four-wave mixing (FWM) and amplified spontaneous emission (ASE) [3], [4].

First, we conducted a detailed study of new-field generation in Rb vapours revealing important properties of the ASE radiation on the $5D_{5/2}$ - $6P_{3/2}$ transition at 5.23 μm.

- Depending on the excitation geometry, the ASE radiation could be spectrally and spatially distinguishable
- Both the FWM and ASE processes could be effectively switched off by an additional resonant laser field
- We find the optimal conditions for generating spatially and temporally coherent backward-directed radiation.

The mechanism of mirrorless lasing investigated in Rb vapours has been extended to Na. A scheme of relevant energy levels of Na is shown in Fig. 1 (a). Directional emission at 2.20 μm that is equally intense in the forward and backward directions has been obtained for Na vapours excited by co-propagating laser fields at 589 and 569 nm. Its directionality, as well as the threshold-like number-density and laser-power dependences (Fig. 1b), are consistent with the mechanism of ASE. The divergence of mirrorless lasing is determined by the aspect ratio of the interaction region and can be as small as 6 mrad (Fig.1c).

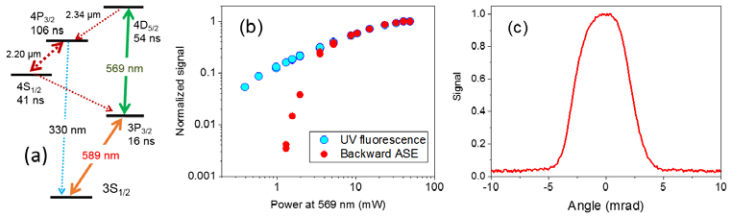

Fig. 1: (a) Relevant energy levels of Na atoms. (b) Backward emission at 2.20 μm and isotropic fluorescence at 330 nm as a function of laser power at 589 nm. (c) Spatial profile of **backward-directed lasing** at 2.20 μm.

We find that the intensity of mirrorless lasing strongly depends on the polarization of the applied laser light and magnetic field in the cell. Under the present experimental conditions, the backward ASE generated by linearly polarized laser light is approximately ten times weaker than the ASE generated by circularly polarized light. This effect, as well as its possible application for remote magnetometry, is the subject of our current study.

The presented results could decisively inform the prospects for achieving directional return from mesospheric sodium atoms that would be beneficial for remote magnetometry and may enable dramatic improvement of the LGS technique.

References

[1] W. Happer, G. J. MacDonald, C. R. Max, and F. J. Dyson, JOSA A **11**, 263-276 (1994).
[2] J. V. Thompson, et al, New J. Phys. **16**, 103017 (2014).
[3] A. Akulshin, D. Budker, and R. McLean, Opt. Lett. **39**, 845–848 (2014).
[4] A. M. Akulshin, N. Rahaman, S. A. Suslov, and R. J. McLean, JOSA B **34**, 2478-2484 (2017).

[*]Corresponding author: aakoulchine@swin.edu.au
[†]Corresponding author: pedreros@uni-mainz.de

Microwave hole-burning spectroscopy and coherent population oscillations in NV^- color centers in diamond

Mariusz Mrózek[1], Krystian Sycz[1], Andrzej Kruk[2], Adam M. Wojciechowski[*1], Wojciech Gawlik[†1]
[1] *Institute of Physics, Jagiellonian University, Łojasiewicza 11, 30-348 Kraków, Polska*
[2] *University of Information Technology and Management, ul. Sucharskiego 2, 35-225 Rzeszów, Polska*

Nitrogen-Vacancy (NV^-) color centers in diamond attract much attention of many research groups and have many applications in physics, biophysics and quantum information [1]. NV^- type defect is characterized by a nonzero electron spin (S = 1) which allows it to be optically pumped (spin polarized) by green light, probed via microwave (MW) resonance spectroscopy, and optically detected.

We present results of our research on two-field (two-frequency) microwave spectroscopy in ensemble of nitrogen-vacancy (NV^-) color centers in diamond. We focus on the case where two microwave fields drive the same transition between two NV− ground state sublevels, $m_s = 0 \leftrightarrow m_s = +1$, (Fig.1a). In this case, the observed spectra exhibit a complex narrow structure (Fig.1b) composed of three Lorentzian resonances positioned at the pump-field frequency [2-3]. The resonance widths and amplitudes depend on the population and coherence lifetimes of the levels involved in the transition. We attribute the spectra to coherent population oscillations induced by the two nearly degenerate microwave fields. We present recent developments of the theory and it's verification in the experiments with various samples of NV ensembles. The observations can be useful for detailed investigation of the NV relaxation mechanisms.

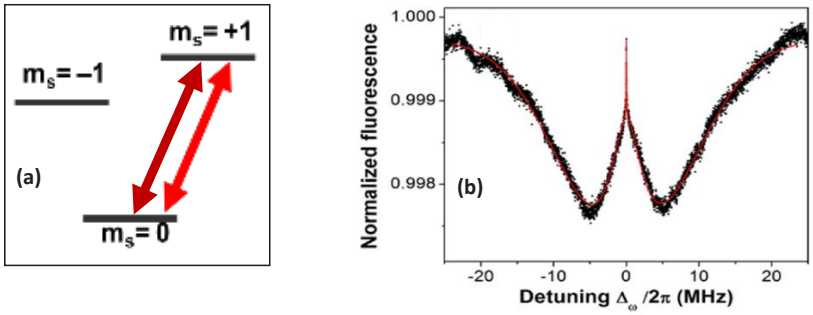

Fig. 1. **(a)** magnetic sublevels of the NV^- ground state $^3A_2$ in a non-zero magnetic field with transitions induced by two (pump and probe) MW fields. **(b)** NV^- fluorescence intensity vs. the probe frequency scanned around the $m_s=0 \leftrightarrow m_s=+1$ transition for pump field tuned to the center of that transition (from Ref.3). Red line shows the theoretical lineshape. The resonance shape reflects contributions associated with different relaxation rates.

This work was sponsored by the ERA-NET Rus+ (DIABASE), Polish National Science Center (grant 2016/21/B/ST7/01430), and MNSW (7150/E-338/M/2015).

References

[1] e.g. M.W. Doherty, N.B. Manson, P. Delaney, F. Jelezko, J. Wrachtrup, L.C.L. Hollenberg, Phys. Rep. **528**, 1-45 (2013) and the references therein
[2] P. Kehayias, M. Mrozek, V. M. Acosta, A. Jarmola, D. S. Rudnicki, R. Folman, W. Gawlik, and D. Budker, Phys. Rev. B **89**, 245202 (2014)
[3] M. Mrozek, A. M. Wojciechowski, D. S. Rudnicki, J. Zachorowski, P. Kehayias, D. Budker and W. Gawlik, Phys. Rev. B **94**, 035204 (2016)

[*]Corresponding author: a.wojciechowski@uj.edu.pl
[†]Corresponding author: gawlik@uj.edu.pl

Probing Topological Matter by «Heating»: From Quantized Circular Dichroism to Tensor Monopoles

N. Goldman[*1]
1. Université Libre de Bruxelles, CP 231, Campus Plaine, B-1050 Brussels, Belgium

The intimate connection between topology and quantum physics has been widely explored in solid-state physics, revealing a plethora of remarkable physical phenomena over the years. Building on their universal nature, topological properties are currently studied in an even broader context, ranging from ultracold atomic gases to photonics, where distinct observables and probes offer a novel view on topological quantum matter.

In this talk, I will discuss how the geometry of quantum states can be revealed using an universal scheme based on excitation-rate measurements upon periodic driving [1,2,3]. When applied to Chern insulators or Landau levels, this approach leads to a quantized circular dichroism phenomenon [1,2], which can be interpreted as the dissipative counterpart of the quantum Hall effect. Besides, we will present protocols allowing for the experimental detection of the quantum metric tensor [3], which could be applied to detect new forms of monopoles in higher dimensions [4]. Finally, I will report on the first experimental observation of quantized circular dichroism in an ultracold Fermi gas [5].

References

[1] D. T. Tran, A. Dauphin, A. G. Grushin, P. Zoller and N. Goldman, Science Advances **3**, e1701207 (2017).
[2] D. T. Tran, N. R. Cooper, and N. Goldman, arXiv:1803.01010 (2018).
[3] T. Ozawa and N. Goldman, arXiv:1803.05818 (2018).
[4] G. Palumbo and N. Goldman, arXiv:1805.01247 (2018).
[5] L. Asteria, D. T. Tran, T. Ozawa, M. Tarnowski, B. S. Rem, N. Fläschner, K. Sengstock, N. Goldman and C. Weitenberg, arXiv:1805.11077 (2018).

[*]Corresponding author: ngoldman@ulb.ac.be

Trapping Single Ions and Coulomb Crystals with Light Fields

J. Schmidt[1], **A. Lambrecht**[1], **P. Weckesser**[1], **M. Debatin**[1], **L. Karpa**[*1] **T. Schaetz**[1]
1. Physikalisches Institut, Albert-Ludwigs Universität Freiburg, Germany

Confining ions in optical dipole traps is a relatively new approach aiming to combine the most prominent advantages of ions or Coulomb crystals with those of optical traps developed for trapping and manipulating ultracold neutral atoms. On one hand, ions feature long-range interaction by means of the Coulomb force and allow for control and coherent coupling of their motional and electronic degrees of freedom on the quantum level [1]. On the other hand, in comparison to the well established radio-frequency (rf) traps, light fields provide versatile nanoscale potential landscapes and state-dependent confinement.

We report on recent experiments demonstrating optical trapping of $^{138}Ba^{+}$ ions for durations of up to a few seconds [2]. The observed lifetimes approach the performance of optical traps for single neutral atoms, improving upon previous results by 3 orders of magnitude [3],[4]. In addition, we find that the prolonged lifetimes are accompanied by low heating and electronic decoherence rates.

More recently, we have extended the presented approach to optically confine multiple ions in a focused beam dipole trap. We investigate the preservation of order in linear strings consisting of up to six ions (as shown in Fig. 1), determine their temperature, and confirm that the ions form one-dimensional Coulomb crystals by performing spectroscopy within the optical dipole trap [5]. The demonstrated properties may be useful for novel experimental studies of many-body physics, investigations of structural quantum phase transitions in Coulomb crystals, and experimental quantum simulations with ions and atoms. We will discuss the prospects of the presented methods for entering the previously inaccessible regime of ultracold interactions in ion-atom collision experiments, where optical trapping of ions may provide trapping potentials while avoiding undesired implications of conventional ion traps, such as rf-driven motion and heating [6],[7].

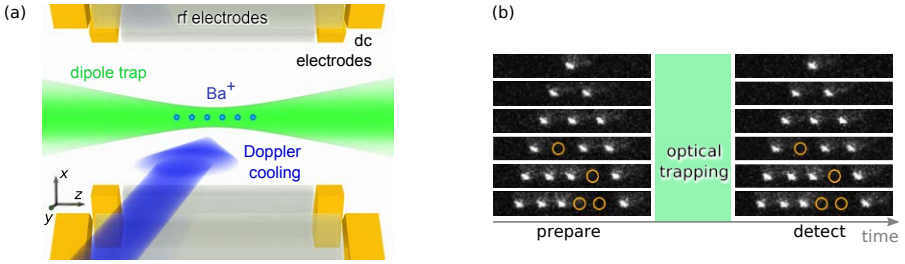

Fig. 1: (a) Set-up for optical trapping of linear ion Coulomb crystals. (b) Images of ion crystals at the end of the preparation phase and after optical trapping. The circles mark the positions of sympathetically cooled barium isotopes other than $^{138}Ba^{+}$ which are embedded into the crystal and appear dark in the image.

References

[1] D. J. Wineland, Rev. Mod. Phys. **85**, 1103 (2013).
[2] A. Lambrecht, J. Schmidt, P. Weckesser, M. Debatin, L. Karpa, and T. Schaetz, Nat. Photonics **11**, 704 (2017).
[3] C. Schneider, M. Enderlein, T. Huber and T. Schaetz, Nat. Photon. **4**, 772 (2010).
[4] T. Huber, A. Lambrecht, J. Schmidt, L. Karpa and T. Schaetz, Nat. Commun. **5**, 5587 (2014).
[5] J. Schmidt, A. Lambrecht, P. Weckesser, M. Debatin, L. Karpa, and T. Schaetz, Phys. Rev. X **8**, 021028 (2018)
[6] M. Cetina, A. T. Grier, and V. Vuletić, Phys. Rev. Lett. **109**, 253201 (2012).
[7] Z. Meir, T. Sikorsky, R. Ben-shlomi, N. Akerman, Y. Dallal, and R. Ozeri, Phys. Rev. Lett. **117**, 243401 (2016).

*Corresponding author: leon.karpa@physik.uni-freiburg.de

Spontaneous emission beyond dipole approximation in nanoscopic environments

K. Słowik[*1], **M. Kosik**[1]
1. Institute of Physics, Faculty of Physics, Astronomy and Informatics, Nicolaus Copernicus University, Grudziadzka 5, 87-100 Torun, Poland

The possibility to control the spontaneous emission lifetime of quantum emitters by tailoring their surroundings was first investigated in the pioneering work of Purcell [1]. An excited quantum emitter can decay to the photonic modes of its environment, whose local density can be modified by the surroundings. Such influence on emitters such as atoms, molecules and quantum dots has been experimentally verified in various types of cavities or band-gap environments, including semiconductor microstructures [2], photonic crystals [3], and plasmonic nanoparticles [4], where the emission rate was boosted by so-far the record 3 orders of magnitude.

Usually only the electric dipole contribution to the spontaneous emission of quantum emitters is considered, which is justified in the case of negligible spatial variations of the electric field over the size of the quantum emitter. However, nanoscopic environments are capable of localizing the electric field into nanometric spatial domains, providing high intensities and spatial modulations at the length scale of the emitter. Thus, higher order multipolar contributions to light-matter coupling may become relevant. Until now, the enhancement by a nanostructure of magnetic dipole emission of lanthanide ions, such as Eu^{3+} and Er^{3+}, was reported [5]. Large enhancement of quadrupole transitions was predicted [6]. Transitions driven with several multipolar mechanisms have been observed in semiconductor quantum dots [7].

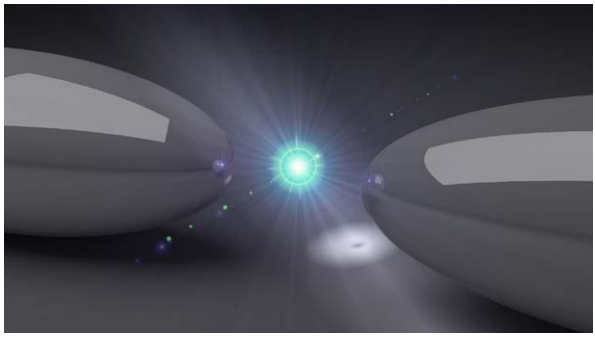

Fig. 1: Artistic impression of a pair of nanoellipsoids influencing radiative properties of a quantum emitter.

Here, we derive expressions for spontaneous emission rates beyond the electric dipole approximation, taking into account the magnetic dipole and electric quadrupole components [8]. Our approach generalizes the one introduced in Ref. [9], based on the Green's tensor formalism applied to quantize electromagnetic fields and account for resulting vacuum fluctuations. A Green's tensor naturally takes into account the structure of electromagnetic surroundings, and is suited to describe nanoparticles made of dispersive and lossy materials such as metals. Exemplary cases will be discussed where the terms beyond the electric dipole significantly influence the emission rate or even dominate it. Finally, we will investigate interference of different multipolar components, which may lead to an even stronger enhancement of the emission rate, or - contrary - to its suppression, leading to enhanced lifetimes of quantum emitters.

References

[1] E.M. Purcell, Phys. Rev. 69, 681 (1946).
[2] Gérard, J. M., et al., Phys. Rev. Lett. 8(5), 1110 (1998).
[3] T.B. Hoang, Thang B. et al., Nature communications 6, 7788 (2015).
[4] S. Noda, M. Fujita, and T. Asano, Nature Photonics 1(8), 449 (2007).
[5] M. Kasperczyk et al., Phys. Rev. Lett. 114(16), 163903, (2015).
[6] R. Filter et al., Phys. Rev. B 86(3), 035404 (2012).
[7] P. Tighineanu et al., Phys. Rev. Lett., 113(4), 043601 (2014).
[8] K. Słowik and M. Kosik, to be published
[9] D. Dzsotjan, et al., Phys. Rev. B 82(7), 075427 (2010).

*Corresponding author: karolina@fizyka.umk.pl

Gold cluster radiation from thermally populated excited electronic states

K. Hansen[*1], **P. Ferrari**[2], **E. Janssens**[2], **P. Lievens**[2]
1. Center for Joint Quantum Studies and Department of Physics, Tianjin University, 92 Weijin Road, Tianjin 300072, China
2. Laboratory of Solid State Physics and Magnetism, KU Leuven, 3001 Leuven, Belgium

Small positively charged gold clusters have been found to emit thermal radiation at a very high rate, with time constants ranging from one to 35 μs for Au_n^+ ($n = 6-13, 15$)[1]. Photon emission time constants of this magnitude are only consistent with emission of thermally excited electronic states. Direct detection of the emitted photons in the analogous process in small carbon clusters have confirmed the nature of this decay [2]. For sizes $n = 14, 16-20$ the radiation occurs on much longer time scales, beyond the reach of the reflectron Time-of-Flight mass spectrometer used in this study.

The clusters were produced neutral in a laser ablation source [3] and excited, ionized and strongly fragmented by laser pulses of either 20 mJ at 355 nm or 140 mJ at 532 nm wavelengths, with no change in the observed quantities. The extensive fragmentation excludes long-lived states as the origin of the photons and allows an analysis based on broad internal clusters energy distributions. Radiative cooling was inferred from the suppression of the metastable evaporation between mass selection and analysis in the reflectron. Fig. shows the results of the measurements.

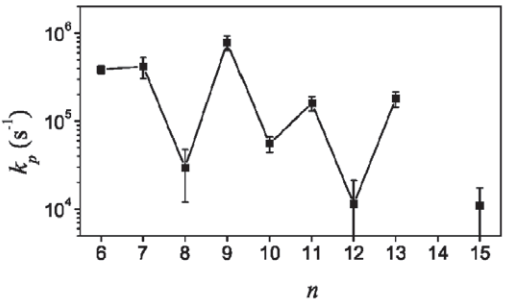

Fig. 1: The fitted values of the photon emission rate constant, k_p. The uncertainties are 1-σ values. The values for n = 14, 16 - 20 are consistent with zero.

The measured data combined with the Thomas-Reiche-Kuhn dipole transition sum rule limit the possible excited state energies, and gives a minimum oscillator strength required. The upper limits of the state energies are given all around 1.5 eV. The necessary oscillator strengths are in all cases below $f = 1$ and usually less than $f = 0.3$, corresponding to 0.3 electron out of the $n-1$ valence electrons.

These and similar results for niobium[4], silicon[5], and carbon[6],[7],[8] suggest that this dissipation mechanism from highly excited clusters may be more widespread that previously anticipated.

References

[1] K . Hansen, P. Ferrari, E. Janssens, and P. Lievens, Phys. Rev. A **96** 022511 (2017)
[2] Y . Ebara, T. Furukawa, J. Matsumoto, H. Tanuma, T. Azuma, H. Shiromaru, and K. Hansen, Phys. Rev. Lett. **117** 133004 (2016)
[3] W . Bouwen, P. Thoen, F. Vanhoutte, S. Bouckaert, F. Despa, H. Weidele, R.E. Silverans, and P. Lievens, Rev. Sci. Instrum. **71** 54-58 (2000)
[4] K . Hansen, Y. Li, V. Kaydashev, and E. Janssens, J. Chem. Phys., **141** 024302 (2014)
[5] P iero Ferrari, Ewald Janssens, Peter Lievens, and Klavs Hansen, J. Chem. Phys. **143** 224313 (2015)
[6] K . Hansen and E.E.B. Campbell, J. Chem. Phys. **104** 5012 (1996)
[7] J . U. Andersen, C. Brink, P. Hvelplund, M. O. Larsson, B. B. Nielsen, and H. Shen, Phys. Rev. Lett. **77** 3991 (1996)
[8] G . Ito, T. Furukawa, H. Tanuma, J. Matsumoto, H. Shiromaru, T. Majima, M. Goto, T. Azuma, and K. Hansen, Phys. Rev. Lett. **112** 183001 (2014)

[*]Corresponding author: klavshansen@tju.edu.cn

Friday

Nonlinear magneto-optics

D. Budker[*1]
1. Johannes Guttenberg University, Mainz, Germany

I plan to talk about nonlinear magneto-optics and the key role Prof. Gawlik has played in its development.

[*]Corresponding author: budker@uni-mainz.de

The optical ^{88}Sr lattice clocks and stabilized fibre links: a frequency reference for the VLBI system

M. Zawada[*1], **P. Krehlik** [2], **Ł. Buczek** [2], **J. Kołodziej** [2], **M. Lipiński** [2], **Ł. Śliwczyński** [2], **J. Nawrocki** [3], **P. Nogaś** [3], **A. Marecki** [4], **E. Pazderski** [4], **P. Ablewski** [1], **M. Bober** [1], **R. Ciuryło** [1], **A. Cygan** [1], **D. Lisak** [1], **P. Masłowski** [1], **P. Morzyński** [1], **B. Campbell** [2], **J. Pieczerak** [6], **A. Binczewski** [7], **K. Turza** [7]

1. Institute of Physics, Faculty of Physics, Astronomy and Informatics, Nicolaus Copernicus University, Grudziądzka 5, PL-87-100 Toruń, Poland

2. Department of Electronics, AGH University of Science and Technology, al. Mickiewicza 30, PL-30-059, Kraków, Poland

3. Time and Frequency Department, Astrogeodynamic Observatory of Space Research Center, Borowiec, Drapałka 4, PL-62-035 Kórnik, Poland

4. Centre for Astronomy, Faculty of Physics, Astronomy and Informatics, Nicolaus Copernicus University, Grudziądzka 5, PL-87-100 Toruń, Poland

5. Joint Institute for VLBI ERIC, Oude Hoogeveensedijk 4, 7991 PD Dwingeloo, The Netherlands

6. Orange Polska S.A., Obrzeżna 7, 02-691 Warszawa, Poland

7. Poznanń Supercomputing and Networking Center, Jana Pawła II 10, 61-139 Poznań, Poland

On 26th Nov. 2015 Toruń Radio Astronomy Observatory (based in Piwnice near Toruń), a part of the Centre for Astronomy of N. Copernicus Univ., Toruń (Poland) was connected to Polish fibre optic network distributing time and frequency (T&F) signals from UTC(PL) and UTC(AOS) laboratories. This paves the way for investigation of alternative methods of T&F synchronization during Very Long Baseline Interferometry (VLBI) observations.

Typically, T&F signals for VLBI observations are provided by the local standard, usually H-maser. Here, we report how the fibre network allows remote synchronizing the station with optical strontium lattice clocks [1][2] operated in National Laboratory of Atomic, Molecular and Optical Physics (KL FAMO) in Toruń and with both Polish UTC laboratories [3]. Additionally, the local H-maser may be disciplined by these two remote sources.

We conducted a proof-of-concept experiment on 15 March 2016 during the test time preceding a regular e-VLBI session of the European VLBI Network (EVN). Besides the Toruń VLBI station, the participating telescopes included Effelsberg (DE), Medicina (IT), and Yebes (ES). We have successfully proved that the remote optical atomic clock can provide the operational synchronization of radio telescopes during VLBI observations.

References

[1] P. Morzyński *et al.*, Sci. Rep. **5**, 17495 (2015)
[2] M. Bober *et al.*, Meas. Sci. Technol. **26** 075201 (2015)
[3] P. Krehlik *et al.*, A&A **603**, A48 (2017)

*Corresponding author: zawada@fizyka.umk.pl

A Single Atom Interacting with Light in Free Space

G. Leuchs

1. Max Planck Institute for the Science of Light, Staudtstrasse 2, 91058 Erlangen, Germany
2. Department of Physics, University of Erlangen-Nürnberg, Staudtstrasse 7 / B2, 91058 Erlangen, Germany
3. Department of Physics, University of Ottawa, 25 Templeton Road, Ottawa, Ontario, K1N 6N5, Canada
4. Institute of Applied Physics, Russian Academy of Sciences, 46 Ul'yanov Street, 603950, Nizhny Novgorod, Russia

One might regard the emission and absorption of light by a single atom in free space as one of the most fundamental processes in quantum optics, which has not yet been fully explored on the experimental side:

1. A single atom should be able to act as an efficient 100% reflector for narrow band coherent light provided the light power is not too high.
1. A single atom should be able to efficiently shift the phase of a narrow band coherent light by up to 180° if the light power is not too high. (First results, see [1].)
2. A single photon should be able to deterministically excite a single atom.

We are developing and testing a set-up for the demonstration of this reversal of spontaneous emission by placing a single atom at the focus of a deep parabolic mirror. Using an ionized atom one can hold it in place by electrodes, a variation of the Paul trap for ions. It is expected that such a 100% excitation by a single atom require sending in the time-reversed version of the photon, which would be emitted by the same atom if it were to decay. Regarding the spatial structure, a parabolic mirror generates the required ingoing spherical wave fronts. Concerning the temporal shape, the single photon wave packet should have an exponentially rising leading edge as opposed to the exponentially falling trailing edge of the wave packet created in a spontaneous emission process [2].

References

[1] M. Fischer, B. Srivathsan, L. Alber, M. Weber, M. Sondermann, G. Leuchs, Appl. Phys. **B 123**, 48 (2017).
[2] M. Stobinska, G. Alber, and G. Leuchs, Euro Phys. Lett. **86**, 14007 (2009).

Our road to optical atomic clock

C. Radzewicz[*1]
1. Department of Physics, Institute of Experimental Physics, University of Warsaw, Pasteura 5, 02-093 Warsaw, Poland

I will speak about the initiative of Polish AMO community aimed at construction the strontium 87 optical atomic clock. Wojtek was one of the leaders of this project from the very beginning to the end and the contribution of his group to the project was absolutely crucial.

[*]Corresponding author: Czeslaw.Radzewicz@fuw.edu.pl

Time Crystals

Krzysztof Sacha[*1]
1. Jagiellonian University in Krakow, Marian Smoluchowski Institute of Physics, ul. Prof. Łojasiewicza 11, 30-348 Kraków, Poland

Time crystals are quantum many-body systems which, due to interactions between particles, are able to self-organize spontaneously their motion in a periodic way in time by analogy with the formation of crystalline structures in space in condensed matter physics [1]. In solid state physics properties of space crystals are often investigated with the help of external potentials that are spatially periodic and reflect various crystalline structures. A similar approach can be applied for time crystals, as periodically driven systems constitute counterparts of spatially periodic systems, but in the time domain [1].

The basic idea of the so-called discrete time crystals [2][3][4], that have been already realized in the experiments [5][6], will be presented. Moreover, it will be shown that condensed matter problems ranging from Anderson localization in time or single particles in potentials of quasi-crystal structure in time to many-body systems with exotic long-range interactions in the time domain can be realized with an appropriate periodic driving [1][7][8][9]. Moreover, it is possible to create molecules where atoms are bound together due to destructive interference if the atomic scattering length is modulated in time [9].

References

[1] K. Sacha and J. Zakrzewski, Rep. Prog. Phys. **81**, 016401 (2018).
[2] K. Sacha, Phys. Rev. A **91**, 033617 (2015).
[3] V. Khemani et al, Phys. Rev. Lett. **116**, 250401 (2016).
[4] D. V. Else et al., Phys. Rev. Lett. **117**, 090402 (2016).
[5] J. Zhang et al., Nature **543**, 217 (2017).
[6] S. Choi et al., Nature **543**, 221 (2017).
[7] K. Sacha, Sci. Rep. **5**, 10787 (2015).
[8] D. Delande, L. Morales-Molina and K. Sacha, Phys. Rev. Lett. **119**, 230404 (2017).
[9] K. Giergiel, A. Miroszewski, and K. Sacha, Phys. Rev. Lett. **120**, 140401 (2018).

[*]Corresponding author: krzysztof.sacha@uj.edu.pl

Cold atoms in Cracow

T. Kawalec[*1]
1. Jagiellonian University in Krakow, Marian Smoluchowski Institute of Physics, ul. Prof. Łojasiewicza 11, 30-348 Kraków, Poland

I will shortly present the role Professor Gawlik played in the development of cold atom physics in Cracow and in Poland.

Then I will focus on our realization of a plasmonic dipole mirror for cold atoms based on a metallic grating coupler. In this case a cloud of atoms is reflected by the repulsive potential generated by surface plasmon polaritons (SPPs) excited on a gold grating by a 780 nm laser beam. Experimentally and numerically determined mirror efficiency is close to 100%. The intensity of SPPs above a real grating coupler and the classical atomic trajectories, are computed.

Using the dipole mirror, we have determined the absolute value of the surface plasmon polariton (SPP) intensity, reaching 90 times the intensity of the excitation laser beam. With an infrared camera we have also directly measured thermo-plasmonic effects accompanying SPPs excitation on gold submicron structures [1], [2].

References

[1] T. Kawalec, D. Bartoszek-Bober, R. Panaś, J. Fiutowski, A. Pławecka, H.-G. Rubahn, Opt. Lett. **39**, 2932 (2014).
[2] T. Kawalec, A. Sierant, R. Panaś, J. Fiutowski, D. Bartoszek-Bober, L. Józefowski, H.-G. Rubahn, Plasmonics **13**, 639 (2018).

[*]Corresponding author: tomasz.kawalec@uj.edu.pl

Title to be announced

Fedor Jelezko[1]
1. Institute for Quantum Optics and Center for Integrated Quantum Science and Technology (IQST), Ulm University, Albert-Einstein-Allee 11, 89081 Ulm, Germany

Concluding remarks

Wojciech Gawlik[1]
1. M. Smoluchowski Institute of Physics, Jagiellonian University, Łojasiewicza 11, 30-348 Kraków, Polska

Poster session A

On photonic spectral entanglement improving quantum communication

K. Sędziak, Mikołaj Lasota, Piotr Kolenderski
Faculty of Physics, Astronomy and Informatics, Nicolaus Copernicus University, Grudziadzka 5, 87-100 Torun, Poland

Single-photon sources are crucial components for the implementation of quantum communication (QC) protocols. However, photons emitted by some of the most popular types of realistic sources, e.g. the ones based on SPDC process [1,2], are spectrally broadband. Due to this drawback, the signal emitted from such sources is typically affected by the effect of temporal broadening during its propagation through telecommunication fibers, exhibiting chromatic dispersion. In the case of long-distance QC this phenomenon can significantly limit the efficiency of temporal filtering [3]. It is a popular method for decreasing the number of registered errors, basing on the reduction of the duration time of the detection windows. Thus, temporal broadening of the signal emitted by realistic single-photon sources negatively affects the security of QC protocols.

In our work we investigate the temporal properties of a pair of photons produced by a SPDC source and subsequently propagated through a pair of standard single-mode fibers. In particular, we study the connection between the type of spectral correlation generated between those photons and their temporal widths. We show that in some realistic scenarios changing the typical negative type of this correlation to the positive one, or decreasing its strength, can lead to narrowing of the temporal wave function of SPDC photons. Therefore, it can increase the effectiveness of the temporal filtering method.

The results of our work can be used to improve the security of QKD systems [4,5]. They can be particularly important for the QKD schemes utilizing commercial telecom fibers populated by strong classical signals. In such situations the temporal filtering method can be utilized to reduce not only the dark counts registered by the detection system, but also the excessive channel noise originating from the process of Raman scattering, which is the main factor limiting their performance [6].

References

[1] T. Lutz et al., Opt. Lett. 38, 697 (2013).
[2] T. Lutz et al., Opt. Lett. 39, 1481 (2014).
[3] K. A. Patel et al., Phys. Rev. X #, 041010 (2012).
[4] K. Sedziak et al., Optica **5**, 84 (2017), K. Sedziak et al, arXiv:1711.06131
[5] M.Lasota, P. Kolenderski, arXiv:1702.05165
[6] P. Eraerds et al., N. J. Phys. 12, 063027 (2009).

Electro-optical effect in dense and cold atomic ensembles

I. M. Sokolov[*1]
1. Peter the Great St. Petersburg Polytechnic University, Polytechnicheskaya st. 29, 195251 St. Petersburg, Russia

This work is devoted to theoretical analysis of the influence of an electrostatic fields on optical properties of nondegenerate atomic gases cooled to sub-Doppler temperatures in atomic traps. We focus our attention on dense atomic ensembles, in which the mean free path of the resonant radiation is comparable with its wavelength. Besides wide range of possible practical applications, such ensembles exhibit a number of unique physical properties, for example, subradince, a collective Lamb shift, random lasing, and possible strong localization of light, which are either impossible or essentially suppressed in low-density media.

Our analysis is based on the consistent quantum approach developed previously in [1], [2]. In the framework of this approach we solve the Schrodinger equation for the wave function of the joint system consisting of all atoms and a weak electromagnetic field. The description of the field takes into account all modes, including the modes of the vacuum reservoir, which allows considering the interaction of the atoms with the external light, resonant dipole–dipole interatomic interaction, and spontaneous decay in a single approach.

On the basis of this approach we study spatial distribution of atomic polarization created by weak monochromatic light in atomic ensembles. On this ground we calculate numerically the wavelength of the light in the dense atomic cloud, its extinction coefficient as well as complex index of refraction and dielectric constant of the medium. We also analyze the dispersion of the permittivity for different values of atomic density and electrostatic field strength.

To find two principal values of the permittivity tensor, we consider two main polarization schemes. In the first case the light is circularly polarized and the electrostatic field is directed along its wavevector $\mathbf{E}\|\mathbf{k}$. The second case corresponds to radiation linearly polarized along the electrostatic field, $\mathbf{E}\perp\mathbf{k}$.

We show that electro-optical effects in dense cold gases essentially differ from those in dilute ones. In a dilute medium, for the two principal polarizations the electrostatic field does not change the shape of the atomic resonance as well as its amplitude and width. Only the resonant frequency is changed. The situation in dense media is fundamentally dissimilar. Electric field changes all parameters of the atomic transition – its shape, amplitude, and width. Besides that the electric field modifies the collective Lamb shift. As an example in Fig. 1 we show spectral dependence of real and imaginary part of the light complex wavenumber in the dense medium for two main polarizations. For comparison we included corresponding dependences in the case of the absence of the electric field.

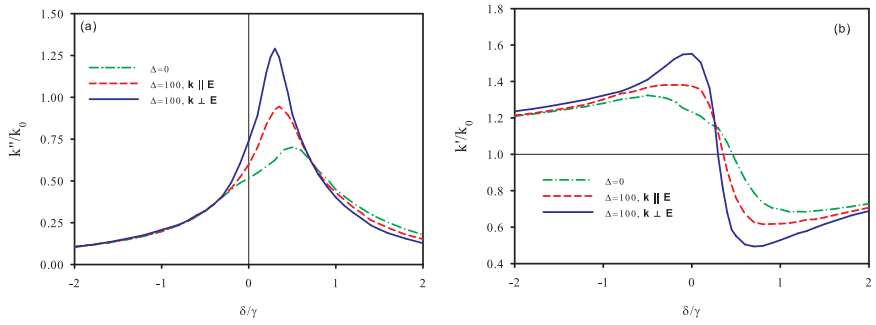

Fig. 1: Spectral dependence of the (a) imaginary and (b) real parts of the complex wavenumber in the medium calculated for cold atomic ensemble with density $n = 0.15k_0^3$. Here Δ is the Stark shift of the transition in units of the linewidth γ of the atomic transition, k_0 is wavenumber of incident light. The detuning δ is the difference between the frequency of the incident light and resonant atomic transition in electric field.

The observed peculiarities of electro-optical effects in dense gases we explain as a result of influence of electric field on the nature of collective polyatomic effects caused by resonant dipole-dipole interatomic interaction.

This work was supported by the Russian Science Foundation, project no. 17-12-01085.

References

[1] I. M. Sokolov, D. V. Kupriyanov, and M. D. Havey, J. Exp. Theor. Phys. **112**, 246 (2011).
[2] Ya. A. Fofanov, A. S. Kuraptsev, I. M. Sokolov, and M. D. Havey, Phys. Rev. A **84**, 053811 (2011).

*Corresponding author: ims@is12093.spb.edu

A – 2

Time resolved measurement of the ultrafast electronic decay of core excited HCL molecules by THz Streaking.

K. Wenig[1] M. Wieland[1,2] S. Walther[1,2] A. Baumann[1,2] A. Dimitriou[*1,2], M. Prandolini[1] O. Schepp[1] I. Bermúdez Macias[3] M. Sumfleth[1,2] N. Stojanovic[3] S. Düsterer[3] J. Röntsch-Schulenburg[3] M. Drescher[1,2] U.Frühling[†1,2]

1. Institut für Experimentalphysik, Universität Hamburg, Luruper Chaussee 149, 22761 Hamburg, Germany
2. Center for Ultrafast Imaging, Luruper Chaussee 149, 22761 Hamburg, Germany
3. Deutsches Electron-Synchrotron DESY, 22761 Hamburg, Germany

The study of ultrafast electronic decays of core excited molecules is a matter of particular interest. The reason for this interest is the fact that nuclear motion and electronic relaxation both take place on similar femtosecond time scales and thus the dynamics cannot be easily understood with the use of simple spectroscopic measurements. Molecules providing such examples are halogen compounds (HI, HBr or HCL). After resonant excitation of a core electron to an antibonding orbital, molecules start to dissociate and at the same time the electronic excitation relaxes via the emission of an Auger electron. This has already been proven in experiments with synchrotron radiation where both atomic and molecular Auger spectra were measured after core hole excitation [1] [2] [3] [4]. In the present work we use the THz streaking technique in order to study these systems directly in the time domain and follow the transition from molecular to atomic decays.

We have used soft-X-ray pulses of femtosecond duration from the free-electron laser in Hamburg (FLASH) to resonantly excite the $2p_{3/2}$ core electrons from HCL molecules to the antibonding σ^* orbital. These pulses were collinearly overlapped with intense THz pulses provided by the FLASH THz undulator. The emitted photoelectrons are accelerated (streaked) by the THz electric field whereby the resulting momentum change is proportional to the THz vector potential at the emission time. Thus, the ionization dynamics can be studied by measuring the streaked electron spectra [5] [6].

In this contribution the experimental setup and the first experimental results will be presented.

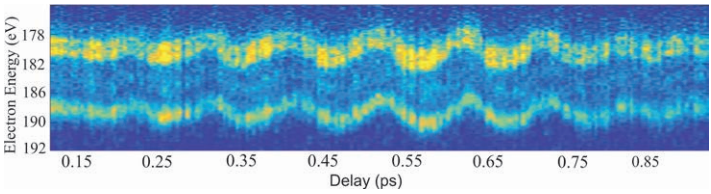

Fig. 1: Series of kinetic Energy spectra of HCL electrons detached by soft-X-ray pulses from FLASH in the presence of THz light from the THz undulator.

References

[1] P. Morin and I. Nenner Phys. Rev. Lett. **56**, 1913 (1987).
[2] P. Morin and I. Nenner Phys. Scr. **T17**, 171 (1987).
[3] A. Menzel *et al.*, Chem. Rev. Lett. **258**, 265 (1996).
[4] A. Menzel *et al.*, Phys. Rev. Lett. **79**, 3150 (1997).
[5] U. Frühling *et al.*, Nat. Phot. **3**, 523 (2009).
[6] U. Frühling, J. Phys. B. **44**, 243001 (2011).

[*]Corresponding author: anastasios.dimitriou@cfel.de
[†]Corresponding author: ulrike.fruehling@uni-hamburg.de

Theoretical investigation of energy levels and transition data for Cl III

P. Rynkun[*1], **G. Gaigalas**[1], **P. Jönsson**[2]

1. Institute of Theoretical Physics and Astronomy, Vilnius University, Saulėtekio av. 3, LT-10222, Vilnius, Lithuania
2. Group for Materials Science and Applied Mathematics, Malmö University, SE-20506, Malmö, Sweden

Chlorine is an important element in various astrophysical environments. The atomic data, such as transition probabilities and collision strengths, are used in the determination of chemical abundances in ionized nebulae. Dios & Rodríguez [1] have computed the ionic abundances of O II, O III, N II, Cl III, Ar III, Ar IV, Ne III, S II and S III, and the total abundances of the corresponding elements. They have observed that the choice of atomic data can have a large impact on the chemical abundances. Schectman *et al.* [2] measured lifetimes and branching fractions with beam-foil techniques and derived oscillator strengths for transitions in Cl II and III. Froese Fischer *et al.* [3] computed energy levels and transition data using Breit-Pauli approximation. Sossah *et al.* [4] used multiconfiguration Hartree-Fock and B-spline Breit-Pauli R-matrix method to calculate transition probabilities and effective collision strengths.

In this work energy spectrum calculations were performed for 52 even states of the $3s3p^4$, $3s^23p^23d$, $3s^23p^24s$, $3s^23p^24d$ configurations and for 35 odd states of the $3s^23p^3$, $3s^23p^24p$, $3s3p^33d$, $3p^5$ configurations in Cl III ion. Also electric dipole transition data were computed between these states. The calculations are in progress, so here are presented results where just valence-valence electron correlations are included.

The calculations were done using multiconfiguration Dirac-Hartree-Fock and relativistic configuration interaction (RCI) methods, which are implemented in the general relativistic atomic structure package GRASP2K [5]. In the RCI calculations the transverse-photon (Breit) interaction, the vacuum polarization, and the self-energy corrections were included. In the present work, the atomic state functions (ASFs) were obtained as expansions over jj-coupled configuration state functions (CSFs). To provide the *LSJ* labeling system the ASFs were transformed from a jj-coupled CSF basis into an *LSJ*-coupled CSF basis using the method provided by Gaigalas *et al.* [6].

In Table 1 is shown the convergence of energy levels of the $3s3p^4(^3_2P)\ ^4P_{5/2,3/2,1/2}$ states. These are compared with data from the NIST [7] database. Table 2 gives the comparison of computed wavelengths and oscillator strengths for the $3s^23p^3(^4_3S)\ ^4S^o_{3/2} \rightarrow 3s3p^4(^3_2P)\ ^4P_{5/2,3/2,1/2}$ transitions with experiment and other theoretical calculations.

Table 1: The convergence of energy levels depending on the expansion of CSFs. Energy levels are given relative to a ground state energy. Computed energies are compared with the values from the NIST database. The CSFs were generated using active set (AS) method and account for valence-valence electron correlation.

Label	AS_1	AS_2	AS_3	AS_4	AS_5	NIST
$3s3p^4(^3_2P)\ ^4P_{5/2}$	98106	98045	98082	98107	98114	98520.34
$3s3p^4(^3_2P)\ ^4P_{3/2}$	98705	98641	98679	98705	98711	99131.40
$3s3p^4(^3_2P)\ ^4P_{1/2}$	99066	99013	99053	99080	99087	99475.22

Table 2: Comparison of wavelengths and oscillator strengths for the $3s^23p^3(^4_3S)\ ^4S^o_{3/2} \rightarrow 3s3p^4(^3_2P)\ ^4P_{5/2,3/2,1/2}$ transitions in Cl III. The oscillator strengths in the RCI column are given in the length gauge. The estimated uncertainty in % of the oscillator strengths are given in parenthesis.

	λ (in Å)				$f\times10^{-2}$			
$J_i \rightarrow J_f$	Exp. [7]	RCI	[3]	[4]	Exp. [2]	RCI	[3]	[4]
3/2 → 5/2	1015.02	1019.22	1023.21	1024.48	2.85±0.11	3.14 (2.6)	3.23	3.21
3/2 → 3/2	1008.78	1013.05	1017.96	1018.74	1.93±0.08	2.10 (2.9)	2.15	2.14
3/2 → 1/2	1005.28	1009.21	1015.04	1015.46	0.96±0.05	1.04 (3.8)	1.07	1.07

Acknowledgments: This research is funded by the European Social Fund under the No 09.3.3-LMT-K-712 Development of Competences of Scientists, other Researchers and Students through Practical Research Activities measure.

References

[1] L. J. Dios and M. Rodríguez, MNRAS **469**, 1036 (2017).
[2] R. M. Schectman, S. R. Federman, M. Brown, S. Cheng, M. C. Fritts, R. E. Irving, and N. D. Gibson, ApJ **621**, 1159 (2005).
[3] C. Froese Fischer, G. Tachiev, and A. Irimia, At. Data Nucl. Data Tables **92**, 607 (2006).
[4] A. M. Sossah and S. S. Tayal, ApJS **202**, 12 (2012).
[5] P. Jönsson, G. Gaigalas, J. Bieroń, C. Froese Fischer, and I.P. Grant, Comput. Phys. Commun. **184**, 2197 (2013).
[6] G. Gaigalas, C. Froese Fischer, P. Rynkun, and P. Jönsson, Atoms **5**, 6 (2017).
[7] A. Kramida, Yu. Ralchenko, J. Reader, and NIST ASD Team (2018). NIST Atomic Spectra Database (ver. 5.5.2), [Online]. Available: http://physics.nist.gov/asd [2018, March 13]. National Institute of Standards and Technology, Gaithersburg, MD.

[*]Corresponding author: pavel.rynkun@tfai.vu.lt

A – 4

Calculated Oscillator Strengths for Radiative Transitions of Cosmochronological Interest in Singly Ionized Uranium (U II)

S. Gamrath[*1], **P. Palmeri**[1], **P. Quinet**[†1,2]

1. Physique Atomique et Astrophysique, Université de Mons, B-7000 Mons, Belgium
2. IPNAS, Université de Liège, B-4000 Liège, Belgium

Up to now, there have been no available calculation of radiative data at all for singly ionized uranium (U II). The main reason is that the complexity of the electron configurations involved in the excited states and the fragmentory knowledge of the experimental spectrum of this ion make theoretical computations extremely difficult [1]. However, transition probabilities and oscillator strengths for U II radiative transitions are expected to be important in astrophysics, in particular in cosmochronology where the age of a star can be determined by the use of a radiaoactive isotope of sufficiently long lifetime. Up until a few years ago, the radioisotope ^{232}Th, with a half-life of 14 Gyr, was used to date galactic stars [2-4] but it decays by only a factor of two over the lifetime of the Universe. It was indeed pointed out by Goriely and Clerbaux [5] that new accurate observations of heavy radioactive elements could improve the accuracy of cosmochronometry analyses. More particularly, ^{238}U, with a half-life of 4.5 Gyr, represents a much more precise age indicator. In 2001, Cayrel *et al*. [6] reported the first detection of a spectral line at a wavelength of 385.957 nm, from singly ionized uranium, in the very metal-poor star CS31082-001. The derived uranium abundance yielded an age of 12.5 ± 3 Gyr, which led to the best estimate of the age of the Galaxy and, consequently provided a lower limit to the age of the Universe.

However, as mentioned in [6], the accuracy of this uranium dating technique is still limited by the lack of available radiative parameters for U II spectral lines. Some reliable oscillator strengths were obtained experimentally by combining branching fraction measurements with laboratory lifetimes determined using laser spectroscopy [7,8] but these data concern only a small number of strong lines. In order to partly fill this gap, we carried out extensive calculations of oscillator strengths for the most intense U II lines of potential cosmochronological interest using two independent theoretical approches, i.e. the pseudo-relativistic Hartree-Fock [9] and the purely relativistic multiconfiguration Dirac-Fock [10] methods. Some preliminary results will be presented at the conference.

References

[1] A. Meftah *et al*., Atoms **5**, 24 (2017).
[2] H.R. Butcher, Nature **328**, 127 (1987).
[3] P. François, M. Spite and F. Spite, Astron. Astrophys. **274**, 821 (1993).
[4] J.J. Cowan *et al*., Astrophys. J. **521**, 194 (1999).
[5] S. Goriely and B. Clerbaux, Astron. Astrophys. **346**, 798 (1999).
[6] R. Cayrel *et al*., Nature **409**, 691 (2001).
[7] H. Lundberg *et al*., Astron. Astrophys. **372**, L50 (2001).
[8] H. Nilsson *et al*., Astron. Astrophys. **381**, 1090 (2002).
[9] R.D. Cowan, *The Theory of Atomic Structure and Spectra*, Univ. California Press, Berkeley (1981).
[10] I.P. Grant, Relativistic Quantum Theory of Atoms and Molecules, Springer-Verlag, New York (2007).

[*]Corresponding author: Sebastien.Gamrath@umons.ac.be
[†]Corresponding author: Pascal.Quinet@umons.ac.be

Wide-range optical magnetometer based on hot alkaline vapor nanocell

E. Klinger,[*1,2] **A. Sargsyan,**[1] **C. Leroy,**[2] **A. Papoyan,**[1] **& D. Sarkisyan**[1]

1. Institute for Physical Research, National Academy of Sciences of the Republic of Armenia, 0203 Ashtarak-2, Armenia
2. Laboratoire Interdisciplinaire Carnot de Bourgogne, UMR CNRS 6303, Université Bourgogne – Franche-Comté, Dijon, France

In the past decade, optical nanocells (NC) of ~ 40 nm to 1 μm thickness in light propagation direction have proven to be efficient spectroscopic tool, allowing to perform linear Doppler-free spectroscopy with a simple one-beam experimental setup. We have recently shown that derivative of the selective reflection (dSR) from an interface formed by a dielectric window and an alkaline vapor allows one to record spectrally narrowed atomic resonances (~ 50 MHz) [1]. The sub-Doppler nature of recorded signals, along with the linearity with respect to the atomic transitions strength make the NC-based dSR technique an extremely convenient tool for studying the splitting of hyperfine atomic transitions in a longitudinal magnetic field and modification of their transition probabilities [2]. Our theoretical model based on articles [3], [4] has shown a very good agreement with the recorded experimental spectra in a wide range of *B*-field variation covering evolution from Zeeman to hyperfine Paschen-Back regime [2] (see the lower graph in Fig.1).

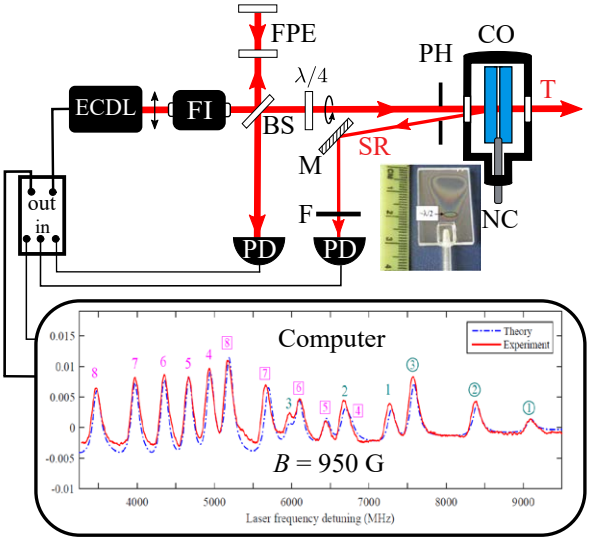

Fig. 1: Experimental setup. ECDL – extended cavity diode laser; FI – Faraday insulator; BS – beam splitter; FPE – Fabry-Pérot etalon; $\lambda/4$ – quarter-wave-plate; PH – pinhole; CO – compact oven; NC – alkaline nanocell; M – mirror; F – filter; PD – photo-detector; SR – selective reflection channel; T – transmission channel. Computer screen shows an example of experimentally recorded spectrum with superimposed modeling curve.

Based on these studies, we have explored the feasibility of designing a nanocell-based optical magnetometer having a measurement range of 50 – 10000 G with a precision of ~ 1 G (10^{-4} T). Measurements are done on a computer driven experimental setup recording the alkali D line spectrum of a NC exposed to measured *B*-field. The sketch of the NC-based magnetometer is schematically depicted in Fig 1. After recording the spectrum, the computer code generates a succession of modeled spectra sorting out the proper one, helped by the FPE reference. The fitting routine terminates when the residuals between calculated and recorded spectra are minimized, thus returning the value of the magnetic field.

References

[1] A. Sargsyan, E. Klinger, Y. Pashayan-Leroy, C. Leroy, A. Papoyan & D. Sarkisyan, J. Exp. Theor. Phys. Lett. **104**, (2016).
[2] A. Sargsyan, E. Klinger, G. Hakhumyan, A. Tonoyan, A. Papoyan, C. Leroy, & D. Sarkisyan, J. Opt. Soc. Am. B **34**, (2017).
[3] P. Tremblay, A. Michaud, M. Levesque, S. Thériault, M. Breton, J. Beaubien & N. Cyr, Phys. Rev. A **42**, 2766 (1990).
[4] G. Dutier, S. Saltiel, D. Bloch & M. Ducloy, J. Opt. Soc. Am. B **20**, 793 (2003).

*Corresponding author: emmanuel.klinger@u-bourgogne.fr

A – 6

Sub-Doppler spectroscopy of the Faraday Rotation effect occurring in nano-layers of alkaline atoms

A. Amiryan[*1,2], **A. Sargsyan**[1], **Y. Pashayan-Leroy** [2,3], **C. Leroy**[2], **D. Sarkisyan**[1]

1. Institute for Physical Research, National Academy of Sciences of Armenia, 0203 Ashtarak-2, Armenia

2. Laboratoire Interdisciplinaire Carnot de Bourgogne, UMR CNRS 6303, Université Bourgogne - Franche-Comté, Dijon, France

3. Université Bourgogne - Franche-Comté, 32 avenue de l'Observatoire, Besançon, France

The plane of polarization is rotated when linearly polarized light passes through a medium in a direction parallel to the applied magnetic field. This effect was discovered by Michael Faraday in 1845 and found many applications in optical isolators, telecommunications, optical current sensors, tomography, magnetometry, spectroscopy *etc*.

In this research the Faraday Rotation effect (FR) was studied both theoretically and experimentally for D lines of alkaline atoms. The theoretical FR model for strong magnetic fields has been elaborated using [1] and [2] and shows a good agreement with the experiments [3]. A special pressure-controlled thickness nano-metric thickness-cell (NTC) filled with alkali atoms and having a variable thickness in the range of 170 nm - 1700 nm has been fabricated and implemented in these experiments. These cells are exclusively fabricated at IPR, Ashtarak, Armenia in the group of Prof. D. Sarkisyan. For the last 15 years many unexpected scientific results have been obtained using the NTC, among which it is worth mentioning sub-Doppler spectroscopy and study of the behaviour of fine and hyperfine structure individual atomic transitions.

For magnetic fields in range of 0.1 - 6 kG, the atomic transitions of Cs are split into a large number of components that are frequency-resolved due to sub-Doppler nature of the recorded spectra. This allows one to investigate the behaviour of an individual atomic transition. With a further increase in magnetic field, the number of FR components remains the same while their frequencies increase monotonously with a constant slope. The FR signal of the Cs D_1 line atomic transitions for 6 kG magnetic field is presented in Fig. 1. Note that due to the small tuning range of the diode laser ~ 5 GHz, only the part of the spectrum can be obtained experimentally. The upper and the middle curves are respectively the theoretical and the experimental FR spectra, while the lower curve is the frequency reference. As one can see the two spectra are in good agreement. The inset shows the diagram for the Cs D_1 line transitions in the case of Hyperfine Paschen-Back (HPB) regime [4].

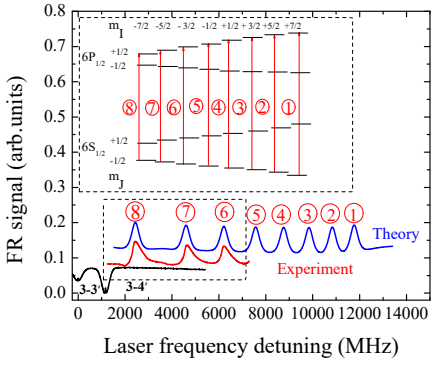

Fig. 1: Cs D_1 line Faraday Rotation spectra for $F_g = 3 \rightarrow F_e = 4$ at $B = 6$ kG applied magnetic field. Upper curve – the theoretical spectrum, middle – the experimental spectrum, lower curve – the reference spectrum. The inset shows the diagram of Cs D_1 line HPB regime (for σ^+ radiation) with the transitions 1 – 8 satisfying the selection rules $\Delta m_I = 0$, $\Delta m_J = +1$. The component labelled 8 arises from the atomic transition $F_g = 4 \rightarrow F_e = 4$.

References

[1] B. Zambon, G. Nienhuis, Opt. Comm., **143**, (1997).

[2] G. Dutier, S. Saltiel, D. Bloch, and M. Ducloy, J. Opt. Soc. Am. B, **20**(5) (2003).

[3] A. Amiryan, A. Sargsyan, Y. Pashayan-Leroy, C. Leroy and D. Sarkisyan, Submitted to J. Mod. Opt. (2018).

[4] Research conducted in the scope of the International Associated Laboratory IRMAS (CNRS France - SCS Armenia) and with the support of the Armenian National Science & Education Fund (ANSEF Opt 4732) grant for the financial support. A. A. acknowledges the support of AGBU France and Philippossian & Pilossian foundation.

*Corresponding author: arevamiryan@gmail.com

A – 7

Long-range Rydberg molecules bound by electron-atom scattering

M. Peper*[1], H. Saßmannshausen[1], F. Merkt[1], J. Deiglmayr†[1]
1. Laboratory of Physical Chemistry, ETH Zürich, Vladimir-Prelog-Weg 2, 8093 Zürich, Switzerland

In 1934, Amaldi and Segré [1] observed pressure-dependent shifts and broadenings in Rydberg spectra. The pressure shift results from interactions of the Rydberg electron with ground-state atoms lying within the Rydberg electron's orbit as shown in Fig. 1.

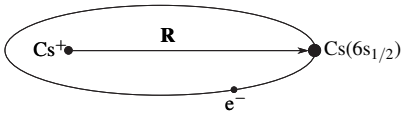

Figure 1: Rydberg electron e^- with its semi-classical orbit around the Cs^+ ion-core scattering at a $Cs(6_{1/2})$ ground-state atom.

Fermi [2] modelled this interaction as arising from the s-wave scattering of the slow Rydberg electron with the ground-state atom using a pseudopotential

$$V(\mathbf{R}) = 2\pi a |\Psi(\mathbf{R})|^2, \tag{1}$$

where a is the s-wave scattering length and $|\Psi(\mathbf{R})|^2$ is the probability density of the Rydberg electron at postion $\mathbf{R}$ with respect to the ion core.

As first predicted by Greene et al. [3] and first observed by Bendkowsky et al. [4], this interaction leads to oscillatory potentials that may support bound states of long-range diatomic molecules in case of a negative s-wave scattering length as depicted in Fig. 1. For the alkali metal atoms, the triplet scattering length is negative whereas the singlet scattering length is very small or even positive. Singlet and triplet scattering channels are, however, mixed by the hyperfine interaction in the ground-state atom [5]. This mixing allowed for the first determination of the zero-energy singlet s-wave scattering length of caesium [6].

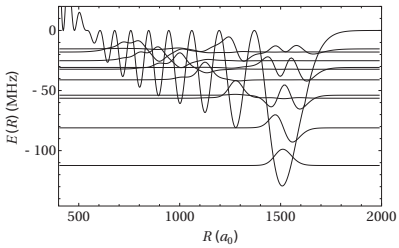

Figure 2: Vibrational wave functions (dashed lines) in the interaction potential including s-wave scattering (solid line) for the $^3\Sigma$ state dissociating to the $32p_{3/2}$,$6s_{1/2}$ asymptote.

The often neglected p-wave contribution is known to lower the potential barrier towards smaller internuclear separations [7], [8]. The excited molecules may therefore decay by tunnelling through the potential barrier. Measurements of the lifetimes of the molecules can provide a sensitive probe of the potential-energy curve. We will present studies on the formation and dynamics of long-range Rydberg molecules in ultracold caesium and potassium gases using high-resolution photoassociation spectroscopy and an outlook towards future experiments with heteronuclear molecules.

References

[1] E. Amaldi, and E. Segré, *Il Nuovo Cimento* **11**, 145 (1934).
[2] E. Fermi, *Il Nuovo Cimento* **11**, 157 (1934). [3] C. H. Greene, A. S. Dickinson, and H. R. Sadeghpour, *Phys. Rev. Lett.* **85**, 2458 (2000).
[4] V. Bendkowsky et al., *Nature* **458**, 1005 (2009).
[5] D. A. Anderson, S. A. Miller, and G. Raithel, *Phys. Rev. A* **90**, 062518 (2014).
[6] H. Saßmannshausen, F. Merkt, and J. Deiglmayr, *Phys. Rev. Lett.* **114**, 133201 (2015).
[7] M. T. Eiles, and C. H. Greene, *Phys. Rev. A* **95**, 042515 (2017).
[8] S. Markson et al., *ChemPhysChem* **17**, 3683 (2016).

*Corresponding author: michael.peper@phys.chem.ethz.ch
†Corresponding author: deiglmayr@xuv.phys.chem.ethz.ch

A – 8

The Atomic Scattering Factor for negative ions in Stabilising Potential Wells

S Y Yousif Al-Mulla*
University of Borås/College of Engineering/ S-50190 Borås/ Sweden
EGAS 50th Conference of the European Group of Atomic Systems/
Jagiellonian University/ Krakow / Poland / July 9-13, 2018

The study of the effectiveness of the crysalline environments on the modification of the atomic scattering factors are presented. This has been done by comparing quantum mechanical calculations of perturbed X-ray scattering form factor of negative ions in an electric field for various stabilising potential wells of various depth. It is known that the polarisability of ions in crystals varies with crystalline environment. Similar effect can be seen in Fig.1 in the comparison of the modification of the X-ray scattering factor for $O^{=}$ and $S^{=}$ subject to an external field in addition to stabilising potential wells of various depth (0,5 , 1,0 , 1,5 and 2 atomic units).

The X-ray atomic scattering factor for an unperturbed atom with N electron is given by:

$$f_0 = \sum_{j=1}^{N} \psi_0^* \exp(i\chi S \cdot r_j)\psi_0 d\tau = \sum_{j=1}^{N} \psi_0^* \exp(iKr_j \cos\theta_j)\psi_0 d\tau$$

In the presence of an electric field F, the wave function is perturbed,

$$f = f_0 + if_1F + O(F^2) \text{ where } if_1F = 2F \sum_{j=1}^{N} \int \psi_0^* \exp(iKS \cdot r_j)\psi_1 d\tau$$

We use the Kirkwood - Pople-Schofield approach for the wave function

$$\psi = \psi_0 \left[1 + \sum_j u(r_j)\right] \text{ where } u(r) = F(\mu r + \nu r^2 + \eta r^3) \text{ and the } f_1 \text{ is given by}$$

$$if_1F = 2F \sum_i \sum_j \psi_0^* \exp(iKS \cdot r_j)(\mu r_i + \nu r_i^2 + \eta r_i^3)\cos\theta_i \psi_0 d\tau$$

The optimal values of μ, ν and η are determined variationally and calculated from various moments of the unperturbed charge distribution using a single Slater determinant[1-5].

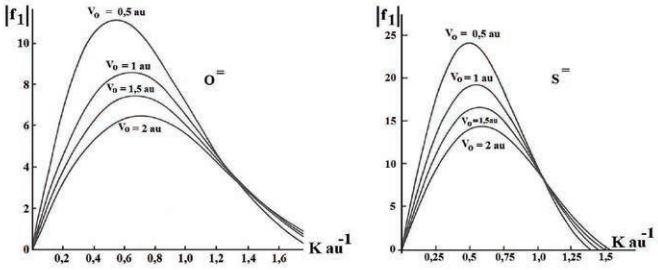

Fig. 1: Comparison of the magnitude of the modified X-ray scattering factor per unit applied field with scattering vector K (au^{-1}) in stabilising potential wells of various depths for $O^{=}$ and $S^{=}$.

References

[1] JAD. Matthew and S.Y. Yousif, , Acta Crys. **A 40**, 716 (1984).
[2] JAD. Matthew and S.Y. Yousif , Molec. Phys. **51**, 175 (1984).
[3] S.Y. Yousif Al-Mulla, Physica Scripta **61**, 417 (2000).
[4] S.Y. Yousif Al-Mulla, EGAS 46th (2014) . [5] S.Y. Yousif Al-Mulla, EGAS 49th (2017)

*samir.al-mulla@hb.se

A – 9

Electron-impact excitation of forbidden and allowed transitions in Fe II

O. Zatsarinny[*1] **and S. Tayal**[†2]
1. Department of Physics, University of Poland, Atomic Physicists Street 10, 30-348 Kraków, Poland
2. Department of Mathematics, Clark Atlanta University, Atlanta, GA 30314, USA

New extensive calculations are reported for electron collision strengths, rate coefficients, and transitions probabilities for a wide range of transitions in Fe II among the 340 fine-structure levels of Fe II, belonging to the lowest $3d^64s$, $3d^54s^2$, $3d^7$, $3d^64p$, and $3d^54s4p$ configurations. The present results considerably expand the existing data sets for Fe II, allowing a more detailed treatment of the available measured spectra from different astrophysical sources. The calculations were carried out in the close-coupling approximation using the B-spline R-matrix code [1].

The Fe II ion is the most abundant of iron-peak elements with a large number of lines in a broad wavelength region from the infrared to ultraviolet and received extra special attention for the theoretical and experimental studies of the transition and collision rates. However, not a single available calculation has yet achieved convergence so as to provide accurate atomic parameters. The problem is mainly computational; the very large number of energy levels and transitions involved in the spectrum requires big CC expansions, whereas the accurate representation of the open 3d-shell target states requires extensive CI expansions. The purpose of the present work is to perform more elaborate and extensive calculations for the electron scattering from Fe II by using highly accurate target wave functions and by including fine-structure effects in the close-coupling expansions through the Breit-Pauli Hamiltonian.

The target states were generated by the multi-configurational Hartree-Fock method. The multiconfiguration expansions include all single and double promotions from the 3d, 4s and 4p orbitals to the 4*l* and 5*l* (*l* =0-4) correlated orbitals. To represent the target states with different configurations, we use term-dependent non-orthogonal orbital sets, which allowed us to include the relaxation effect directly.

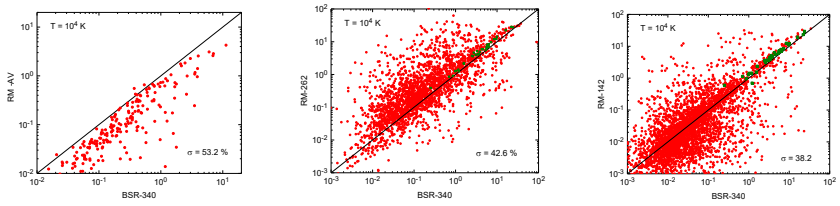

Fig. 1: Comparison of effective collision strengths obtained in the present BSR-340 model with the RM-AV results of Bautista *et al*. [2], RM-262 calculations of Ramsbottom [3] and RM-142 calculations of Zhang and Pradhan [4]). Also indicated in the panels is the average deviation σ from the BSR-340 resultsthe caption. The squares in the left panel represent transitions from the ground level only.

The global comparison of the present effective collision strengths with available data sets is presented in figure 1. The comparison shows that previous calculations of collision strengths for many transitions are much more uncertain than previously thought. We offer arguments in favor of our results being the most accurate, where differences occur. It is based on the more accurate representation of target states and more extensive close-coupling expansions. To further improve the accuracy of our final collision rates, experimental energies through the fine-tuning process have been used, not only for target level energies, but also to enhance the accuracy of the term-mixing coefficients in the wave functions. This is a distinctive and novel feature of the present calculations, that allowed us to generate a more accurate description of the Fe II target states than those employed before.

References

[1] O. Zatsarinny, Comp. Phys. Commun. **174** , 273 (2006).
[2] M. A. Bautista, V. Fivet, C. Ballance, P. Quinet, G. Ferland, C. Mendoza, and T. R. Kallman, Astroph. J. **808**, 174 (2015).
[3] C. Ramsbottom, At. Data Nucl. Data Tables **95**, 910 (2009).
[4] H. Zhang and A. Pradhan, A&A **293**, 953 (1995).

[*]Corresponding author: oleg.zatsarinny@drake.edu
[†]Corresponding author: stayal@cau.edu

A – 10

Fourier transform emission spectroscopy and *ab initio* calculations on the visible spectrum of AlD^+

W. Szajna*[1], R. Hakalla[1], K. Moore[2], I. C. Lane[2], M. Ostrowska−Kopeć[1], I. Piotrowska[1], P. Kolek[1], M. Zachwieja[1] and R. Kępa[1]

1. Materials Spectroscopy Laboratory, Department of Experimental Physics, Faculty of Mathematics and Natural Science, University of Rzeszów, Pigonia 1 Street, 35-959 Rzeszów, Poland

2. School of Chemistry and Chemical Engineering, Queen's University Belfast, Stranmillis Road, Belfast BT9 5AG, UK

The emission spectrum of the AlD^+ ion has been studied by Fourier transform spectroscopy technique, as a further step of our investigation of the AlD neutral molecule [1]. The $0-0$ and $1-1$ bands of the $A^2\Pi - X^2\Sigma^+$ system have been recorded in the $27,000 - 29,000$ cm^{-1} region with an instrumental resolution of 0.03 cm^{-1}. In total, almost 500 rotational frequencies were measured with an absolute accuracy of about 0.005 cm^{-1}. It improved the experimental accuracy of the determined frequencies by the factor 10 compared to the previous work [2]. The rotational analysis has shown irregularities in the $\Lambda-$ doubling splitting of the $A^2\Pi$ $v = 0, 1$. Consequently, the $A^2\Pi$ state has been represented by the rotational term values, while the regular $X^2\Sigma^+$ state by the molecular constants. The causes of the irregularities were identified in the interaction between the $A^2\Pi$ state the lying higher the $B^2\Sigma^+$ state.

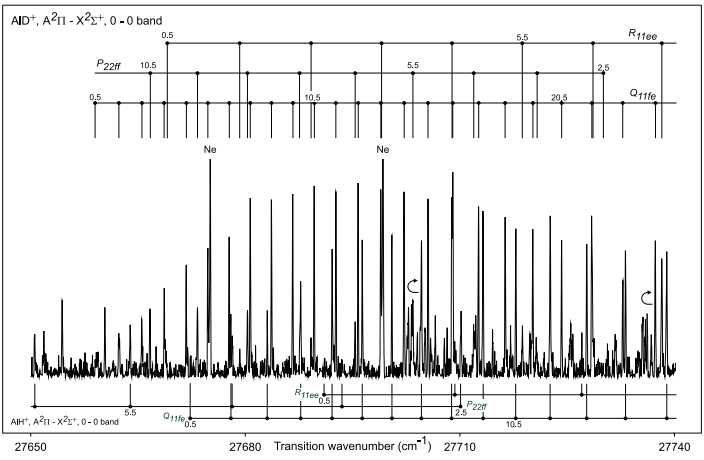

Fig. 1: The VIS-FT emission spectrum of the AlD^+ $A^2\Pi - X^2\Sigma^+$ $(0,0)$ band recorded with an instrumental resolution of 0.03 cm^{-1}. Signal-to-noise ratio was ca. $50:1$. Lines of the AlH^+ $A^2\Pi - X^2\Sigma^+$ $(0,0)$ band, occurring in the same spectral region, are marked at the bottom. Two characteristic features distinguished by turning back arrows are the P_{11} and P_{22} branch heads of the AlD^+ $A^2\Pi - X^2\Sigma^+$ $(1,1)$ band at the 27,703 cm^{-1} and 27,735 cm^{-1}, respectively.

Ab initio calculations on the ion were performed using a parallel version of the MOLPRO [3] (version 2010.1) suite of quantum chemistry codes. The static electron correlation was calculated using SA−CASSCF method [4]. The active space consisted of all the occupied valence orbitals of the aluminum atom plus the $1s$ orbital from the deuterium atom. The $1s$ orbital of the Al^+ atom is kept frozen while the $2s2p$ orbitals are closed (kept doubly occupied in all configurations). In addition, SA−CASSCF can be used to calculate the excited electronic states corresponding to the $Al^+(^3P) + D(^2S)$ asymptote so a total of five states are included $(2\times\ ^2\Sigma^+, ^2\Pi, ^4\Sigma^+, ^4\Pi)$. The accuracy of the potentials can be improved by including dynamic electron correlation, that was handled here by using MRCI method [5].

References

[1] W. Szajna, K. Moore, I.C. Lane. J. Quant. Spectrosc. Radiat. Transf. **196**, 103 – 11 (2017).
[2] W.J. Balfour, B. Lindgren. J. Phys. B: At. Mol. Phys. **17**, L861−6 (1984).
[3] H.J. Werner,P.J. Knowles, R. Lindh,F.R. Manby et.al. MOLPRO (2010), http://www. molpro.net.
[4] P. Siegbahn ,A. Heiberg, B. Roos, B. Levy. Phys. Scr. **21**, 323 – 30 (1980).
[5] H.J. Werner, P.J. Knowles. J. Chem. Phys. **89**, 5803 – 8 (1988).

*Corresponding author: szajna@ur.edu.pl

A – 11

Deperturbation analysis of the $A^1\Pi(v=0)$ level in the $^{12}C^{17}O$ isotopologue

R. Hakalla*[1], W. Szajna[1], A. N. Heays[2,3,4], N. de Oliveira [5], E. J. Salumbides [2], M. Ostrowska−Kopeć[1], I. Piotrowska[1], P. Kolek[1], M. Zachwieja[1], R. Kępa[1], R. W. Field [6], and W. Ubachs [2]

1. Materials Spectroscopy Laboratory, Department of Experimental Physics, Faculty of Mathematics and Natural Science, University of Rzeszów, Pigonia 1 Street, 35-959 Rzeszów, Poland

2. Department of Physics and Astronomy, and LaserLaB, Vrije Universiteit, De Boelelaan 1081, 1081 HV Amsterdam, The Netherlands

3. LERMA, Observatoire de Paris, PSL Research University, CNRS, Sorbonne Universités, UPMC Univ. Paris 06, F-92190, Meudon, France

4. School of Earth and Space Exploration, Arizona State University, Tempe, AZ 85281, USA

5. Synchrotron SOLEIL, Orme de Merisiers, St. Aubin, BP 48, F-91192 Gif sur Yvette Cedex, France

6. Department of Chemistry, Massachusetts Institute of Technology, Cambridge, MA 02139, USA

The present study focuses on a first analysis of spectroscopic data for the $A^1\Pi(v=0)$ level in the $^{12}C^{17}O$ isotopologue. Fourier-transform spectroscopy (1.71 m Bruker IFS 125HR) was used to obtain the Ångström $(B^1\Sigma^+ - A^1\Pi)(0,0)$ band spectrum under 0.018 cm^{-1} resolution. The discharge was conducted in the air-cooled, carbon hollow-cathode lamp. The temperature of dc-plasma at the center of the cathode was about 1000 K. The estimated absolute calibration uncertainty (1σ) was 0.005 cm^{-1}. The fitting uncertainty of the line frequency measurements was estimated to be 0.005 cm^{-1}. The spectrum was combined with high-resolution photoabsorption measurements of the $^{12}C^{17}O$ $B^1\Sigma^+ - X^1\Sigma^+(0,0)$ and $C^1\Sigma^+ - X^1\Sigma^+(0,0)$ bands [1] recorded with an accuracy of 0.01 cm^{-1} using the vacuum ultraviolet Fourier-transform spectrometer, installed on the DESIRS beamline at the SOLEIL synchrotron. An effective Hamiltonian used in deperturbation analysis was performed up to $J=39$, quantitatively addressing complex, multistate interactions with the $e^3\Sigma^-(v=1)$, $d^3\Delta(v=4)$, $a'^3\Sigma^+(v=9)$, $D^1\Delta(v=0)$, and $I^1\Sigma^-(v=0,1)$ rovibrational levels. The comprehensive data set, 281 spectral lines belonging to 3 bands, was included in the fit. The $A^1\Pi$ and perturber states were described in terms of a set of deperturbed molecular constants, spin-orbit and *L*-uncoupling interaction parameters, individual and equilibrium constants, term values, as well as isotopologue-independent spin-orbit and rotation-electronic perturbation parameters. This work is a member of a sequence of studies analysing the $A^1\Pi(v=0)$ level in the CO isotopologues [2],[3],[4],[5],[6].

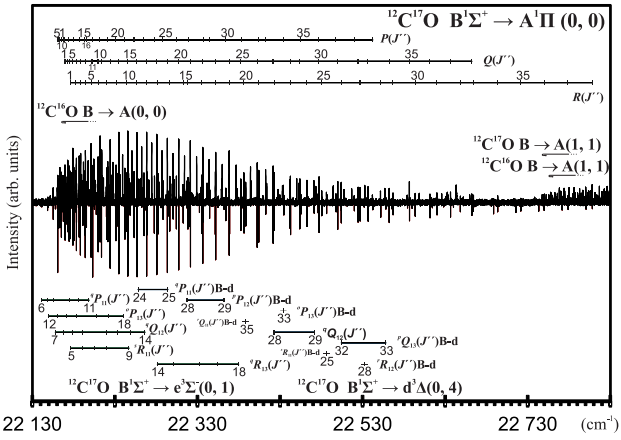

Fig. 1: Upper trace presents VIS-FT emission spectrum of the $^{12}C^{17}O$ $B^1\Sigma^+ - A^1\Pi(0,0)$ band, as well as the $B^1\Sigma^+ - e^3\Sigma^-$ (0, 1) and $B^1\Sigma^+ - d^3\Delta$ (0, 4) extra-bands gaining intensity from the Ångström system. Lower trace shows simulation of the $^{12}C^{17}O$ $B^1\Sigma^+ - A^1\Pi(0,0)$ band.

References

[1] R. Hakalla et al., *Roy. Soc. Chem. Adv.*, **6**, 31588 (2016).
[2] M. L. Niu et al., *Mol. Phys.*, **111**, 2163 (2013).
[3] M. L. Niu, R. Hakalla, T. M. Trivikram, A. N. Heays, N. de Oliveira, E. J. Salumbides, and W. Ubachs, *Mol. Phys.*, **114**, 2857 (2016).
[4] T. M. Trivikram, R. Hakalla, A. N. Heays, M. L. Niu, S. Scheidegger, E. J. Salumbides, N. de Oliveira, R. W. Field, and W. Ubachs, *Mol. Phys.*, **115**, 3178 (2017).
[5] R. Hakalla, M. L. Niu, R. W. Field, A. N. Heays, E. J. Salumbides, G. Stark, J. R. Lyons, M. Eidelsberg, J. L. Lemaire, S. R. Federman, N. de Oliveira, and W. Ubachs, *J. Quant. Spectr. Rad. Transfer*, **189**, 312 (2017).
[6] R. Hakalla, T. M. Trivikram, A. N. Heays, E. J. Salumbides, N. de Oliveira, R. W. Field, and W. Ubachs, *Mol. Phys.*, (2018) - submitted.

*Corresponding author: hakalla@ur.edu.pl

A – 12

Optical Lattice Clocks with Weakly Bound Molecules

M. Borkowski[*1]
1. Institute of Physics, Faculty of Physics, Astronomy and Informatics, Nicolaus Copernicus University, Grudziadzka 5, 87-100 Torun, Poland

Molecular optical clocks promise unparalleled sensitivity to proton-to-electron mass ratio and in searches for physics beyond the Standard Model. We propose to observe clock $^1S_0$-$^3P_0$ transitions in weakly bound bosonic $^{174}Yb_2$ molecules [1]. As in bosonic atomic clocks, a small transition dipole moment could be induced by means of a weak external magnetic field (Fig. 1a) [2]. The positions of molecular clock lines (Fig. 1b) can be determined to high accuracy: ground bound state positions have been measured with two-color photoassociation spectroscopy [3], while excited $^1S_0$+$^3P_0$ 0_u^- vibrational states can be predicted accurately using an interaction potential with *ab initio* long range parameters [4] and fitted to the experimental ^{174}Yb $^1S_0$-$^3P_0$ scattering length of $a_{ge} = 94.84(0.14)\,a_0$ (refs. [5] and [3]). The necessary ground state Yb_2 molecules could be efficiently produced by STIRAP. Thanks to favorable Franck-Condon factors (Fig. 1c) the magnetically induced molecular Rabi frequencies can be comparable to the atomic Rabi frequencies under same laser intensities and magnetic fields (Fig. 1d). A successful observation of the proposed clock transitions could pave the way towards Hz-level molecular spectroscopy.

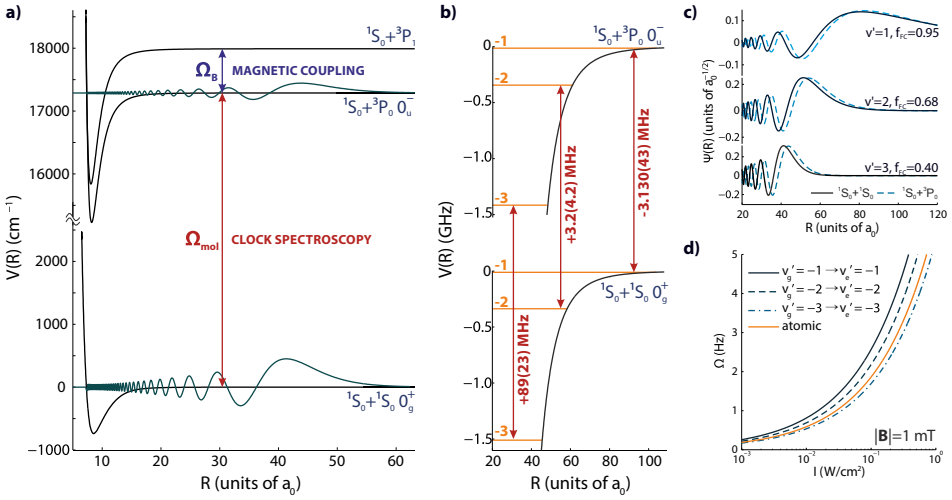

Fig. 1: Magnetically induced clock spectroscopy of weakly bound molecules. a) Magnetic coupling between molecular states correlating to $^1S_0$+$^3P_0$ and $^1S_0$+$^3P_1$ induces an artificial transition dipole moment that can be used to observe optical Rabi flipping between ground and "clock" $^1S_0$+$^3P_0$ 0_u^- states. b) Predicted molecular clock line positions in $^{174}Yb_2$, numbers in parentheses denote standard uncertainties; only the strongest lines are shown. c) Ground and excited state radial wavefunctions for weakly bound states show significant overlap thanks to similar long range interactions and bound state positions which leads to favorable Franck-Condon factors f_{FC}. d) The magnetically induced molecular Rabi frequencies $\Omega_{mol} \approx \sqrt{2}\sqrt{f_{FC}}\,\Omega_{at}$, shown as a function of laser intensity I, can be as large, or even larger than the atomic Rabi frequency under the same magnetic and optical fields.

References

[1] M. Borkowski, Phys. Rev. Lett. **120**, 083202 (2018)
[2] A.V. Taichenachev, V. I. Yudin, C.W. Oates, C.W. Hoyt, Z.W. Barber, and L. Hollberg, Phys. Rev. Lett. **96**, 083001 (2006)
[3] M. Borkowski, A. A. Buchachenko, R. Ciuryło, P. S. Julienne, H. Yamada, Y. Kikuchi, K. Takahashi, Y. Takasu, and Y. Takahashi, Phys. Rev. A **96**, 063405 (2017)
[4] S. G. Porsev, M. S. Safronova, A. Derevianko, and C.W. Clark, Phys. Rev. A **89**, 012711 (2014)
[5] L. Franchi, L. F. Livi, G. Cappellini, G. Binella, M. Inguscio, J. Catani, and L. Fallani, New J. Phys. **19**, 103037 (2017)

*Corresponding author: mateusz@fizyka.umk.pl

$N^+(^3P_J)$ Mobility in Cooled Helium Gas

L. Aissaoui[*1], Peter Knowles[2] and M. Bouledroua[3]
[1]*Physics Department, Batna 1 University, Algeria.*
[2]*School of Chemistry, Cardiff University, Cardiff, United Kingdom.*
[3]*Physics Department, Badji Mokhtar University, Annaba, Algeria.*

Based on the recent ion mobility measurements, performed by Matoba *et al*., [1] and Sandreson *et al.*, [2] with a mass-selected-ion-injected drift tube mass spectrometer, of ionic open-shell systems such as C^+, N^+ and O^+ ions, evolving in a helium gas at very low temperatures (4.3 and 77 K), the results could not be explained at 4.3 K. The authors suggested to improve the calculations by using *full quantum-mechanical* transport cross sections and a higher-level kinetic theory of gas mobility.

On the light of the quantum-mechanical [3] and the classical [4] calculations of the ground and the metastable-excited C^+ ion mobility in helium at temperatures 77 and 4.3 K, we have aimed to show the effect of the Spin-Orbit on the quantum-mechanical calculations of the N^+ ions in a cooled buffer helium gas. For this reason, we use the interaction potentials corresponding to the ground state $N^+(^3P_J)$ ions which are performed with MOLPRO. Then we use the computed quantum-mechanical and classical transport cross sections in the Viehland gram-char Fortran code as to get the mobility of $N^+(^3P_J)$ ions at 4.3K and 77K helium gas temperatures.

References

[1] S. Matoba, H. Tanuma, and K. Ohtsuki, J. Phys. B **41,** 145205 (2008).
[2] J. Sanderson, H. Tanuma, N. Kobayashi, Y. Kaneko, J. Chem. Phys. **103,** 16 (1995).
[3] L. Aissaoui, M. Bouledroua, K. Alioua, Mol. Phys. **113,** N°. 23, 3740 (2015).
[4] W.D. Tuttle, R. L. Thoringtona, L. A. Viehland, T. G. Wrighta, Mol. Phys. **113,** N°. 23, 3767 (2015).

[*]Corresponding author: lamia.aissaoui@univ-batna.dz

A – 14

FT spectroscopy of the comet−tail ($A^2\Pi_i \rightarrow X^2\Sigma^+$) system bands in $^{12}C^{17}O^+$

I. Piotrowska*, M. Ostrowska-Kopeć, W. Szajna, R. Hakalla, M. Zachwieja, P. Kolek, M. Rusznica and R. Kępa

Materials Spectroscopy Laboratory, Department of Experimental Physics, Faculty of Mathematics and Natural Science, University of Rzeszów, ul. Prof. S. Pigonia 1, 35-959 Rzeszów, Poland

In the emission spectrum of $^{12}C^{17}O^+$ molecule new observations and analyses were performed. Two bands, $(1,0)$ and $(1,1)$, of the comet−tail ($A^2\Pi_i \rightarrow X^2\Sigma^+$) system in the 18,900 to 22,100 cm^{-1} region were recorded with the Fourier transform spectrometer (BRUKER IFS 125−HR). The absolute accuracy of wavenumbers was about 0.005 cm^{-1}. The measurement cycle included 128 scans within 1.5 h. As a source of the studied spectrum an air−cooled, carbon hollow−cathode lamp operated at 780 V and 60 mA dc was used. The lamp was filled with a static mixture of $^{17}O_2$ (70 %) and $^{16}O_2$ (30 %) at a pressure of ∼1 Torr. During the discharge process, the O_2 molecules react with the ^{12}C atoms ejected from the carbon filler placed inside the cathode, thus forming $^{12}C^{17}O$ and $^{12}C^{17}O^+$ molecules in the gas phase, in amounts sufficient to finally achieve a signal−to−noise ratio of 100 : 1 for the $^{12}C^{17}O^+$ ion. Spectra were analyzed using a commercial software OPUS^{TM} [1], which finds peaks and calculates various spectral parameters (wavenumbers, FWHM, etc). As a result of a detailed spectral analysis the individual molecular constants of both $A^2\Pi_i$ and $X^2\Sigma^+$ states were obtained. For the upper $A^2\Pi_i$ state all these constants were delivered for the first time. The parameters for the lower $X^2\Sigma^+$ state were also calculated and can be compared with these determined previously [2],[3],[4].

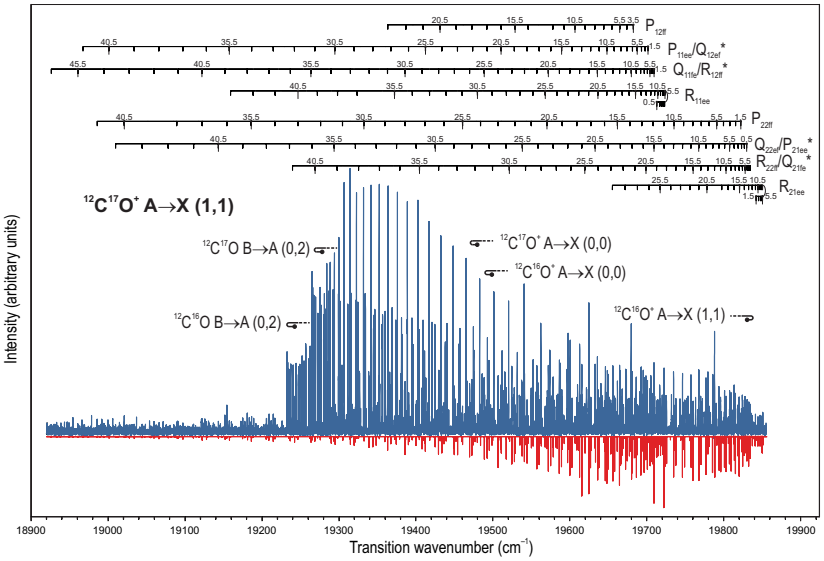

Fig. 1: High-resolution emission spectrum (upper trace) of the $(1,1)$ band of the comet – tail ($A^2\Pi_i \rightarrow X^2\Sigma^+$) system in the rare $^{12}C^{17}O^+$ isotopologue together with the other bands: $^{12}C^{16}O$ and $^{12}C^{17}O$ B – A system $(0,2)$ bands, $^{12}C^{16}O^+$ and $^{12}C^{17}O^+$ A – X system $(0,0)$ bands and $^{12}C^{16}O^+$ A – X system $(1,1)$ band, as well as simulated spectrum [5] (lower trace) of the $^{12}C^{17}O^+$ A – X system ($(1,1)$) band. In case of P_{11}/Q_{12}, Q_{11}/R_{12}, Q_{22}/P_{21} and R_{22}/Q_{21} main/sattelite branches (denoted by an asterisk) the values of the rotational quantum number J are provided just for the main branches.

References

[1] OPUS^{TM}. Computer program by Bruker Optik GmbH; 2014. v.7.5.18.
[2] W. Szajna and R. Kępa, Spectrochim. Acta A. **65**, 1014 (2006).
[3] W. Szajna, R. Kępa, R. Hakalla, and M. Zachwieja, J. Mol. Spectrosc. **240**, 75 (2006).
[4] W. Szajna, R. Kępa, R. Hakalla, and M. Zachwieja, Spectrosc. Lett. **40**, 667 (2007).
[5] C. M. Western, J. Quant. Spectrosc. Radiat. Transf., **186**, 221 (2016).

*Corresponding author: ipiotrowska@ur.edu.pl

A – 15

Magnetic field imaging of magnetic micro structures by using a layer of nitrogen vacancy centers in diamond crystal

A. Berzins[*1], **K. Erglis**[2] **J. Smits**[1] **M. Auzins**[1] **R. Ferber**[1] **A. Cebers**[2]
1. Laser Centre, University of Latvia, Zellu Street 25, Riga, Latvia
2. Laboratory of Magnetic Soft Materials, University of Latvia, Zellu Street 25, Riga, Latvia

Nitrogen-vacancy (NV) centers in diamonds have proven to be useful for the imaging of magnetic fields created by various magnetic structures [1],[2],[3]. The reason is that the NV center has a triplet ground state with a zero-field splitting between the $m_s = 0$ and $m_s = \pm 1$ ground-state sublevels of 2.87 GHz. Moreover, in the presence of a local magnetic field the $m_s = \pm 1$ energies components are shifted by 2.8 MHz/G. Due to a non-radiative decay path via a singlet state that preferentially populates the $m_s = 0$ ground-state sublevel, thus the NV center can be polarized optically. The fluorescence from exciting $m_s = 0$ sublevel is more intense than the fluorescence from exciting the $m_s = \pm 1$ sublevels. As a result one can read out the polarization state from the fluorescence intensity.

When a thin layer of NV centers is created close to the surface of a diamond, magnetic field distributions at the position of the NV layer can be imaged. We have constructed a magnetic field microscope and are using it to study magnetic field distributions from magnetic spheres, magnetic labyrinths and magnetic thin films made from different materials.

As an example of our measurements we present (Fig. 1) results we obtained from mix of 500 nm paramagnetic and 4 μm ferromagnetic particles.

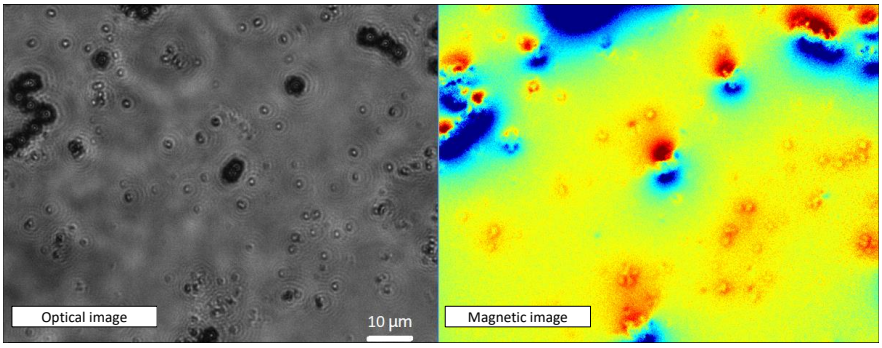

Fig. 1: On the left optical image and an the right magnetic image of mix of 500 nm paramagnetic and 4 μm ferromagnetic particles. Paramagnetic particles align their magnetic fields along the external field, but ferromagnetic particles maintain their initial magnetization.

Acknowledgments: A. Berzins gratefully acknowledges support from PostDoc Latvia project 1.1.1.2/VIAA/1/16 "Two-way research of thin-films and NV centres in diamond crystal" and LLC "MikroTik" donation, administered by the UoL foundation, for opportunity to improve experimental set-up. Other authors acknowledges support by M-ERA-NET project "Metrology at the Nanoscale with Diamonds" (MyND) and Base/Performance Funding Project Nr. AAP2016/B013, ZD2010/AZ27.

References

[1] J. Smits *et al.*, Eur. Phys. J. Appl. Phys. **73** 20701 (2016).
[2] L. M. Pham *et al.*, New Journal of Physics **13** 045021 (2011).
[3] D. Le Sage *et al.*, Nature **496** 486 (2013).

*Corresponding author: andris.berzins@lu.lv

A – 16

Near-threshold Stark spectra of strontium: Single- and two-photon excitation schemes

P. Kalaitzis[*1], D. Spasopoulos[1], S. Cohen[†1]

1. Atomic and Molecular Physics Laboratory, Physics Department, University of Ioannina, 45110 Ioannina, Greece

When an atom is placed in a uniform static electric field of strength F its ionization threshold (originally at E=0) is lowered by the saddle point energy, classically given by E_{sp}=–$2F^{1/2}$ au [1]. Within the E_{sp}≤E≤0 energy range quasi-bound Stark states (resonances) and continuum ones coexist [2]. Hydrogenic resonances are characterized by the excited electron's escape to infinity solely via tunnelling [3]. On the contrary, in non-hydrogenic atoms resonances are coupled to the degenerate continua and the electron escapes via autoionization [2]. Furthermore, the coupling between resonances leads to avoided crossings of the resonance energies as a function of F [1]. Remarkably, in the vicinity of an avoided crossing one of the resonances partially decouples from the continua (stabilization) and the outgoing photoelectron escapes again solely via tunnelling [4]. This situation was found very appealing for Photoionization Microscopy (PM) studies, the term denoting probability density measurements of slow (meV) electrons photoionized in the presence of the static electric field. The PM images are proportional to the squared modulus of the electronic wave function [5].

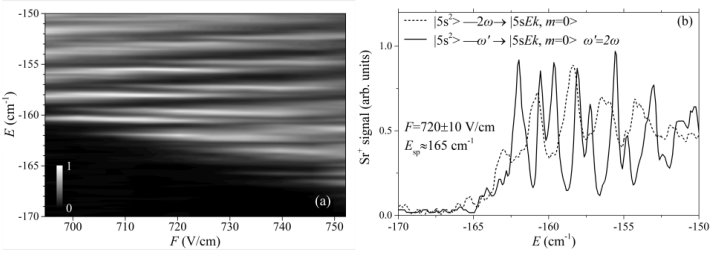

Fig. 1. (a) Stark map of single-photon excitation spectra of Sr out of its $5s^2$ ground state. Several avoided crossings and stabilization effects are evident. (b) Single-(solid line) and two-photon (dashed line) excitation Stark spectra of Sr. Linear laser light polarization parallel to the electric field (azimuthal quantum number m=0).

It would be highly interesting to observe PM images of resonances decoupled from the continua in atoms heavier then He [4] and in conjunction with the application of phase sensitive coherent control techniques [6], for the purpose of further reducing the continuum excitation [7]. As a first step towards this goal, we have employed single- and two-photon laser excitation schemes out of the ground state of Sr, in order to record (using a typical atomic beam/time-of-flight ion spectrometer setup) Stark spectra just above E_{sp} and as a function of F. The single-photon spectra revealed several avoided crossings and stabilization effects (Fig. 1(a)). These effects are not easily identified in the (considerably different) two-photon spectra (Fig. 1(b)). These observations will be presented and discussed at the conference.

The research (MIS: 5005247) is implemented through the Operational Program "Human Resources Development, Education and Lifelong Learning" and is co-financed by the European Union (European Social Fund) and Greek national funds.

References

[1] T. F. Gallagher, *Rydberg Atoms* (Cambridge University Press, Cambridge, 1994) and references therein.
[2] D. A. Harmin, Phys. Rev. A **24**, 2491 (1981).
[3] A. S. Stodolna et al, Phys. Rev. Lett. **110**, 213001 (2013).
[4] A. S. Stodolna et al, Phys. Rev. Lett. **113**, 103002 (2014).
[5] V. D. Kondratovich and V. N. Ostrovsky, J. Phys. B **23**, 3785 (1990).
[6] A. Bolovinos, S. Cohen, and I. Liontos, Phys. Rev. A **77**, 023413 (2008).
[7] S. Cohen, J. Phys. B **44**, 205402 (2011).

[*]Corresponding author: pkalaitz@cc.uoi.gr
[†]Corresponding author: scohen@uoi.gr

Fourier transform study of the RbCs $(4)^1\Pi$ state using the two-step Ti:Saphire laser excitation

A. Kruzins*[1], I. Klincare[1], M. Tamanis[1], R. Ferber[1], E.A. Pazyuk [2], A.V. Stolyarov [2]
1. Laser Centre, University of Latvia, Rainis blvd. 19, Riga, Latvia, LV-1586
2. Department of Chemistry, Lomonosov Moscow State University, 119991 Moscow, Leninskie gory 1/3, Russia

We performed a high resolution spectroscopic study of the regularly perturbed $(4)^1\Pi$ state of RbCs molecule by applying two-step optical excitation $(4)^1\Pi \leftarrow A-b \leftarrow X^1\Sigma^+$ followed by observation of the $(4)^1\Pi \rightarrow X^1\Sigma^+$ laser induced fluorescence (LIF) spectra. The main aim of this work was to extend the experimental rovibronic term values data set, if compare with [1], in order to perform direct-potential-fit (DPF) of the highly excited RbCs $(4)^1\Pi$ state. As intermediate state we have used strongly mixed by spin-orbit interaction $A^1\Sigma^+$ and $b^3\Pi$ states ($A-b$ complex for short). It was shown [2] that a rigorous coupled-channel deperturbation analysis allows to reproduce the rovibronic term values of the $A-b$ complex with the spectroscopic accuracy. Hence, the $A-b$ complex in RbCs can be used as a convenient intermediate state to reach higher excited singlet and triplet states manifold.

The RbCs molecules were produced in a linear stainless-steel heat pipe, that was loaded with 7g Cs and 10g Rb. Work temperature during experiments was around 310^oC. Two-step excitation in both steps ($A^1\Sigma^+ - b^3\Pi \leftarrow X^1\Sigma^+$ and $(4)^1\Pi \leftarrow A^1\Sigma^+ - b^3\Pi$) was realized by two Ti:Saphire lasers (Coherent MBR-110) operating within the frequency range 9800-11000 cm^{-1}. LIF spectra were recorded by high resolution Fourier transform spectrometer (IFS 125-HR, Bruker). The $(4)^1\Pi \rightarrow X^1\Sigma$ transitions were recorded in the 18000-22000 cm^{-1} spectral range using photomultiplier tube while the $A^1\Sigma^+ - b^3\Pi \rightarrow X^1\Sigma^+$ LIF spectra were detected by InGaAs diode in the range 6000 - 11000 cm^{-1}.

Overall 69 $(4)^1\Pi \rightarrow X^1\Sigma$ LIF progressions were recorded. Assignment of these progressions provided termvalues and rotational quantum numbers of directly excited rovibronic levels. In many spectra rotational satellite lines were observed thus increasing the amount of term values and allowing to estimate the rotationally induced Λ-splitting of the $(4)^1\Pi$ state. All resulting 780 term values were included in the robust DPF procedure and analytical Expanded Morse Oscillator (EMO) potential was constructed. The DPF analysis reveals numerous regular shifts in the experimental level positions of the $(4)^1\Pi$ state. At the same time, relative intensity distributions measured from the most observed levels of the $(4)^1\Pi$ state are in very good agreement with their theoretical counterparts.

The support from Base/Performance Funding project no. AAP2016/B013, ZD2010/AZ27 and project 1.1.1.2/VIAA/1/16/068 is gratefully acknowledged by Riga team. The work is partly supported by the RFBR grant N 16-03-00529.

References

[1] T. Gustavsson,*et al.*, Molecular Physics **64** No 2, 293 (1988).
[2] A. Kruzins, *et al.*, J. Chem. Phys. **141**, 184309 (2014).

*Corresponding author: artis.kruzins@lu.lv

A – 18

Non-linear resonances of calcium ions in a linear quadrupole trap

M. Piwiński[1], **D. Lisak**[1], **K. Pleskacz**[1], **S. Wójtewicz**[1], **Ł. Kłosowski***[1]
1. Institute of Physics, Faculty of Physics, Astronomy and Informatics, Nicolaus Copernicus University in Torun, Grudziadzka 5, 87-100 Torun, Poland

Non-linear resonances are well known effect observed in ion traps since the early stage of development of the trapping techniques [1]. They occur, when trapping potential is not perfectly harmonic and some higher multipole terms are present in the field's expansion series. Such non-harmonicity can lead to energy gain by an ion trapped inside such potential well.

In our recent paper [2] we described such resonances in a linear, segmented Paul trap, where the central segments of electrodes are relatively short comparing to their transversal dimensions.

The trapped ion stability is usually described using Mathieu equations:

$$\ddot{x} = (2q\cos\Omega t + a)x \tag{1}$$

with defined q and a stability parameters:

$$q = \frac{2QU_0}{M\Omega^2R^2}, \tag{2}$$

$$a = \frac{4QV}{M\Omega^2R^2}, \tag{3}$$

where M and Q are ion's mass and charge respectively, Ω is angular frequency of the used AC electric field, R is trap's radius and U_0 and V are AC and DC voltages driving the trap. In the experiment we observed that, besides the two standard trapping parameters, a third one Δa is necessary to describe the stability in a more reliable way:

$$\Delta a = \frac{3.8QV_{end}}{M\Omega^2R^2}, \tag{4}$$

where V_{end} is additional voltage used for confinement of ions along the trap's main axis and 3.8 factor results from geometry of the electrodes. In the 3-dimensional $(q,a,\Delta a)$ parameter space we explored its $a = 0$ cross section, where we observed several strong lines of non-linear resonances. The $(q,\Delta a)$ stability diagram is presented in Fig. 1.

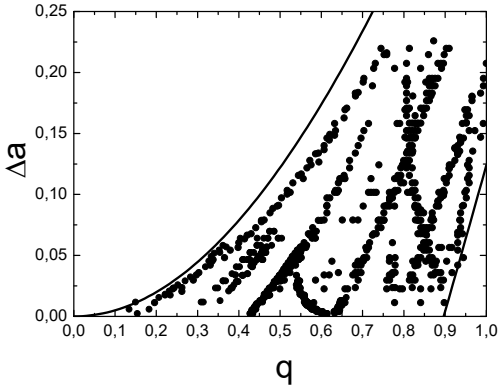

Fig. 1: Stability diagram of the linear Paul trap. Solid lines are theoretical boundaries of the main stability domain. Experimental points show parameters where ion ensembles are unstable.

The apparatus and experimental procedure will be presented. The theoretical model of resonance mechanism in the used trap's geometry will be discussed and the experimental resonance lines will be identified using the model.

References

[1] F. von Busch and W. Paul Z. Phys. **154** 588-594 (1961).
[2] Ł. Kłosowski *et al.* Journal of Mass Spectrometry (2018) In press.

*Corresponding author: lklos@fizyka.umk.pl

An optical atomic clock using a single $^{171}Yb^{+}$ ion with a characterisation of thermal systematic effects

C. F. A. Baynham*[1,2], E. A. Curtis[1], R. M. Godun[1], J. M. Jones[1,3], P. B. R. Nisbet-Jones[1], P. E. G. Baird[2], P. Gill[1,2], T. Fordell[4], T. Hieta[4], T. Lindvall[4],

1. National Physical Laboratory, Hampton Road, Teddington TW11 0LW, United Kingdom
2. Clarendon Laboratory, University of Oxford, Parks Road, Oxford OX1 3PU, United Kingdom
3. School of Physics and Astronomy, University of Birmingham, Birmingham B15 2TT, United Kingdom
4. VTT Technical Research Centre of Finland Ltd, Centre for Metrology MIKES, P.O.Box 1000, FI-02044 VTT, Finland

Optical frequency standards operate by measuring to high precision the frequency associated with an optical atomic transition. Recent improvements in ultra-stable lasers, trapping technology and probe schemes have resulted in these systems approaching fractional systematic frequency uncertainties of $\sim 1 \times 10^{-18}$.

These astounding levels of accuracy allow clocks to be used for more than just timekeeping. Modern optical clocks are used to measure gravity potential differences through the relativistic time-dilation of general relativity [1]. They can measure the fractional rate of change of the fine structure constant (α) and proton:electron mass ratio $\mu = m_p/m_e$ [2], and probe for violation of Lorentz symmetry [3], effects that are predicted by some variants of the Standard Model Extension.

To make a repeatable frequency measurement at the $\sim 1 \times 10^{-18}$ level, environmental perturbations to the atomic sample must be strictly characterised or eliminated. Amongst the effects that must be considered is the ac Stark shift. Any atom exposed to an electric field will experience Stark shifts of its internal energy levels, proportional to their polarizabilities. It is desirable therefore to minimise any radiation incident on the atomic sample, but the background black-body radiation (BBR) due to the temperature of the trapping structure is an unavoidable source. The operation of a clock using singly-ionised ytterbium therefore requires careful characterisation of both the thermal environment of the trapped ion [4] and its intrinsic response to that radiation: the differential polarizability.

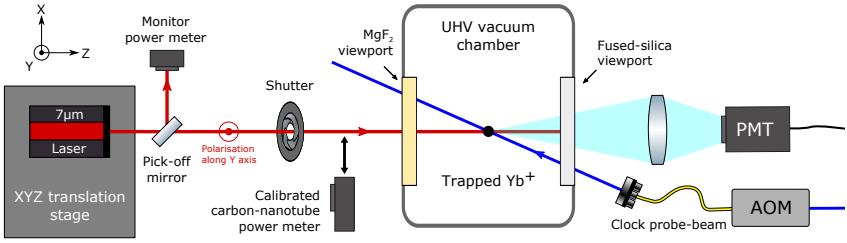

Fig. 1: The frequency of the two clock transitions at 436 nm and 467 nm in $^{171}Yb^{+}$ can be perturbed by incident light at near-IR wavelengths (here $\lambda = 7.17\,\mu$m). This light couples to the clock frequencies in the same way as background BBR: via the ion's differential polarizability. The perturbing laser is mounted on an automated translation stage so that all parts of the beam can be sampled by the ion. A shutter allows the 7 μm beam to be toggled so that the induced shift is measured differentially avoiding many common-mode errors on the two frequency servos.

The complex structure of $^{171}Yb^{+}$ makes the differential polarizability difficult to calculate theoretically; instead we present an experiment to measure the differential polarizabilities of two ultra-narrow optical clock transitions present in $^{171}Yb^{+}$, performed by exposing the ion to an oscillating electric field at a wavelength in the region of the room temperature BBR spectrum: $\lambda = 7.17\,\mu$m. This field is produced by a quantum cascade laser incident on the ion and can be blocked using a shutter, permitting a differential measurement with common-mode insensitivity to systematic effects from the ion's environment.

References

[1] Chou, C. W., *et. al.* (2010). Optical clocks and relativity. Science, 329(5999), 1630–1633.
[2] Godun, R. M., *et. al.* (2014). Frequency Ratio of Two Optical Clock Transitions in $^{171}Yb^{+}$ and Constraints on the Time Variation of Fundamental Constants. Physical Review Letters, 113(21), 210801.
[3] Dzuba, V. A., *et. al.* (2016). Strongly enhanced effects of Lorentz symmetry violation in entangled Yb^{+} ions. Nature Physics, 12(5), 4–9.
[4] Nisbet-Jones, P. B. R., *et. al.* (2016). A single-ion trap with minimized ion–environment interactions. Applied Physics B, 122(3), 57.

*Corresponding author: charles.baynham@npl.co.uk

Elastic Electron Scattering by the SF_n $(n = 1-6)$ Molecular Systems

S. Demes[*1], **V. Kelemen**[2], **E. Remeta**[†2]
1. Institute for Nuclear Research of the Hungarian Academy of Sciences (ATOMKI), Bem tér 18/c, 4026 Debrecen, Hungary
2. Institute of Electron Physics of the Ukrainian Academy of Sciences, Universitetska St. 21, 88017 Uzhhorod, Ukraine

The elastic scattering of electrons by the SF_6 molecule and its SF_n $(n = 1-5)$ fragments has been studied theoretically in a wide energy range of $5-700$ eV in the framework of independent-atom model (IAM) [1-3]. The relativistic, parameter-free, real optical potential approximation (RSEP) [1,4] is used to calculate the electron scattering amplitudes of the S and F atoms. It consists of static, relativistic local exchange, local correlation-polarization, scalar-relativistic and spin-orbit interaction potentials [4]. The differential and integral cross sections are calculated using the ground-state equilibrium internuclear distances of the sulphur fluorides in the IAM and Additivity Rule (IAM-AR) approximations. In the IAM framework the differential cross sections (DCSs) are obtained by averaging over the vibrational and rotational degrees of freedom of the target molecules (see [1-3]). They could be expressed with the direct $f(\theta,k)$ and spin-flip $g(\theta,k)$ atomic scattering amplitudes:

$$\frac{d\sigma_{\rm el}^{\rm IAM}}{d\Omega} = \sum_m \left[|f_m(\theta,k)|^2 + |g_m(\theta,k)|^2\right] + \sum_m \sum_{n\neq m} \left[f_m(\theta,k) f_n^*(\theta,k) + g_m(\theta,k) g_n^*(\theta,k)\right] \times e^{-\ell_{mn}^2 s^2/2} \frac{\sin(s r_{nm})}{s r_{nm}}, \quad (1)$$

where r_{nm} is the internuclear distance between n-th and m-th atoms of the molecule, ℓ_{mn} is the average amplitude of the corresponding vibrations, while $s(\theta,k) = 2k\sin(\theta/2)$, θ – scattering angle, $k = \sqrt{2E}$ (in a.u.), E – collision energy. The first sum of Eq. 1 is the direct term, which corresponds to the IAM-AR approximation. The r_{nm} internuclear distances for all SF_n $(n = 1-6)$ molecules are calculated by the GAMESS-US quantum chemistry package at the DFT/B3LYP level of theory.

In Fig. 1 we present DCSs for $e^- + SF_n$ $(n = 6,4,1)$ processes at 10 and 50 eV impact energies, comparing with experimental [5,6] and theoretical [7,8] data for $e^- + SF_6$ scattering. At 10 eV the angular behaviour and the magnitude of our DCSs are similar, they slightly differs only at small angles, up to 70°. In this region there is a higher deviation between our calculated and the measured DCSs of [5,6]. At 50 eV a better qualitative and quantitative agreement is seen between these cross sections in general, even at small scattering angles. However, our DCSs for the $e^- + SF_n$ $(n = 6,4,1)$ processes differ more distinctly. Integral cross sections of scattering are also calculated by direct integration of the corresponding DCSs in the IAM and IAM-AR framework.

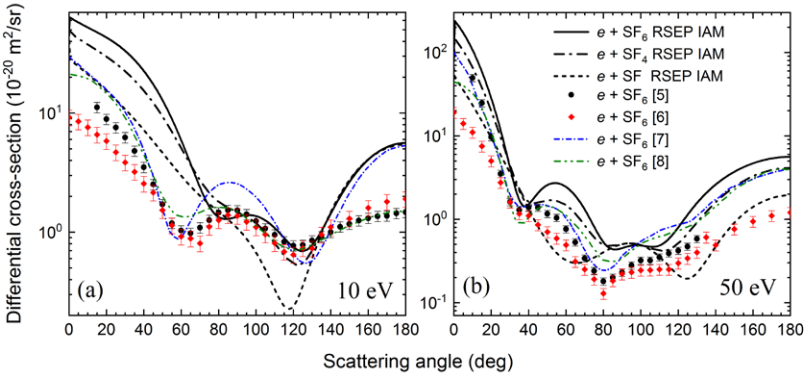

Fig. 1: Angular behaviour of differential cross sections of $e^- + SF_n$ $(n = 6,4,1)$ scattering at 10 (a) and 50 (b) eV.

References

[1] Sh. Demesh, V. Kelemen and E. Remeta, J. Phys. B: At. Mol. Opt. Phys. **50**, 135201 (2017).
[2] J. Raj, Phys. Lett. A **160**, 571 (1991).
[3] P. Możejko, B. Żywicka-Możejko and C. Szmytkowski, Nucl. Instr. Meth. B **196**, 245 (2002).
[4] V. I. Kelemen and E. Yu. Remeta, J. Phys. B: At. Mol. Opt. Phys. **45**, 185202 (2012).
[5] H. Cho, R. J. Gulley, K. W. Trantham, L. J. Uhlmann, C. J. Dedman *et al.*, J. Phys. B: At. Mol. Opt. Phys. **33**, 3531 (2000).
[6] S. Trajmar, D. F. Register and A. Chutjian, Physics Reports **97**, (5), 219-356 (1983).
[7] F. A. Gianturco and R. R. Lucchese, J. Chem. Phys. **114**, 3429 (2001).
[8] C. Winstead and V. McKoy, J. Chem. Phys. **121**, 5828 (2004).

[*]Corresponding author: demes.sandor@atomki.mta.hu
[†]Corresponding author: remetoveyu@gmail.com

A – 21

Theoretical Study of Elastic Electron Scattering by Sulphur Clusters

S. Demes[*1], **V. Kelemen**[2], **E. Remeta**[†2]
1. Institute for Nuclear Research of the Hungarian Academy of Sciences (ATOMKI), Bem tér 18/c, 4026 Debrecen, Hungary
2. Institute of Electron Physics of the Ukrainian Academy of Sciences, Universitetska St. 21, 88017 Uzhhorod, Ukraine

The elastic scattering of electrons by the sulphur atom and the S_n $(n = 2-4)$ clusters has been studied theoretically in a wide energy range of $10-700$ eV in the framework of independent-atom model (IAM) [1-3]. The relativistic, parameter-free, real optical potential approximation (RSEP) [1,4] is used to calculate the electron scattering amplitudes of the S atom. It consists of static, relativistic local exchange, local correlation-polarization, scalar-relativistic and spin-orbit interaction potentials [4]. The molecular differential and integral cross sections are calculated using the ground-state equilibrium internuclear distances of the sulphur clusters in the IAM and Additivity Rule (IAM-AR) approximations. In the IAM framework the differential cross sections (DCSs) are obtained by averaging over the vibrational and rotational degrees of freedom of the target molecules (see [1-3]). They could be expressed with the direct $f(\theta,k)$ and spin-flip $g(\theta,k)$ atomic scattering amplitudes:

$$\frac{d\sigma_{\rm el}^{\rm IAM}}{d\Omega} = \sum_m \left[|f_m(\theta,k)|^2 + |g_m(\theta,k)|^2\right] + \sum_m \sum_{n\neq m} \left[f_m(\theta,k) f_n^*(\theta,k) + g_m(\theta,k) g_n^*(\theta,k)\right] \times e^{-\ell_{mn}^2 s^2/2} \frac{\sin(sr_{nm})}{sr_{nm}}, \quad (1)$$

where r_{nm} is the internuclear distance between n-th and m-th atoms of the molecule, ℓ_{mn} is the average amplitude of the corresponding vibrations, while $s(\theta,k) = 2k\sin(\theta/2)$, θ – scattering angle, $k = \sqrt{2E}$ (in a.u.), E – collision energy. The first sum of Eq. 1 is the direct term, which corresponds to the IAM-AR approximation. The r_{nm} internuclear distances for all S_n $(n = 2-4)$ molecules are calculated by the GAMESS-US quantum chemistry package at the DFT/B3PW91 level of theory. The calculated cross sections are compared with the available experimental and theoretical data for elastic electron scattering by the S atom as well as by CS_2 and H_2S molecules [5-8].

In Fig. 1 we present DCSs for $e^- + S_n$ $(n = 1,2,4)$ processes at 20 and 100 eV impact energies, comparing with the data of [5-8]. The angular behaviour of our DCSs are similar, they slightly differs only at small angles, however the magnitude of the cross sections strongly changes with the target molecules. The relative difference between the cross sections primarily depends on the number of sulphur atoms of the target, the DCS of $e^- + S_2$ scattering about 2 times higher, than the corresponding atomic scattering cross section. The structure of our DCSs are very similar to those observed in [5-8], hovewer they differs strongly in magnitude at some angles, especially in the minima. Taking into account the absorbtion effects (see [6]) leads to somewhat lower cross sections.

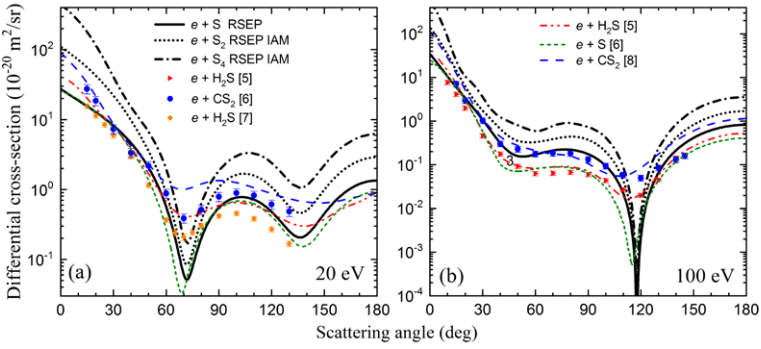

Fig. 1: Angular behaviour of differential cross sections of $e^- + S_n$ $(n = 1,2,4)$ scattering at 20 (a) and 100 (b) eV.

References

[1] Sh. Demesh, V. Kelemen and E. Remeta, J. Phys. B: At. Mol. Opt. Phys. **50**, 135201 (2017).
[2] J. Raj, Phys. Lett. A **160**, 571 (1991).
[3] P. Możejko, B. Żywicka-Możejko and C. Szmytkowski, Nucl. Instr. Meth. B **196**, 245 (2002).
[4] V. I. Kelemen and E. Yu. Remeta, J. Phys. B: At. Mol. Opt. Phys. **45**, 185202 (2012).
[5] P. Rawat, I. Iga, M.-T. Lee, L. M. Brescansin, M. G. P. Homem and L. E. Machado, Phys. Rev. A **68**, 052711 (2003).
[6] H. Murai, Y. Ishijima, T. Mitsumura, Y. Sakamoto, H. Kato, M. Hoshino, F. Blanco, G. García *et al.*, J. Chem. Phys. **138**, 054302 (2013).
[7] R. J. Gulley, M. J. Brunger and S. J. Buckman, J. Phys. B: At. Mol. Opt. Phys. **26**, 2913-2925 (1993).
[8] M. T. Lee, S. E. Michelin, T. Kroin and E Veitenheimer, J. Phys. B: At. Mol. Opt. Phys. **32**, 3043–3053 (1999).

[*]Corresponding author: demes.sandor@atomki.mta.hu
[†]Corresponding author: remetoveyu@gmail.com

A – 22

Dielectronic Satellites of the Tl^+ Ion 132.2 nm Resonance Line

A.N. Gomonai*[1], S. Demes[2], A.I. Gomonai[1], Yu. Hutych[1], V. Zvenihorodsky[1], A. Mylymko[1],
1. Institute of Electron Physics , National Academy of Sciences of Ukraine, Universitetska Street 21, 88017 Uzhgorod, Ukraine
2. Institute for Nuclear Research of the Hungarian Academy of Sciences (ATOMKI), Bem tér 18/c, 4026 Debrecen, Hungary

Dielectronic recombination (DR) is a resonant process in which a free electron is captured by an ion whereas a bound electron in the ion is promoted forming a multiply excited intermediate state situated above the autoionization threshold. As a consequence one or few photons are released to stabilize the recombined ion. The dielectronic satellite (DS) radiation coming from this process can give a significant contribution to both the apparent width and intensity of a resonance line.

We report the experimental observation of the DS in the near-threshold electron-impact excitation of the Tl^+ ion λ = 132.2 nm resonance line ($6s6p\ ^1P_1^o \rightarrow 6s^2\ ^1S_0$). The experiment was performed by a VUV-spectroscopy method using the crossed (at right angle) monoenergetic electron and ion beams technique which was previously described elsewhere [1].

Strong resonance features observed in the energy dependence of the effective excitation cross-section for this line are due to the emission of the DS $6s6p\ (^1P_1^o)nl \rightarrow 6s^2nl$ ($n \geq 7$) of the resonance line below the threshold and the resonance excitation due to electron decay of the autoionizing states (AIS) above the threshold. The analysis of the results using the data on the energy positions and configurations of the Tl atom AIS [2] has shown that the isolated maxima at 7.4 eV (**a**) and at 8.4 eV (**b**) in the energy dependence under study are most likely related to the decay of the Tl^{**} $6s6p\ (^1P_1)7p$ and $6s6p\ (^1P_1)8p$ AIS while the maximum at 9.0 eV (**c**) to that of the Tl^{**} AIS of the $6s6p\ (^1P_1)np$ (n = 10, 11) configurations.

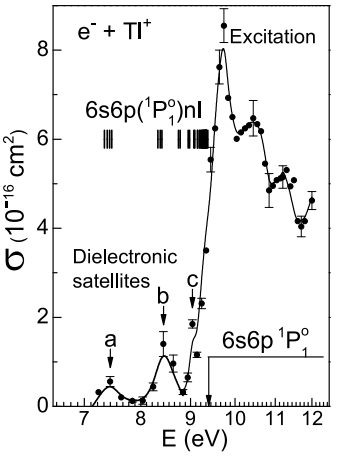

Fig. 1: Energy dependence of the near-threshold electron-impact excitation.

The absolute values of the excitation cross-sections for the DS of the resonance Tl^+ ion line were determined at the threshold taking into account the absolute value of the resonance line excitation cross-section obtained by normalizing to the theoretical calculation at E = 100 eV energy using the close-coupling method, taking into account two stages [3].

It is worth noting that the DS of the resonance λ = 132.2 nm line ($6s6p\ ^1P_1^o \rightarrow 6s^2\ ^1S_0$) were found to be much less intensive then those of the resonance intercombination λ = 190.8 nm line ($6s6p\ 3P_1^o \rightarrow 6s^2\ ^1_0$) of the Tl^+ ion [4].

The work is supported by the grant program of scientific research of the National Academy of Sciences of Ukraine "Advanced research on plasma physics, controlled thermonuclear fusion, and plasma-based technologies".

References

[1] E. Ovcharenko, A. Imre, A. Gomonai et al., J. Phys. B: At. Mol. Opt. Phys. **43**, 175206 (2010).
[2] M. Baig and S. Ahmad, J. Phys. B: At. Mol. Phys. **25**, 1719 (1992).
[3] A. Imre, A.N. Gomonai et al., XVI ICPEAC, Abstracts of Contributed Papers, 876 (1989).
[4] A. Gomonai, A. Imre and E. Kontrosh, Opt. and Spectrosc. **81**, 22 (1996).

*Corresponding author: annagomonai@gmail.com

Coherent and efficient microwave-to-optical conversion via six-wave mixing in Rydberg atoms

Thibault Vogt[*1,2], **C. Gross**[1], **J. Han**[1], **D. Jaksch**[3], **M. Kiffner**[1,3], **W. Li**[1,4]

1. Centre for Quantum Technologies, National University of Singapore, 3 Science Drive 2, Singapore 117543
2. MajuLab, CNRS-UNS-NUS-NTU International Joint Research Unit UMI 3654, Singapore 117543
3. Clarendon Laboratory, University of Oxford, Parks Road, Oxford OX1 3PU, United Kingdom
4. Department of Physics, National University of Singapore, 117542, Singapore

Frequency interconversion between microwave and optical fields will be important in future quantum information networks for connecting superconducting qubits and optical photons. To achieve the transfer of quantum states between microwave and optical photons, coherent, efficient, and broadband conversion is essential. Here we demonstrate a coherent microwave-to-optical conversion via frequency mixing in Rydberg atoms [1]. In contrast to other physical systems being explored, our scheme requires no cavity and allows free-space and broadband conversion due to the strong coupling of microwaves to atomic transitions between Rydberg states. Moreover, using electromagnetically induced transparency strongly enhances the efficiency of the process. Our results are in excellent agreement with theoretical predictions based on an independent atom model, which indicates a limited effect of interactions.

In this presentation, I will introduce these results, and discuss the strategies that we are developing for reaching near-unit conversion efficiency, which include using collinear frequency mixing, three-photon electromagnetically induced transparency (EIT) [2], and improved energy level schemes.

References

[1] J. Han, T. Vogt, C. Gross, D. Jaksch, M. Kiffner, and W. Li, Phys. Rev. Lett. 120, 093201 (2018).
[2] T. Vogt, C. Gross, T. F. Gallagher, and W. Li, Opt. Lett. 43, 1822 (2018).

*Corresponding author: cqttv@nus.edu.sg

A – 24

Atomic double core holes produced in electron K-capture

M.D. Kiselev[*1], O.I. Zatsarinny[2], M. Bilal[3,4], S. Fritzsche[3,4], E.V. Gryzlova[5], A.N. Grum-Grzhimailo[†5]

1. Faculty of Physics, Lomonosov Moscow State University, Leninskie Gory 1-2, 119991 Moscow, Russia
2. Department of Physics and Astronomy, Drake University, Des Moines, IA 50311, USA
3. Theoretisch-Physikalisches Institut, Friedrich-Schiller-Universität Jena, Max-Wien-Platz 1, D-07743 Jena, Germany
4. Helmholtz-Institut Jena, Fröbelstieg 3, D-07743 Jena, Germany
5. Skobeltsyn Institute of Nuclear Physics, Lomonosov Moscow State University, Leninskie Gory 1-2, 119991 Moscow, Russia

Physics of the double core holes (DCH) currently attracts interest due to new possibilities of their creation by X-ray free electron lasers and advanced synchrotron sources, and due to applications in chemical analysis. In the case of electron capture, which is one more mechanism of the DCH production, a DCH is formed after one K-electron is captured by the nucleus, and the second K-electron is either shaken off (SO) to a continuum, or shaken up (SU) to an unoccupied shell due to a change of the nuclear charge. Theoretical models of such electron shell rearrangements are based on sudden approximation, with the overlap integrals between wave functions of many-electron atoms (ions) both before and after electron absorption by the nucleus as main elements for calculations. In atomic processes involving internal electron shells the relaxation phenomena of electron orbitals play a key role. Relaxations could be most effectively taken into account by using sets of atomic orbitals for the initial and final states with non-orthogonal orbitals from different sets. Such an approach requires the representation of overlap integrals in terms of one-particle wave functions from different non-orthogonal sets. Nowadays, it can be done with the help of specialized program packages.

The goal of this work is to take into account the full non-orthogonality (FNO) of many-electron initial and final states' wave functions of the system to determine double K-vacancy production probability per K-capture, P_{KK} (as a sum of two channels: SU and SO) in order to improve the existing theoretical calculations in less advanced models. We have chosen isotopes ^{37}Ar, ^{54}Mn and ^{65}Zn for the analyses and used code [1] for the expansion of many-electron overlap integrals in terms of one-particle overlaps. Pilot calculations were made with relativistic hydrogen-like wave functions with effective charges for each subshell (FNO-C model), determined from the average radii of the relativistic orbitals obtained in the Dirac-Fock calculations [2]. Accounting for the non-orthogonality of the orbitals above the K-shell was found crucial. For more accurate calculations we used Hartree-Fock wave functions. SU-probabilities were found by means of the BSR complex [3], and SO-probabilities were calculated with the combination of Hartree-Fock wave functions for bound states and Coulomb wave functions for continuum (FNO-HF model). The latter model improves the results of the previous calculations (see Table 1). More details will be presented at the conference.

Table 1: Double K-vacancy production probability per K-capture.

	P_{KK}, 10^{-4}			
	Other calculations	FNO-C	FNO-HF	Experiment
^{37}Ar	2.58 [4], 3.86 [5], 5.30 [6]	7.77	3.87	3.7 ± 0.9 [7] 4.4 ± 0.8 [8]
^{54}Mn	1.13 [4], 1.35 [5], 2.43 [6]	5.45	2.46	3.6 ± 0.3 [9] $2.3^{+0.8}_{-0.5}$ [10]
^{65}Zn	0.87 [5], 1.53 [6]	3.17	2.37	2.2 ± 0.2 [11]

References

[1] O. Zatsarinny, Comp. Phys. Comm. **98**, 235 (1996).
[2] P. Jönsson et al., Comp. Phys. Comm. 184, 2197 (2013).
[3] O. Zatsarinny, Comp. Phys. Comm. **174**, 273 (2006).
[4] R.L. Intemann, Phys. Rev. C **31**, 1961 (1985).
[5] H. Primakoff and F.T. Porter, Phys. Rev. **89**, 930 (1953).
[6] A. Suzuki and J. Law, Phys. Rev. C **25**, 2722 (1982).
[7] J.A. Miskel and M.L. Perlman, Phys. Rev. **94**, 1683 (1954).
[8] R.W. Kiser and W.H. Johnston, J. Am. Chem. Soc. **81**, 1810 (1959).
[9] H.J. Nagy and G. Schupp, Phys. Rev. C **30**, 2031 (1984).
[10] M.M. Hindi, C.A. White and R.L. Kozub, Phys. Rev. C **68**, 014306 (2003).
[11] H.J. Nagy and G. Schupp, Phys. Rev. C **27**, 2887 (1983).

[*]Corresponding author: md.kiselev94@gmail.com
[†]Corresponding author: grum@sinp.msu.ru

Circular dichroism in electron-hydrogen scattering in a two-color bicircular laser field

Gabriela Buica*
1. Institute of Space Science, P.O. Box MG-36, R-77125, Bucharest, Romania

We study circular dichroism in laser assisted electron-hydrogen scattering by two-color circularly polarized (CP) fields with the same or different helicities, at high projectile energies, where the first order Born approximation is reliable for the evaluation of the scattering amplitude [1]. Obviously, the physical mechanism occurring in laser-assisted processes for two-color fields is the interference among different photon channels leading to the same final state. For the bicircular laser the polarization vector of the first laser beam is defined as $(\mathbf{e}_x + i\mathbf{e}_y)/\sqrt{2}$, while the second laser beam has the same polarization (corotating polarization), or is CP in the opposite direction (counterrotating polarization). We calculate the differential cross section (DCS) in the UV photon energy range, where the dressing of the target is important and the laser assisted signal is sensitive to the helicity of the photons of the two-color bicircular laser field [2]. In this framework the two-photon circular dichroism in angular distribution [3], is a second-order effect in the laser intensity. In figure 1 we present the relative dichroism in angular distribution, $R(\theta,\varphi) = \left(\frac{d\sigma_2^{LL}}{d\Omega} - \frac{d\sigma_2^{LR}}{d\Omega}\right)\left(\frac{d\sigma_2^{LL}}{d\Omega} + \frac{d\sigma_2^{LR}}{d\Omega}\right)^{-1}$, as a function of the scattering and azimuthal angles, θ and φ, of the projectile electron. We aim to establish the origin of the dichroic effect in elastic scattering of electrons by hydrogen atoms in the presence of a two-color circularly polarized laser field in the domain of moderate intensities below 10 TW/cm^2, for commensurate photon energies $\omega_3 = 3\omega_1$, and high projectile energies. Because of the strong second-order atomic dressing effects at small scattering angles ($\theta < 20°$), we found out a clear enhancement of DCSs for corotating compared to counterrotating CP fields. As a preliminary result, we are able to demonstrate that the circular dichroism at these photon energies originates from the nonzero atomic dressing at small scattering angles.

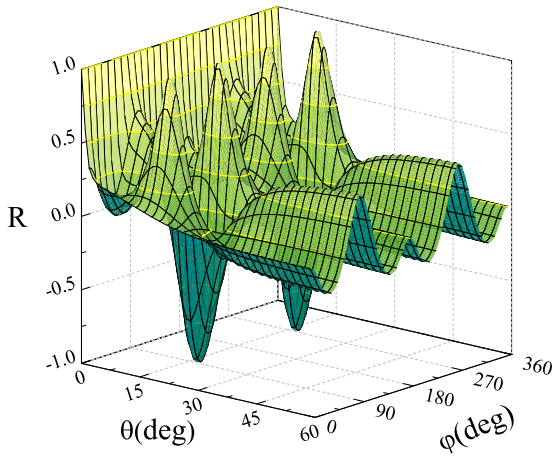

Fig. 1: Relative two-photon circular dichroism in angular distribution, R, as a function of the scattering and azimuthal angles. The projectile electron energy is $E_p = 100$ eV, the laser field intensities are $I_1 = I_3 = 1$ TW/cm^2, and the photon energies are $\omega_1 = 3$ eV and $\omega_3 = 3\omega_1$.

References

[1] F. W. Byron Jr. and C. J. Joachain, J. Phys. B **17**, L295 (1984).
[2] G. Buica, Phys. Rev. A **96**, 043419 (2017).
[3] A. Cionga, F. Ehlotzky, and G. Zloh, Phys. Rev. A **61**, 063417 (2000).

*Corresponding author: buica@spacescience.ro

A – 26

Positron Elastic Scattering off Half-Filled Shell Atoms: the Mn case

V. Dolmatov[*1], **M. Amusia**[†2,3], **L. Chernysheva**[‡3]
1. Department of Physics and Earth Science, University of North Alabama, 1 Harrison Plaza, 35630 Florence, Alabama, U. S. A.
2. Racah Institute of Physics, Hebrew University, 91904 Jerusalem, Israel
3. A. F. Ioffe Physical-Technical Institute, 124021 St. Petersburg, Russia.

Positron-atom ($e^+ + A$) scattering is an interesting and important process the study of which has a long history. Compared to electron scattering ($e^- + A$), $e^+ + A$ scattering is a much more subtle elementary process owing to the possibility of the formation of a virtual positronium during the scattering process [1]. Many methods have been developed and attempts made to study $e^+ + A$ scattering off atoms with account for the positronium formation. However, to the best of the authors' knowledge, $e^+ + A$ scattering has not been studied for the case of collision with atoms with a $n\ell^{2\ell+1}$ multielectron half-filled subshell in the ground-state. Meanwhile, its presence results in the introduction of an additional novel, interesting aspect into scattering theory. Owing to the presence of the $n\ell^{2\ell+1}$ subshell in the atom, like the $3d^5$ in Mn, each of used to be closed subshells of the atom splits into two different $n'\ell'^{2\ell'+1}\uparrow$ spin-up and $n'\ell'^{2\ell'+1}\downarrow$ spin-down levels [2]. This is owing to differences in exchange interaction of $n'\ell'^{2\ell'+1}\uparrow$ and $n'\ell'^{2\ell'+1}\downarrow$ electrons with the electrons from the $n\ell^{2\ell+1}$ half-filled subshell, where the electronic spins are co-directed, say, pointing upward ($\uparrow$), according to Hunds's rule. Not only are $n'\ell'^{2\ell'+1}\uparrow$ and $n'\ell'^{2\ell'+1}\downarrow$ split by energy, but spatially as well. This contributes to an important novel aspect into $e^\pm + A$ scattering. It is the main aim of the present work to learn about $e^+ + A$ scattering off a half-filled shell atom and unravel differences between $e^+ + A$ and $e^- + A$ scattering by such atom. We choose the Mn atom as a case study, since $e^- +$ Mn scattering has been detailed earlier [3],[4]. During $e^+ + A$ scattering, the positronium formation [1] occurs in a virtually excited state of an atomic electron, thus being a multielectron effect. In this work, perturbation of the atomic states by a positron is accounted in the framework of the spin-polarized self-energy part, Σ, of the Green function (referred to, herein, as the "Σ-approximation") of a positron, as in [3] for $e^- +$ Mn scattering, with the necessary correction to remove electron-positron exchange correlation. The effect of the positronium formation is calculated in a simple and yet surprisingly efficient approximation [1], where accounting for the effect is equivalent to a simple reduction of the energy of the e^-e^+ virtual pair by the binding energy of the positronium. On Fig. 1, depicted are calculated elastic scattering cross sections for $e^+ +$ Mn scattering as well as for $e^- +$ Mn scattering of spin-up and spin-down polarized electrons off Mn (the $3d^5$ electrons are assumed to be spin-up polarized, for the sake of certainty). The results are self-explanatory. Note how strong are quantitative and qualitative differences between $e^+ +$ Mn and $e^- +$ Mn scattering calculated in any of the utilized approximations.

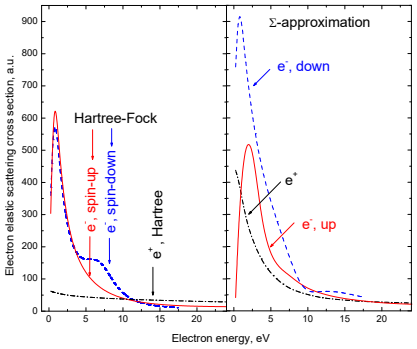

Fig. 1: $e^+ +$ Mn and $e^- +$ Mn elastic scattering cross sections, calculated in the spin-polarized Hartree and Hartree-Fock approximations, respectively, and in the multielectron Σ-approximation (see main text), as marked. In the Σ-approximation, perturbation of only 4*s*-electrons of Mn by incident $e^\pm$ was accounted in the present calculation.

V. K. D. acknowledges a travel support by the University of North Alabama Research Committee.

References

[1] M. Ya. Amusia, N. A. Cherepkov, L. V. Chernysheva, and S. G. Shapiro, J. Phys. B, **9**, L531 (1976).
[2] M. Ya. Amusia, V. K. Ivanov, and V. K. Dolmatov, Sov. Phys. - JETP **58**, 67 (1983).
[3] V. K. Dolmatov, M. Ya. Amusia, and L. V. Chernysheva, Phys. Rev A **88**, 042706 (2013).
[4] V. K. Dolmatov, Phys. Rev. A **96**, 052704 (2018).

[*]Corresponding author: vkdolmatov@una.edu
[†]Corresponding author: amusia@012.net.il
[‡]Corresponding author: larissa.chernysheva@mail.ioffe.ru

A – 27

Experimental and Calculated Lifetimes for highly excited levels in Nb^+

L. Engström[1*], H. Lundberg[1], H. Nilsson[2], H. Hartman[2,3], V. Fivet[4], P. Palmeri[4], P. Quinet[4,5]

1. Department of Physics, Lund University, P.O. Box 118, S-221 00 Lund, Sweden
2. Lund Observatory, Lund University, P.O. Box 43, S-221 00 Lund, Sweden
3. Material Sciences and Applied Mathematics, Malmö University, 20506 Malmö, Sweden
4. Physique Atomique et Astrophysique, Université de Mons - UMONS, 20 Place du Parc, B-7000 Mons, Belgium
5. IPNAS, Université de Liège, B15 Sart Tilman, B-4000 Liège, Belgium

We report experimental lifetimes for 10 highly excited levels in Nb II between 68000 and 73200 cm^{-1} [1], from an ongoing study. The lifetimes were obtained by the time-resolved laser-induced fluorescence technique on ions produced by laser ablation from an Nb target. To reach these high energies we employed a two-step laser excitation scheme. The experimental set-up is described in detail in [2, 3]. In this case, the first laser excited different levels in the odd $3d^3(^4F)5p\ ^5G$ term, around 35000 cm^{-1}, from which the second laser reached the investigated even levels in the $3d^3(^4F)5d$ and 6s configurations. The experimental lifetimes are compared with preliminary theoretical values obtained with a relativistic Hartree-Fock method that includes core polarization.

References

[1] A. N. Ryabtsev, S.S. Churilov and U. Litzén, Physica Scripta **62**, 368 (2000).
[2] L. Engström, H. Lundberg, H. Nilsson, H. Hartman and E. Bäckström, A&A, 570, A34 (2014).
[3] H. Lundberg *et.al.* MNRAS **460,** 356 (2016).

*Corresponding author: lars.engstrom@fysik.lth.se

A – 28

Intense molecular beams to test fundamental physics

P. Aggarwal*[1], H. L. Bethlem[2], A. Borschevsky[1], M. Denis[1], K. Esajas[1], P. A. B Haase[1], Y. Hao [1], S. Hoekstra[1], K. Jungmann[1], T. Meijknecht[1], M. Mooij[2], R. G. E Timmermans[1], W. Ubachs[2], L. Willmann[1], A. Zapara[1]

1. Van Swinderen Institute for Particle Physics and Gravity (VSI), University of Groningen, The Netherlands and Nikhef, National Institute for Subatomic Physics, Science Park 105, 1098 XG Amsterdam, The Netherlands

2. Laser lab, Department of Physics and Astronomy, Vrije Universiteit, De Boelelaan 1081, 1081 HV Amsterdam, The Netherlands

Advances in the production and cooling of molecules have given an impetus to the search for the electric dipole moment (EDM) of the electron in the past decade (see Table 1). This has enabled the testing of beyond the Standard Model (BSM) theories upto an energy scale of 1 TeV [1]. Future experiments hold potential to test BSM theories at even higher energy scales.

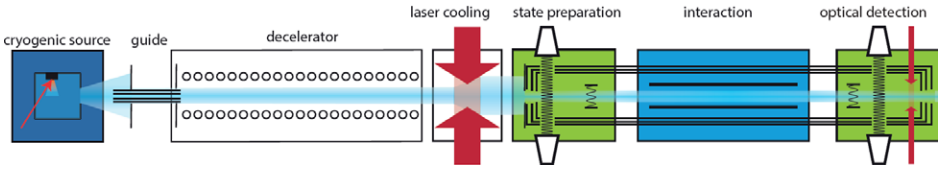

Fig. 1: Planned setup for the electron EDM search using a BaF molecular beam

Our group is starting an experiment [2] to measure the electric dipole moment (EDM) of the electron using a cold, slow and intense barium fluoride molecular beam, the experimental layout is depicted in Fig. 1. We plan to Stark decelerate and laser cool the cryogenic barium fluoride molecular beam. The molecule will be prepared in a superposition of two hyperfine states and be made to interact with an electric field inside the interaction zone. The two hyperfine states develop a phase difference which is directly proportional to the electron EDM.

Table 1: eEDM experiments; currently with the best upper bounds on the electron EDM

Molecule	eEDM upper bound (in e·cm)
ThO (Harvard/Yale University)	8.7×10^{-29} [1]
HfF^+ (JILA)	1.3×10^{-28} [3]
YbF (Imperial College)	1.05×10^{-28} [4]

I will present the work done on the first part of the experiment, which is the beam production. To start with, we are developing a cryogenic and supersonic molecular beam source. The beam from a cryogenic source is slower and denser compared to the beam from a supersonic source. The cryogenic source is under construction and will be coupled to the decelerator according to the planned setup. The supersonic source will be used to perform spectroscopy on barium fluoride molecules and to explore the best possible rotational states for laser cooling. We built a supersonic source which is a combination of pulsed even lavie valve [5] with laser ablation. I will present the optimization results on strontium fluoride molecules from this source.

To sum up, I will present the motivation for eEDM searches, details of our planned experiment and my own work in the construction and optimization of the supersonic source.

References

[1] The ACME Collaboration, J. Baron et al. *Order of magnitude smaller limit on the electric dipole moment of the electron.* Science 343, p. 269-272 (2014)

[2] P. Aggarwal et al. *Measuring the electric dipole moment of the electron in BaF*, arxiv: 1804.10012

[3] William B. Cairncross et al. *Precision measurement of the Electron's Electric Dipole Moment using trapped molecular ions.* PRL 119, 153001 (2017)

[4] J.J Hudson et al. *Improved measurement of the shape of the electron.* Nature 473, 493(2011)

[5] U. Even. *Pulsed Supersonic beams from high pressure source: Simulation results and Experimental Measurements.* Advances in Chemistry, vol. 2014 (2014), pp. 1-11

*Corresponding author: p.aggarwal@rug.nl

Non-adiabatic effects in the $c^3\Sigma^+_\Omega$ state of the LiK, LiRb, and LiCs molecules: homogeneous and heterogeneous perturbations

S.V. Kozlov[*1], **E.A. Bormotova**[1]
1. Chemistry Department, Lomonosov Moscow State University, Moscow 119991, Russia

Energetic and dynamic properties of rovibronic levels of electron-excited states can not be properly described without taking non-adiabatic interactions into account [1]. The non-adiabatic matrix elements (such as spin-orbit or *L*-coupling functions) can be computed using high level *ab initio* methods with an accuracy of 5-10 %. As a result, these *ab initio* matrix elements are widely used for modelling of energetic and dynamic properties and as an initial estimate for direct deperturbation treatment.

In this work, we systematically investigate the influence of both homogeneous spin-orbit and heterogeneous electron-rotational interactions on the $c^3\Sigma^+_\Omega$ state of the LiK, LiRb, and LiCs molecules using *ab initio* calculations. According to the selection rules [1], the $c^3\Sigma^+$ state is perturbed by the $^1\Pi$ and $^3\Pi$ states. Their corresponding non-adiabatic matrix elements between states converging to the second and third dissociation limits are calculated as follows: The small-core effective core potentials (ECPs) with 9 electrons (1 valence + 8 subvalence) are used for K, Rb, and Cs while Li is described using an ECP with a single valence electron [2]. The internally contracted multi-reference configuration interaction (MRCI) method with preliminary state-averaged complete active space self-consistent field (SA-CASSCF) optimization is used to compute the potential energy curves as well as non-adiabatic matrix elements. Core polarization effects are taken into account using *l*-independent core polarization potentials (CPPs) [3]. It is found that electron-rotational effects are stronger than the spin-orbit effects in the case of LiK, have a same magnitude in the case of LiRb, and are much weaker in the case of LiCs. However, both interactions should be taken into account for a precise description of rovibronic level properties for each molecule. The energetic levels of the $c^3\Sigma^+_\Omega$ state are affected with regular and local perturbations. For the regularly perturbed low-lying levels of $c^3\Sigma^+_\Omega$ the Van Vleck perturbation theory is applied to take interactions with the $^{1,3}\Pi$ states into account while Ω-components of the state are treated explicitly using only the Coupled Channels method. On the other hand, strong local perturbations in the $c^3\Sigma^+ - b^3\Pi$ crossing region are described using the Coupled Channels method.

The study was funded by RFBR according to the research project N 18-33-00753.

References

[1] H. Lefebvre-Brion and R. W. Field, *The Spectra and Dy- namics of Diatomic Molecules: Revised and Enlarged Edition*, Academic Press, 2004.
[2] M. M. Hurley, L. F. Pacios, P. A. Christiansen, R. B. Ross and W. C. Ermler, J. Chem. Phys., **84**, 6840–6853 (1986).
[3] W. Muller, J. Flesch and W. Meyer, J. Chem. Phys., **80**, 3297–3310 (1984).

[*]Corresponding author: sevlakoz@phys.chem.msu.ru

A – 30

Calculations of line-shape parameters from first principles in the CO-N_2 system

H. Jóźwiak[*1], **H. Cybulski**[1], **F. Thibault**[2], **N. Stolarczyk**[1], **P. Wcisło**[1]

1. Faculty of Physics, Astronomy and Applied Informatics, Nicolaus Copernicus University in Toruń, Grudziadzka 5, 87-100 Toruń, Poland
2. Institut de Physique de Rennes, UMR CNRS 6251, Universite de Rennes 1, Campus de Beaulieu, Bât.11B, F-35042 Rennes, France

Collisional line-shape effects play an important role in optical spectroscopy. Molecular collisions manifest as a perturbation of the optical line shapes. Proper treatment of these effects is important to reach high accuracy in spectroscopy-based optical metrology [1,2]. The CO-N_2 system is of particular importance for terrestrial atmospheric measurements. Here we report the first line-shape parameters for this system based on quantum scattering calculations performed on an accurate *ab initio* potential energy surface (PES) [4].

The four-dimensional PES [4], with the interatomic distances in N_2 and CO set to the experimental values (1.09768 and 1.128323 Å, respectively [3]) is used. The interaction energies are calculated with the coupled-cluster CCSD(T) method and Dunning's aug-cc-pVQZ basis set extended further with midbond functions for more than 10 100 *ab initio* points, corresponding to 12 values of θ_{N_2}, 13 values of θ_{CO} in a range of 0-180°, 5 values of ϕ in a range of 0-90° and 14 values of R in a range of 4-40 a_0.

The calculated PES is expanded over bispherical harmonics [5] leading to 205 radial coupling terms. The close-coupling equations are solved for a wide range of kinetic energies using the MOLSCAT code [6]. The calculations of generalized spectroscopic cross sections are performed for several purely rotational lines from the R branch. Finally, the standard pressure broadening and shifting coefficients are obtained. The data provided through this investigation can be used for upgrading the HITRAN database [7] and the HITRAN Application Programming Interface (HAPI) [8].

References

[1] L. Moretti *et al.* Phys. Rev. Lett. **111**, 060803 (2013)
[2] P. Wcisło *et al.* Phys. Rev. A **93**, 022501 (2016)
[3] H. Cybulski *et al.*, Phys. Chem. Chem. Phys., **20**, 12624 (2018)
[4] K. P. Huber and G. Herzberg, *Molecular Spectra and Molecular Structure: IV Constants of Diatomic Molecules*, Springer Berlin Heidelberg, 1979
[5] L. A. Surin *et al.*, J. Chem. Phys., **148**, 044313 (2018)
[6] J. M. Hutson and S. Green, MOLSCAT version 14, Collaborative Computational Project 6 of the UK Science and Engineering Research Council, Daresbury Laboratory, UK, 1995
[7] I. E. Gordon *et al.* J Quant. Spectrosc. Radiat. Transf. **203**, 3 (2017)
[8] R. V. Kochanov *et al.* J Quant. Spectrosc. Radiat. Transf. **177**, 15 (2016)

*Corresponding author: hubj96@gmail.com

A – 31

Line-shape parameters of the H_2-He system: *ab initio* calculations

H. Jóźwiak[*1], **F. Thibault**[2], **N. Stolarczyk**[1], **P. Wcisło**[1]
1. Faculty of Physics, Astronomy and Applied Informatics, Nicolaus Copernicus University in Toruń, Grudziadzka 5, 87-100 Toruń, Poland
2. Institut de Physique de Rennes, UMR CNRS 6251, Universite de Rennes 1, Campus de Beaulieu, Bât.11B, F-35042 Rennes, France

Hydrogen molecule is the most abundant molecule in the Universe. It is investigated in various physical fields, ranging from astrophysics and the analysis of gas giants' atmospheres [1,2], to ultra-accurate measurements in molecular spectroscopy [3,4,5], and even in the search for physics beyond Standard Model [6]. Recently [7] it was pointed out, that the available data regarding the line-shape parameters of hydrogen is rather sparse. The development of experimental techniques in molecular spectroscopy requires a sub-percent accuracy of the theoretical calculations. It is believed that fully quantum calculations, based on the *close-coupling* scheme, could fulfill such requirements.

The collisional system of hydrogen molecule and helium atom is a perfect benchmark system for performing complex, *ab initio* investigation line-shape parameters. It involves only four electrons, allowing researchers to calculate the potential energy surface of such system with highly accurate methods of quantum chemistry. Moreover, because of the small mass of the system and large rotational constant of the hydrogen molecule, the dynamical calculations can be performed in reasonable computational time.

Using the recently reported ultra-accurate potential energy surface for the H_2-He system [8], we performed *close-coupling* calculations of generalized cross sections for lines of the S and O branches. We investigated 60 lines in total, for vibrational bands from 0-0 to 0-5 and rotational levels up to j=5. Generalized spectroscopic cross sections were obtained from S-matrix elements for a wide range of kinetic energies (from 0.1 to 9000 cm^{-1}). The cross sections were later averaged over the relative speed distribution of the colliding pair, leading to the final line-shape parameters: pressure broadening and shifting coefficients and real and imaginary part of the Dicke contribution to the Hess profile. The parameters are obtained for 17 temperatures, ranging from 5 to 2000 K. This is the first complex investigation of the S and O branches in the H_2-He system using *ab initio* methods.

References

[1] W. M. Hayden Smith *et al.*, Icarus **81**, 429 (1989)
[2] K. H. Baines *et al.*, Icarus **114**, 328 (1995)
[3] S. Kassi and A. Campargue, Journal of Molecular Spectroscopy **300**, 55 (2014)
[4] S.-M. Hu *et al.*, The Astrophysical Journal **749**, 76 (2012)
[5] P. Wcisło *et al.*, Journal of Quantitative Spectroscopy and Radiative Transfer **213** 41 (2018)
[6] W. Ubachs *et al.*, Journal of Molecular Spectroscopy **320**, 1 (2016)
[7] P. Wcisło *et al.*, Journal of Quantitative Spectroscopy Radiative Transfer **177** 75 (2016)
[8] F. Thibault *et al.*, Journal of Quantitative Spectroscopy Radiative Transfer **202** 308 (2017)

*Corresponding author: hubj96@gmail.com

A – 32

Electron-Collisional Spectroscopy of Multicharged Ions in plasmas: Relativistic Energy Approach

V. Buyadzhi[*1,2]

1. Department of Mathematics, Odessa State Environmental University, L'vovskaya Street 15, 65016 Odessa, Ukraine
2. Int. Res. Centre of Quantum, Optics and Laser Physics, Odessa State Environmental University, L'vovskaya Street 15, 65016 Odessa

We have applied a generalized relativistic energy approach (REA) [1-3] combined with the relativistic many-body perturbation theory [4,5] to studying spectroscopic parameters (transition energies, oscillator strengths, collision cross-sections, collision strengths) of the few-body atomic systems (ions) in plasmas with taking into account of a shielding effect (in a Debye shielding approximation) and inter-particle correlations within many-body perturbation theory. In fact the uniform quantum energy approach is firstly used in a theory of spectra and spectral lines shape for the multicharged ions in a plasma. By introducing the Yukawa- Debye type potential, the 0-th order electronic Hamiltonian for a few-body system in a plasmas is given as :

$$H_0 = \sum_i [\alpha cp - \beta mc^2 - Z\exp(-\mu r_i)/r_i],$$

where μ is connected with the plasma parameters such as the temperature T and the charge density n as follows: $\mu \sim \sqrt{e^2 n / k_B T}$. The energy shift due to the collision is arisen at first in the second PT order in the form of integral on the scattered electron energy ε_{sc} : $\mathrm{Im}\Delta E = \pi G(\varepsilon_{iv}, \varepsilon_{ie}, \varepsilon_{in}, \varepsilon_{sc})$, where G is the squared combination of the two-particle matrix elements, which contain the amplitudes $Q_\lambda^{\mathrm{Qul}}, Q_\lambda^{\mathrm{Br}}$ (the corresponding Coulomb part $exp(i|\omega|r_{12})/r_{12}$ and the Breit part $exp(i|\omega|r_{12})\alpha_1\alpha_2/r_{12}$ (α_i are the Dirac matrices) of the inter-particle interaction). Transition probability is determined within REA [1-3].

We have carried out a studying the transition energies, oscillators strengths, collision cross-sections for a group of the low lying (plus Rydberg) transitions in spectra of the Li- and Be-like ions with a charge of a nucleus Z=26-42 and plasma parameters: density n_e= 10^{22}-10^{24}cm^{-3} and temperature T=0.5-2keV. A part of the data has been firstly presented. To test the results of calculations we have compared the obtained data for some ions with other authors' calculations (within multiconfiguration Dirac-Fock method and relativistic coupled-cluster theory) and available experimental data [6,7]. In table 1 we list our results of calculation of the energy shifts ΔE (cm^{-1}) for $2s^2$-$[2s_{1/2}2p_{1/2,3/3}]_1$ transitions for different plasma parameters. Comparison is performed with the multiconfiguration Dirac-Fock (DF) data [6]. In Table 2 we present our calculation data on oscillator strengths for the $2s^2$-$[2s_{1/2}2p_{3/2}]_1$ transition in spectra of the Be-like ions Fe and Zn for different values of the n_e (см$^{-3}$) and T (in eV)

Table 1: Energy shifts ΔE (cm^{-1}) for $2s^2$-$[2s_{1/2}2p_{3/2}]_1$ transition in spectra of the Be-like Ni for different values of n_e (см$^{-3}$), T (in keV)

n_e	10^{22}	10^{24}	10^{22}	10^{24}
kT	[6]	[6]	Our data	Our data
0.5	31.3	2639.6	33.8	2655.4
1.0	23.4	2030.6	25.7	2046.1
2.0	18.0	1597.1	20.1	1612.5

Table 2: Oscillator strengths gf for the $2s^2$-$[2s_{1/2}2p_{3/2}]_1$ transition in spectra of the Be-like ions of Fe and Zn for different values of the n_e (см$^{-3}$) and T (in keV)

n_e	10^{22}(Fe)	10^{24}(Fe)	10^{22}(Zn)	10^{24}(Zn)
kT	Our data	Our data	Our data	Our data
1.0	0.15406	0.15488	0.14356	0.14396
2.0	0.15404	0.15467	0.14355	0.14383

References

[1] A. Glushkov, and L.N. Ivanov, Phys. Lett. A **170**, 33 (1992).
[2] E.P. Ivanova, L.N. Ivanov, and L. Knight, Phys.Rev.A. **48**, 365 (1993).
[3] S. Malinovskaya, A. Glushkov, O. Khetselius *et al.*, Int.J.Quant.Chem. **111**, 288 (2011).
[4] V.V.Buyadzhi, P.A.Zaichko, O.A.Antoshkina, *et al.*, J.Phys.: Conf. Ser. **905**, 012003 (2017).
[5] V.V. Buyadzhi, P.A. Zaichko, M. Gurskaya, *et al.*, J.Phys.: Conf. Ser. **810**, 012047 (2017).
[6] Yongqiang Li, Jianhua Wu, Yong Hou, and Jianmin Yuan, J. Phys. B. **41**, 145002 (2008).
[7] M. Das, R.K. Chaudhuri, S. Chattopadhyay, Phys. Rev. A. **85**(4), 042506 (2012).

[*]Corresponding author: buyadzhivv@gmail.com

A – 33

Multi-photon spectroscopy of the Debye plasmas atomic systems in a one- and two-color laser fields

V. Buyadzhi[*1,2], **A. Kuznetsova**[1] , **A. Svinarenko**[1,2]
1. Department of Mathematics, Odessa State Environmental University, L'vovskaya Street 15, 65016 Odessa, Ukraine
2. Int. Res. Centre of Quantum, Optics and Laser Physics, Odessa State Environmental University, L'vovskaya Street 15, 65016 Odessa

The interaction of a high intensity laser field with an atomic system results in multi-photon excitation, ionization and shifts of the energy levels [1]. A great number of physically different effects occur in atomic systems (ensembles) in dependence upon a intensity, frequency, multi-colority of laser field, energy spectrum structure of an atomic system etc. In the last decade a considerable interest has attracted studying of the elementary atomic processes in plasma environments because of the plasma screening effect on the plasma-embedded atomic systems.

In this paper one-and two-color multi-photon spectroscopy of a number of transitions in a hydrogen, lithium and caesium atoms and ions (free and immersed in a Debye plasmas) is studied theoretically. The theoretical approach is based on the relativistic energy approach and relativistic operator perturbation theory [2-5]. The energy shift and width of the multiphoton resonances are calculated within an energy approach, which is based on the Gell-Mann and Low adiabatic formalism and formalism of the relativistic Green function for the Dirac equation. The plasmas medium screening effects are taken into account by introducing the Yukawa-type electron-nuclear attraction and electron-electron repulsion potentials into the electronic Hamiltonian for N-electron atom (ion) in a plasma [5-8].

The calculations have been performed for a plasmas with the typical corresponding parameters: the Debye lengths λ_D=5a.u. (solar core: temperature T=10^7K; density 10^{32} m^{-3}) and 25 a.u. (inertial confinement: temperature T=10^4K; density 10^{28} m^{-3}) . It has been quantitatively determined a variation of the multi-photon resonance enhancement frequencies in a few atomic systems (hydrogen, lithium) in dependence upon the plasmas parameters (the Debye length). For example, the corresponding values for the resonance enhancement frequencies ω_{r1}, ω_{r2} and ω_{r3} for the 1s–4f transition in the hydrogen for different Debye lengths (λ_D=5-50 a.u.) are between 0.009 and 0.023a.u. The obtained results reveal the plasma effects on the multi-photon transition amplitudes for the plasma-imbedded atoms (ions). The hydrogen plasma results are compared with the similar data, presented in [9,10].

References

[1] N. Delone, M. Fedorov, and V. Kraynov, Phys. Usp. **158**, 215 (1989); **169**, 753 (1999).
[2] A. Glushkov, and L.N. Ivanov, Phys. Lett. A **170**, 33 (1992).
[3] E.P. Ivanova, L.N. Ivanov, and L. Knight, Phys.Rev.A. **48**, 365 (1993).
[4] A.V. Glushkov, Adv. in the Theory of Quantum Systems in Chem. and Phys. (Springer) **26**, 231 (2012);
[5] V.V. Buyadzhi, Photoelectr. **21**, 57 (2013).
[6] S. Malinovskaya, A. Glushkov, O. Khetselius *et al.*, Int.J.Quant.Chem. **111**, 288 (2011).
[7] V.V.Buyadzhi, P.A.Zaichko, O.A.Antoshkina, *et al.*, J.Phys.: Conf. Ser. **905**, 012003 (2017).
[8] V.V. Buyadzhi, P.A. Zaichko, M. Gurskaya, *et al.*, J.Phys.: Conf. Ser. **810**, 012047 (2017).
[9] K.Wang, T.-S. Ho and S.-I. Chu, J. Phys. B: At. Mol. Phys. **18**, 4539 (1985);
[10] S. Paul and Y.K. Ho, J. Phys. B: At. Mol. Opt. Phys. **43**, 065701 (2010);

*Corresponding author: buyadzhivv@gmail.com

A – 34

Spectroscopy of Rydberg atoms in a Black-Body Radiation Field: Relativistic Theory of Excitation and Ionization

O. Khetselius[*1,2], V. Buyadzhi[1,2], A. Ignatenko[1,2], A. Glushkov[1,2], A. Svinarenko[1,2]

1. Department of Mathematics, Odessa State Environmental University, L'vovskaya Street 15, 65016 Odessa, Ukraine

2. Int. Res. Centre of Quantum, Optics and Laser Physics, Odessa State Environmental University, L'vovskaya Street 15, 65016 Odessa

In this paper we present the results of computing the spectra, radiation amplitudes for the Rydberg Na, K, Rb, Cs atoms, ionization rates of states with n = 10-100 in the field of blackbody radiation (BBR). The starting master method is the combined energy approach and relativistic many-body perturbation theory with the zeroth model potential and quantum defect approximation [1-5]. It provides sufficiently correct and simultaneously simplified numerical procedure to determination of the corresponding radiative transition and ionization properties. Interaction of the Rydberg atom A(nL) with the BBR induces transitions to the bound states and states of continuum: $A(nL)+\hbar\omega_{BBR} \rightarrow A^{+}+e^{-}$, where $\hbar\omega_{BBR}$- an energy of the BBR photon; A^{+} is the corresponding atomic ion and e^{-} is a free electron,which is emitted during the Rydberg atom ionization. Probability of induced BBR transition between the nlj and $n'l'j'$ states is determined by the standard radiative matrix element and number of photons for $\omega_{nn'}$, $W(nl \rightarrow n'L') = \Gamma(nL \rightarrow n'L') / [\exp(\omega_{nn'} / kT) - 1]$. A rate of ionization in the initial bound Rydberg state nl is determined by an intergral (integration is carrying out on the BBR frequency) of the kind: $\int_{|E_{nl}|}^{\infty} \sigma_{nl}(\omega)\rho(\omega,T)d\omega, \sigma_{nl}(\omega) \sim \omega[lM^2_{nl\rightarrow El-1} + (l+1)M^2_{nl\rightarrow El+1}]$, where E_{nL} –is the threshold frequency of ionization of the atom in the Rydberg state nL with the corresponding quantum defect. The calculated data (as example in table 1 there are our data on the BBR rates for Na) on the energy parameters, radiation amplitudes for RA Na, K, Rb, Cs, their ionization rates of states with n = 10-100 in the BBR field (T=300-600K) are listed and compared with available experimental data (Kleppner et al; Burkhardt et al) and some results of the alternative theories [6-9].

Table 1. Rates (s^{-1}) of BBR ionization for Na (T=300K; see text)

state/n	10	20	30	40	state/n	50	70	100
Na S	2.86	169	187	448	Na S	106	61.4	29.5
Na P	49	1207	1147	2610	Na P	576	311	141
Na D	124	1205	1038	2365	Na D	496	268	122

Analysis of the temperature dependence for the BBR-ionization of 17D Na state and the Coulomb approximation data by Kleppner etal shows that at temperatures above 150K our theory data and the Coulomb model ones very close to each other and fairly good agreement with experimental measurements, but at below 150K there is a deviation of the Coulomb model data from experimental data, while our theory gives good agreement. There are received (a part of data is firstly obtained) data for radiation amplitudes, effective lifetimes, BBR-ionization velocities for $nS_{1/2}$, $nP_{1/2,3/2}$, $nD_{3/2,5/2}$ (n=5-100) states of the Rydberg atoms Na, K,Rb, Cs, in a wide temperature interval 0-600K. It is performed a detailed comparison of some obtained data for lifetimes and BBR-ionization rates with available data of advanced quasiclassical calculations by Beterov et al, Glukhov-Ovsiannikov, model calculation results by Kleppner et al, Theodosiou et al. It is established that despite on a good agreement between experimental and theoretical (on the basis of quasiclassical and other models) there is a serious deviation these data from the experiment for a number of Rydberg states n = 25-45, which is provided by no-accounting important exchange-polarization effects, including an effect of essentially non-Coulomb grouping of Rydberg levels, pressure continuum and others. These effects are taken into account in the presented approach.

References

[1] A. Glushkov, and L.N. Ivanov, Phys. Lett. A **170**, 33 (1992).
[2] A.V. Glushkov, Adv. in the Theory of Quantum Systems in Chem. and Phys. (Springer) **26**, 231 (2012);
[3] O.Yu. Khetselius, *Progress in Theoretical Chemistry and Physics* (Springer) **26,** 217 (2013).
[4] O.Yu. Khetselius, Int. J. Quant.Chem. **109,** 3330(2009).
[5] V.V. Buyadzhi, P.A. Zaichko, M. Gurskaya, *et al.*, J.Phys.: Conf. Ser. **810**, 012047 (2017).
[6] D.Kleppner etal, Phys.Rev.A**26**, 1490 (1982).
[7] L.Lehman, J.Phys.B**16**, 2145 (1983).
[8] V. Glukhov, and D. Ovsiannikov, J.Phys. B**42**, 075001 (2009),
[9] I.Beterov etal, New J. Phys. **1**1, 013052 (2009).

[*]Corresponding author: okhetsel@gmail.com

A – 35

Effects of molecular vibrations on the binding of a positron to polyatomic molecules

Yukiumi KITA[*1], Yurika YAMADA[1], Umihiro URAKAWA[1], and Masanori TACHIKAWA[2]
1.Division of Theoretical Chemical Physics, Yokohama City University, 22-2 Seto, Kanazawa-ku, Yokohama 236-0027, Japan
2. Data Science Center, Yokohama City University, 22-2 Seto, Kanazawa-ku, Yokohama 236-0027, Japan

The positron, which is the anti-particle of the electron, is now widely used in both scientific and technological areas such as physics, chemistry, material science, medical science, and their interdisciplinary areas. The detailed mechanism of fundamental processes of positrons at a molecular level, however, still leave a great deal to be clarified, so that the understanding for the interactions between positrons and molecules is a central issue in the field of positron chemical physics.

A positron affinity (PA), which is a binding energy of a positron to a molecule, is one of the most important properties for studying a positron-molecular complex as with a pair-annihilation rate. The PA values have now been experimentally measured by Surko and co-workers for many molecular species such as hydrocarbons (alkanes, alkenes, and aromatics), alcohols, nitrile, and carbonyl compounds [1,2]. They have succeeded in revealing properties inherent in each molecule with respect to the binding of a positron, with vibrational Feshbach resonance (VFR) spectrum measurements by incident low-energy positrons. To understand such specific properties of each positron-molecular complex in more detail, theoretical analyses based on first-principles calculations must be quite useful.

Recently, we have proposed a first-principles based method that enable us to calculate whole degrees of freedom (positronic, electronic, and nuclear motions) quantum mechanically, in order to elucidate the effect of molecular vibrations on molecular positron affinities. Our method is based on both the anharmonic vibrational state theory with quantum Monte Carlo method [3], and *ab inito* multi-component molecular orbital theory [4,5] that enable us to solve the electronic and positronic wave functions simultaneously. Applying our method to some small molecules such as hydrogen cyanide (HCN) [3] and formaldehyde (CH_2O) [6] molecules, we demonstrated the effect of molecular vibrations to PA values of these molecules. For instance, we found that (i) for HCN molecule, the vibrational excitations of CN and CH stretching modes enhance the PA value compared to the value at the ground state, whereas the excitation of HCN bending mode deenhances it, and (ii) for CH_2O molecule, the vibrational excitation of C=O stretching mode enhances the PA value, whereas the excitation of CH_2 rocking mode deenhances it. We confirmed that such PA variations (enhancement or deenhancement) arise from the change in both the permanent dipole moments and dipole-polarizability by vibrational excitations. In this presentation, we also show theoretical results of H/D isotope effects on PA values of these molecules.

References

[1] G. F. Gribakin, J. A. Young, C. M. Surko, *Rev. Mod. Phys.* **82** (2010) 2557.
[2] J. R. Danielson, A. C. L. Jones, J. J. Gosselin, M. R. Natisin, and C. M. Surko, *Phys. Rev. A* **85** (2012) 022709.
[3] Y. Kita and M. Tachikawa, *Eur. Phys. J. D* **68** (2014) 116.
[4] M. Tachikawa, Y. Kita, and R. J. Buenker, *Phys. Chem. Chem. Phys.* **13** (2011) 2701.
[5] M. Tachikawa, Y. Kita, and R. J. Buenker, *New J. Phys.* **14** (2012) 035004.
[6] Y. Yurika, Y. Kita, and M. Tachikawa, *Phys. Rev. A* **89** (2014) 062711.

[*]Corresponding author: ykita@yokohama-cu.ac.jp

A – 36

Sympathetic cooling of OH^- by a laser-cooled buffer gas

M. Nötzold[1], J. Tauch[2], S. Z. Hassan[2,3], E. Endres[2], H. Lopez[2], B. Höltkemeier[2], M. Weidemüller[*2,3,4], R. Wester[†1]

1. Institut für Ionenphysik und Angewandte Physik, Universität Innsbruck, Innsbruck, Austria
2. Physikalisches Institut, Ruprecht-Karls-Universität Heidelberg, Heidelberg, Germany
3. International Max Planck Research School for Quantum Dynamics in Physics, Chemistry and Biology, Heidelberg, Germany
4. University of Science and Technology of China, Shanghai Branch, Shanghai, China

Cold molecules offer new opportunities for precision spectroscopy and for studying ultracold chemistry at temperatures close to 0 K. A common method to cool molecular ions is to confine them in high-order multipole radio frequency traps and cool them sympathetically using a cryogenic buffer gas at about 4 K [1]. In order to reach lower temperatures a laser-cooled buffer gas can be utilised, which has been demonstrated for different cationic species. We have begun to investigate the combination of laser-cooled atoms and molecular anions [2].

We have recently developed a theoretical description which predicts that efficient cooling beyond the critical atom-ion mass ratio can be achieved by a localized buffer gas cloud and/or a higher order radio frequency trap [3,4]. We developed a Hybrid Atom-Ion Trap (HAI-Trap), combining an 8-pole radio frequency trap and a Dark Spontaneous-Force Optical Trap (Dark-SPOT) to study the interaction of ultracold Rb atoms with OH^-. In our experiment we use photodetachment tomography not only to measure the spatial ion-distribution in our trap but also determine the internal temperature of the sympathetically cooled ensemble [5]. The external temperature is derived from the time-of-flight distribution of the ions extracted from the trap by comparison with numerical simulations.

In this contribution the most recent results of the observed sympathetic cooling are presented and future prospects will be given.

References

[1] R. Wester , J. Phys. B 42, 154001 (2009)
[2] J. Deiglmayr et al , Phys. Rev. A 86 , 043438 (2012)
[3] B. Höltkemeier et al , Phys. Rev. A 94, 062703 (2016)
[4] B. Höltkemeier et al , Phys. Rev. Lett . 116, 233003 (2016)
[5] R. Otto et al , Phys. Chem. Chem. Phys. 15 , 612 (2013)

*Corresponding author: weidemueller@uni-heidelberg.de
†Corresponding author: roland.wester@uibk.ac.at

On the heading error of optically pumped magnetometers operated in Earth magnetic field

G. Oelsner*[1], V. Schultze[1], R. IJsselsteijn[2], F. Wittkämper[1], R. Stolz[1]
1. Leibniz Institute of Photonic Technology, P.O. Box 100239, D-07702 Jena, Germany
2. Supracon AG, An der Lehmgrube 11, D-07751 Jena, Germany

In the context of atomic magnetometers the term "heading error" summarizes any falsification of the measured magnetic-field strength in dependence on the orientation of the pump beam direction with respect to the magnetic field B_0 to be measured. Thus, the heading error is a great challenge in the use of such detectors concerning geomagnetism. Special operational modes offering in principle tens of fT per root Hz resolution in Earth magnetic field strengths have been recently introduced [1,2]. These Light Narrowing (LN) and Light-Shift Dispersed M_z (LSD-Mz) modes require large off-resonant pumping and thus exploit large light shifts. Therefore, in our investigations of the heading error we focused on two main contributions, namely the non-linear Zeeman splitting in Earth magnetic field and the light shift.

Our experimental investigation is thus aimed for an independent estimation of both effects. The measurements were performed with setups of cesium vapour atomic magnetometers cleaned from any magnetic pollution that are rotated in a stable and uniform artificial magnetic field well shielded from the outside.

Using a glass-blown vacuum cell [3] the sole action of the non-linear Zeeman effect in the conventional M_x mode at B_0=50µT is investigated. The measured Larmor frequencies as a function of the angle between the pump laser beam direction and the magnetic field are shown in Fig. 1 for both circular polarizations. In the Light Narrowing (LN) [1] and the Light-Shift Dispersed M_z (LSD-Mz) mode [2] strong detuned pumping of a micro-fabricated Cs cell with high buffer-gas pressure is used. The orientation dependence shown in Fig. 2 is a superposition of scalar, vector and tensor light shift.

We support our experimental findings with a theoretical analysis and demonstrate that both dependencies result from the scalar product of the electric field vector of the pump laser and the dipole moment of the atoms in the magnetic field B_0. Our description is based on the modification of the transition dipole moment for different optical transitions when the orientation of the laser beam to the magnetic field is changed. In that frame, the population of the cesium atoms' ground-state levels is calculated following rate equations. This allows a qualitative description of the measured heading error due to the non-linear Zeeman effect. The light shift of the ground state levels is modified when the atomic magnetometer is rotated in the B_0 field due to the modification of interaction strengths between a single ground and different excited state levels. For parameters consistent to the experiment we achieve good quantitative agreement of the theoretical curves with the experimental results. Our analysis suggest that by the use of both circular polarizations the heading error caused by both, the non-linear Zeeman effect and the light shift, can be compensated when both, amplitude and grade of polarization, are accurately balanced between the two channels.

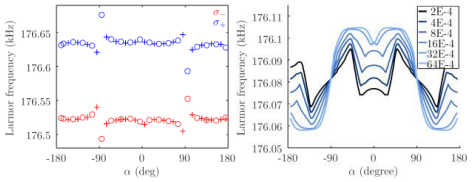

Fig. 1: Measured Larmor frequencies for both circular polarizations in dependence of the orientation angle (left) and calculated Larmor frequency for + light.

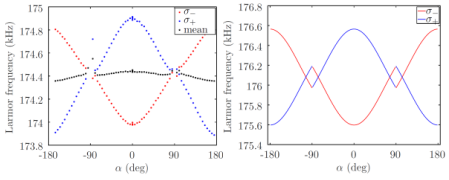

Fig. 2: Measured (left) and calculated (right) heading error caused by light shift in the LSD-Mz operational mode for both circular polarizations.

References

[1] N. Castagna *et al*., Appl. Phys. B **96**, 763 (2009).
[2] T. Scholtes *et al*., Phys. Rev. A **84**, 043416 (2011); **86**, 059904 (E) (2012).
[3] V. Schultze *et al*., Sensors **17**, 561 (2017).

*Corresponding author: volkmar.schultze@leibniz-ipht.de

A – 38

Continuum contributions to the atomic electric dipole moments

P. Syty[*1], **J.E. Sienkiewicz**[1], **G. Gaigalas**[2], **L. Radžiūtė**[2], **J. Bieroń**[3]
1. Department of Theoretical Physics and Quantum Information, Gdańsk University of Technology, Narutowicza 11/12, 80-233 Gdańsk, Poland
2. Institute of Theoretical Physics and Astronomy, Vilnius University, Saulėtekio Al. 3, 10257 Vilnius, Lithuania
3. Department of Atomic Optics, Jagiellonian University, Stanisława Łojasiewicza 11 , 30-348 Kraków, Poland

In last years the electric dipole moments (EDM) of elementary particles, nuclei, atoms and molecules have been subject of intensive experimental and theoretical studies. The importance of these studies relies in fact that if the EDM does not exist than the prediction of T, P and CP violations by unification theory is not correct. In other words eventual existence of EDM violates the CP invariants due to the CPT invariance. Significant enhancement of the electron EDM makes hopes for decisive measurements. Nevertheless, the current experimental limits significantly constrain the validity of unification theory.

The main purpose of present work was to estimate contribution of the continuum states to the atomic EDM. Nowadays, the focus is on EDM of diamagnetic atoms like Xe, Y or No, and as the example system the ^{129}Xe was chosen. The measurements of the EDM of Xe have significant potential for improvements in the experimental limit by using a nuclear spin maser technique [1], [2]. Very recent experimental studies in newly designed EDM cell indicate the possibility of improving the EDM upper limit by at least of one order in magnitude to achieve the accuracy as low as 10^{-28} $e$cm [4], while the most precise measurement of the EDM [3] gives the value of $d(^{129}\mathrm{Xe}) = (0.7 \pm 3.3 \pm 0.1) \times 10^{-27} e\mathrm{cm}$.

Discrete states of ^{129}Xe were calculated with the relativistic atomic structure package GRASP2K [5], based on multiconfiguration Dirac-Hartree-Fock (MCDHF) approach. Continuum states were calculated using the COWF code, prepared in frames of the RATIP package [6], adapted to the GRASP2K. Let us stress, that the contribution to EDM coming from continuum electrons is calculated for the first time in a variational approach. To ensure correctness of our approach we get detailed insight into behavior of electron wave function while passing through the ionization energy.

In the next step, EDM arising from (P;T)-odd e-N tensor-pseudotensor and pseudoscalar-scalar interactions, nuclear Schiff moment, interaction of electron electric dipole moment with nuclear magnetic moments, and atomic electric dipole matrix elements, were calculated for both discrete and continuum states (see Fig. 1).

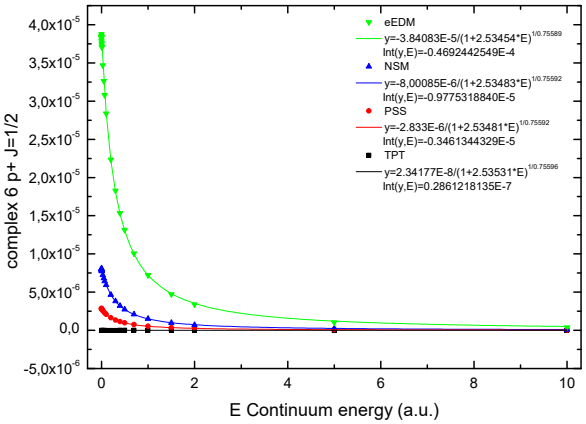

Fig. 1: Dependence of EDM values for all interaction from continuum energy (in a.u.), for p+ orbital in DF approximation, state of ground configuration for Xe^+ is $J = 1/2$ with fitted equations and values of integrals.

The results show small contribution of continuum state electron to the final EDM value.

References

[1] T. Inouea *et al.*, Phys, Proc. **17**, 100 (2011)
[2] T. Furukawa *et al.*, J. Phys.: Conf. Ser. **312**, 102005 (2011)
[3] M.A. Rosenberry, T. E. Chupp, Phys. Rev. Lett. **86**, 22 (2001)
[4] F. Kuchler *et al.*, Hyperfine Interactions **237**, 95 (2016)
[5] P. Jönsson, G. Gaigalas, J. Bieroń, C. Froese Fischer, I.P. Grant, Comp. Phys. Comm. **184**, 2197 (2013)
[6] S. Fritzsche, Comp. Phys. Comm. **183**, 1525 (2012)

*Corresponding author: pawel.syty@pg.edu.pl

Dissociation suppression in methylated nitroimidazole anions

F. Kossoski[1,2] **M. T. do N. Varella**[*3]
1. Institute of Physics , State University of Campinas, 13083-859 Campinas, Sãoo Paulo, Brazil
2. Aix Marseille Université, CNRS, ICR, Marseille, France
3. Institute of Physics, University of São Paulo, Rua do Matão 1731, 05508-090, São Paulo, Brazil

Nitroimidazoles are efficiently decomposed by slow electrons. This process, known as dissociative electron attachment (DEA), involves the formation of transient negative ions (resonances) that undergo dissociation reactions. Electron-induced dissociation is believed to account, at least partially, for the bioactivity of nitroimidazoles as radiosensitizers, *i.e.*, drugs that can enhance the efficiency of radiation or havy-ion treatments of tumour cells [1][2].

The DEA data recently reported by Tanzer *et al*. [3] revealed that 4-nitroimidazole (4NI) has a rich fragmentation branching below 2V, including single-bond cleavages and more complex reactions. Even at those low collision energies, many dissociation channels were observed, producing the H, OH and NO2 radicals, in addition to HNO_2 and CN^-. The most striking result was the full suppression of those reactions in 1-methyl-4-nitroimidazole (1M4NI), along with a significant quenching of the dissociation reactions induced by faster electrons, with incident energies around 3 eV. The DEA suppression was also observed for 1-methyl-5-nitroimidazole (1M5NI) in subsequent experiments [4]. As the DEA yields showed a series of narrow peaks for H abstraction below 1 eV, Tanzer *et al*. proposed that vibrational Feshbach resonances (VFRs) would trigger the H-loss reaction, as expected from previous measurements, and the authors further considered that VFRs would also be doorways for more complex reactions, involving the cleavage of the C4–NO_2 bond.

We report a theoretical study on the anion state spectra of 4NI, 5-nitroimidazole (5NI), 1M4NI, and 1M5NI, obtained from electron scattering and bound state calculations. Our results point out that five anion states would trigger the DEA dynamics in 4NI, namely a dipole bound state (DBS), a valence bound state, and three resonances, the latter formed by electron attachment into either π^* or σ^* virtual orbitals. While the DBS binding energy and the fundamental frequency of the ν_{NH} stretch mode were found consistent with the VFR progression for H elimination, as previously proposed, our computations strongly suggest that the formation of a π^* resonance would initiate the cleavage of both the N1–H and C4–NO_2 bonds around 1.5 eV. The lifetime estimates, obtained with the Schwinger Multichannel Method [5], indicate that the methylated species (1M4NI and 1M5NI) would have shorter-lived π^* resonances than 4NI and 5NI. The shorter lifetimes, which favour autoionization against vibrational relaxation in the methylated forms, would account for the suppression of DEA reactions around 1.5 eV.

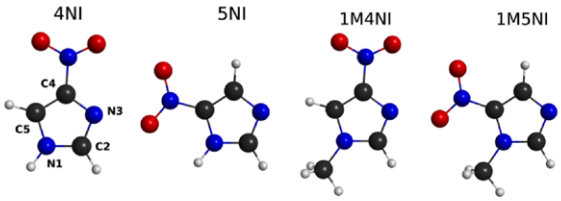

Fig. 1: Structures of 4NI, 5NI, 1M4NI and 1M5NI. The hydrogen atoms are indicated in white, carbon atoms in grey, nitrogen atoms in blue and oxygen atoms in red. The labelling of the ring positions is indicated for 4NI.

References

[1] P. Wardman, Clin. Oncol. (R. Coll. Radiol). **19**, 397 (2007).
[2] J. Overgaard, Radiother. Oncol., **100**, 22 (2011).
[3] K. Tanzer,L. Feketeová, B. Puschnigg, P. Scheier, E. Illenberger, S. Denifl, Angew. Chem. Int. Ed., **53**, 12240 (2014).
[4] K. Tanzer,L. Feketeová, B. Puschnigg, P. Scheier, E. Illenberger, S. Denifl, J. Phys. Chem. A, **119**, 6668 (2015).
[5] R. F. Costa, M. T. do N. Varella, M.H. F. Bettega, M. A. P. Lima, Eur. Phys. J. D, **69**, 159 (2015).

*Corresponding author: mvarella@if.usp.br

Ab Initio Collisional Calculations For Providing The Line-Shape Parameters For The HITRAN Database.

P.Wcisło[1], F. Thibault[2], N. Stolarczyk*[1], H. Jóźwiak [1], M. Słowiński [1], M. Konefał [1,3,4], S. Kassi [3,4], A. Campargue [3,4], Y. Tan [5,7], J. Wang [5], A.-W. Liu [5], S.-M. Hu [5], K. Patkowski [6], R. Ciuryło [1], D. Lisak [1], R.V. Kochanov [7], I.E. Gordon [7]

1. Institute of Physics, Faculty of Physics, Astronomy and Informatics, Nicolaus Copernicus University, Grudziadzka 5, 87-100 Torun, Poland
2. Institut de Physique de Rennes, UMR CNRS 6251, Université de Rennes 1, Campus de Beaulieu, Bât.11B, Rennes F-35042, France
3. University of Grenoble Alpes, LIPhy, F-38000 Grenoble, France
4. CNRS, LIPhy, F-38000 Grenoble, France
5. Hefei National Laboratory for Physical Sciences at Microscale, iChEM, University of Science and Technology of China, Hefei, 230026 China
6. Department of Chemistry and Biochemistry, Auburn University, Auburn, AL 36849 USA
7. Atomic and Molecular Physics Division, Harvard-Smithsonian Center for Astrophysics, Cambridge, Massachusetts 02138, USA

Molecular collisions are manifested as a perturbation of the shapes of molecular optical resonances. Therefore, on the one hand, the line-shape analysis of accurate molecular spectra constitutes an important tool for studying quantum scattering and testing ab initio molecular interactions [1]. On the other hand, the collisional effects can deteriorate the accuracy of atmospheric measurements of the Earth and other planets, modify the opacity of the exoplanetary atmospheres as well as influence the accuracy in optical metrology based on molecular spectroscopy [2],[3]. Recently a new relational structure has been introduced to the most extensively-used line-by-line spectroscopic database HITRAN [4],[5], enabling the collisional, beyond-Voigt line-shape effects to be represented. It is, however, extremely challenging to populate the entire database with purely experimental parameters for all the molecular transitions and thermodynamical conditions (all the bands, branches and temperature ranges). We demonstrate a new methodology of generating a comprehensive dataset of the beyond-Voigt line-shape parameters from fully ab initio quantum-scattering calculations. We also demonstrate first such a complete dataset for the benchmark system of helium-perturbed H_2 line. We provide the temperature dependences for the pressure broadening and shift parameters, as well as for the Dicke parameter using generalized spectroscopic cross sections resulting from quantum scattering calculations on accurate ab initio potential energy surfaces. The results are consistent with the recently adapted HITRAN parameterisation of the Hartmann-Tran profile [4]. The calculations and methodology are also validated on the ultra-accurate experimental data of the H_2-He system.

References

[1] P. Wcisło et al. Phys. Rev. A **91**, 052505, (2015)
[2] L. Moretti et al. Phys. Rev. Lett. **111** 060803 (2013)
[3] P. Wcisło et al. Phys. Rev. A **93**, 022501, (2016)
[4] P. Wcisło et al. J. Quant Spectrosc. Radiat. Transfer **177**, 75-91, (2016)
[5] I. E. Gordon et al. J. Quant Spectrosc. Radiat. Transfer **203**, 3 – 69. 3, (2017)

*Corresponding author: 280301@stud.umk.pl

A – 41

Ro-vibrational cooling of diatomic molecules

T. Urbańczyk*, **J. Koperski**
Smoluchowski Institute of Physics, Jagiellonian University, ul. Łojasiewicza 11, 30-348 Kraków, Poland

We present a method of ro-vibrational cooling of diatomic molecules which initially are in an excited ro-vibrational level of its ground electronic state. This contribution is an extension of the method reported in [1]. The method employs an example of cooling scheme for Cd_2 using the $X^1 0_g^+ (5^1S_0)$ and $c^3 1_u (5^3P_2)$ states. The cooling relies on a successive decreasing of population of υ and J levels using a series of laser-induced excitations of the molecule: from a selected (υ'',J'') ro-vibrational level in the $X^1 0_g^+$ to ($\upsilon' = \upsilon'' - 1$, $J' = J'' - 1$) ro-vibrational level in the $c^3 1_u$ state, and fluorescence decays to the ground state.

Because distribution of Franck-Condon factors (F-Cf) for fluorescence from the $c^3 1_u$ to the $X^1 0_g^+$ state strongly prefers transitions without changing of υ, a vibrational cooling occurs i.e. υ'' is reduced in excitation to the $c^3 1_u$ state. Due to the fact, that the molecules are excited while decreasing of J and, during fluorescence from the $c^3 1_u$ state, the $\Delta J = -1, 0, 1$ selection rule is valid, also rotational cooling occurs (see Fig. 1). In Fig. 2 we present result of rotational cooling for group of 16 000 Cd_2 molecules, which initially occupy a group of ($J'' = 2, 3, 4, 5, 6, 7, 8$) rotational levels in $\upsilon'' = 4$ vibrational level. We will present a similar process applied for Yb_2 or Hg_2.

Support from the National Science Centre Poland under grant number UMO-2015/17/B/ST4/04016 is acknowledged.

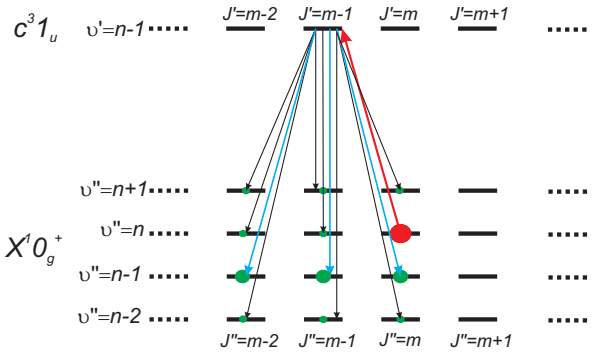

Fig. 1: Schematic representation of one excitation-fluorescence step in the ro-vibrational cooling process. Initially, the large number of molecules occupy ($\upsilon'' = n$, $J'' = m$) ro-vibrational level in the $X^1 0_g^+$ state (red full circle). The molecules are excited to ($\upsilon' = n - 1$, $J'' = m - 1$) level in the $c^3 1_u$ state by laser radiation (red arrow). Due to the fluorescence from the excited state, the molecules are transferred (black arrows) to different ro-vibrational levels in the $X^1 0_g^+$ state (green full circles). Due to the distribution of F-Cf, the majority of molecules is transferred to $\upsilon'' = n - 1$ vibrational level (blue arrows).

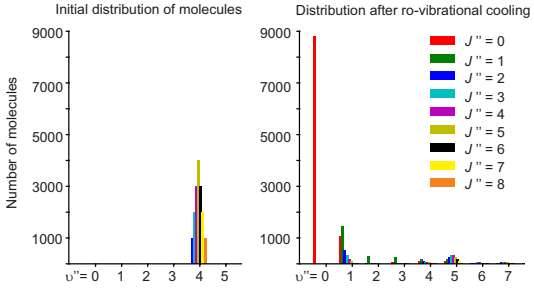

Fig. 2: Result of ro-vibrational cooling of group of 16 000 Cd_2 molecules using the $c^3 1_u \leftrightarrow X^1 0_g^+$ transition. After cooling process, 55% of molecules is in the desired ($\upsilon'' = 0$, $J'' = 0$) level.

References

[1] T. Urbańczyk, M. Strojecki, J. Koperski, *Mol. Phys.* (2018), in print.

*Corresponding author: tomek.urbanczyk@uj.edu.pl

Spectroscopy of CdRg complexes using OODR method: New analysis of the $E^3\Sigma^+_{1\,out}(6^3S_1)$ Rydberg state potential in CdKr

T. Urbańczyk*, **J. Koperski**
Smoluchowski Institute of Physics, Jagiellonian University, ul. Łojasiewicza 11, 30-348 Kraków, Poland

In molecular spectroscopy, the low-lying Rydberg electronic state can be excited using so-called optical-optical double resonance (OODR) method. In the method, two laser beams are used to excite the selected Rydberg state from the ground *via* the intermediate state. We have used this method to study the energy structure of the $E^3\Sigma^+_{1\,out}(6^3S_1) \leftarrow B^3\Sigma^+_1(5^3P_1), \upsilon'' = 6$ bound $\leftarrow$ bound and free $\leftarrow$ bound transitions in CdKr van der Waals (vdW) complex produced employing a supersonic molecular beam technique and high-temperature high-pressure pulsed source [1]. Here, we present the analysis of new laser induced fluorescence (LIF) excitation spectrum of the studied transition (see Fig. 1) as well as new characteristics of the $E^3\Sigma^+_{1\,out}$ Rydberg state potential obtained using e.g. inverted perturbation approach (IPA) methodology.
Support from the National Science Centre Poland under grant number UMO-2015/17/B/ST4/04016 is acknowledged.

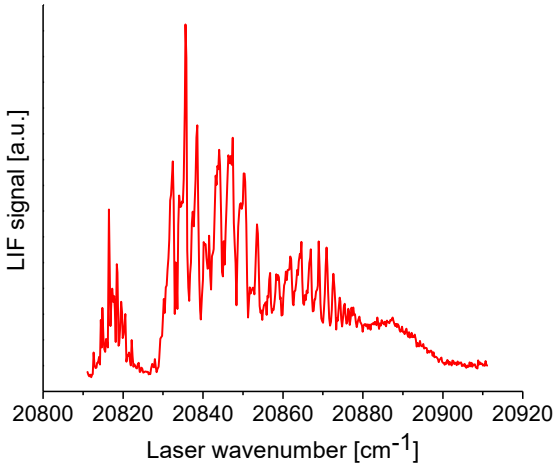

Fig. 1: Experimental LIF excitation spectrum of the $E^3\Sigma^+_{1\,out} \leftarrow B^3\Sigma^+_1, \upsilon'' = 6$ transition in CdKr vdW complex.

References

[1] T. Urbańczyk and J. Koperski, *Rev. Sci. Instrum.* **83**, 083114 (2012).

*Corresponding author: tomek.urbanczyk@uj.edu.pl

Propagation of short twin pulses in four-wave mixing in hot Potassium vapor

I. S. Radojičić[L], M. Ćurčić[1], B. Zlatković[1], Ž.Nikitović[1], A. Krmpot[1], D. Arsenović[1], and B. Jelenković[1]
1. Photonic Center, Institute of physics, University of Belgrade, Belgrade, Pregrevica 118, 11000 Belgrade, Serbia

In this work we investigate, theoretically and experimentally, slowing of light pulses due to four wave mixing (FWM) in hot Potassium. Slow light is valuable for all signal processing, but in order to be really useful, the system has to produce fractional delays large than one, with the small broadening and absorption. Absorption and distortion are alleviated in the system with the gain, like in FWM, which opens possibilities for stacking many delay lines. Special feature of FWM is simultaneously slowing of incident probe pulse and a new beam that emerges from the vapor at quite different frequency, a conjugate beam.

We use off- resonant double Lambda scheme for FWM to investigate propagation of 80 ns probe pulse, and generation and propagation of conjugate pulse, which typically separates from the probe pulse at the end of the cell. This atomic scheme was used before to investigate slow light in Rb [1], Na [2]. The model derives atomic populations, coherences, pulse gains and wave forms solving first optical Bloch equations, and then phenomenological Maxwell equations, taking into account Doppler broadening of transitions. In the experiment, we tune probe laser to Raman resonance with the pump laser by a pair of AOMs, and generate probe Gaussian 80 ns pulse, by EOM before it is combined with the pump laser and send to the hot K vacuum vapor cell. Group velocities were measured by recording the arrival times of the probe and the conjugate relative to the reference pulse.

Potassium has smaller hyperfine structure, smaller than Doppler width then other alkali atoms. It wasn't so far used for slowing light pulses. Comparison between theory and experiment provides more insights into the dynamics of pulses propagation through this FWM medium. Agreement between theory and experiment, both qualitative in terms of similar pulse waveforms after the cell, and quantitative in terms of fractional delays and broadening, revels proper values of fitted parameters, like collisional and transit time dephasing. Moreover, by following location of the small perturbation (placed at the peak of input probe pulse) vs the location of the pulse peak at different distances in the vapor from the entrance, we can follow behavior of the probe pulse in the cell. We show that depending on the FWM parameters, pulses behave quite differently, in some cases showing complete disappearance, and revival of the pulse later in time.

All our results are given as a function of one photon pump detuning, two Raman pump-probe detuning, gas density, laser power and Rabi frequency.

References

[1] V. Boyer, C. F. McCormick, E. Arimondo, and P. D. Lett, Phys. Rev. Lett. **99**, 143601 (2007).
[2] J. Okuma, N. Hayashi, A. Fujisawa, and M. Mitsunaga, Opt. Lett. 34, 1654–1656 (2009).

Strong-field atomic dynamics numerical simulations within Two- and Three- Active Electron models

Dmitry K. Efimov[*1], **Jan H. Thiede**[2], **Artur Maksymov**[1], **Jakub S. Prauzner-Bechcicki**[1], **Bruno Eckhardt**[2], **Alexis Chacon**[3,4], **Maciej Lewenstein**[4,5], **Jakub Zakrzewski**[1,6],

1. Instytut Fizyki imienia Mariana Smoluchowskiego, Uniwersytet Jagiellonski, Lojasiewicza 11, 30-348 Krakow, Poland
2. Philipps-University Marburg, Biegenstrasse 10, 35037 Marburg, Germany
3. Los Alamos National Laboratory, New Mexico 87544, USA
4. ICFO-Institut de Ciencies Fotoniques, The Barcelona Institute of Science and Technology, 08860 Castelldefels (Barcelona), Spain
5. ICREA, Passeig de Lluis Companys, 23, 08010 Barcelona, Spain
6. Mark Kac Complex Systems Research Center, Jagiellonian University, Lojasiewicza 11, 30-348 Krakow, Poland

The interaction of a strong femtosecond laser pulse with atoms and molecules yields ionization of them and generates light characterized by a very wide spectral range (High Harmonics Generation). Theoretical descriptions of corresponding effects and phenomena are frequently compared not with the results of experiments, but with that of numerical simulations. Recently a number of efficient and trusted tools for making simulations in the framework of the Single Active Electron approximation were developed [1,2], they work well for a range of problems, but can not account for multi-electron dynamics. The full-dimensional scheme for the two electron problem was developed by Taylor et al [3], but was too computationally demanding to be used for practical cases of IR carrier laser frequencies. Therefore, usually one is concerned with reduced dimensionality models that are nevertheless able to bring light to a number of strong-field processes. The reasonable question is to which degree one can trust the results obtained with exploiting them.

Here we investigate the performance of several reduced dimensionality models. Results of quantum mechanical simulations are compared with those of the classical ensemble method. First, we run and analyze the two numerical schemes within the two-active-electron approximation: the Center-of-Mass and Eckhardt-Sacha models [4].Two important kinds of experimentally measurable parameters are considered: ionization yields and momenta distribution. Second, we perform the first grid computational scheme for three electron dynamics in the IR field based on the Eckhardt-Sacha model [5]. Advances of all the schemes are discussed and major results obtained are presented.

References

[1] Bauer, D. and Koval, P., 2006. *Qprop: A Schrödinger-solver for intense laser–atom interaction.* Computer physics communications, 174(5), pp.396-421.
[2] Patchkovskii, S. and Muller, H.G., 2016. *Simple, accurate, and efficient implementation of 1-electron atomic time-dependent schrödinger equation in spherical coordinates.* Computer Physics Communications, 199, pp.153-169.
[3] Parker, J.S., Moore, L.R., Dundas, D. and Taylor, K.T., 2000. *Double ionization of helium at 390 nm.* Journal of Physics B: Atomic, Molecular and Optical Physics, 33(20), p.L691.
[4] Efimov, D.K., Maksymov, A., Prauzner-Bechcicki, J.S., Thiede, J., Eckhardt, B., Chacon, A., Lewenstein, M. and Zakrzewski, J., 2018. *Restricted space ab initio models for double ionization by strong laser pulses.* arXiv preprint arXiv:1803.08364.
[5] Thiede, J.H., Eckhardt, B., Efimov, D.K., Prauzner-Bechcicki, J.S. and Zakrzewski, J., 2018. *Strong field three electron ionization-ab initio time-dependent study.* arXiv preprint arXiv:1804.05773.

*Corresponding author: dmitry.efimov@uj.edu.pl

Measurements of the longitudinal relaxation of a large potassium cell with anti-relaxation coating

Yucheng Yang[1], **Wenhao Li**[1], **Xiang Peng**[1], **Jingbiao Chen**[1], **Hong Guo**[*1]

1. State Key Laboratory of Advanced Optical Communication Systems and Networks, School of Electronics Engineering and Computer Science, and Center for Quantum Information Technology, Peking University, Beijing 100871, China

Alkali metal atom cells with anti-relaxation wall coating, which have a long ground-state spin polarization lifetime, are widely used in various atomic physics experiments. The relaxation properties of small alkali metal atom cells have been studied extensively, while those of cells with comparably larger size (diameter > 10 cm), which are thought to have a better performance due to longer mean free paths for atoms, have not been explored sufficiently.

We manufactured a potassium cell with a diameter of 16 cm and measured the pump power and probe power dependence of relaxation properties using a modified "relaxation in the dark" (RID) method [1] (see in Fig. 1). The pump beam and the probe beam were generated by a 770 nm (K D1 line) laser whose frequency is set at the Doppler boradened $F_g = 2 \rightarrow F_e = 1, 2$ transitions.

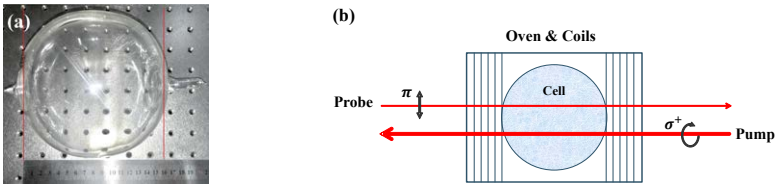

Fig. 1: The K cell with a diameter of 16 cm (a) and the experimental setup of the modified "RID" method (b).

According to the previous work [2], when measuring the pump power dependence of relaxation properties, in order to keep a proper balance between a higher signal-to-noise ratio (SNR) and lower probe-beam-induced relaxation, the probe power was set to about 6 μW. We can see from Fig. 2(a) that when the pump power is below 70 μW, the atomic polarization increases with pump power, so the amplitude of the optical rotation signal will increase and reach its maximum. When the pump power is above 70 μW, the amplitude will decrease, which may be caused by some nonlinear effects. Besides, we can observe that the relaxation rate stays flat at about 1 s^{-1} almost throughout the pump power range explored in the experiment.

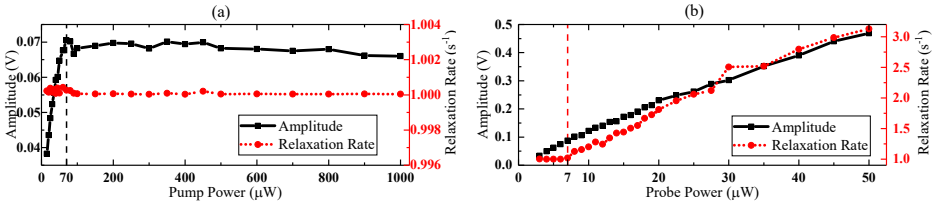

Fig. 2: The pump power dependence (a) and the probe power dependence (b) of relaxation properties.

When measuring the probe power dependence, the pump power is set at 215 μW, where both signal amplitude and relaxation rate are insensitive to the power fluctuation, to maximize the amplitude of the optical rotation signal. The amplitude will increase with the probe power as we can see in Fig. 2(b). For the large potassium cell, its relaxation rate increases linearly with the probe power when the probe power is above 7 μW.

In conclusion, for the large K cell, its relaxation rate is 1 s^{-1} when the probe power is below 7 μW and not affected by the pump power, while the amplitude of optical rotation signal will increase with the pump power when the pump power is below 70 μW and decrease with the pump power when the pump power is above 70 μW.

References

[1] M. Graf, D. Kimball, S. Rochester, K. Kerner, C. Wong, D. Budker, E.Alexandrov, M. Balabas, and V. Yashchuk, Phys. Rev. A **72**, 023401 (2005).

[2] W. Li, M. Balabas, X. Peng, S. Pustelny, A. Wickenbrock, H. Guo, and D. Budker, Journal of Applied Physics **121**, 063104 (2017).

*Corresponding author: hongguo@pku.edu.cn

New odd-parity electronic levels in the holmium atom

B. Furmann*, **D. Stefanska, M. Suski, and S. Wilman**
Division of Quantum Engineering and Metrology, Institute of Materials Research and Quantum Engineering, Faculty of Technical Physics, Poznan University of Technology, Piotrowo 3, 60-965 Poznań, Poland

Electronic level system in the holmium atom is characteristic for the lanthanides. Collapse of the $4f$ orbital results in the occurrence of numerous electronic levels with close energy values. Due to this fact, along with the extraordinary magnetic properties of the holmium atom, the electronic transitions can be applied for a number of interesting experiments in the fields of metrology and quantum optics. A proposal of an experiment of this kind is presented in another contribution to this conference [1].

The perspectives of the use of holmium in the investigations, as well as of obtaining of the concise description of the interactions in this atom, are determined by knowledge of a possibly large number of the electronic levels, in particular the knowledge of their physical properties, such as the Lande factors and the hyperfine structure constants. In this context the holmium atom belongs to those less studied [2]. Among the theoretically predicted ca. 600 electronic levels belonging to the odd-parity configurations, only for 30% the energy values were experimentally determined [3]. The statistics of the knowledge of the constants A and B is similar; in the case of the g_J the situation is still worse [4]. All these facts constituted the motivation for undertaking an attempt of determination of the energies for new electronic levels.

In the history of investigations of the atoms numerous variations of two methods of the search for new electronic levels were applied. In the first method the levels' energies were determined on the basis of the coincidences of the wavelengths of unclassified spectral lines. This method totally fails for lanthanides due to the large number of accidental coincidences. In the second method the hyperfine structure of the unclassified lines is recorded, and the values J, A and B for both levels involved are calculated; moreover, a possibly highest number of the fluorescence channels' wavelengths should also be determined. The line classification is accomplished by comparison of the results obtained with the known experimental or theoretically predicted values [5],[6].

After performing the preliminary studies it proved that in the case of the holmium atom also the latter method is not efficient. The reason is insufficient number of the observed fluorescence channels, as well as not sufficiently precise theoretical predictions. Thus a method constituting a specific combination of the two standard methods described was described. On the basis of coincidences of unclassified spectral lines [7],[8] a hypothetic energy and J quantum number values of a new level were calculated. Then the wavenumbers of all the spectral lines, which should occur if the level existed, were calculated, and attempts were made to record the structure of these lines with the method of laser induced fluorescence in a hollow cathode discharge lamp, with the use of the tunable lasers available in the laboratory.

As a result, the values of energies, J quantum numbers and the hyperfine structure constants for over 20 new electronic levels were obtained. Each of the levels was confirmed by at least 3 observed spectral lines, in which it was involved.

The work was supported by Poznan University of Technology under the Project 06/65/DSPB/5183.

References

[1] D. Stefanska, B. Furmann, and P. Głowacki, "Possibilities of investigations of the temporal variation of the fine structure constant α in the holmium atom", contribution to this conference; D. Stefanska, B. Furmann, and P. Głowacki, JQSRT **213**, 159–168 (2018).
[2] D. Stefanska, J. Ruczkowski, M. Elantkowska, and B. Furmann, JQSRT **209**, 180–195 (2018).
[3] D. Stefanska and B. Furmann, JQSRT **206**, 286–295 (2018).
[4] D. Stefanska, S.Werbowy, A.Krzykowski, and B.Furmann JQSRT **210**, 136–140 (2018).
[5] W. J. Childs, D. R. Cok, and L. S. Goodman, JOSA **73**(2), 151–155 (1983).
[6] S. Kröger, J. F. Wyart, and P. Luc, Phys. Scr. **55**(5), 57 (1997).
[7] J. F. Wyart, P. Camus, and J. Verges, Physica C **92**(3), 377–396 (1977).
[8] N. Al-Labady, *et al*., Astrophys.J. Suppl. Ser **228**(2), 16 (2017).

*Corresponding author: boguslaw.furmann@put.poznan.pl

Magnetic multipole shielding constants of the ground state of the relativistic hydrogenlike atom: application of the Sturmian expansion of the generalized Dirac–Coulomb Green function

G. Łukasik[*1], **R. Szmytkowski**[†1],
1. Department of Atomic, Molecular and Optical Physics, Faculty of Applied Physics and Mathematics, Gdańsk University of Technology, Narutowicza 11/12, 80-233 Gdańsk, Poland

The knowledge of the Dirac–Coulomb Green function is required for many physical problems. Among several well-known representations of that function, a particularly convenient one is that in the form of the Sturmian expansion, constructed in [1]. It has been already used to derive closed-form expressions for various electromagnetic properties of relativistic hydrogenlike atoms in electric or magnetic multipole fields [2,3].

Consider a relativistic hydrogenlike atom. Within the framework of the perturbation theory, one can calculate the magnetic field at the nucleus:

$$\boldsymbol{B} \simeq \boldsymbol{B}^{(0)} + \boldsymbol{B}^{(1)}, \tag{1}$$

where $\boldsymbol{B}^{(0)}$ is the magnetic field in the unperturbed atom, while

$$\boldsymbol{B}^{(1)} = -\sigma_L \boldsymbol{B}_L^{ext} \tag{2}$$

is the first-order approximation to the induced magnetic field, proportional to the perturbing external 2^L-pole magnetic field $\boldsymbol{B}_L^{ext}$. The factor σ_L is the multipole magnetic shielding constant.

Using the Sturmian expansion of the generalized Dirac–Coulomb Green function [1], we derive a closed-form expression for the multipole magnetic shielding constant of the ground state of the Dirac one-electron atom placed in a weak, static, 2^L-pole magnetic field. For $L = 1$ (the magnetic dipole field), we obtain

$$\sigma_1 = -\alpha^2 Z \frac{2(4\gamma_1^3 + 6\gamma_1^2 - 7\gamma_1 - 12)}{27\gamma_1(\gamma_1+1)(2\gamma_1-1)}, \tag{3}$$

while for $L \geqslant 2$ we find

$$\begin{aligned}\sigma_L \;=\; & -\alpha^2 Z \frac{2}{(2L+1)^2}\left[\frac{(L+1)(\gamma_L+\gamma_1)}{(L-1)(\gamma_L+\gamma_1-L)}\,{}_3F_2\left(\begin{matrix}-L,\,1,\,\gamma_L-\gamma_1-L\\ \gamma_L-\gamma_1+1,\,\gamma_L+\gamma_1-L+1\end{matrix};1\right)\right. \\ & \left. -\frac{L(\gamma_{L+1}+\gamma_1)}{(L+2)(\gamma_{L+1}+\gamma_1-L)}\,{}_3F_2\left(\begin{matrix}-L,\,1,\,\gamma_{L+1}-\gamma_1-L\\ \gamma_{L+1}-\gamma_1+1,\,\gamma_{L+1}+\gamma_1-L+1\end{matrix};1\right)\right],\end{aligned} \tag{4}$$

where $\gamma_\kappa = \sqrt{\kappa^2 - (\alpha Z)^2}$ (α is the Sommerfeld's fine structure constant) and ${}_3F_2$ is the generalized hypergeometric function. Equation (3) confirms previous results [4-6], while Eq. (4) is much simpler than its counterpart in [4]. It is worth to emphasize that the ${}_3F_2$ functions in Eq. (4) are truncating ones and consequently for each particular value of $L \geqslant 2$ the formula for σ_L may be expressed in terms of elementary functions.

References

[1] R. Szmytkowski, J. Phys. B **30**, 825 (1997) [erratum: J. Phys. B, **30**, 2747 (1997); addendum: arXiv:physics/9902050].
[2] R. Szmytkowski, G. Łukasik, At. Data Nucl. Data Tables, **111-112**, 41 (2016).
[3] R. Szmytkowski, G. Łukasik, Phys. Rev. A, **93**, 062502 (2016).
[4] S. A. Zapryagaev, N. L. Manakov, L. P. Rapoport, Yad. Fiz., **19**, 1136 (1974) [English translation: Sov. J. Nucl. Phys., **19**, 582 (1974)].
[5] V. G. Ivanov, S. G. Karshenboim, R. N. Lee, Phys. Rev. A, **79**, 012512 (2009).
[6] P. Stefańska, R. Szmytkowski, Int. J. Quantum Chem., **112**, 1363 (2012).

*Corresponding author: grzegorz.lukasik@pg.edu.pl
†Corresponding author: radoslaw.szmytkowski@pg.edu.pl

Level dynamics in spin-1/2 system during transition from delocalized to localized phase

A. Maksymov*[1] , P. Sierant[1], J. Zakrzewski[1]
1. Instytut Fizyki im. Mariana Smoluchowskiego, Uniwersytet Jagielloński, ul. Lojasiewicza 11, PL-30059 Kraków, Poland

The many body localization of a system can be interpreted as a transition from quantum chaos to integrability. Therefore two different statistics of energy levels are applicable: the Wigner-Dyson statistics for delocalized system with quantum chaos and Poisson statistics for many body localized system that has integrable properties [1], [2].

In XXZ Heisenberg spin chain with external random field a smooth transition is observed crossing the border between localized and extended states. For studied by us model (1) the transition occurs due to increase the strength of external disorder. We characterize the parametric motion of energy levels, obtained by means of full exact diagonalization technique. The focus has been put on the distribution of first and second derivatives of level dynamics over the control parameter, i.e. their velocities and curvatures [3]. The following Hamiltonian is considered

$$\hat{H} = J\sum_{i=1}^{L}\left(S_i^x S_{i+1}^x + S_i^y S_{i+1}^y\right) + \Delta\sum_{i=1}^{L} S_i^z S_{i+1}^z + \sum_{i=1}^{L} h_i S_i^z, \tag{1}$$

where J and Δ are the coupling for XY and Z components respectively, and h_i is the Zeeman splitting that describes the uniformly distributed random field within the range $[-W;W]$, where W is field strength.

For delocalized and transient regimes the curvatures of energy levels were numerically obtained and the distribution of curvatures and their ratio (the ratio of two consequent curvatures) were analyzed. In Fig. 1 are given the results of our analysis which indicate the qualitative statistical changes in level dynamics during localization.

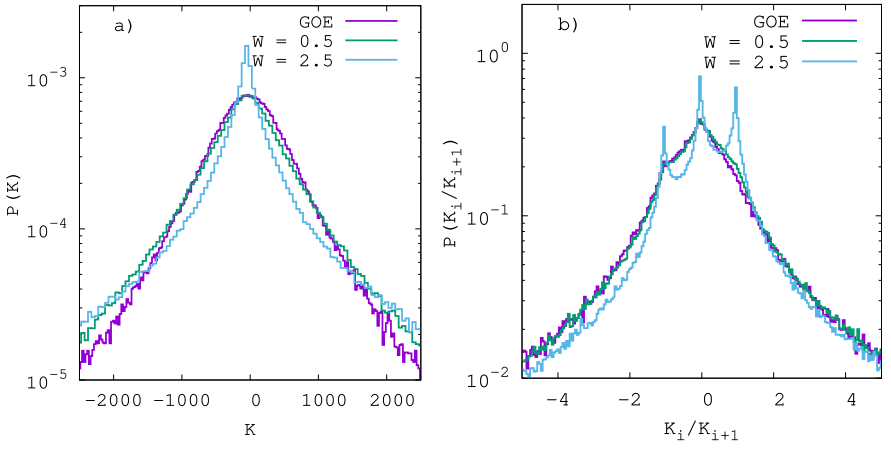

Fig. 1: The curvatures distribution of energy levels (a) and the distribution of curvatures ratio (b) for GOE ensemble and for fixed field strengths. The value of filed strength is changing from delocalized system ($W = 0.5$) to the transient state where the many body localization phase is prevailed ($W = 2.5$).

From the distribution of curvatures ratio the additional peaks in the distribution were detected, which become more pronounced during the transition to localized regime.

We hope that observed features may be used along with level spacing statistics as additional characteristic of many body system's localization.

Work supported by National Science Center (Poland) grant 2015/19/B/ST2/01028.

References

[1] M. Serbyn, J. E. Moore, Phys. Rev. E 93, 041424(R) (2016).
[2] P. Sierant, J. Zakrzewski, New J. Phys. 20, 043032 (2018).
[3] J.Zakrzewski, D. Delande, Phys. Rev. E 47, 1650 (1993).

*Corresponding author: maxyartur@gmail.com

A – 49

Collective effects in spin-optomechanics

Simon B. Jäger*[1], John Cooper[2,3], Murray J. Holland[2,3], and Giovanna Morigi[1]

1. Theoretische Physik, Universität des Saarlandes, D-66123 Saarbrücken, Germany

2. JILA, National Institute of Standards and Technology and Department of Physics, University of Colorado, Boulder, Colorado 80309-0440, USA

3. Center for Theory of Quantum Matter, University of Colorado, Boulder, Colorado 80309, USA

We theoretically analyse the collective dynamics of N particles, whose spins couple to a single-mode optical resonator. The particles' spins are driven by an incoherent pump and move along the cavity axis. Previous studies show that their spin and motion can synchronize by means of the dynamics following the collective emission into the cavity [1][2]. We study the onset of this synchronization dynamics as a function of the initial kinetic energy by means of a mean-field treatment. We also analyse the dynamics when the particles initially form a Bose-Einstein condensate and observe that deep in the quantum regime synchronization becomes unstable on longer timescales.

References

[1] Minghui Xu, Simon B. Jäger, S. Schütz, J. Cooper, Giovanna Morigi, and M. J. Holland, Phys. Rev. Lett. **116**, 153002 (2016).

[2] Simon B. Jäger, Minghui Xu, Stefan Schütz, M. J. Holland, and Giovanna Morigi, Phys. Rev. A **95**, 063852 (2017).

*Corresponding author: simonjaeger1@aol.com

LIF excitation and emission spectra of CdAr van der Waals complexes: Novel possibilities

J. Dudek[*1], **T. Urbańczyk**[†1], **M. Krośnicki**[2], **A. Kędziorski**[3], **J. Koperski**[1]
1. Smoluchowski Institute of Physics, Jagiellonian University, ul. Łojasiewcza 11, 30-348 Kraków, Poland
2. Institute of Theoretical Physics and Astrophysics, Faculty of Mathematics, Physics and Informatics, University of Gdansk, Wita Stwosza 57 80-952 Gdańsk, Poland
3. Institute of Physics, Faculty of Physics, Astronomy and Informatics, Nicolaus Copernicus University, Grudziądzka 5/7 87-100 Toruń, Poland

Interatomic potentials of Rydberg electronic energy states of CdAr van der Waals complex were recently calculated using *ab initio* method [1]. The main goal of the presented work is to determine these Rydberg-state potentials experimentally employing both laser induced fluorescence (LIF) excitation and emission spectra, and verify accuracy of the *ab initio* method. Using results of *ab initio* calculations, two experimental approaches were analysed. Firstly, LIF excitation spectra from the $C^1 1(5^1P_1)$ to higher Rydberg states using optical-optical double resonance method (OODR) were taken into consideration. Secondly, LIF emission spectra from the $E^3 1(6^3S_1)$ Rydberg state were simulated for both bound→bound and bound→free transitions. To be able to record the emission spectra in the experiment, it is necessary to exite CdAr complex to the $E^3 1$ state. Thus, a few possibilites of the excitation of the complex were simulated. It is planned to realize the experiment using CdAr complexes cooled vibrationally in a supersonic beam produced using pulsed-operating source.

This work was supported by the National Science Centre Poland under a grant number UMO-2015/17/B/ST4/04016.

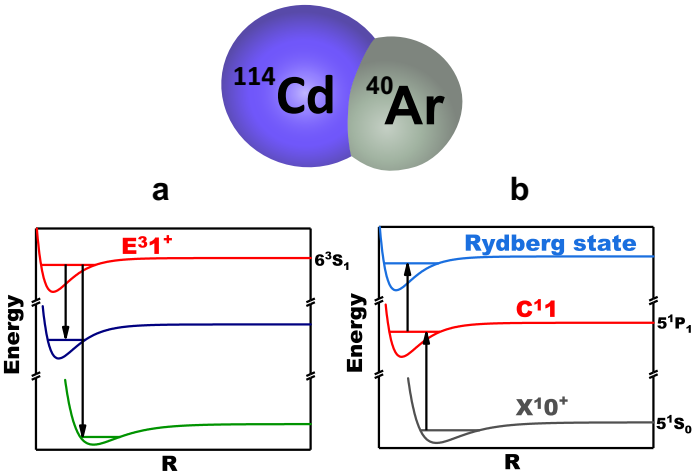

Fig. 1: Proposal for novel experimental study of CdAr van der Waals complex: a) LIF emission spectra from the $E^3 1(6^3S_1)$ Rydberg state. b) Laser excitation from the $C^1 1(5^1P_1)$ to higher Rydberg states.

References

[1] M. Krośnicki, A. Kędziorski, T. Urbańczyk and J. Koperski, *Valence and Rydberg states of CdAr within ab initio approach*, in preparation.

*Corresponding author: joanna.b.dudek@doctoral.uj.edu.pl
†Corresponding author: tomek.urbanczyk@uj.edu.pl

Influence of Comprehensive Atomic Structure and Continuum Lowering on the Ionization Balance of a High-Density Tungsten Plasma

M. Bernardi[1], J. Deprince[1], S. Gamrath[1], P. Quinet[*1,2]

1. Physique Atomique et Astrophysique, Université de Mons, B-7000 Mons, Belgium

2. IPNAS, Université de Liège, B-4000 Liège, Belgium

A correct determination of the ionization balance, i.e. the fractional abundance of different charge states of a particular element, is of paramount importance for describing the physical conditions inside a plasma. For a plasma in local thermodynamic equilibrium (LTE), the Saha equation (see e.g. [1]) is a well known expression that relates the ionization state to the temperature and electron density. As an example, this equation was recently used to estimate the electron temperature (T_e) and the electron density (n_e) characterizing a laser-produced tungsten plasma observed by Kubkowska *et al*. [2]. However, these latter authors considered only the atomic data available at that time for neutral and singly ionized tungsten atoms, namely the few experimental energy levels and the ionization potentials compiled by Kramida and Shirai [3,4]. Since then, the situation has evolved. More precisely, new laboratory measurements were carried out in W I [5], while extensive atomic structure calculations were performed in lowly charged tungsten, from W I to W VI, using the semi-empirical pseudo-relativistic Hartree-Fock method [6-11]. In these studies, numerical values for many energy levels, not yet determined experimentally, were obtained.

The main goal of the present work is to estimate the influence of the use of a comprehensive set of energy levels, including all the experimentally known values completed with the computed ones, on the ionization balance of a high density tungsten plasma, from $n_e = 10^{17}$ to 10^{21} cm^{-3} within the framework of the Saha equation. Moreover, it is well established that, at sufficiently high densities, neighboring charged particles deform the confining potential of an ion immersed in a plasma. As a consequence, its effective ionization potential is lowered. In our study, this effect, usually called *ionization potential lowering* or *continuum lowering*, has also been estimated as regards the determination of the ionization balance using the Saha equation.

References

[1] H. Bradt, *Astrophysics Processes*, Cambridge University Press (2008).
[2] M. Kubkowska *et al*., Eur. Phys. J. D 54, 463 (2009).
[3] A.E. Kramida and T. Shirai, J. Phys. Chem. Ref. Data 35, 423 (2006).
[4] A.E. Kramida and T. Shirai, At. Data Nucl. Data Tables 95, 305 (2009).
[5] J.-F. Wyart, J. Phys. B : At. Mol. Opt. Phys. 43, 074018 (2010).
[6] H. Nilsson H. *et al*., Eur. Phys. J. D 49, 13 (2008).
[7] P. Palmeri *et al*., Phys. Scr. 78, 015304 (2008).
[8] P. Quinet *et al*., J. Phys. B : At. Mol. Opt. Phys. 44, 145005 (2011).
[9] S. Enzonga Yoca *et al*., J. Phys. B : At. Mol. Opt. Phys. 45, 035001 (2012).
[10] S. Enzonga Yoca *et al*., J. Phys. B : At. Mol. Opt. Phys. 45, 065001 (2012).
[11] S. Enzonga Yoca *et al*., J. Phys. B : At. Mol. Opt. Phys. 45, 035002 (2012).

[*]Corresponding author: Pascal.Quinet@umons.ac.be

Study of Stark broadened hydrogen line profiles using laser-induced plasma, laser Thomson scattering and *ab initio* computer simulations

F. Sobczuk[*1], K. Dzierżęga[†1], E. Stambulchik[2], T. Pięta[1], B. Pokrzywka[3]

1. Marian Smoluchowski Institute of Physics, Jagiellonian University, ul. Łojasiewicza 11, 30-348 Kraków, Poland
2. Faculty of Physics, Weizmann Institute of Science, Rehovot 7610001, Israel
3. Institute of Physics, Pedagogical University, ul. Podchorążych 2, 30-084 Kraków, Poland

The analysis of the Stark broadened line profiles emitted by hydrogen atoms is the basic method of plasma diagnostics. This is due to the strong sensitivity of their widths to the charged particle concentration in plasma. However, it turns out that much more information about plasma can be inferred by examining **full profiles of hydrogen lines**, as shapes of practically all of them also depend upon the kinetics of the emitter-perturber system, the so-called **ion dynamics effect**. Despite the fact that such profiles have been the subject of many theoretical models for several decades, their results have never been unambiguously confirmed experimentally.

This work concerns detailed investigations of the profiles of the Balmer hydrogen spectral lines in the laser-induced plasma. The measured emission profiles, together with independently determined plasma parameters - electron concentration, their temperature and the temperature of perturbing atoms and ions - are used to verify the calculations performed by the *ab initio* computer simulations [1].

In our studies the laser-induced plasma (LIP) is generated as a result of the laser breakdown in pure hydrogen gas under reduced pressure. High precision plasma diagnostics is achieved using the laser Thomson scattering (TS), with a second harmonic of a Nd:YAG laser as the probe beam, as described in [2]. TS is characterized by high spatial and temporal resolution and most importantly the scattering spectra are directly related to the plasma parameters. Therefore they are independent of the accepted and at the same time difficult to verify hypotheses about the equilibrium state of the plasma.

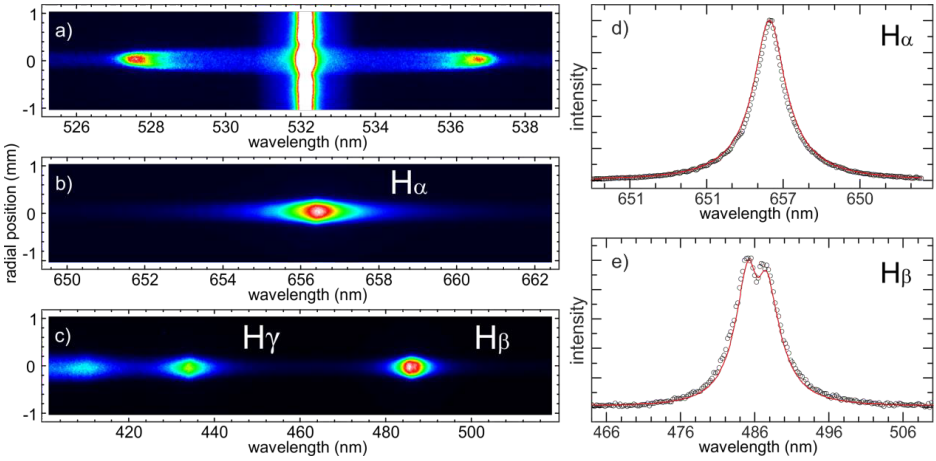

Fig. 1: The spectrum of the Nd:YAG 532 nm laser beam Thomson scattering on LIP generated by the laser breakdown in hydrogen gas (a), the spectrum of the H_α emission line (b), the spectrum of the H_β and H_γ emission lines (c), the measured profile of the H_α line (black circles) and the simulated profile of that line convoluted with the apparatus profile (red line) (d), the measured profile of the H_β line (black circles) and the simulated profile of that line convoluted with the apparatus profile (red line) (e).

References

[1] E. Stambulchik and Y. Maron, J. Quant. Spectr. Rad. Transfer **99**, 730 (2006).
[2] K. Dzierżęga, A. Mendys, and B. Pokrzywka, Spectrochim. Acta Part B, **98**, 76-86 (2014).

[*] Corresponding author: franciszek.sobczuk@student.uj.edu.pl
[†] Corresponding author: krzysztof.dzierzega@uj.edu.pl

Atomic Structure, Radiative and Auger Parameters for Modelling Oxygen K-Lines in High-Density Astrophysical Plasma Environments

J. Deprince[1], M.A. Bautista[2], S. Fritzsche[3,4], J. Garcia[5], T.R. Kallman[6], C. Mendoza[2], P. Palmeri[1], P. Quinet[*1,7]

1. Physique Atomique et Astrophysique, Université de Mons, B-7000 Mons, Belgium
2. Department of Physics, Western Michigan University, Kalamazoo, MI 49008, USA
3. Helmholtz Institut Jena, 07743 Jena, Germany
4. Theoretisch Physikalisches Institut, Friedrich Schiller University at Jena, 07743 Jena,Germany
5. Department of Astronomy, California Institute of Technology, Pasadena, CA 91125,USA
6. NASA Goddard Space Flight Center, Code 662, Greenbelt, MD 20771, USA
7. IPNAS, Université de Liège, B-4000 Liège, Belgium

The emission lines in the X-ray spectral region from accreting black holes, most notably K-lines, have observed widths and shifts which imply an origin very close to the compact object [1]. The intensity of these lines can provide insight into the effects of special and general relativity in the emitting region as well as insight into some properties of the compact object itself. Magnetohydrodynamics simulations of accreting black holes with 10 solar masses, computed by Schnittman *et al.* [2], seem to reveal that the plasma conditions in such an environment should be characterized by an electronic temperature ranging from 10^5 to 10^7 K and an electronic density ranging from 10^{18} to 10^{21} cm^{-3}. Such physical conditions may affect the atomic structure and processes corresponding to the ionic species present in the plasma. However, atomic data used in the standard programs to model astrophysical X-ray spectra arise from isolated ion approximation calculations. This shortcoming is thought to be the major reason of inconsistencies observed in the results [3].

The main goal of the present work is to estimate the effects of high-density plasma environment on the atomic parameters, such as the ionization potentials, the radiative decay and Auger rates, associated with the K-vacancy states along the oxygen isonuclear sequence within the astrophysical context of accretion disks around black holes. In this purpose, relativistic atomic structure calculations have been carried out using the multiconfiguration Dirac-Fock (MCDF) method, in which a time averaged Debye-Hückel potential has been considered for both the electron-nucleus and electron-electron interactions in order to model the plasma environment, using a combination of the GRASP92 [4] and of the RATIP [5] codes. A comparison with the results obtained by another independent computational method, namely the Breit-Pauli relativistic approximation as implemented in the AUTOSTRUCTURE code [6, 7], has also been carried out, showing that both approaches are in very good agreement as far as the influence of plasma environment on the different atomic parameters is concerned.

References

[1] C.S. Reynolds and M.A. Nowak, Phys. Rep. 377, 389 (2003).
[2] J.D. Schnittman, J.H. Krolik and S.C. Noble, Astrophys. J. 769, 156 (2013).
[3] J. Garcia *et al.*, Mon. Not. Roy. Astron. Soc. 462, 751 (2016).
[4] F.A. Parpia, C. Froese Fischer and I.P. Grant, Comput. Phys. Commun. 94, 249 (1996).
[5] S. Fritzsche, Comput. Phys. Commun. 183, 1523 (2012).
[6] N.R. Badnell, J. Phys. B : At. Mol. Opt. Phys. 30, 1 (1997).
[7] N.R. Badnell, Comput. Phys. Commun. 182, 1528 (2011).

[*]Corresponding author: Pascal.Quinet@umons.ac.be

Correction of the frequency of velocity-changing collision parameter in the Hartmann-Tran profile

M. Konefał[*1,2], **M. Słowiński**[1], **M. Zaborowski**[1], **D. Lisak**[1], **P. Wcisło**[1]

1. Institute of Physics, Faculty of Physics, Astronomy and Informatics, Nicolaus Copernicus University in Toruń, ul. Grudziadzka 5, 87-100 Toruń, Poland

2. University of Grenoble Alpes, CNRS, LIPhy, 38000 Grenoble, France

We model an analytical extension of the frequency of the velocity-changing collision parameter in recently recommended line-shape profile - the Hartmann-Tran Profile (HTP) [1]. HTP includes all significant effect used in line-shape modeling nowadays. Nevertheless, HTP gives unsatisfactory results in the analysis of high-resolution spectra with a prominent effect of the Dicke narrowing, particularly in H_2 spectra [2]. The proposed method allows reducing the discrepancy between HTP and more physically justified, but numerically complicated line-shape profile originated in the transport-relaxation equation, the Speed Dependent Billiard Ball Profile (SDBBP) [3][4]. As shown in Fig. 1 the correction reduces HTP fit residuals fivefold, while keeping the computational time of the line-shape profile comparable to the standard Voigt profile. We introduce the correction in regards to commonly analyzed atmospheric and planetary molecular systems.

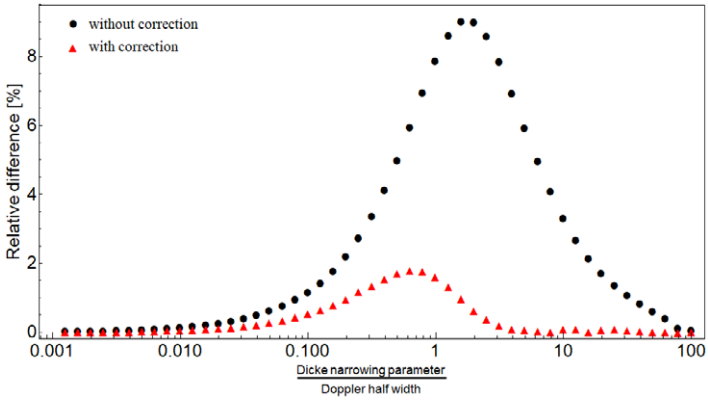

Fig. 1: The relative difference between SDBBP and HTP without and with applied correction, dots and triangles respectively. The correction enables to reproduce the molecular spectra by HTP within two percent to SDBBP.

Acknowledgments

This work has the support of the National Science Centre Poland, Projects No. 2014/15/D/ST2/05281, 2015/19/D/S and 2015/18/E/ST2/00585.

References

[1] J. Tennyson, P.F. Bernath *et al.*, Pure Appl. Chem. **86**, 1931-1943 (2014).
[2] P. Wcisło, I.E. Gordon *et al.*, J. Quant. Spectrosc. Radiat. Transf. **177**, 75-91 (2016).
[3] A.D. May, W-K. Liu *et al.*, Can. J. Phys. **91**, 879 (2013).
[4] R. Ciuryło, D.A. Shapiro *et al.*, Phys. Rev. A **65**, 012502 (2002).

*Corresponding author: konefal@fizyka.umk.pl

Determination of lower state energy values of $^{13}CH_4$ transitions near 1.73 μm from absorption spectra at 80 K and 296 K

M. Konefał[*1,2], **M. Ghysels**[1], **D. Mondelain**[1], **S. Kassi**[1], **A. Campargue**[1]
1. University of Grenoble Alpes, CNRS, LIPhy, 38000 Grenoble, France
2. Institute of Physics, Faculty of Physics, Astronomy and Informatics, Nicolaus Copernicus University in Toruń, ul. Grudziadzka 5, 87-100 Toruń, Poland

The spectroscopy of methane is of particular interest for astronomical studies, for instance Titan's atmosphere, giant planets, brown dwarfs. In this work we extend the experimental spectroscopic study of the minor isotopologue of methane $^{13}CH_4$ near 1.73 μm (5695-5850 cm^{-1}) providing a list of more than 3300 spectral lines, mostly observed for the first time. The spectra were recorded by direct absorption spectroscopy (DAS) at 296 K and 80 K [1]. The achieved noise equivalent absorption of the spectra is 5×10^{-8} cm^{-1} leading to line intensity detectivity threshold on the order of 10^{-25} cm/molecule at 296 K and 10^{-26} cm/molecule at 80 K. The empirical values of lower state energy and rotational quantum number J were derived from the ratio of the line intensities measured at 80 K and 296 K (2T-method) [2]. We add over 1500 new and revise some of incorrect J values included in the HITRAN spectroscopic database [3]. Furthermore, we compare our line list with the theoretical calculations [4] showing that the *ab initio* positions will have to be tuned according to our experimental values.

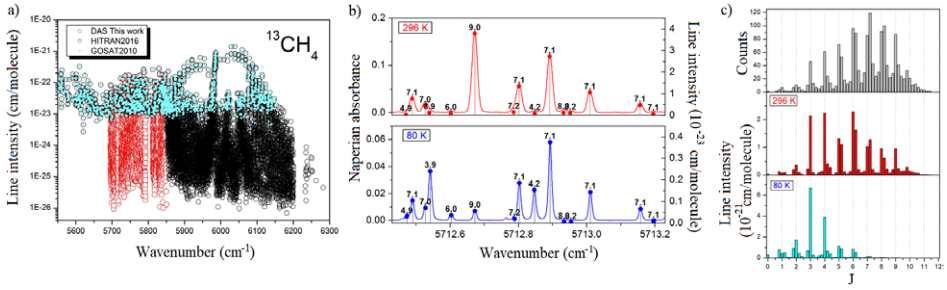

Fig. 1: a) Overview of the room temperature spectrum of $^{13}CH_4$ as provided by the HITRAN2016 database [3] (black open circles), the GOSAT2009 line list [5] and the present DAS data are plotted in light cyan and red, respectively. The HITRAN2016 line list in this region is formed by the GOSAT2009 list and the DAS line list of [6] below and above 5850 cm^{-1}, respectively. b) Example of empirical lower state J values derived by the 2T-method for transitions near 5713 cm^{-1}. c) Histograms of the empirical lower J values. Upper panel: Counts of the obtained J values with a step interval of 0.2. Medium and lower panels: Corresponding sum of line intensities at 296 K and 80 K.

Acknowledgments
This work was performed in the frame of the LabexOSUG2020 (ANR10 LABEX56) and of the ANR project e_PYTHEAS (ANR-16-CE31-0005). M. K. acknowledges the financial support of the French Government and the French Embassy in Poland.

References
[1] O.M. Lyulin, S. Kassi *et al.*, J. Mol. Spectrosc. **261**, 91-100 (2010).
[2] S. Kassi, B. Gao *et al.*, Phys. Chem. Chem. Phys. **10**, 4410-19 (2008).
[3] I.E. Gordon, L.S. Rothman *et al.*, J. Quant. Spectrosc. Radiat. Transf. **203**, 3-69 (2017).
[4] M. Rey, A.V. Nikitin *et al.*, Icarus **303**, 114-130 (2018).
[5] A.V. Nikitin, O.M. Lyulin *et al.*, J. Quant. Spectrosc. Radiat. Transf. **111**, 2211-2224 (2010).
[6] E. Starikova, A.V. Nikitin *et al.*, J. Quant. Spectrosc. Radiat. Transf. **177**, 170-180 (2016).

*Corresponding author: konefal@fizyka.umk.pl

A – 56

Experimental Observation of H_2-He Scattering States with Accurate Spectroscopic Measurements

M. Słowiński*[1], F. Thibault[2], Y. Tan[3], J. Wang[3], A.-W. Liu[3], S.-M. Hu[3], S. Kassi[4], A. Campargue[4], M. Konefał[1,4], H. Jóźwiak[1], K. Patkowski[5], P. Żuchowski[1], R. Ciuryło[1], D. Lisak[1], P. Wcisło[1]

1. Institute of Physics, Faculty of Physics, Astronomy and Informatics, Nicolaus Copernicus University in Toruń, Grudziadzka 5, 87-100 Torun, Poland

2. Institut de Physique de Rennes, UMR CNRS 6251, Université de Rennes 1, Campus de Beaulieu, Bât. 11B, F-35042 Rennes, France

3. Hefei National Laboratory for Physical Sciences at Microscale, iChEM, University of Science and Technology of China, Hefei, 230026 China

4. University of Grenoble Alpes, CNRS, LIPhy, F-38000 Grenoble, France

5. Department of Chemistry and Biochemistry, Auburn University, Auburn, AL 36849 USA

We employ highly accurate cavity-enhanced molecular spectroscopy to study the H_2-He collisions and interactions [1]. Hydrogen molecule in its ground electronic state perturbed by the helium atom constitutes the simplest system of perturbed molecule (it contains only four electrons). This gives possibility to make a link between the experiment and the theory from first principles, allowing to use *ab initio* calculations to make the physical interpretation of the experimental spectra.

In contrast to most of the previous studies, we do not fit spectra with phenomenological line shapes, but directly [2] superimpose theoretical profiles (originating from our *ab initio* calculations) on the raw experimental spectra without fitting any of the line-shape parameters. Within this approach not only the shapes of experimental lines are reliably reproduced, but also the underlying physics of molecular collisions can be traced. Besides the analysis of the basic line-shape effects (such as relaxation or phase changes of the internal states of the molecule), we also analyse the more sophisticated ones such as speed-dependent effects or velocity-changing collisions (complex Dicke narrowing parameter) [3-4], which are particularly pronounced for the H_2-He system [1,5-7]. We achieved good agreement between raw experiment data and *ab initio* calculations reaching the differences at the 1% level, as shown in Fig. 1.

According to our knowledge, this is the first comparison of highly accurate experimental spectra with advanced *ab initio* models which includes the speed-dependent effects and velocity-changing collisions. It allows us to study quantum scattering for molecules as well as to validate *ab initio* quantum potentials in ranges very challenging for quantum chemistry methods (for instance, for highly stretched molecules).

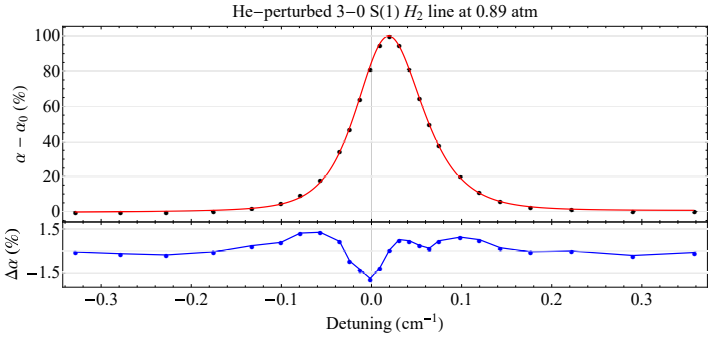

Fig. 1: *Upper panel:* Experimental points (black dots) and the billiard-ball profile (red line) with fitted area of the line, unperturbed frequency position and experimental background. No line-shape parameter was fitted. *Lower panel:* Residuals of the fit.

References

[1] F. Thibault, K. Patkowski et al., 2017, *J. Quant. Spectrosc. Radiat. T*, **202**, 308.
[2] A. D. May, W.-K. Liu et al., 2013, *Can. J. Phys.*, **91**, 879.
[3] S. Hess, 1972, *Physica*, **61**, 80.
[4] R. Ciuryło, D. Saphiro et al., 2002, *Phys. Rev. A*, **65**, 012502.
[5] P. Wcisło, H. Tran et al., 2014, *J. Chem. Phys.*, **141**, 074301.
[6] F. Thibault, P. Wcisło et al., 2016, *Eur. Phys. J. D*, **70**, 236.
[7] R. Z. Matrínez, D. Bermejo et al., *J. Raman Spectrosc.* (accepted).

*Corresponding author: suowik@fizyka.umk.pl

Lowering thermal noise of ultrastable cavities to 10^{-17} level of fractional frequency instability

N. Zhadnov[*1,2], **K. Kydeyarov**[1,2], **D. Kruchkov**[1,2], **I. Semerikov**[1,2], **K. Khabarova**[†1,2], **N. Kolachevsky**[1,2]
1. P.N. Lebedev Physical Institute of the Russian Academy of Sciences, 53 Leninskiy Prospekt, Moscow, 119991, Russia
2. Russian Quantum Center, Business-center "Ural", 100A, Novaya street, Skolkovo, Moscow, 143025, Russia

Development of ultrastable lasers is vital for many areas of modern spectroscopy, especially for advancement of optical clocks. Unprecedented frequency stability of such laser systems is usually provided by a finely stabilized Fabry-Perot cavity. During last decades the fractional frequency instability of such systems was decreasing by an order of magnitude every ten years. State-of-the-art ultrastable lasers have reached fractional frequency instability of $4 \cdot 10^{-17}$ [1]. The achievable instability in their case is completely determined by the fundamental thermal Brownian noise of the mirror coatings.

The thermal Brownian noise of the reference cavity parts causes fluctuations of the cavity length and thus limits the achievable stability of the laser frequency. However, there are some ways to decrease the thermal noise floor since it's level depends on different factors:

$$\sigma_y(\tau) \propto \frac{\sqrt{T \cdot \phi_{coat}}}{L^{5/4} \cdot \lambda^{1/2} \cdot E^{1/2}}. \tag{1}$$

Here, $\sigma_y(\tau)$ — Allan variance of thermal noise, T — temperature, ϕ_{coat} — loss angle of mirror coating, L — cavity length, λ — laser wavelength, E — Young's modulus of mirror's substrate. Thus there are several possibilities to decrease thermal noise limit by using high-Q materials for cavities, lowering temperature and increasing distance between mirrors.

Today one of the promising concepts is mono crystalline cavities consisting of crystalline silicon spacer and mirror substrates and multilayer crystalline GaAs/AlGaAs mirror coatings. The crystalline silicon has two zero points of thermal expansion at 124 K and 17 K and high Young's modulus. Our group works on development of 1.5 μm ultrastable laser systems, based on monocrystalline silicon Fabry-Perot cavities with both dielectric and crystalline GaAs/AlGaAs coatings. The cavities with finesses up to 250000 are placed in UHV chambers and are operated at first CTE zero point of 124 K. To perform the instability comparison both cavities have the same design. Estimated thermal noise level of crystalline silicon cavity with crystalline coatings is $5 \cdot 10^{-17}$ [2].

We also work on alternative approach: long cavities, less sensitive to Brownian thermal noise. Two different concepts of long ultrastable ULE cavities are under investigation: horisontally and vertically oriented 48 centimeter long cavities with dielectric mirrors on fused silica substrates. The horisontal cavity exploits a novel mount design, analyzed using finite element method. Estimated thermal noise floor for the laser stabilized to a long ULE cavity is $7 \cdot 10^{-17}$ [2].

References

[1] D. Matei et al. Phys. Rev. Lett. 118, 263202 (2017)
[2] N. Zhadnov et al. Quantum Electronics, 48 (5), 425–430 (2018)

[*]Corresponding author: nik.zhadnov@yandex.ru
[†]Corresponding author: kseniakhabarova@gmail.com

Non-Destructive Structural Imaging of Steelwork with Atomic Magnetometers

P. Bevington[*1,2], **R. Gartman**[1], **W. Chalupczak**[1]
C. Deans[3], **L. Marmugi**[3], **F. Renzoni**[3]
1. National Physical Laboratory, Hampton Rd, Teddington, London, TW11 0LW, United Kingdom
2. Department of Physics, University of Strathclyde, Glasgow, G1 1XQ, United Kingdom
3. Department of Physics and Astronomy, University College London, London WC1E 6BT, United Kingdom

Eddy current testing is a widely used non-destructive evaluation (NDE) method to identify cracks and fatigue-related damage in metallic structures [1],[2]. It relies on the generation of eddy currents by an oscillating magnetic field (the primary field, referred to as the "rf field") in the object of interest and on the detection of the magnetic field produced by those eddy currents (the secondary field). In the case of ferromagnetic metallic objects, which have a relatively high permeability and low conductivity, the secondary field originates from an oscillating local magnetisation induced by the primary field and not from eddy currents. Changes in the material, such as a defect, can be detected by monitoring the secondary field produced in the material.

Here, we demonstrate imaging of ferromagnetic carbon steel samples, Fig 1, using an ultra-sensitive radio-frequency (rf) atomic magnetometer [3] to monitor the secondary field induced by the rf field [4],[5],[6]. An active magnetic field compensation system [7] and a dedicated measurement geometry is used, making it suitable for industrial monitoring. Images are obtained at room temperature, in a magnetically unscreened environment. We demonstrate imaging and measurement of changes in the thickness of pipeline-grade carbon steel profile with a sensitivity of 0.1 mm, and the detection of concealed defects. This measurement, accepted by industry as a benchmark, represents a proof-of-concept demonstration of the relevance of the atomic magnetometer technology in steelwork NDE and corrosion under insulation detection.

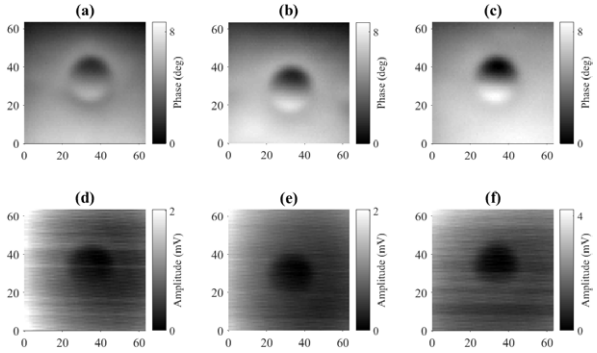

Fig. 1: Phase (a, b, c) and amplitude (d, e, f) change in rf signal generated by the scans of 64×64 mm^2 area of carbon steel plate with a defect (24.5 mm diameter) in a form of recess - 20% (a, d), 40% (b, e) and 60% (c, f) of the plate thickness. The images have been recorded at 12.6 kHz.

References

[1] H. Griffiths, *Meas. Sci. Technol.*, **12**, 1126 (2001).
[2] A. Sophian, G. Tian, M. Fan, *Chin. J. Mech. Eng.*, **30**, 500 (2017).
[3] W. Chalupczak, R. M. Godun, S. Pustelny, and W. Gawlik, *Appl. Phys. Lett.* **100**, 242401 (2012).
[4] A. Wickenbrock, S. Jurgilas, A. Dow, L. Marmugi, and F. Renzoni, *Opt. Lett.* **39**, 6367 (2014).
[5] C. Deans, L. Marmugi, S. Hussain, and F. Renzoni, *Appl. Phys. Lett.* **108**, 103503 (2016).
[6] A. Wickenbrock, N. Leefer, J. W. Blanchard, and D. Budker, *Appl. Phys. Lett.* **108**, 183507 (2016).
[7] C. Deans, L. Marmugi, and F. Renzoni, *Opt. Exp.* **25**, 17911 (2017).

*Corresponding author: patrick.bevington@npl.co.uk

Local minima suppression in octupole linear RF traps

J. Pedregosa-Gutierrez[*1], **C. Champenois, G. Hagel, M. Houssin, M. Knoop**
1. Aix-Marseille Université, CNRS, PIIM, UMR 7345, 13397 Marseille, France

Multipole radiofrequency RF traps offer new possibilities for tailoring well-defined ion crystals and in particular the potential to create pure 2D-structures [1]. However, multipole traps have also been shown to be very sensitive to geometrical misalignments of the trap rods [2], leading to additional local trapping minima. The present work proposes a method to correct the potential create by non-ideal geometries, by tuning the radiofrequency amplitudes applied on each trap rod. This approach is discussed for the octupole trap, leading to the restitution of a pseudo-potential which locally copy the one expected in multipole traps. The goodness of the compensation method is discussed in terms of the corrected error, the potential variations, the applied voltage amplitudes and the impact on the trapped ion structures. Experimental implementation is also discussed, in order to propose a diagnostic method and with respect to the resolution and stability of the trap drive. As a benchmark, the feasibility of generating a homogeneous ion ring crystal using the proposed compensation technique is evaluated with Molecular Dynamic simulations.

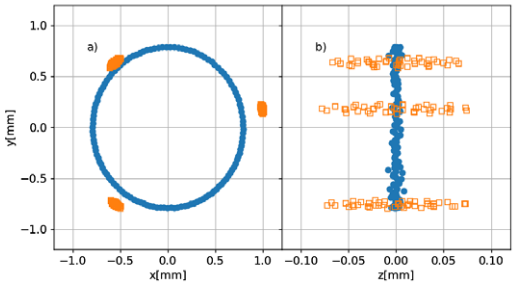

Fig. 1: Ion positions simulated with a full RF potential and laser cooling. The simulation parameters are: 128 Ca^+ ions, a nominal value of RF amplitude (before corrections) of $V_{rf} = 300V$, $\Omega/2\pi = 3.5MHz$, $\omega_z/2\pi = 100kHz$ and $r_0 = 3.93mm$. a) XY projection, b) ZY projection. Full circles correspond to the compensated potential while the empty squares correspond the uncompensated potential.

References

[1] K. Okada, K. Yasuda, T. Takayanagi, M. Wada, H.A. Schuessler, S. Ohtani, Phys. Rev. A 75, 033409 (2007)
[2] J. Pedregosa-Gutierrez, C. Champenois, M. R. Kamsap, G. Hagel, M. Houssin, and M. Knoop, Journal of Modern Optics 65, 529 (2018).

*Corresponding author: jofre.pedregosa@univ-amu.fr

Oxygen B-band investigation with cavity ring-down spectroscopy

K. Bielska[*1], **J. Domysławska**[1], **S. Wójtewicz**[1], **A. Cygan**[1], **P. Morzyński**[1], **M. Słowiński**[1], **P. Masłowski**[1], **R. Ciuryło**[1], **D. Lisak**[1]

1. Institute of Physics, Faculty of Physics, Astronomy and Informatics, Nicolaus Copernicus University in Toruń, Grudziadzka 5, Torun 87-100, Poland

Until recently only A-band transitions were used in an oxygen remote sensing in the Earth's atmosphere. This was due to lack of laboratory reference data for the B-band as well as low line intensities, which are below $6 \cdot 10^{-25}$ cm/molecule for the entire band. However, many recent investigations show that simultaneous measurements of the A and B bands lead to significantly more accurate results in various atmospheric applications such as stratospheric wind detection, clouds observations as well as pressure and temperature profiles determination.

Precise measurements of such weak transitions are technically demanding. In laboratory conditions they can be realized with the use of a high-finessee optical cavity which provides long absorption path length. We present results of our O_2 B-band lineshape measurements performed with a cavity ring-down spectroscopy (CRDS), which is among the most sensitive absorption-based measurement techniques.

We determined line positions, intensities as well as lineshape parameters for nearly 50 transitions [1] with an optical frequency comb (OFC) assisted, Pound-Drever-Hall (PDH) locked, frequency stabilized cavity ring-down spectrometer (FS-CRDS) [2]. The above self-perturbed transitions were sufficiently well described with a relatively simple speed-dependent Voigt profile (SDVP) [3] within a quadratic approximation of the speed dependence [4]. We obtained line positions characterized by uncertainties of less than 200 kHz in most cases and relative line intensity uncertainties between 0.3% and 0.6%.

The spectrometer has been modified recently so that the probe laser beam is divided into two beams of orthogonal polarizations, that is the locking beam and the actual probe beam detuned from each other by one cavity free spectral range (FSR), similarly as in Ref. [5]. With this system we investigated the systematic errors which might be introduced by incomplete optical power switching during collecting ring-down decays and the probe beam detuning from the cavity resonance. Using a simple analytical model and experimental data we show that phase shift occurring in the optical signal during the beam power switching is crucial to understand the shape of ring-down signals. In such case the magnitude of systematic errors in the ring-down time constant strongly depends on the probe beam detuning from the cavity mode center [6].

Spectra recorded with the modified spectrometer are characterized by QF (quality of the fit) factor as high as nearly 40000 from single scan. This makes possible investigation of subtle lineshape effects even in a low pressure range. We show that with increased experimental signal-to-noise ratio simultaneously with the speed dependence, also the Dicke narrowing [7] needs to be taken into account even in the low pressure range. For one of the strongest transitions in the band, P9 P9, we observe the Dicke narrowing in the pressure range below 10 Torr (1.3 kPa). It is also clearly visible in a higher pressure range, 100 Torr (13 kPa) for R35 Q36 transition which is nearly 3 orders of magnitude weaker. Our spectrometer provides sensitivity high enough to detect quadrupole transition T5 S6 with intensity of about $1.4 \cdot 10^{-30}$ cm/molec.

References

[1] J. Domysławska, S. Wójtewicz, P. Masłowski *et al.*, J. Quant. Spectrosc. Radiat. T. **169**, 111 (2016).
[2] A. Cygan, S. Wójtewicz, J. Domysławska *et al.*, Eur. Phys. J.-Spec. Top., **222**, 2119 (2013).
[3] P. R. Berman, J. Quant. Spectrosc. Radiat. T. **12**, 1331 (1972).
[4] F. Rohart, H. Mader, and H. W. Nicolaisen, J. Chem. Phys. **101**, 6475 (1994).
[5] A. Cygan, P. Wcisło, S. Wójtewicz *et al.*, Opt. Expr. **23**, 14472 (2015).
[6] S. Wójtewicz, A. Cygan, J. Domysławska *et al.*, Opt. Expr. **26**, 5644 (2018).
[7] B. Lance, G. Blanquet, J. Walrand, and J.-P. Bouanich, J. Mol. Spectrosc.**185**, 262 (1997); A. Pine, J. Quant. Spectrosc. Radiat. T. **62**, 397 (1999); R. Ciurylo, and J. Szudy, J. Quant. Spectrosc. Radiat. T. **57**, 411 (1997).

*Corresponding author: kasia@fizyka.umk.pl

A – 61

Line Shape Study of the Second Overtone Band of CO Using Cavity-Enhanced Comb-Based Fourier-Transform Spectroscopy

A. Nishiyama[1,2,3], G. Kowzan[1], D. Charczun[1], V. S. de Oliveira[4], A. Ruehl[4,5], I. Hartl[4], K. Minoshima[2], R. S. Trawiński[1], P. Masłowski[†1]

1. Institute of Physics, Faculty of Physics, Astronomy and Informatics, Nicolaus Copernicus University in Toruń, ul. Grudziadzka 5, 87-100 Toruń, Poland

2. Department of Engineering Science, Graduate School of Informatics, The University of Electro-Communications (UEC), 1-5-1 Chofugaoka, Chofu, Tokyo 182-8585, Japan

3. Japan Society for the Promotion of Science (JSPS)

4. Deutsches Elektronen-Synchrotron (DESY), Notkestrasse 85, 22607 Hamburg, Germany

5 Leibniz University Hannover, QUEST-Leibniz-Research School, Institute for Quantum Optics, Welfengarten 1, 30167 Hannover

Direct frequency comb spectroscopies provide precise molecular spectra over a wide wavelength range thanks to the precisely determined comb mode frequencies and broadband comb spectra. In this study, we applied frequency comb-based cavity-enhanced absorption spectroscopy (FC-CEAS) and sub-nominal resolution Fourier-transform spectroscopy (FC-FTS) [1,2] to a line shape study of CO in Ar. The FC-CEAS was applied to measure weak absorption transitions of the second overtone band (0 3) of CO with high signal-to-noise ratio, and we obtained precise collisional line-shape parameters of multiple lines in the near infrared region.

A schematic of our experimental setup is shown in Fig. 1(a). We used an erbium-doped-fiber laser based comb, and the output was coupled into a cavity with a finesse of around 20000. The comb modes were locked by the two-point PDH locking scheme [3] to match every cavity resonance mode. Furthermore, the cavity length was stabilized to keep the comb repetition frequency (f_{rep}) constant. The cavity was filled with a sample gas which was a CO-Ar mixture with CO concentration of 1000 ppm, and the measurements were performed in the pressure range from 10 to 700 Torr. Cavity transmission spectra were acquired with a FTS system calibrated by a stabilized He-Ne laser. We obtained interferograms with length of about 1.2 m corresponding to c/f_{rep}, and treated the data according to the procedure in [2] to remove instrumental line shape of the FTS system and utilize high frequency accuracy of comb modes.

The top of Fig. 1 (b) shows a normalized cavity transmission spectrum around the P4 line measured at a sample pressure of 450 Torr. Fit residuals of the Voigt profile (VP) and the speed-dependent VP (SDVP) are shown below the spectrum, and the quality factors (QF) of the fits are 661 and 1178, respectively. The fitting model included a molecular dispersion term [4] which described the asymmetric spectral shapes caused by molecular dispersion of the gas sample inside the cavity. The fits with high QF values were performed on multiple lines in P and R branches observed at every pressures. As a result, we obtained precise collision-induced line shape parameters for multiple lines.

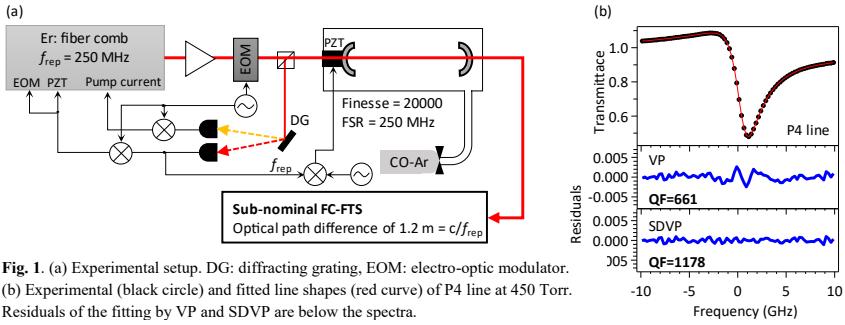

Fig. 1. (a) Experimental setup. DG: diffracting grating, EOM: electro-optic modulator. (b) Experimental (black circle) and fitted line shapes (red curve) of P4 line at 450 Torr. Residuals of the fitting by VP and SDVP are below the spectra.

This work was supported by National Science Centre, Poland (No.UMO-2016/23/B/ST2/00730, 2016/21/N/ST2/00334) and JSPS KAKENHI Grant Numbers 16J02345, 17K14435. Silva de Oliveira acknowledges CNPq–Brazil. G.K was supported by National Science Centre, Poland scholarship 2017 /24/T/ST2/00242.

References

[1] P. Masłowski, et al., Phys. Rev. A 93, 021802(R) (2016).
[2] L. Rutkowski, et al., Journal of Quantitative Spectroscopy & Radiative Transfer 204, 63 (2018).
[3] A. Foltynowicz, et al., Physical Review Letters 107, 233002 (2011).
[4] A. Foltynowicz, et al., Applied Physics B 110, 163 (2013).

[†]Corresponding author: pima@fizyka.umk.pl

Complex Gas Spectroscopy Through Hz-Level Cavity Mode Measurements With a Comb-Based VIPA Spectrometer

G. Kowzan[*1], **D. Charczun**[1], **A. Cygan**[1], **D. Lisak**[1], **R. S. Trawiński**[1], **P. Masłowski**[1]
1. Institute of Physics, Faculty of Physics, Astronomy and Informatics, Nicolaus Copernicus University in Toruń, Ul. Grudziądzka 5, 87-100 Toruń, Poland

Cavity mode-width spectroscopy [1] and cavity mode-dispersion spectroscopy [2] techniques provide a way to simultaneously determine absorption and dispersion of a sample by measuring widths and positions of enhancement cavity resonances. It was shown recently that the latter can also be efficiently combined with optical frequency combs (OFCs) to perform dispersion measurements in a broad spectral range [3]. Here, we present broadband measurements of 7-kHz-wide cavity resonances at Hz-level precision, resulting in complex spectra of CO second overtone transitions [4]. To the best of our knowledge, the 7-kHz-wide cavity resonances shown in this work are the narrowest spectral features measured directly with a frequency comb. Moreover, the presented technique is capable of retrieving shapes of such cavity modes in several seconds, enabling future ultra-precise, broadband and time-resolved spectroscopic measurements.

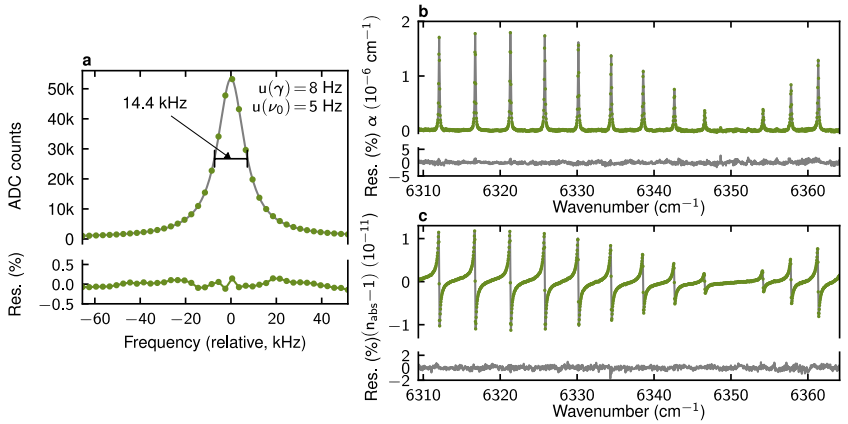

Fig. 1: Left part: (a) Measured cavity mode shape with a Lorentzian fit and fit residuals. The uncertainties for mode width γ (HWHM) and ν_0 are 1σ fit uncertainties. Right part: absorption (b) and dispersion (c) spectrum of the 0-3 band of CO-N_2 at 714 Torr with fit residuals based on complex Voigt profiles..

We couple a near-infrared OFC into a high-finesse optical cavity ($\mathscr{F} = 18500$) and tightly lock the comb teeth to the cavity modes, while absolute frequencies of the cavity modes are stabilized to an Rb frequency standard. The OFC is Vernier-filtered by the cavity to obtain 4-GHz spacing between comb modes and transferred to a VIPA spectrometer [5]. The VIPA spectrometer with resolution of 600 MHz and spectral bandwidth of 20 nm clearly resolves individual comb lines. The shapes of the cavity modes are retrieved by tuning their positions with respect to the OFC and recording the transmitted spectra. Each of the modes is subsequently fitted to a Lorentzian function (shown on Fig. 1a) to obtain its width and position. The mode widths are converted to absorption coefficient and the mode position shifts to refractive index and both are fitted to the complex Voigt profiles of probed transitions. We obtain signal-to-noise ratio of 190 for absorption spectrum and of 380 for dispersion spectrum with expected better performance for longer averaging times. We also report on broadband determination of group-delay dispersion of the cavity mirrors based on observed cavity mode positions.

The research was supported by the National Science Center, Poland, project nos. 2015/18/E/ST2/00585, 2016/21/N/ST2/00334. G. K. was supported by the National Science Centre, Poland scholarship 2017/24/T/ST2/00242.

References

[1] A. Cygan, D. Lisak, P. Morzyński, M. Bober, M. Zawada, E. Pazderski, and R. Ciuryło, Opt. Express **21**, 29744 (2013).
[2] A. Cygan, S. Wójtewicz, M. Zaborowski, P. Wcisło, R. Guo, R. Ciuryło, and D. Lisak, Meas. Sci. Technol. **27**, 045501 (2016).
[3] L. Rutkowski, A. C. Johansson, G. Zhao, T. Hausmaninger, A. Khodabakhsh, O. Axner, and A. Foltynowicz, Opt. Express **25**, 21711 (2017).
[4] G. Kowzan, D. Charczun, A. Cygan, R. S. Trawiński, D. Lisak, and P. Masłowski, Conference on Lasers and Electro-Optics (2018), Paper STu3N.8 (Optical Society of America, 2018)
[5] S. A. Diddams, L. Hollberg, and V. Mbele, Nature **445**, 627 (2007).

*Corresponding author: gkowzan@fizyka.umk.pl

A – 63

Saturated configuration interaction calculations for five-valent Ta and Db.

A. J. Geddes[*1], **D. A. Czapski**[1], **E. V. Kahl** [1], **J. C. Berengut** [1]
1. School of Physics, University of New South Wales, Sydney, New South Wales 2052, Australia

Accurate *ab initio* atomic structure calculations of complicated atoms with 4 or more valence electrons begin to push the memory and time limits of modern supercomputers. Hence, we present a robust method of decreasing the size of configuration interaction and many-body perturbation theory calculations without undermining the accuracy of the resulting atomic spectra. This method, referred to as "emu CI", has been implemented directly within the existing AMBiT CI+MBPT program [1]. Emu CI can allow for more accurate structure calculations in atoms with many valence electrons without the need for major modifications to existing code.

Emu CI makes it possible to saturate the CI matrix in atoms with many valence electrons which have otherwise resulted in prohibitively large calculations. We test our method on the five-valence-electron atom tantalum, verify the convergence of the calculated energies and compare the Emu CI method with a usual CI calculation as depicted in Figure 1. Next, emu CI was used alongside MBPT to calculate the spectra and isotope shifts of tantalum's superheavy analogue dubnium [2].

Theoretical predictions of spectra and ionisation energies for super-heavy atoms can be used to interpret experimental data and extract ionisation potentials from measurements; the heaviest elements that have been characterised in this manner are nobelium and lawrencium [3] [4]. Experimental techniques developed for Lr and No are expected to be applied to even heavier elements of $Z \geq 104$, making it necessary to perform theoretical calculations for super-heavy elements.

Additionally, isotope-shift calculations can be used to search for the spectra of superheavy isotopes which may be produced in astrophysical phenomena. It has been proposed in [5] that it is possible to predict the spectra of stable superheavy atoms using the spectra of the neutron-deficient isotope produced on Earth combined with accurate isotope shift calculations.

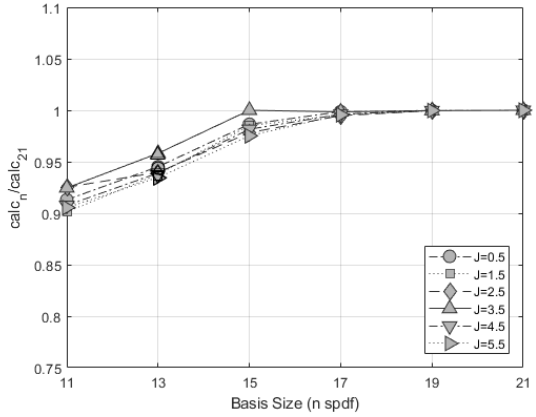

Fig. 1: Convergence of select even states when CI basis set is increased from $11spdf$ to $21spdf$ and MBPT is included. Open shapes denote results of the largest non-emu calculations performed.

References

[1] E. V. Kahl, J. C. Berengut, arXiv:1805.11265 (2018)
[2] A. J. Geddes, D. A. Czapski, E. V. Kahl, J. C. Berengut, arXiv:1805.06615 (2018)
[3] M . Laatiaoui, W. Lauth, H. Backe, M. Block, D. Ackermann, B. Cheal, P. Chhetri, C. Düllmann, P. van Duppen, J. Even, R. Ferrer, F. Giacoppo, S. Götz, F. Heßberger, M. Huyse, O. Kaleja, J. Khuyagbaatar, P. Kunz, F. Lautenschläger, A. Mistry, S. Raeder, E. Ramirez, T. Walther, C. Wraith and A. Yakushev, Nature, **538**, 495–498, (2016)
[4] T . K. Sato, M. Asai, A. Borschevsky, T. Stora, N. Sato, Y. Kaneya, K. Tsukada, Ch. E. Düllmann, K. Eberhardt, E. Eliav, S. Ichikawa, U. Kaldor, J. V. Kratz, S. Miyashita, Y. Nagame, K. Ooe, A. Osa, D. Renisch, J. Runke, M. Schädel, P. Thörle-Pospiech, A. Toyoshima and N. Trautmann Nature, **520**, (209–211), (2015)
[5] V. A. Dzuba, V. V. Flambaum, and J. K. Webb, Phys. Rev. A **95**, 062515 (2017)

*Corresponding author: a.geddes@unsw.edu.au

Hz-level Resolution Fourier Transform Spectrometry for Complex Refractive Index Spectroscopy

D. Charczun*[1], G. Kowzan[1], A. Nishiyama[1,2], M. Debus[3], P. Huke[3], D. Tomaszewska[4], G. Soboń[4], A. Cygan[1], D. Lisak[1], R. S. Trawiński[1], P. Masłowski[1],

1. Institute of Physics, Faculty of Physics, Astronomy and Informatics, Nicolaus Copernicus University in Toruń, ul. Grudziadzka 5, 97-100 Toruń, Poland

2. Department of Engineering Science, Graduate School of Informatics, The University of Electro-Communications (UEC), 1-5-1 Chofugaoka, Chofu, Tokyo 182-8585, Japan

3. Institut für Astrophysik, Georg-August-Universität, Friedrich Hund-Platz 1, D-37077 Göttingen, Germany

4. Faculty of Electronics, Laser Fiber Electronics Group, Wrocław University of Science and Technology, Wybrzeże Wyspiańskiego 27, 50-370 Wrocław, Poland

For over half a century Fourier Transform Spectroscopy (FTS) has been the constant element of spectroscopic landscape, providing a reliable way to obtain broadband absorption spectra in the infrared range, but at some point progress in this field halted, seemingly reaching its limits. Invention of the optical frequency comb (OFC) changed the equation, enabling the development of a method surpassing the optical path difference resolution limit [1,2] and opening the possibility for inventing more advanced methods.

Cavity Mode Dispersion Spectroscopy (CMDS) and Cavity Mode Width Spectroscopy (CMWS) [3,4] are two recently developed spectroscopic techniques, which yield information about molecular dispersion and absorption from measuring the positions and widths of cavity resonances. Previously they were demonstrated with continuous wave lasers, showing signal-to-noise ratio and resolution similar to the well-established cavity ring-down spectroscopy. However in this implementation they also shared the same limits of measurement range and relatively slow acquisition. The new sub-nominal resolution OFC-based FTS [1,2] is a great match for those methods, as it enables measuring thousands of cavity modes simultaneously. It also overcomes the limitations of OFC-based Cavity-Enhanced Absorption Spectroscopy (OFC-CEAS), which are cavity dispersion limiting the bandwidth and a requirement for a reference measurement [5]. Here we present the measurements of 10 kHz HWHM cavity resonances, which are some of the narrowest features ever measured by the FTS, from which we derive the absorption and dispersion spectra of the 0-3 band transitions of CO in Ar.

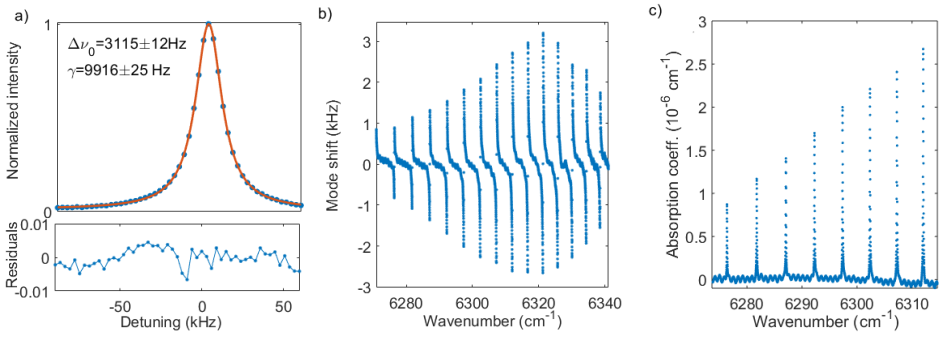

Fig. 1: a) Close-up of a single cavity mode measurement. Blue dots: measured points. Orange line: fitted Lorentzian curve. $\Delta\nu_0$ - cavity mode shift compared to the comb tooth position. γ - half-width of the cavity mode. b) Cavity mode shifts after subtracting mirror dispersion, giving the molecular dispersion spectrum of the P-branch of the 0-3 CO band. c) Absorption spectrum obtained from fitted mode widths. Note the narrower useful range compared to the dispersion spectrum, coming from the better precision of the mode position measurement compared to mode width measurement.

References

[1] P. Maslowski et al., Phys. Rev. A 93, 021802(R), (2016).
[2]] L. Rutkowski et al., J. Quant. Spec. Radiat. Transf. 204 63-73, (2018).
[3] A. Cygan et al., Opt. Express 21, 29744-29754 (2013).
[4] A. Cygan et al., Opt. Express 23, 14472-14486 (2015).
[5] L. Rutkowski et al. Opt. Express 25, 21711-21718 (2017).

*Corresponding author: charczun@fizyka.umk.pl

A – 65

Positron scattering from benzene

J. Franz[*1], **K. Fedus**[2], **G. P. Karwasz**[2]

1. *Department of Theoretical Physics and Quantum Informatics, Faculty of Applied Physics and Mathematics, Gdansk University of Technology, Narutowicza 11/12, 80-233 Gdańsk, Poland*
2. *Institute of Physics, Faculty of Physics, Astronomy and Informatics, Nicolaus Copernicus University, Grudziadzka 5/7, 87-100 Toruń, Poland*

We are presenting calculations of cross sections for collisions of positrons with benzene molecules in the gas-phase. Several sets of cross sections are computed with multi-component density functional theory [1], [2] and the molecular R-matrix method [3] for collision energies below 10 eV. Our results are compared with cross sections from calculations by Occhigrossi and Gianturco [4] and from experiments by Sueoka [5], Makochekanwa *et al.* [6], Karwasz *et al.* [7], [8] and Zecca *et al.* [9].

This work is supported by the grant 2014/15/D/ST2/02358 of the Narodowe Centrum Nauki (National Science Center Poland) and by computer grants from the computer centers WCSS (Wroclawskie Centrum Sieciowo-Superkomputerowe, Politechnika Wroclawska) and TASK (Trójmiejska Akademicka Sieć Komputerowa Gdańsk).

References

[1] J. Franz, J. Math. Phys. **56**, 012104 (2015).
[2] J. Franz, Eur. J. Phys. D **71**, 44 (2017).
[3] J. Tennyson and J. Franz, *Low-energy electron and positron collisions with the R-matrix method* in E. A. G. Armour, J. Franz and J. Tennyson (Eds.), *Explicitly correlated wavefunctions*, CCP2, Daresbury, 32-38 (2006).
[4] A. Occhigrossi and F. A. Gianturco, J. Phys. B: At. Mol. Opt. Phys. **36**, 1383 (2003).
[5] O. Sueoka, J. Phys. B: At. Mol. Opt. Phys **21**, L631 (1988).
[6] C. Makochekanwa, O. Sueoka and M. Kimura, Phys. Rev. A **68**, 32707 (2003).
[7] G. P. Karwasz, D. Pliszka, A. Zecca and R. S. Brusa, J. Phys. B: At. Mol. Opt. Phys. **38**, 1 (2005).
[8] G. P. Karwasz, A. Karbowski, Z. Idziaszek and R. S. Brusa, Nucl. Instr. and Meth. in Phys. Res. B **266**, 471 (2008)
[9] A. Zecca A, N. Moser, C. Perazzolli, A. Salemi and M. J. Brunger, Phys. Rev. A **76**, 022708 (2007)

[*]Corresponding author: janfranz@pg.edu.pl

Doppler-limited and sub-Doppler cavity-enhanced complex refractive index spectroscopy

A. Cygan*[1], P. Wcisło[1], S. Wójtewicz[1], G. Kowzan[1], M. Zaborowski[1], D. Charczun[1], K. Bielska[1], R. S. Trawiński[1], R. Ciuryło[1], P. Masłowski[1], D. Lisak[1]

1. Institute of Physics, Faculty of Physics, Astronomy and Informatics, Nicolaus Copernicus University in Toruń, Grudziadzka 5, Torun 87-100, Poland

A full spectroscopic characterization of the analyte properties requires knowledge at the same time about absorptive and dispersive parts of the spectrum. In practice, however, due to straightforward experimental realization, absorption spectroscopy is much more extensively used to collect data on our Universe than dispersion. On the other hand, development of optical cavities and sub-Hz-level control of laser light frequency allows a convenient way to simultaneously measure absorption and dispersion of the sample with an excellent precision. This gave rise to new calibration-free spectroscopy techniques: cavity mode-width spectroscopy (CMWS) [1] and cavity mode-dispersion spectroscopy (CMDS) [2]. While the first method measures broadening of cavity modes due to absorption, the latter one records dispersive changes in cavity modes positions. The CMDS has an intrinsic advantage over widely used absorption spectroscopies. Its dependence on only one physical quantity - frequency enables to avoid fundamental limitations of light intensity measurements typical for absorption.

A sub-per-mille accuracy of spectral line-shape parameters is important for many applications, e.g providing reference data for interpretation of Earth [3] and other planets atmospheres [4], determination of molecules structure [5], isotopes mass ratio measurements [6] as well as basic study of molecular hydrogen [7],[8] important for QED tests [9] and constraints on some hypotheses on physics beyond the Standard Model [10]. In order to find a spectroscopy method most suitable for delivering high-accuracy reference spectra of weak molecular transitions we compared three cavity-enhanced techniques: CMWS, CMDS and well-established in high-accuracy measurements cavity ring-down spectroscopy (CRDS). Measurement conditions were chosen to cover both low-pressure Doppler and high-pressure collisional regime. With an excellent signal-to-noise ratio exceeding 20000 we have demonstrated that CMDS does not show any tendencies towards systematic errors in contrast to absorption methods. A sub-per-mille accuracy of line-shape parameters obtained in CMDS for a weak R23 transition in $3-0$ CO band has been shown in the full range of measurement conditions, including high-opacity of the sample for which accuracy of absorption methods drastically decreases. Moreover, application of the popular CRDS has to be limited to low absorptions due to limited-bandwidth of optical switches and detection systems [11],[12],[13]. We have also shown a wide dynamic range of CMDS that spans nearly six orders of magnitude up to absorptions of 10^{-4} cm^{-1}, not achievable for CRDS method.

Doppler-free saturation spectroscopy is a well-known tool for obtaining the most precise data on spectral line positions. This field of research is also dominated by measurements based on light intensity. To probe the weakest transitions cavity-enhanced absorption techniques are mostly used. As a consequence of saturation, both the decays of light measured in CRDS as well as the shapes of cavity modes recorded in CMWS experience distortion of shapes due to variable optical power in the cavity. We observed, increasing with the saturation parameter, systematic deviations from a Lorentzian profile of absorptive Lamb dips of R23 CO transition measured by CRDS and CMWS. Interestingly, in case of CMDS measurements the dispersive profiles of Lamb dips have shown very good agreement with the dispersive Lorentzian profile in the full investigated range of pressures (saturation parameters). This points to a high potential of CMDS for high-accuracy spectroscopy applications also under saturation conditions.

References

[1] A. Cygan *et al.*, Opt. Express **21**, 29744 (2013).
[2] A. Cygan *et al.*, Opt. Express **23**, 14472 (2015).
[3] D. R. Thompson *et al.*, J. Quant. Spectrosc. Radiat. Transfer **113**, 2265 (2012).
[4] P. F. Bernath, Phil. Trans. R. Soc. A **372**, 20130087 (2014).
[5] O. L. Polyansky *et al.*, Phys. Rev. Lett. **114**, 243001 (2015).
[6] I. Galli *et al.*, Phys. Rev. Lett. **107**, 270802 (2011).
[7] L.-G. Tao *et al.*, Phys. Rev. Lett. **120**, 153001 (2018).
[8] F. M. J. Cozijn *et al.*, Phys. Rev. Lett. **120**, 153002 (2018).
[9] E. J. Salumbides *et al.*, Phys. Rev. Lett. **107**, 043005 (2011).
[10] E. J. Salumbides *et al.*, Phys. Rev. D **87**, 112008 (2013).
[11] H. Huang, K. K. Lehmann, Appl. Phys. B **94**, 355 (2009).
[12] S. Wójtewicz *et al.*, Phys. Rev. A **84**, 032511 (2011).
[13] S. Wójtewicz *et al.*, Opt. Express **26**, 5644 (2018).

*Corresponding author: agata@fizyka.umk.pl

A – 67

SiO_2 microsphere whispering gallery mode resonators coated with ZnO

I. Brice[1], A. Atvars[1], K. Grundsteins[1], R. Viter[1], I. Iatsunskyi[2], J. Alnis[*1]
1. Institute of Atomic Physics and spectroscopy of the University of Latvia, Rainis Blvd. 19,Riga, LV-1586, Latvia
2. NanoBioMedical Centre, Adam Mickiewicz University, 85 Umultowska str., 61-614, Poznan, Poland

Optical whispering gallery mode resonators (WGMR) keep circulating light wave circulating inside thanks to the total internal reflection. WGMRs allow to significantly increase the effective path length of the light allowing to make gas sensors, or to detect molecules attaching to the surface in liquid [1].

We are melting SiO_2 microsphere resonators from a telecom fiber *Corning SMF-28* with an oxy-hydrogen torch or with a CO_2 laser. Spheres with diameters 300-500 μm are obtained (Fig. 1a) . We introduce light into the WGMR by prism coupling. For the excitation we use a tunable external cavity diode laser at 780 nm. We achieve optical Q factors at the 1E8 range (Fig. 1b).

For biosensing applications it is necessary to functionalize the surface to facilitate attachment of molecules. As the first layer we are coating the WGMR surface with ZnO and investigate the changes of optical Q factor. Atomic layer deposition technique was used to cover resonators with ZnO nanolayers of 5, 10, 20 and 100 nm thickness. Results show that the sharpest resonances (in the region of 780 nm) are seen when 20 nm ZnO nanolayer is used (Fig. 1c). It was observed that resonators covered with ZnO, unlike uncovered resonators, are not electrically attracted to the surface of prisms, which is an advantage for finding the best prism-resonator coupling distance. In future we plan to add antibody coatings on the top of ZnO.

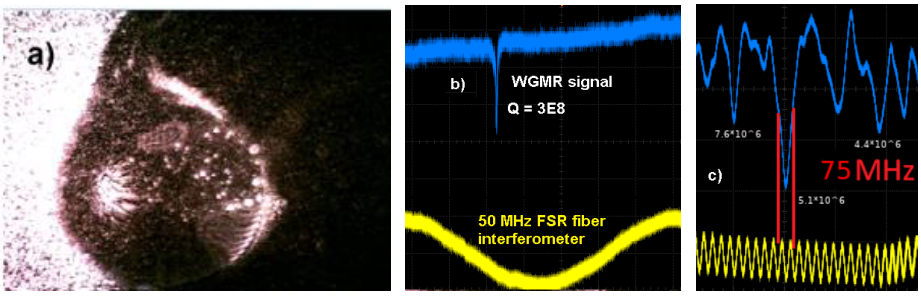

Fig. 1: a) 0.5 mm diameter SiO_2 microsphere with prism coupling of the light. On the right lower side a periodic annual ring structure is visible indicating that a higher order WGM resonance is excited. b) A resonance with Q = 3E8 and a 50 MHz interferometer trace used for the laser scan calibration. c) Resonances from a sphere coated with a 20 nm layer of ZnO have Q in the 10^6 range.

LV team thanks for support ERAF project Nr.1.1.1.1/16/A/259: “Development of novel WGM microresonators for optical frequency standards and biosensors, and their characterization with a femtosecond optical frequency comb”.

References

[1] F. Vollmer, S. Arnold, “Whispering-gallery-mode biosensing: label-free detection down to single molecules”, Nature Methods 5, 591–596 (2008).
[2] I. Brice, A. Pirktina, A. Ubele, K. Grundsteins, A. Atvars, R. Viter, J. Alnis, “Development of optical WGM resonators for biosensors”, Proc. of SPIE, 105920B-1 (2017).

[*]Corresponding author: janis.alnis@lu.lv

High-accuracy deuterium spectroscopy and comparison with *ab initio* line-shape calculations

M. Zaborowski*[1], F. Thibault[2], S. Wójtewicz[1], A. Cygan[1], G. Kowzan[1], P. Masłowski[1], M. Słowiński[1], A. Nishiyama[1,3], N. Stolarczyk[1], D. Lisak[1], R. Ciuryło[1], P. Wcisło[1]

1. Institute of Physics, Faculty of Physics, Astronomy and Informatics, Nicolaus Copernicus University in Toruń, Grudziadzka 5, 87-100 Torun, Poland

2. Institut de Physique de Rennes, UMR CNRS 6251, Université de Rennes 1, Campus de Beaulieu, Bât.11B, F-35042 Rennes, France

3. Department of Engineering Science, Graduate School of Informatics, The University of Electro-Communications (UEC), 1-5-1 Chofugaoka, Chofu, Tokyo 182-8585, Japan

Molecular hydrogen is the simplest chemically neutral system and therefore most appropriate for testing quantum electrodynamics (QED) for molecules as well as for searching for physics beyond the Standard Model [1]. The uncertainties of the *ab initio* calculated wave-numbers corresponding to H_2, HD or D_2 rovibrational transitions are reaching a few times 10^{-5} cm^{-1} [2], [3], [4]. It puts high demands on spectroscopic meassurements [3], [5], [6]. With our experimental strategy utilizing cavity-enhanced spectroscopy, we have accomplished sub-MHz accuracy on the weak quadrupole line position, despite operating in the Doppler-limited regime [4]. However, the determination of the line position was heavily affected by the line-shape effects leading to its asymmetry [7].

We present new results of applying this approach to the experimental determination of the energies of weak quadrupole transitions in molecular hydrogen isotopologues. We applied *ab initio* quantum scattering calculations to describe the collisional line-shape effects and performed measurements in several pressures to obtain determination of the line position free from systematic errors caused by incorrect line-shape characterisation. Furthermore, we extended our experiments to a wide range of temperatures and validated temperature dependences of line-shape effects. Line S(2) 2-0 of D_2 has been measured by the frequency-stabilized cavity ring-down spectroscopy (FS-CRDS) assisted by an optical frequency comb (OFC) [8], [9], using experimental setup described in Refs. [10], [11].

The project is supported by the National Science Centre, Poland, Project Nos. 2015/19/D/ST2/02195 and 2015/17/B/ST2/02115. The research effort is part of the program of the National Laboratory FAMO in Torun, Poland. The research effort is also supported by the COST Action CM1405 MOLIM.

References

[1] W. Ubachs, J.C.J. Koelemeij, K.S.E. Eikema, and E.J. Salumbides, J. Mol. Spec. *320*, 1-12 (2016).
[2] M. Puchalski, J. Komasa, and K. Pachucki, Phys. Rev. A **95**, 052506 (2017).
[3] L.-G. Tao, A.-W. Liu, K. Pachucki, J. Komasa, Y. R. Sun, J. Wang, and S.-M. Hu, Phys. Rev. Lett. **120**, 153001 (2018).
[4] P. Wcisło, F. Thibault, M. Zaborowski, S. Wójtewicz, A. Cygan, G. Kowzan, P. Masłowski, J. Komasa, M. Puchalski, K. Pachucki, R. Ciuryło, and D. Lisak, J. Quant. Spectrosc. Radiat. T **213**, 41-51 (2018).
[5] D. Mondelain, S. Kassi, T. Sala, D. Romanini, D. Gatti, and A. Campargue, J. Mol. Spectrosc. **326**, 5 (2016).
[6] F. M. J. Cozijn, P. Dupre, E. J. Salumbides, K. S. E. Eikema, and W. Ubachs, Phys. Rev. Lett. **120**, 153001 (2018).
[7] P. Wcisło, I. E. Gordon, C.-F. Cheng, S.-M. Hu, and R. Ciuryło, Phys. Rev. A **93**, 022501 (2016).
[8] J. Domysławska, S. Wójtewicz, D. Lisak, A. Cygan, F. Ozimek, K. Stec, Cz. Radzewicz, R. S. Trawiński, and R. Ciuryło, J. Chem. Phys. **136**, 024201 (2012).
[9] D. A. Long, A. Cygan, R.D. van Zee, M. Okumura, C.E. Miller, D. Lisak, and J.T. Hodges, Chem. Phys. Lett. **536**, 1 (2012).
[10] A. Cygan, S. Wójtewicz, M. Zaborowski, P. Wcisło, R. Guo, R. Ciuryło, and D. Lisak , Meas. Sci. Technol. **27**, 045501 (2016).
[11] M. Zaborowski, P. Wcisło, F. Thibault, S. Wójtewicz, A. Cygan, G. Kowzan, P. Masłowski, D. Lisak, and R. Ciuryło, J. Phys. Conf. Ser. **810**, 012042-1-4 (2017).

*Corresponding author: zaborowski@fizyka.umk.pl

Unshielded Atomic Magnetometry – Building a Portable, Compact Device

C. O'Dwyer*[1], S.J. Ingleby, A.S. Arnold, P.F. Griffin, E. Riis
1. Department of Physics, SUPA, University of Strathclyde, 107 Rottenrow East, Glasgow, UK

The field of optically-pumped magnetometry has seen rapid progress in the past decade. In order to move from well established lab-based experiments to field-ready instruments we are developing an unshielded, portable Mx magnetometer for use in a range of environments, from medical, (e.g. magnetocardiography, magnetoencephalography) to maritime defence and geophysical applications, (e.g. geology, archaeology). The double resonance technique presented here uses a single laser beam to pump thermal caesium vapour as well as phase sensitively probe its coherent precession in the presence of an RF field [1].

We aim to minimise hardware while prioritising sub-picoTesla sensitivities. Component miniaturisation is key – optimisation and characterisation of micro-fabricated alkali vapour cells is reported, and the effects of operation temperature and buffer gas pressure discussed. We introduce a novel feed-forward noise suppression technique for operation in magnetically noisy environments, in particular those dominated by 50 Hz noise.

We have achieved signal resolution in the parts per million against a background comparable to the Earth's field, observing noise suppression of 20 dB. Here we present the techniques used to achieve this, as well as potential applications.

This work is funded by the UK Quantum Technology Hub in Sensors and Metrology.

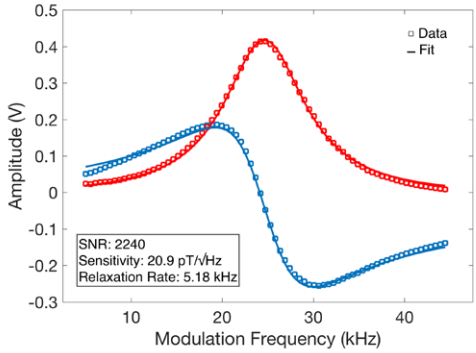

Fig. 1: Measured data and fits to the in-phase and quadrature components of the magnetic resonance signal. A 300 nT RF modulation field is applied across a range of frequencies and a resonant response observed in the presence of a 7 μT static field.

References

[1] S. J. Ingleby, P. F. Griffin, A. S. Arnold, M. Chouliara, E. Riis, *High-precision control of static magnetic field magnitude, orientation, and gradient using optically pumped vapour cell magnetometry*, Review of Scientific Instruments. **88**, (2017).

*Corresponding author: carolyn.odwyer@strath.ac.uk

Optically-pumped cesium magnetometer in a semi-shielded magnetic environment

Marek Kopciuch [1], **Irena Rodzoń** [1], **Szymon Pustelny** [1]
1. Marian Smoluchowski Institute of Physics, 11, Kraków 30-348, Poland

One of the most practicable feature of a hot atomic vapour is the prospect of very precise and sensitive measurement of a weak magnetic field. Magnetometry in the hot atomic vapour is based on the fact that external magnetic fields may modify the optical properties of a magneto-optically active medium, such as optically-pumped alkali vapour, and by the detection of the light state, the magnetic field can be determined. [1].

We present our activities aiming at a construction of an optically-pumped magnetometer employing hot cesium vapour as a magneto-optically active medium. The device is operated in a semi-shielded magnetic environment and hence becomes the sensor predominantly driven by external magnetic field (field noise). In our scheme, the optically-pumped magnetometer operates in the so-called M_x scheme, i.e., it uses absorption of resonant light propagating through the cesium vapour subjected to the external magnetic field, to measure magnetic-level splitting arising due to the Zeeman effect. Placing the sensor in a single-layer mumetal tube without endcaps provides reduction of transversal fields, which deteriorate on the magnetometerperformance, while the sensor itself operates in a field determined by the Earth magnetic field.

The described sensor is designed to operate as a veto sensor for the Krakow station of the Global Network of Optical Magnetometer for Exotic physics search [2]. The network searches for hitherto undiscovered exotics spin couplings, which would induce a torque on spins and hence affect readouts of the main sensor which is magnetometer enclosed in a 4-layer mumetal shield. Application of the M_x magnetometer enables discrimination of the main sensor associated with real magnetic fields and identify false-positive signals recorded by the network.

References

[1] D. Budker, D. Jackson Kimball, (Eds.), *Optical Magnetometry*, Cambridge, Cambridge University Press, (2013).
[2] S. Pustelny et.al., Ann. Phys. (Berlin) 525, 659-670, (2015).

Autoionizing States of Mg in the Problem of Electron-impact Ionization of Atom

I. Moshkola[*1], **V. Simulik**[†2], **T. Zajac**[1]

1. Department of Electronic Systems, Engineering-technical Faculty, Uzhgorod National University, Kapitulna Street 13, 88000 Uzhgorod, Ukraine

2. Institute of Electron Physics, National Academy of Sciences, Universitetska Street 21, 88000 Uzhgorod, Ukraine

The method of interacting configurations in complex numbers representation (MICCNR) has been developed in [1]–[4]. The first application to the photoionization and electron-impact ionization of He has been suggested. Below the investigated atomic system is more complicated. For instance, the MICCNR is applied to the investigation of the electron-impact ionization of Mg in the autoionizing states (AIS) formation region. The spectra of losses in the problem of electron-impact ionization of atom are considered. The calculations of that kind are relevant in the analysis of radiation and elementary particles interaction with matter including the interaction of cosmic rays with metallic surfaces. In addition to the MICCNR the energetic positions and widths of AIS are calculated in the method of interacting configurations in real numbers representation (MICRNR), in the diagonalization approximation (DA) and in the complex diagonalization approximation (CDA) [2].

The energetic positions and widths of the lowest ^{1}S, ^{1}P, ^{1}D, ^{1}F AIS of Mg calculated in the problem of electron-impact ionization of Mg are presented in the Table below. The four different approximations are used: MICCNR, MICRNR, DA and CDA.

Table 1: The energetic positions and widths of the lowest ^{1}S, ^{1}P, ^{1}D, ^{1}F AIS of Mg in the problem of electron-impact ionization of atom. Calculations in different methods: MICCNR is the method of interacting configurations in complex numbers representation, MICRNR is the method of interacting configurations in real numbers representation, DA is the diagonalization approximation, CDA is the complex diagonalization approximation.

Methods	MICCNR	MICCNR	MICRNR	MICRNR	DA	DA	CDA	CDA
Lowest AIS	E, eV	Γ, eV	E, eV	Γ, eV	E, eV	Γ, eV	E, eV	Γ, eV
^{1}S	13,08	0,0987	13,09	0,0981	13,06	0.0329	0.0329	0.0329
^{1}P	14,15	0,1574	14,16	0,1570	14,17	0.0329	0.0329	0.0329
^{1}D	13,62	0.2633	13,64	0,2623	13,65	0.0329	0.0329	0.0329
^{1}F	14,63	0,0225	14,66	0,0220	14,64	0.0329	0.0329	0.0329

Some results of other atomic systems investigations can be found in [5]. The different modern calculation methods of AIS are observed briefly. The choice of the ground state wave function for the calculation of AIS is discussed in [6].

References

[1] S. Burkov, N. Letyaev, S. Strakhova and T. Zajac, J. Phys. B: At. Mol. Opt. Phys. **21**, 1195 (1988).
[2] S. Burkov, S. Strakhova and T. Zajac, J. Phys. B: At. Mol. Opt. Phys. **23**, 3677 (1990).
[3] T. Zajac, Uzhgorod Univ. Sci. Herald, Ser. Phys. **11**, 72 (2002).
[4] T. Zajac and V. Simulik, Int. J. Pure. Appl. Phys. **3**, 243 (2007).
[5] V. Simulik, R. Tymchyk, and T. Zajac, Univ. J. Phys. Appl. **11**, 162 (2017).
[6] T. Zajac, V. Simulik and R. Tymchyk, Tech. Phys. **88**, 970 (2018).

[*]Corresponding author: moshkola96@gmail.com
[†]Corresponding author: vsimulik@gmail.com

Magnetocardiography

I. Rodzoń[*1], **M. Kopciuch**[1], **S. Pustelny**[1]
1. Department of Photonics, Institute of Physics, Jagiellonian University, S. Łojasiewicza Street 11, 30-348 Kraków, Poland

Magnetocardiography (MCG) is a relatively new and incredibly precise medical diagnostic method. It was discovered by Baule and McFee in 1966, over 60 years after the first electrocardiographic (ECG) measurement performed by Einthoven [1]. Compared to traditional diagnostic methods, such as heart echo or ECG, MCG allows completely non-invasive, contact-free measurements. Detection of the magnetic field produced by a human heart makes possible diagnose of possible cardiopathies in fetus as well as implementation of the technique for people with burned chests [2]. In addition, by performing the MCG examination, it is possible to have a much earlier detection of myocardial ischemic diseases and perform precise location of the arrhythmia foci [3].

Detection of biomagnetic fields, which just next to the human body reach a maximum field of to 100 pT, requires application of the most sensitive magnetometers. With this respect, optical magneomteters, routinly reaching sensitivity at a $\mathrm{fT/Hz^{1/2}}$ level, are promising candidates for the application. The devices are based on detection of properties of light (intensity or polarization) traversing a medium subjected to the magnetic field. An example of the phenomenon exploited in optical magnetometers is non-linear magneto-optical rotation. In this case, the polarization rotation of linearly polarized light, passing a medium (atomic vapor), provides information about the magnetic field.

In the Photonics Department of the Institute of Physics of the Jagiellonian University in Kraków, we measure the magnetic field from a human heart using optical magnetometers using rubidium vapor. The field is measured by detecting polarization rotation but a novel scheme for optical pumping of atoms, using a rotating linear polarization, is implemented. If the rotation is synchronized with the magnetically-induced precession of spins, strong, dynamic anisotropy of the medium is induced. The anisotropy is stronger than the one generated with intensity or amplitude-modulated light. This difference is particularly pronounced at the Earth magnetic field, i.e. the field important for many practical applications [4]. In our presentation, we will also describe experimental apparatus in details, and present the recent results obtained with the rotating-polarization magnetometer. During the presentation, we will demonstrate detection of the magnetic signals from a human heart, in particular, mapping of the field above the chest will be presented. We will also present our plans, aiming at generation of three-dimensional maps of the magnetic field generated by the heart as well as detection of possible lesions in the organ.

References

[1] G. Baule, R. McFee, *Detection of the magnetic field of the heart*, American Heart Journal, 66, 95-96, 1963.
[2] D. Budker, D. F. Jackson Kimball, *Optical magnetometry*, Cambridge University Press, Cambridge 2013.
[3] P. Augustyniak, *Elektroniczna aparatura medyczna*, Wydawnictwo Akademii Górniczo – Hutniczej, Kraków 2015.
[4] P. Włodarczyk, *Podzespoły elektroniczne i optoelektroniczne w magnetometrii atomowej*, praca doktorska, Akademia Górniczo – Hutnicza, 2016.

*Corresponding author: irena.rodzon@gmail.com

Poster session B

Time Crystal Behavior of Excited Eigenstates

A. Syrwid[*1], **J. Zakrzewski**[1,2], **K. Sacha**[1,2]

1. Instytut Fizyki imienia Mariana Smoluchowskiego, Uniwersytet Jagielloński, ulica Profesora Stanisława Łojasiewicza 11, PL-30-348 Kraków, Poland

2. Mark Kac Complex Systems Research Center, Uniwersytet Jagielloński, ulica Profesora Stanisława Łojasiewicza 11, PL-30-348 Kraków, Poland

In analogy to spontaneous breaking of continuous space translation symmetry in the process of space crystal formation, it was proposed that spontaneous breaking of continuous time translation symmetry could lead to time crystal formation. In other words, a time-independent system prepared in the energy ground state is expected to reveal periodic motion under infinitely weak perturbation. In the case of the system proposed originally by Wilczek [1], spontaneous breaking of time translation symmetry cannot be observed if one starts with the ground state. We point out that the symmetry breaking can take place if the system is prepared in an excited eigenstate. The latter can be realized experimentally in ultracold atomic gases. We simulate the process of the spontaneous symmetry breaking due to measurements of particle positions and analyze the lifetime of the resulting symmetry broken state [2].

References

[1] F. Wilczek, Phys. Rev. Lett. **109**, 160401 (2012).

[2] A. Syrwid, J. Zakrzewski, K. Sacha, Phys. Rev. Lett. **119**, 250602 (2017).

*Corresponding author: asyrwid@gmail.com

Dynamical quantum phase transitions in discrete time crystals

A. Kosior[*1], **K. Sacha**[1,2]
1. Instytut Fizyki imienia Mariana Smoluchowskiego, Uniwersytet Jagielloński, ul. Łojasiewicza 11, PL-30-348 Kraków, Poland
2. Mark Kac Complex Systems Research Center, Uniwersytet Jagielloński, ul. Łojasiewicza 11, PL-30-348 Kraków, Poland

Discrete time crystals are related to non-equilibrium dynamics of periodically driven quantum many-body systems where the discrete time translation symmetry of the Hamiltonian is spontaneously broken into another discrete symmetry [1]. Recently, the concept of phase transitions has been extended to non-equilibrium dynamics of time-independent systems induced by a quantum quench, i.e. a sudden change of some parameter of the Hamiltonian. There, the return probability of a system to the ground state reveals singularities in time which are dubbed dynamical quantum phase transitions [2]. We show that the quantum quench in a discrete time crystal leads to dynamical quantum phase transitions where the return probability of a periodically driven system to a Floquet eigenstate before the quench reveals singularities in time [3]. It indicates that dynamical quantum phase transitions are not restricted to time-independent systems and can be also observed in systems that are periodically driven.

References

[1] K. Sacha, J. Zakrzewski, Rep. Prog. Phys. **81**, 016401 (2018)
[2] M. Heyl, arXiv:1709.07461
[3] A. Kosior, K. Sacha, arXiv:1712.05588

*Corresponding author: arkadiusz.kosiork@euj.edu.pl

Cooperative Effects in Atomic Ensembles Located in a Fabry-Perot cavity and near a Single Mirror

A. S. Kuraptsev[*1], **I. M. Sokolov**[1,2]

1. Peter the Great St. Petersburg Polytechnic University, Polytechnicheskaya st. 29, 195251 St. Petersburg, Russia
2. Institute for Analytical Instrumentation, Russian Academy of Sciences, Ivana Chernykh st. 31, 198095 St. Petersburg, Russia

Since the seminal work of Purcell [1] light interaction with atoms localized inside a cavity or waveguide as well as near its surface has attracted a considerable attention. Now it is understood that a cavity modifies the spatial structure of modes of electromagnetic field. This leads to modification in radiative properties of atoms, in particular, to the enhancement and inhibition of the spontaneous decay rate. Therefore one has an exciting tool to control over the atomic radiative properties by choosing the cavity parameters appropriately. Light matter interaction in the presence of nanophotonic structures, such as nanofibers, photonic crystal cavities and waveguides propose future applications for quantum metrology, scalable quantum networks and quantum information science.

Modification of the spatial structure of field modes causes changes not only in the spontaneous decay rate but also in the nature of photon exchange between different atoms. In its turn it leads to alteration in dipole-dipole interatomic interaction as well as associated cooperative effects. Dipole-dipole interaction plays an important role in the case of dense atomic ensembles, in which the interatomic distance is comparable with the wavelength of resonant radiation. Cooperative effects cause density-dependent shifts of atomic transition as well as distortion of spectral line shape. This influences both on the properties of atoms as well as on scattered radiation characteristics.

In fact, not only cavity can modify the modes of electromagnetic field, but also any conductive device has this property, in particular, metallic conductive surface. For this reason optical properties of atomic ensemble located near a single mirror differ from ones in the case of the same ensemble in free space.

We have developed a consistent quantum approach to describe cooperative polyatomic effects in dense atomic ensembles located in a Fabry-Perot cavity or near a single mirror [2],[3]. This approach is based on the solution of the non-steady-state Schrodinger equation for the wave function of the joint system consisting of all atoms and a weak electromagnetic field including the vacuum reservoir. On the basis of the general theory we study the excitation dynamics of an ensemble of motionless point atoms located in a Fabry-Perot cavity with perfectly conducting mirrors as well as near a single mirror.

Fig. 1 shows the time dependence of the total excited state population and the cooperative decay rate both for the ensemble in free space and in the Fabry-Perot cavity with the distance between the mirrors $d = 3$. We consider the inversed wave number of radiation resonant to the atomic transition, k_0^{-1}, as a unit of length. Wee see that cooperative decay dynamics is described by multiexponential law, and the cooperative decay rate depends on time. Furthermore, we observe, that all the curves differ from each other. The total excited state population in the case of a microcavity decreases slower than one in the case of free space. Besides that, the decay rate of Zeeman sublevels $m = \pm 1$ in a cavity is less than one of the sublevel $m = 0$. It is connected with mentioned features of the field modes structure in the cavity.

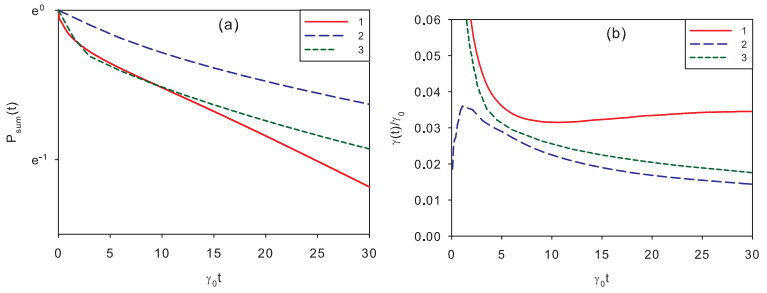

Fig. 1: Time dependence of the total excited state population (a), cooperative decay rate (b). Atomic density $n = 0.1$, the radius a sample $R = 14$. 1, free space; 2, microcavity, $d = 3$, $m = \pm 1$; 3, microcavity, $d = 3$, $m = 0$.

References

[1] E. M. Purcell, Proceedings of the American Physical Society **69**, 681 (1946).
[2] A. S. Kuraptsev, and I. M. Sokolov, Journal of Experimental and Theoretical Physics **112**, 237 (2016).
[3] A. S. Kuraptsev, and I. M. Sokolov, Phys. Rev. A **94**, 022511 (2016).

*Corresponding author: aleksej-kurapcev@yandex.ru

B – 3

Time-resolved Analysis of the NV Centers' Fluorescence Dynamics

M. Gieysztor*[1], M. Mrózek[2], K. Sycz[2], A. Kruk[2], W. Gawlik[2], P. Kolenderski [1]

1. Institute of Physics, Faculty of Physics, Astronomy and Informatics, Nicolaus Copernicus University, Grudziadzka 5, 87-100 Toruń, Poland

2. Institute of Physics, Faculty of Physics, Astronomy and Informatics, Jagiellonian University, Reymonta 4, 30-059 Kraków, Poland

Nitrogen-vacancy (NV) center emerges as an important system exhibiting promising properties for applications in quantum technologies, including quantum information processing, quantum metrology as well as single photon sources. Research on these defects is held since 60's, but the underlying physics is still not fully understood.

In our work, we investigate the dynamics of NV centers excited by pulsed laser (140 fs, 80 MHz repetition rate) tuned over the 382-530 nm range. By means of time-resolved fluorescence measurements we are able to establish the fluorescence decay rate. The experimental setup is shown in Fig. 1. The sample is studied in a home-built confocal microscope. Photon detection is realized by single photon detection modules.

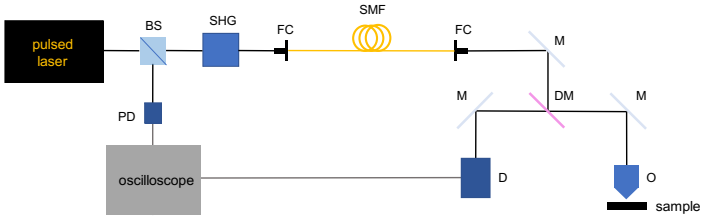

Fig. 1: Experimental setup. BS - beam splitter, SHG - second harmonic generation, FC - fiber coupler, SMF - single mode fiber, M - mirror, DM - dichroic mirror, PD - photodiode, D - detector, O - objective.

As a result, we obtain a histogram of the delay of the single photon detector (D) click with respect to the reference photodiode (PD) signal. To model NV centers' behaviour we use a double-exponential decay model, assuming fast non-radiative decay followed by a radiative one (time constants τ_C and τ_N). A very peculiar wavelength dependence of τ_C and τ_N is observed, as shown in Fig. 2.

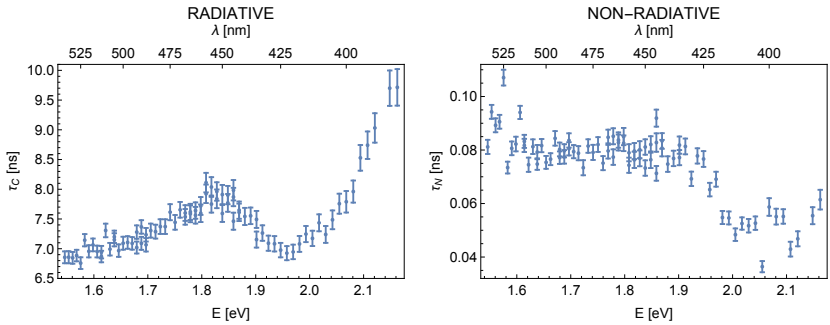

Fig. 2: Radiative (τ_C) and non-radiative (τ_N) decay rates as a function of λ/E.

*Corresponding author: maria.gieysztor@fizyka.umk.pl

B – 4

Photoionization Microscopy: Energy Dependence of Slow-Photoelectron Momentum Distributions

P. Kalaitzis[*1], S. Danakas[1], F. Lépine[2], C. Bordas[2], S. Cohen[†1]
1. Atomic and Molecular Physics Laboratory, Physics Department, University of Ioannina, 45110 Ioannina, Greece
2. Institut Lumière Matière, Université Lyon 1, CNRS, UMR 5306, 10 rue Ada Byron 69622 Villeurbanne Cedex, France

Photoionization microscopy [1,2,3,4,5,6] (PM) is an experimental method allowing for the measurement of the slow (meV) electron current probability density in the case of photoionization of an atom in a static electric field. PM provides access to the quantum oscillatory, radial as well as angular, spatial structure of the outgoing electron flux. The structure of the angularly-integrated differential ionization cross-section of the photoelectron is also of great interest. The latter corresponds to the electron's momentum distribution transversely to the electric field. We examine this distribution as a function of electron energy and radius of impact on the detector. Near the ionization threshold, this two-dimentional map is dominated by intense quantum interference and beating effects. Quantum mecahnical calculations concerning the hydrogen atom will be presented at the conference. They will include maps obtained for the ground and excited initial states and single- and two-photon ionization. Furthermore, these results will be discussed in connection with other calculations at very high DC-field strengths [7], experimental data concerning the hydrogen atom [8] and our magnesium atom measurements [9].

Authors acknowledge support of this work by the project ''ELI - LASERLAB Europe Synergy, HiPER & IPERION-CH.gr" (MIS 5002735) which is implemented under the Action ''Reinforcement of the Research and Innovation Infrastructure", funded by the Operational Programme ''Competitiveness, Entrepreneurship and Innovation" (NSRF 2014-2020) and co-financed by Greece and the European Union (European Regional Development Fund).

References

[1] V. D. Kondratovich and V. N. Ostrovsky, J. Phys. B **23**, 3785 (1990).
[2] C. Nicole, H. L. Offerhaus, M. J. J. Vrakking, F. Lépine, and C. Bordas, Phys. Rev. Lett. **88**, 133001 (2002).
[3] S. Cohen, M. M. Harb, A. Ollagnier, F. Robicheaux, M. J. J. Vrakking, T. Barillot, F. Lépine, and C. Bordas, Phys. Rev. Lett. **110**, 183001 (2013).
[4] S. Cohen, M. M. Harb, A. Ollagnier, F. Robicheaux, M. J. J. Vrakking, T. Barillot, F. Lépine, and C. Bordas, Phys. Rev. A **94**, 013414 (2016).
[5] A. S. Stodolna, A. Rouzée, F. Lépine, S. Cohen, F. Robicheaux, A. Gijsbertsen, J. H. Jungmann, C. Bordas, and M. J. J. Vrakking, Phys. Rev. Lett. **110**, 213001 (2013).
[6] A. S. Stodolna, F. Lépine, T. Bergeman, F. Robicheaux, A. Gijsbertsen, J. H. Jungmann, C. Bordas, and M. J. J. Vrakking, Phys. Rev. Lett. **113**, 103002 (2014).
[7] S. Ohgoda, O. I. Tolstikhin and T. Morishita, Phys. Rev. A **95**, 043417 (2017).
[8] A. S. Stodolna, F. Lépine, A. Rouzée, S. Cohen, A. Gijsbertsen, J. H. Jungmann-Smith, C. Bordas and M. J. J. Vrakking, J. Phys. B **50**, 164001 (2017).
[9] P. Kalaitzis, S. Danakas, F. Lépine, C. Bordas, and S. Cohen, submitted.

[*]Corresponding author: pkalaitz@cc.uoi.gr
[†]Corresponding author: scohen@uoi.gr

Autoionization cross section of Sr atoms excited by electron impact

V. Borovik[*1], **A. Kupliauskienė**[†2], **I. Shafranyosh**[1], **O. Borovik**[1,3]
1. Uzhgorod National University, Voloshina Street 54, 88000 Uzhgorod, Ukraine
2. Institute of Theoretical Physics and Astronomy, Vilnius University, Saulėtekio av. 3, LT-10257 Vilnius, Lithuania
3. Institute of Electron Physics, Universitetska Street 21, 88017 Uzhgorod, Ukraine

Excitation of outer p^6-shell electrons into autoionizing levels followed by electron decay (excitation-autoionization process) enhances significantly the single ionization cross section of alkali-earth atoms [1], [2]. In strontium, the rapid rise of the cross section by more than 16% is observed just above the excitation threshold of the $4p^6$ shell [2]. As was shown earlier for alkali atoms [3], the excitation-autoionization cross section for a particular inner-shell excitation process can be obtained experimentally by accurate measuring the total intensity of ejected-electron spectra arising from the decay of contributed autoionizing states. In the present work we report the first data on the $4p^6$-shell autoionization cross section of strontium atoms.

The ejected-electron spectra arising from the decay of the $4p^5 n_1 l_1 n_2 l_2 n_3 l_3$ atomic autoionizing states in strontium were measured at the 'magic' angle of 54.7° for the incident electron energies from the $4p^6$ excitation threshold at 20.98 eV up to 600 eV. The measurements were performed by using the apparatus described in detail elsewhere [4]. The obtained relative data were put on the absolute scale by normalizing the excitation function of the $4p^5 4d5s^2\ ^3P_1$ state to the calculated cross section at 600 eV [4]. The summary relative error did not exceed 30%.

Figure 1 shows the autoionization cross section σ_{aut} of strontium atoms in an impact energy range 15-650 eV. As can be seen, the dominant feature of the cross section is the strong near-threshold maximum containing "fine" structures *a*, *b*. The cross section reaches the maximum value $1.6\times10^{-16} cm^2$ at 24.8 eV (feature *a*).

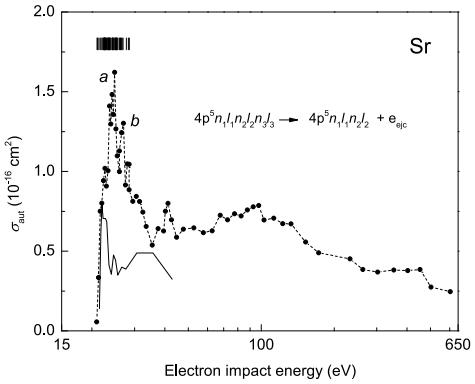

Fig. 1: The $4p^6$ autoionization cross section σ_{aut} (dots) and the sum of excitation cross sections of the states $4p^5 4d5s^2\ ^3P_1$, $^3P_2$ and $^3F_4$ (line) of Sr atoms excited by electron impact. Bars on top mark the location of the $4p^5 n_1 l_1 n_2 l_2 n_3 l_3$ *LSJ* autoionizing states [4].

The comparison of the σ_{aut} cross section with the sum of excitation cross sections of the states $4p^5 4d5s^2\ ^3P_1$, $^3P_2$ and $^3F_4$ [5] (which are the most effectively excited states at low impact energies) shows that just they contribute to the autoionization cross section in a narrow impact energy region up to 3 eV above the $4p^6$ excitation threshold. The strong resonance behavior of the σ_{aut} cross section reflects the presence of strong negative-ion resonances in the near-threshold excitation of the $4p^5 n_1 l_1 n_2 l_2 n_3 l_3$ states.

References

[1] Y. Okuno J. Phys. Soc. Jap. **31**, 1189 (1971).
[2] L. Veinshtein *et al.*, Sov. Phys. -JETP **34**, 271 (1972).
[3] M. Evrij *et al.*, Nucl. Instrum. Methods B **233**, 280 (2005).
[4] A. Kupliauskienė *et al.*, J. Phys. B: At. Mol. Opt. Phys. **50**, 225201 (2017).
[5] A. Borovik, V. Vakula, A. Kupliauskienė Lith. J. Phys. **47**, 129 (2007).

*Corresponding author: v.borovik@gmx.de
†Corresponding author: alicija.kupliauskiene@tfai.vu.lt

Precision Mass Measurements of Neon Isotopes at THe-Trap

T. Segal[*1], **M. Hoecker**[†1], **J. Ketter**[‡1], **M. Schuh**[§1], **S. Streubel**[¶1], **K. Blaum**[‖1]
1. Max-Planck-Institut für Kernphysik, Heidelberg, Germany

THe-Trap is a precision Penning-trap mass spectrometer [1] installed at the Max-Planck-Institut für Kernphysik (MPIK) in Heidelberg. It aims to solve the 4-σ discrepancy in the mass measurements of helium-3 [2][3]. Left unresolved, the discrepancy increases the uncertainties of the hydrogen and deuterium masses, as well as the values of physical constants such as h, k_B and N_A. To check for systematic uncertainties which might explain the discrepancy, a precision mass measurement of ^{20}Ne will be performed which will utilize the methods of the two latest He-3 mass measurements called “sweeps” [1] and “PnP” (Pulse n’ Phase) [4]. In addition, a precision mass measurement of ^{22}Ne with a relative uncertainty of 10^{-10} is planned which will improve upon the existing value by about an order of magnitude. A new gas injection system was developed in preparation for the measurement. To test it, neon gas was successfully injected into the trap region and ionized by a field emission point. The produced ions were trapped and their cyclotron frequency measured. The measurement process will be presented, as well as preliminary mass results for ^{20}Ne and ^{22}Ne.

References

[1] S. Streubel *et al.*, Applied Physics B: Lasers and Optics (2014), 114(1-2), 137-145
[2] R.S. Van Dyck *et al.*, Metrologia (2015), Volume 52, Number 2
[3] E.G. Meyers *et al.*, Phys. Rev. Lett (2015), 144, 013003
[4] S. Sturm *et al.*, Phys. Rev. Lett (2011), 107, 143003

[*]Corresponding author: tom.segal@mpi-hd.mpg.de
[†]Corresponding author:
[‡]Corresponding author:
[§]Corresponding author:
[¶]Corresponding author:
[‖]Corresponding author:

On the use of the Partition Correlation Function Interaction method for atomic properties

S. Schiffmann[*1], **G. Gaigalas**[2], **M. Godefroid**[1], **P. Jönsson**[3]
1. Chimie Quantique et Photophysique, C.P. 160/09, Université Libre de Bruxelles (ULB), B-1050 Brussels, Belgium
2. Vilnius University, Institute of Theoretical Physics and Astronomy, Saulėtekio av. 3, LT-10222, Vilnius, Lithuania
3. Material Science and Applied Mathematics, Malmö University, S-20506 Malmö, Sweden

We investigate the electron correlation in various systems such as Be I or Ne I with the Partition Correlation Function Interaction (PCFI) method [1]. This approach was successfully implemented a few years ago in the non-relativistic framework of the Atomic Structure Package (ATSP2K) [2] and is currently developed in the general-purpose relativistic atomic structure package (GRASP2K) [3]. When applying this methodology, the active space built to describe the atomic state is partitioned in different Partition Correlation Functions (PCFs) targeting specific correlation effects. Since each PCF is optimized independently, the orthogonality constraints between orbitals of different PCFs are no longer needed. These non-orthogonalities provide additional freedom in the orbitals basis to capture more efficiently the electron correlation [4] but their treatment requires the application of biorthonormal transformations followed by counter-weight transformations [5] in order to compute matrix elements. The latter might be time consuming, especially when the PCFs are deconstrained, strenghtening the need to develop new methodologies.

To gain efficiency, the PCFs should be shaped for the targeted correlation. As illustrated in Fig. 1, the correlation orbitals basis optimized to describe core correlation or valence correlation are spatially different. Therefore, computing these effects separately with the PCFI method, should be more efficient than classical multi-configurational approaches. In addition, the relative influence of the excitation families depends on the atomic property considered. For this reason, we investigate the PCFI method through specific mass shifts as well as hyperfine structures, in addition to the total energies.

The closed-shell structures of Ne I and Be I allow to investigate specific pair correlations [6] and develop new strategies to include triple and quadruple excitations. Amongst them, we explore the possibility to include these excitations explicitly in the few first layers before generating the PCFs, creating a large reference orbital basis. This approach reduces the benefit of the PCFI method by raising the number of orthogonality constraints for each correlation orbitals, leading to less spatial flexibility. To recover variational freedom, these reference orbitals can be included in the self-consistent field process. This forces us to treat the PCFI interaction problem as the generalized eigenvalue problem.

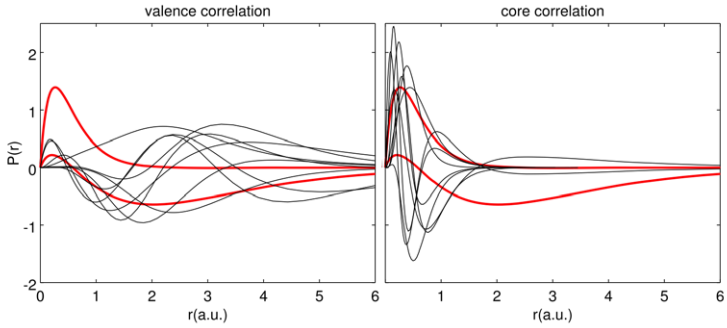

Fig. 1: Hartree-Fock 1*s* and 2*s* orbitals (thick lines) and correlation orbitals (thin lines) in the Be I $1s^2 2s^2\ ^1S$ ground state. Correlation orbitals are spatially different when describing core correlation (contracted orbitals) or valence correlation (diffused orbitals).

References

[1] S. Verdebout, P. Rynkun, P. Jönsson, G. Gaigalas, C. Froese Fischer, M. Godefroid, J. Phys. B: At. Mol. Opt. Phys. **46**, 085003 (2013).
[2] C. Froese Fischer, G. Tachiev, G. Gaigalas, M. R. Godefroid, Comput. Phys. Commun. **176**, 559 (2007).
[3] P. Jönsson, G. Gaigalas, J. Bieroń, C. Froese Fischer and I. P. Grant, Comp. Phys. Commun. **184**, 2197 (2013).
[4] S. Verdebout, P. Jönsson, G. Gaigalas, M. Godefroid, C. Froese Fischer, J. Phys. B: At. Mol. Opt. Phys. **43**, 074017 (2010).
[5] J. Olsen, M. R. Godefroid, P. Jönsson, P. Å. Malmqvist, C. Froese Fischer, Phys. Rev. E **52**, 4499 (1995).
[6] C. F. Bunge, Mol. Phys. **108**, 3279 (2010).

*Corresponding author: saschiff@ulb.ac.be

B – 8

Role of Polarizability of C_{60} in $A@C_{60}$ Photoionization

V. Dolmatov[*1], **C. Parasiliti**[†1]
1. Department of Physics and Earth Science, University of North Alabama, 1 Harrison Plaza, 35630 Florence, Alabama, U.S.A.

Photoionization of, and other processes with, $A@C_{60}$ endohedral fullerenes is a topic of intense scrutiny by modern theoretical and experimental studies [1],[2],[3] (and references therein). Many theoretical results on this topic have been obtained in the framework of a simple and yet surprisingly efficient theoretical model, where the C_{60} carbon cage is modelled by a $U_C(r)$ attractive spherical potential of certain inner radius, r_0, thickness, Δ, and depth, U_0, with A being placed at the center of the cage [1],[2],[3]. However, neither of the thus performed calculations of $A@C_{60}$ photoionization has accounted for polarization of C_{60} by the outgoing photoelectron. Meanwhile, it is known [2] that C_{60} polarization has a drastic impact on electron scattering off C_{60}. Now, upon photoionization of $A@C_{60}$, the outgoing photoelectron, too, scatters off the C_{60} cage on its way out of $A@C_{60}$. Hence, photoionization of $A@C_{60}$ depends on polarizability of C_{60} as well, somehow. But... how? Our study provides the insight into this problem. We choose the $Xe@C_{60}$ as the case study and calculate the $Xe(4d)@C_{60}$ photoionization cross section, σ_{4d}, and corresponding photoionization time delay, τ_{4d}, both with and without account for polarizability of C_{60}. In addition, we explore the effect of atomic-core relaxation of encapsulated Xe on the photoionization quantities. Calculations were performed in the framework of both the random phase approximation with exchange (RPAE) and generalized RPAE (GRPAE) [4]. GRPAE not only accounts for the effects of electron correlation, as RPAE, but, as well, includes the effect of atomic-core relaxation as the photoelectron leaves the atom. The polarization potential of C_{60}, $V_p(r)$, "felt" by the outgoing photoelectron, was approximated by the Bates potential expressed via the static dipole polarizability of C_{60}, α_C, and added to the $U_C(r)$ potential, as in [2]. Photoionization time delay was calculated as the energy derivative of the phase of the $4d$ photoionization amplitude, as in [1]. Calculated σ_{4d} and τ_{4d} are depicted in Fig. 1 along with experimental data for σ_{4d} [3]. A surprising result of the study is that the impact of C_{60} polarization on σ_{4d} and τ_{4d} is weak: calculated results with and without account for α_C differ little from each other. We believe this finding is *general*, i.e., unrelated to the specificity of an encapsulated atom. A possible explanation for the finding is proposed. The overall agrement between each of the calculated GRPAE σ_{4d}'s and experiment is good, in contrast to calculated RPAE σ_{4d}. The latter reveals the importance of the effect of atomic-core relaxation in $Xe@C_{60}$ photoionization – a *particular* effect which is due to the specificity of Xe.

V. D. acknowledges a travel grant from the University of North Alabama Research Committee.

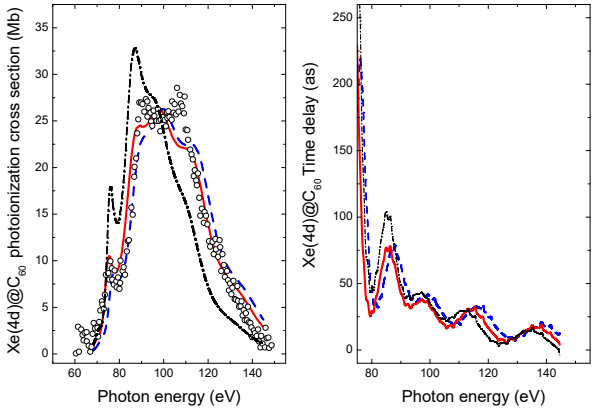

Fig. 1: Calculated GRPAE σ_{4d} and τ_{4d} for $Xe@C_{60}$ photoionization obtained with (solid lines) and without (dashed lines) account for polarizability of C_{60}. Dashed-dotted lines: calculated RPAE results for σ_{4d} and τ_{4d}, obtained without regard for both polarizability of C_{60} and Xe-core relaxation. Open circles: experiment [3]. Parameters of $U_C(r)$: $r_0 = 5.8$ a. u. $\Delta = 1.9$ a. u., $U_0 = 8.2$ eV. Static dipole polarizability: $\alpha_C = 850$ a. u. [2].

References

[1] A. Mandal *et al.*, Phys. Rev. A **96**, 053407 (2017).
[2] V. K. Dolmatov, M. Ya. Amusia, and L. V. Chernysheva, Phys. Rev. A **95**, 012709 (2017).
[3] R. A. Phaneuf *et al.*, Phys. Rev. A **88**, 053402 (2013).
[4] M. Ya. Amusia, *Atomic Photoeffect*, Plenum, New York 1990.

[*]Corresponding author: vkdolmatov@una.edu
[†]Corresponding author: cparasiliti1@una.edu

B – 9

Electron – zinc atom collisions

M. Piwiński[*1], **Ł. Kłosowski** [1], **S. Chwirot** [1], **D. V. Fursa** [2], **I. Bray** [2], **Tapasi Das** [3,4] **R. Srivastava** [4]

1. Institute of Physics, Faculty of Physics, Astronomy and Informatics, Nicolaus Copernicus University in Toruń, Grudziądzka 5, 87-100 Toruń, Poland

2. ARC Centre for Antimatter-Matter Studies, Curtin University, GPO Box U1987, Perth, WA 6845, Australia

3. Department of science and humanities, University of Engineering and Management (UEM), Kolkata, 700160 West Bengal, India

4. Department of Physics, Indian Institute of Technology, Roorkee 247 667 Uttarakhand, India

Electron Impact Coherence Parameters (EICP) enable precise description of the electron-atom collision process [1]. Their values can be obtained in two kind of experiments: electron-photon coincidence [2] and superelastic scattering studies [3]. In both cases there are various technical difficulties connected with a long integration time or efficient UV laser light sources, which cause lack of wide range of EICP data sets. In case of zinc atoms due to relatively short wavelength (213.9 nm) associated with examined first excited P - state, only the coincidence technique is available.

In this work we present EICP for electron impact excitation of 4^1P_1 state of zinc atoms for collision energies 40 eV, 60 eV, 80 eV and 100 eV. The experimental results are presented together with Convergent Close Coupling (CCC) and Relativistic Distorted Wave Approximation (RDWA) theoretical predictions [4].

Comparison of the EICP data for broader range of collision energies allowed formulation three general conclusions:

(1) The differences between CCC, RDWA and experimental data are more clear for lower collision energies,

(2) The characteristic structures in alignment angle, shape and angular momentum transfer parameters shift in the direction of larger scattering angles with decreasing collision energy,

(3) The characteristic structures of γ are observed at slightly lower scattering angle for RDWA predictions than CCC results (see Fig.1).

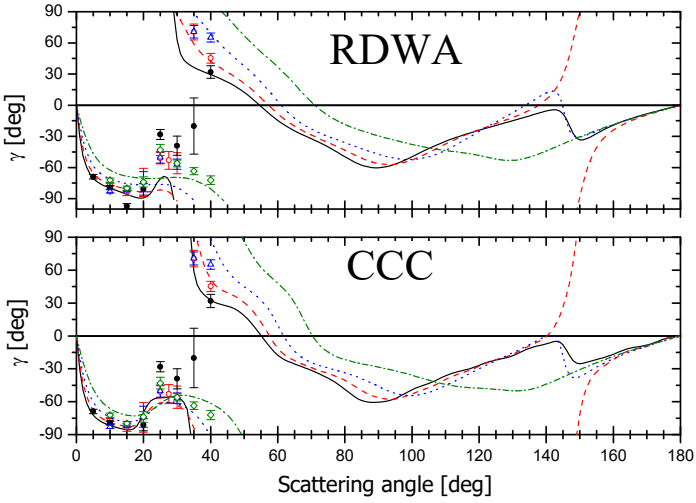

Fig. 1: Alignment angle γ for electronic excitation of 4^1P_1 Zn state. Experimental data: (●) 100 eV, (○) 80 eV, (△) 60 eV, (◇) 40 eV. Theoretical data: (CCC and RDWA): (—) 100 eV, (– –) 80 eV, (· · ·) 60 eV, (– · –) 40 eV [4].

References

[1] N. Andersen, J.W. Gallagher, I.V. Hertel, Phys. Rep. **165** 1-188 (1988).
[2] M. Piwiński *et al.*, J. Phys. B **39**, 1945-1953 (2006).
[3] M. Hussey, S. Jhumka, A. Murray, Phys Rev. A **86**, 042705 (2012).
[4] M. Piwiński *et al.*, J. Phys. B **51**, 085002 (2018).

*Corresponding author: Mariusz.Piwinski@fizyka.umk.pl

B – 10

Helical structures of alignment angle function

M. Piwiński[*1], **Ł. Kłosowski** [1], **S. Chwirot** [1]
1. Institute of Physics, Faculty of Physics, Astronomy and Informatics, Nicolaus Copernicus University in Toruń, Grudziądzka 5, 87-100 Toruń, Poland

Electronic excitation process from S to P atomic state can be characterised by Electron Impact Coherence Parameters (EICP): alignment angle of the electron charge cloud γ, its shape parameter P_L and angular momentum transfer $L_\perp$ [1]. Information of such parameters can be obtained using so-called complete experiments on electron-atom collisions. In the natural reference frame (the quantization axis is perpendicular to the scattering plane) the excited P state of the atom can be described as:

$$|P\rangle = a_{-1}\,|m_j = -1\rangle + a_{+1}\,|m_j = +1\rangle\,, \tag{1}$$

where the complex coefficients $a_{\pm 1}$ represent the relevant excitation amplitudes. In such conditions the alignment angle and shape parameter are defined as follows:

$$\gamma = \frac{1}{2}\arg\left(-a^*_{-1}a_{+1}\right), \tag{2}$$

$$P_L = 2\left|a^*_{-1}a_{+1}\right|. \tag{3}$$

Thus, P_L and γ parameters can be seen as representing polar components of a complex product of the scattering amplitudes $a^*_{-1}a_{+1}$. The product is a function of the scattering angle and impact energy:

$$a^*_{-1}a_{+1} = f(\Theta, E) \tag{4}$$

Therefore some helical structures in γ function in energy and scattering angle domains are expected. Analysing EICP data for zinc [3] and cadmium [2] atoms, such structures were found. They are accompanied by zeros of the shape parameter value, where the maximum angular momentum transfer occurs. Similar patterns were also observed in the scattering angle-impact energy dependence of the alignment angle for other atoms with two valence electrons such as Mg, Ca, Sr and Ba. These narrow structures can be used as a precise tool for verification theoretical models with experimental results.

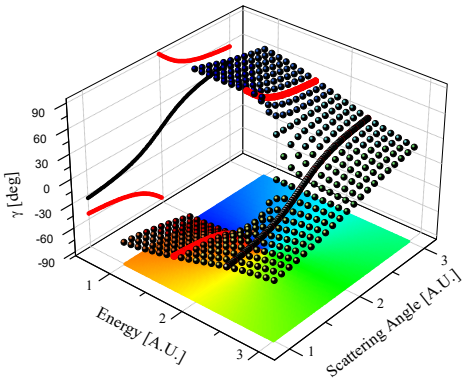

Fig. 1: Illustration of the predicted behaviour of the alignment angle for the impact energy and the scattering angle in the neighbourhood of arbitrarily chosen values of these parameters (see equations (2) and (4)). The 2–d colour map represents the same function (from $-90°$ red to $+90°$ blue). Additionally 2–d projections are presented for two values of the impact energy corresponding to two different modes in changes of the alignment angle with the scattering angle: discontinuous descending (red points) and continuous ascending (black points).

References

[1] N. Andersen, J.W. Gallagher, I.V. Hertel, Phys. Rep. **165**, 1-188 (1988).
[2] M. Piwiński *et al.*, J. Phys. B **39**, 1945-1953 (2006).
[3] M. Piwiński *et al.*, J. Phys. B **51**, 085002 (2018).

*Corresponding author: Mariusz.Piwinski@fizyka.umk.pl

Integral cross sections for electron impact ionization of calcium

M. Piwiński[1], D. Lisak[1], K. Pleskacz[1], S. Wójtewicz[1], Ł. Kłosowski*[1]
1. Institute of Physics, Faculty of Physics, Astronomy and Informatics, Nicolaus Copernicus University in Torun, Grudziadzka 5, 87-100 Torun, Poland

Detailed knowledge on ionization processes is crucial for ion trapping experiments, where ions need to be produced at some stage of the experimental procedure. In our experiment we load various kinds of atomic and molecular ions in a linear Paul trap using electron impact ionization, less common technique than photoionization, however presenting some advantages over optical ionization. The ions trapped are Ca^+ or mixed ensembles containing calcium and other ions. Calcium can be optically cooled in a Doppler scheme and detected using their fluorescence recorded with a CCD camera [1]. Other ions are sympathetically cooled by calcium and detected indirectly by observation of their influence on Ca^+ cloud.

From the rates of trap loading with ions at various electron impact energies, some data on ionization cross sections can be extracted [2]. As the calcium ions are optically accessible, determination of the number of ions inside trap with high precision is possible. Determining number of ions of other species can be more difficult, as they require mass-identification, which can be achieved applying for example resonance phenomena [3].

Integral cross sections (ICS) for electron impact ionization of calcium were measured in the collision energy range from 16 to 160 eV. The measurement results are presented in Fig. 1.

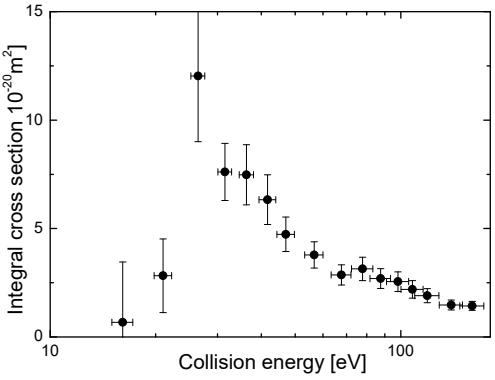

Fig. 1: Integral cross section function for electron impact ionization of calcium atoms determined in the described experiment.

Details of the apparatus, the experimental procedure and data analysis method will be presented and discussed. The obtained values of cross sections will be compared with available theoretical and experimental data.

References

[1] Ł. Kłosowski *et al.* Photonics Letters of Poland **9(4)**, 119-121 (2017).
[2] Ł. Kłosowski *et al.* ArXiv 1802.07111 (2018) To be published.
[3] Ł. Kłosowski *et al.* Journal of Mass Spectrometry (2018) In press.

*Corresponding author: lklos@fizyka.umk.pl

Path integral simulation for muoniated molecules

Yuki Oba, Tsutomu Kawatsu, and Masanori Tachikawa*
Graduate School of NanoBioScience, Yokohama City Unviersity, Yokohama 236-0027, Japan

A considerable amount of knowledge for muonium (Mu; complex of positive muon and electron) chemistry has been accumulated for over 30 years [1]. Compared with a proton, positive muon (μ^+) has a smaller mass and larger magnetic moment. Because of these unique features, Mu is used as the muon spin resonance/rotation/relaxation (μSR), where hyperfine coupling constant (HFCC) is a good index for the magnetic interaction between electron and muon spins.

For instance, the HFCC value of muoniated acetone radical (Mu-ACE, Figure 1) is measured by Percival et al [2] as 10.27 MHz at 300 K (reduced using the proton magnetic moment). However, the reduced HFCC value for Mu-ACE is calculated as -5.8 MHz with the conventional DFT calculation [3], where the quantum effect of nuclei and thermal effect are excluded.

In this study, thus, we performed *on-the-fly ab initio* path integral molecular dynamics (PIMD) simulation [4, 5], which can include these effects, to Mu-ACE and hydrogenated acetone radical (H-ACE). Our HFCC values for Mu-ACE and H-ACE are calculated as 32.1 and 3.97 MHz, respectively, which are in reasonable agreement with the corresponding experimental values of 10.3 and 1.51 MHz. Such mass-dependence on HFCC values is due to the large quantum effect of muon. We will also show other results for other muoniated molecular species.

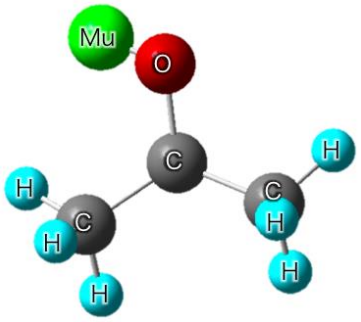

Fig. 1: Structure of Mu-ACE.

References

[1] P. W. Percival, Radiochemica Acta, **26**, 1 (1979).
[2] P. W. Percival, J.-C. Brodovitch, K. Ghandi, B. M. McCollum and I. McKenzie, J. Am. Chem. Soc. **127**, 13715 (2005).
[3] R. M. Macraea and I. Carmichael, Physica B, **326**, 81 (2003).
[4] K. Yamada, Y. Kawashima, and M. Tachikawa, J. Chem. Theory Comput., **10**, 2005 (2014).
[5] Y. Oba, T. Kawatsu, and M. Tachikawa, J. Chem. Phys., **145**, 064301 (2016).

* Corresponding author: tachi@yokohama-cu.ac.jp

Multi-second magnetic coherence in a single domain spinor Bose-Einstein condensate

S. Palacios[*1], **Pau Gomez**[1], **Simon Coop**[1], **Chiara Mazzinghi**[1], **Ferran Martin**[1], **Morgan Mitchell**[1,2]
1. ICFO–Institut de Ciencies Fotoniques, The Barcelona Institute of Science and Technology, 08860 Castelldefels (Barcelona), Spain
2. ICREA–Institució Catalana de Recerca i Estudis Avançats, 08010 Barcelona, Spain

In ordinary spin systems, spin-destruction collision limit the coherence time of the system in general to the ms scale. In ultracold ensembles, these spin-spin interactions are fully coherent, and the relaxation time is expected to be unbounded. Here we show a polarized ferromagnetic single-domain spinor Bose-Einstein condensate (SD SBEC) exhibit no relaxation of the macroscopic spin state other than atoms losses [1]. To characterize the coherence properties, we use standard nomenclature: in a experiment with many spins (condensed or otherwise), the spin component along the field direction (**x**), experiences the longitudinal relaxation time $\mathscr{T}_1$, defined by $\langle F_x\rangle \propto \exp[-t/\mathscr{T}_1]$. Similarly, the transverse components relax according to $\langle F_z\rangle \propto \exp[-t/\mathscr{T}_2^*]$ (and similar for $F_z \to F_y$, cos → sin). $\mathscr{T}_2^*$ accounts for homogeneous effects, i.e., irreversible randomizations affecting all spins in the same way, and inhomogeneous effects, i.e., apparent randomization due to reversible effects such as differences in the local field. The lack of relaxation mechanisms in the SD SBEC implies $\mathscr{T}_2^* = \mathscr{T}_1$. There is another relaxation mechanism, loss of atoms, and this affects both F_x and $F_{y,z}$ in the same way, is truly irreversible, and affects all atoms in the same way. We assign the rate $1/\mathscr{T}_0$ to this loss of atoms: $N_A(t) \propto \exp[-t/\mathscr{T}_0]$.

We create SD SBECs with $N_A = 4\times10^4$ in a compact spherical trap of mean oscillation frequency 50 Hz. $\rho = 3\times10^{19}$ atoms/m^3. This system is well described by the single-mode approximation (SMA) provided the bias field is $B < 1\times10^{-4}$ T: the validity of the SMA depends on both, the spin interaction energy and the quadratic Zeeman energy, and is guaranteed when the condensate R is smaller than the bound $\lambda = h/\sqrt{2M(2|c_2|\rho+q)}$ [2], where ρ represents the mean density and for Rb^{87}, $M = 1.44\times10^{-25}$ kg, $c_2 = -2.39\times10^{-53}$ Jm^3 (spin-dependent interaction strength), and $q = (\gamma B)^2\hbar/\omega_{\rm hf}$ (quadratic Zeeman energy), $\omega_{\rm hf} = 2\pi\times6.83$ GHz (hyperfine frequency splitting) and $\gamma = 2\pi(-7\,\text{GHz/T})$ (gyromagnetic ratio). When the quadratic Zeeman energy dominates over the spin contact interaction energy, the SD SBEC is expected to follow a trivial precession about the magnetic field. We polarize the atoms in the $F = 1, m_F = 1$ state with a bias field $B = 29\,\mu$T defining the quantization axes along x. We then apply two MW pulses to prepare the state $(1,1,0)^T/\sqrt{2}$. Using non-destructive Faraday rotation probing we observe spin dynamics along z. The one-particle dynamics of this system is $f_z(t) = -\cos(\omega_L+\omega_Q)t/\sqrt{2}$. We observe the multiparticle system evolves as $N(t)[-\cos(\omega_L+\omega_Q)t/\sqrt{2}]$, as shown in Fig. 1 and therefore we associate $\mathscr{T}_2^* \equiv \mathscr{T}_0$. Using absorption imaging we have measured $N(t) = N_A\exp[-t/\mathscr{T}_0]$ with $\mathscr{T}_0 = 7.7$ s. This shows in our system only atom losses degrade the macroscopic spin polarization, giving a spin coherence time equal to the trap lifetime. At the used densities, the lifetime is set only by one-body losses. The trap lifetime time can in principle be extended with better vacuum conditions up to the three-body loss time ≈ 70 s.

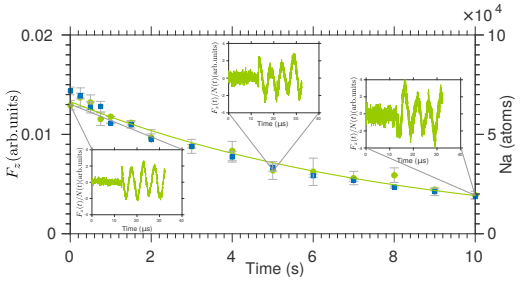

Fig. 1: Amplitude of the Faraday signal ∝ F_z (circles, left axis) and N_A (squares, right axis) as a function of time. Insets: normalized Faraday signal ∝ F_z/N_A showing constant amplitude in time.

This result removes an important limitation of neutral atoms as decoherence is the most significant obstacle for applications in quantum information science. Demonstrating long coherence and scalability of the quantum system, would make the single domain SBEC interesting for long-lived entanglement or spin-squeezing. Additionally, one can profit from the small size of the condensate for applications such as high-resolution magnetic sensing.

References

[1] Palacios, S. et al, S. Coop, P. Gomez, T. Vanderbruggen, Y. N. Martinez de Escobar, M. Jasperse and M. W. Mitchell, New J. Phys. **20**, 053008 (2018). [2] H. Mäkelä, M. Johansson, M. Zelan, and E. Lundh, Phys. Rev. A **84**, 043646 (2011).

*Corresponding author: silvana.palacios@icfo.eu

B – 14

Ultracold rare-earth magnetic atoms with an electric dipole moment

M. Lepers[*1,2], **H. Li**[2], **J. F. Wyart**[2], **G. Quéméner**[2], **O. Dulieu**[2]
1. Laboratoire Interdisciplinaire Carnot de Bourgogne, CNRS, Université de Bourgogne Franche-Comté, 21078 Dijon, France
2. Laboratoire Aimé Cotton, CNRS, Université Paris-Sud, ENS Paris-Saclay, Université Paris-Saclay, 91405 Orsay, France

In the field of ultracold atoms and molecules, dipolar gases, *i.e.* gases composed of particles carrying a dipole moment, are promising candidates to observe new phenomena related to many-body physics, quantum simulation [1] and ultracold chemistry [2]. A particular attention is paid to gases with both an electric and a magnetic dipole moment, consisting up to now in paramagnetic polar molecules [3]. At the single-particle scale, an electric dipole is induced by an external electric field which mixes even- and odd-parity levels of the energy spectrum, with respect to the inversion operation. A magnetic dipole is obtained by preparing a sample of non-zero angular-momentum particles, like lanthanide atoms [4], in a well-defined Zeeman sublevel.

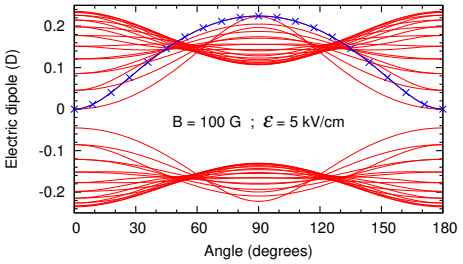

Fig. 1: Induced electric dipole moment of dysprosium as a function of the angle between the electric and magnetic fields, for an electric field of 5 kilovolt per centimeter and a magnetic field of 100 gauss. Each curve corresponds to a field-mixed level converging to the Zeeman sublevels of $|a\rangle$ and $|b\rangle$ for a vanishing angle. The blue curve with crosses corresponds to the lowest sublevel of $|a\rangle$.

In this work, we propose a new method to produce an electric and magnetic dipolar gas composed of ultracold dysprosium atoms. The pair of nearly degenerate energy levels of opposite parity, $|a\rangle$ at 17513.33 cm^{-1} with electronic angular momentum $J_a = 10$, and $|b\rangle$ at 17514.50 cm^{-1} with $J_b = 9$, can be mixed with an external electric field, thus inducing a sizeable electric dipole moment in the laboratory frame. For field amplitudes relevant to current-day experiments, we predict, using our high-level semi-empirical electronic-structure calculations based on the Cowan codes [5], a large magnetic dipole moment up to 13 Bohr magnetons for the blue field-mixed level of Fig. 1, and a sizeable electric dipole moment up to 0.22 debye for the same level. When a magnetic field is present, we show that the induced electric dipole moment strongly depends on the angle between the fields (see Fig. 1). The radiative lifetime of the field-mixed levels is found in the millisecond range, thus allowing for suitable experimental detection and manipulation. Our method is applicable for bosonic as well as fermionic isotopes of dysprosium [6].

References

[1] M. Baranov, M. Dalmonte, G. Pupillo, and P. Zoller, Chem. Rev. **112**, 5012 (2012).
[2] O. Dulieu and A. Osterwalder, *Cold Chemistry: Molecular Scattering and Reactivity Near Absolute Zero*, Royal Society of Chemistry (2017).
[3] T. Rvachov, H. Son, A. Sommer, S. Ebadi, J. Park, M. Zwierlein, W. Ketterle, and A. Jamison, Phys. Rev. Lett. **119**, 143001 (2017).
[4] J. Becher, S. Baier, K. Aikawa, M. Lepers, J.-F. Wyart, O. Dulieu, and F. Ferlaino, Phys. Rev. A **97**, 012509 (2018).
[5] R. Cowan, *The Theory of Atomic Structure and Spectra*, University of California Press (1981).
[6] M. Lepers, H. Li, J.-F. Wyart, G. Quéméner, and O. Dulieu, arxiv preprint arxiv:1803.04159 (2018).

*Corresponding author: maxence.lepers@u-bourgogne.fr

Positron covalent bonding: the e^+-dihydride molecule

J. A. Charry[1], **M. T. do N. Varella**[*2], **A. Reyes**[1]
1. Chemistry Department, National University of Colombia, Bogotá Cundinamarca 111321, Colombia
2. Institute of Physics, University of São Paulo, Rua do Matão 1731, 05508-090, São Paulo, Brazil

Recent experimental advances have allowed for the production and manipulation of antiparticles at very low energies. A wealth of interesting problems in atomic and molecular sciences arise from the interaction of electrons, atoms and molecules with slow antiparticles, *e.g.*, antiprotons [1], muons [2] and positrons [3]. Among the interesting aspects of the research on positrons, one could mention the production of positronium (Ps) atoms in Rydberg states [7] and Ps_2 molecules [8], and as well as the production of positronic compounds, i.e., bound states formed in collisional experiments wherein a positron attaches to a vibrationally excited molecule. The formation of about 60 positronic molecules has been reported [4], and theoretical models [5][6] have also been proposed to describe the attachment and vibrational dynamics underlying the formation of such compounds.

We report on the compound formed by two hydride anions and a positron, $e^+[H_2^{2-}]$. Our high-level computational simulations [9] indicate that the system is energetically stable, *i.e.*, the positron binds the otherwise repelling H^- anions. More importantly, the calculated potential energy curve and positron density provide compelling evidence of the formation of a positronic covalent bond. This covalently bonded system is fundamentally distinct from the positronic molecules produced in collision experiments. In the latter case, the positron attaches to a stable molecule, essentially in result of charge-dipole and charge-induced dipole interactions. Finally, the $e^+[H_2^{2-}]$ is also distinct from the Ps_2 molecule, as the interaction of four light particles with equal probability densities does not involve bond formation, at least in the usual sense [10].

The calculations were performed with the Any-Particle Molecular Orbital (APMO) approach [11] implemented in the LOWDIN [12] code, which allows for the extension of several electronic structure techniques to systems comprising more than a single fermion species. The methodology was previously employed to obtain positron binding energies to ordinary atoms and molecules [13]. In the present study, the results were obtained with several APMO approximations, namely Hartree-Fock, Second-Order Møller-Plesset Perturbation Theory, and Configuration Interaction with different excitation levels. Essentially all calculations indicated the existence of a stable $e^+[H_2^{2-}]$ molecule, as long as the latter complex and the dissociation products were described at the same level of theory. Our most reliable estimate for the bonding energy was 74 kJ/mol (0.77 eV), taking into account the zero-point vibrational energy, which is expected to be a lower bound.

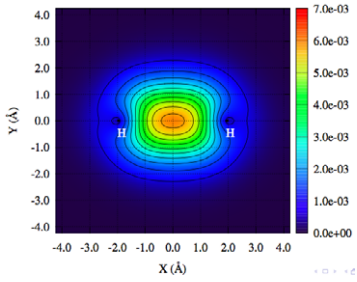

Fig. 1: Positron density in the $e^+[H_2^{2-}]$ molecule. The plot was generated from the APMO/Hartree-Fock positronic orbital. The positions of the hydride nuclei are indicated by H.

References

[1] G. B. Andresen *et al.*, Nature **468**, 673 (2011).
[2] D. G. Fleming *et al.*, Science **331**, 448 (2011).
[3] J. R. Danielson, D. H. E. Dubin, R. G. Greaves, and C. M. Surko, Rev. Mod. Phys. **87**, 247 (2015).
[4] G. F. Gribakin, J. Young, and C. M. Surko, Rev. Mod. Phys. **82**, 2557 (2010).
[5] G. F. Gribakin, and C. M. R. Lee, Phys. Rev. Lett. **97**, 193201 (2006).
[6] S. d'A. Sanchez, M. A. P. Lima, and M. T. do N. Varella, Phys. Rev. Lett. **107**, 103201 (2011).
[7] D. B. Cassidy, T. H. Hisakado, H. W. K. Tom, and A. P. Mills, Phys. Rev. Lett. **108**, 043401 (2012).
[8] D. B. Cassidy, and A. P. Mills, Nature **449**, 195 (2007).
[9] J. A. Charry, M. T. do N. Varella, and A. Reyes, Angew. Chem. Int. Ed., accepted, https://doi.org/10.1002/anie.201800914.
[10] M. Nic, J. Jirat, and B. Kosata, *IUPAC compendium of chemical terminology (gold book)*, online version (2012).
[11] S. A. González, N. F. Aguirre, and A. Reyes, Int. J. Quatum Chem. **108**, 1742 (2008 .
[12] R. Flores-Moreno *et al.*, Int. J. Quatum Chem. **114**, 50 (2013).
[13] J. Romero, J. A. Charry, R. Flores-Moreno, M.o T. do N. Varella, and A. Reyes, J. Chem. Phys. **141**, 114103 (2014).

[*]Corresponding author: mvarella@if.usp.br

Enhanced nuclear spin dependent parity violation effects using the ^{199}HgH molecule

A. J. Geddes[*1], **L. V. Skripnikov** [2,3], **A. Borschevsky** [4], **J. C. Berengut** [1], **V. V. Flambaum** [1], **T. P. Rakitzis** [5,6]

1. School of Physics, University of New South Wales, Sydney, New South Wales 2052, Australia

2. National Research Centre "Kurchatov Institute" B.P. Konstantinov Petersburg Nuclear Physics Institute, Gatchina, Leningrad district 188300, Russia

3. Department of Physics, Saint Petersburg State University, Saint Petersburg, Petrodvoretz 198904, Russia

4. Van Swinderen Institute, University of Groningen, Nijenborgh 4, 9747 AG Groningen, The Netherlands

5. Department of Physics, University of Crete, 71003 Heraklion-Crete, Greece

6. Institute of Electronic Structure and Laser, Foundation for Research and Technology-Hellas, 71110 Heraklion-Crete, Greece

The violation of symmetry under a parity operation is known as parity non-conservation (PNC) which, in atoms and molecules, can be classified as nuclear spin dependent (NSD) or nuclear spin independent (NSI) PNC. The nuclear anapole moment is one example of a manifestation of NSD PNC in atoms and molecules [1][2] and has been detected only once within the ^{133}Cs atom [3], where NSD PNC is sub-dominant. This is because experimental techniques have lacked the sensitivity to detect NSD PNC effects with certainty.

NSD PNC calculations in molecules provide a new window of opportunity to study the parity violating nuclear forces that create the nuclear anapole moment. Importantly, PNC effects are enhanced within diatomic molecules due to closely spaced rotational levels of opposite parity [4] [5]. Mercury hydride (HgH) in particular is a promising choice for the study of PNC effects, not only because it gives an enhanced, pure NSD PNC signal but also because it is easy to make at room temperature.

A low-energy optical rotation experiment is being proposed with the aim of observing NSD PNC interactions in HgH. Using the relativistic coupled cluster method, we present a complete calculation of the circular polarization parameter $P = 2\mathrm{Im}(E1_{PNC})/M1 \approx 3 \times 10^{-6}\ \kappa$ for the $^2\Sigma_{1/2} \rightarrow ^2\Pi_{1/2}$ optical transition of HgH, where κ is a dimensionless constant determined by the nuclear anapole moment [6]. This provides an improvement in sensitivity to NSD PNC by 2 – 3 orders of magnitude over the leading atomic Xe, Hg, Tl, Pb and Bi optical rotation experiments, and shows that the proposed measurement will be sensitive enough to extract the ^{199}Hg anapole moment and shed light on the underlying theory of hadronic parity violation.

References

[1] V.V. Flambaum, I.B. Khriplovich. ZhETF **79**, 1656, 1980. [JETP **52**, 835, (1980)].
[2] V.V. Flambaum, I.B. Khriplovich, O.P. Sushkov. Phys. Lett. B. **146**, 367, 1984.
[3] C. S. Wood, S. C. Bennett, D. Cho, B. P. Masterson, J. L. Roberts, C. E. Tanner, and C. E. Wieman, Science **275**, 1759 (1997)
[4] O. P. Sushkov and V. V. Flambaum, Sov. Phys. JETP **48**, 608 (1978).
[5] L. N. Labzowsky, Sov. Phys. JETP **48**, 434 (1978).
[6] A. J. Geddes, L. V. Skripnikov, A. Borschevsky, J. C. Berengut, V. V. Flambaum, T. P. Rakitzis, (2018) arXiv:1804.05475 [physics.atom-ph]

*Corresponding author: a.geddes@unsw.edu.au

Isotope shift, non-linearity of King plots and the search for new particles

A. J. Geddes[*1] , **A. V. Viatkina** [2], **V. V. Flambaum**[1,2]
1. School of Physics, University of New South Wales, Sydney 2052, Australia
2. Helmholtz Institute Mainz, Johannes Gutenberg University, 55099 Mainz, Germany

It has been recently suggested to use the measurements of the King plot non-linearity in a search for hypothetical new light bosons [1]. However, in order to extract and put limits on the effect on new bosons, one must find the non-linear corrections to the King-plot already arising in the Standard Model framework. A King plot is constructed from the isotope shifts between four isotopes of a given atom for two different transitions; the points are conventionally fitted with a line in order to extract nuclear parameters and electronic isotope shift terms.

We investigate the notion of a non-linear King plot and focus on contributions to the non-linearity arising from relativistic effects in the isotope field-shift, the nuclear polarizability and many-body effects [2]. It is found that the nuclear polarizability contribution can lead to the significant deviation of the King plot from linearity. Therefore, the measurements of the non-linearity of King plots may be applied to obtain the nuclear polarizability change between individual isotopes. We then proceed to provide a rough analytical estimate of the non-linearity arising solely from the effect of a hypothetical scalar boson. Our predictions give theoretical limitations on the sensitivity of the search for new interactions and should help to identify the most suitable atoms for corresponding experiments.

In addition, we derive a mean-field relativistic formula for the isotope shift of an electronic energy level for arbitrary angular momentum; we then use it to predict the spectra of superheavy metastable neutron-rich isotopes belonging to the hypothetical island of stability [2]. Our results may be applied to the search for superheavy atoms in astrophysical spectra using the known values of the transition frequencies for the neutron deficient isotopes produced in the laboratory [3]. An example of a relevant astrophysical system may be the spectra of the Przybylski's star where superheavy elements up to $Z = 99$ have been possibly identified [4].

References

[1] , J. C. Berengut, D. Budker, C. Delaunay, V. V. Flambaum, C. Frugiuele, E. Fuchs, C. Grojean, R. Harnik, R. Ozeri, G. Perez, and Y. Soreq, Phys. Rev. Lett. **120**, 9 091801 (2018)
[2] V . V. Flambaum, A. J. Geddes and A. V. Viatkina, Phys. Rev. A **97**, 3 032510 (2018)
[3] V . A. Dzuba, V. V. Flambaum, and J. K. Webb, Phys. Rev. A **95**, 062515 (2017)
[4] V . F. Gopka, A. V. Yushchenko, V. A. Yushchenko, I. V. Panov and C. Kim, Kinematics and Physics of Celestial Bodies **24**, 89 (2008)

*Corresponding author: a.geddes@unsw.edu.au

High-temperature superconductors within oscillation electron model

N.P. Netesova*
M.V. Lomonosov Moscow State University, Physics Faculty, Lenin-Sparrow Hills, 119991 Moscow, Russia.

An oscillation electron plasma model of superconductors has been proposed for binary crystals [1]. Within oscillation electron model the superconducting crystal AB is considered consisting of two subsystems for phase separation. Free electrons couple to lower system energy. When molecules are formed from identical atoms, energy is released. This law leads to an energy balance. It is necessary, that square electron energy in a local phase Φ^2_{ab} was essentially much less, than the one Φ^2_a, Φ^2_b in an initial phase. This is the condition for the superconducting phase transition in the crystal AB

$$\Phi^2_{ab} \le \Phi^2_a, \qquad \Phi^2_{ab} \le \Phi^2_b,$$

$$\Phi^2_{ab} = k \bullet \rho_{ab} \bullet s_{ab} / M_{ab}, \qquad \Phi^2_a = k \bullet \rho_a \bullet s_a / M_a, \qquad \Phi^2_b = k \bullet \rho_b \bullet s_b / M_b,$$

where Φ^2_{ab}, Φ^2_a, Φ^2_b are square interaction energy an initial phase AB, the local again formed phases A2 and B2, ρ_{ab}, ρ_a, ρ_b, and s_{ab}, s_a, s_b, and M_{ab}, M_a, M_b are mass density, number of valence electrons, molecule mass for AB, A, B, respectively, $q(AB) = \Phi^2(AB) / \sum\Phi^2$ is interaction parameter for AB, k is a constant.

A plasma electron model for four-component superconductors was developed. Square plasma energies of mixed copper oxides containing mercury and their composite atoms are considered. Mixed copper oxides containing mercury, Hg Ba2 Ca n-1 Cu n O 2n+2+œ, known since 1993, are characterized by the highest superconducting phase transition temperatures. These oxides have the highest critical temperatures (Tc) of all presently known superconductors: 94, 128, and 135 K for HgBa2Cu04+œ, (Hg 1201), HgBa2CaCu206+œ, (Hg 1212), and HgBa2Ca2Cu3O8+œ, (Hg 1223), respectively.
For four-component crystals ABCD = 0.5A2+0.5B2+0.5C2+0.5D2, the interaction parameter was calculated by the formula $q(ABCD) = \Phi^2(ABCD) / \sum\Phi^2$.
Equation of the phase transition curve for superconductors was received
$Tc=40.05687q^2 - 234.44056q+191.51842$.
Plasma parameters of the compound $HgBa_2CuO_{4+œ}$, Tc=94-95, at optimum doping œ=0.12 were given.
$HgBa_2CuO_{4+œ}$ = 0.5 Hg2 + Ba2 + 0.5Cu2+2O2+0.5œ O2.
$\Phi^2(Hg) = 111.9364$, $\Phi^2(Ba) = 45.6976$, $\Phi^2(Cu) = 232.8676$, $\Phi^2(O) = 354.9456$, $\Phi^2(HgBa_2Cu0_{4+œ}) = 242.4249$.

$\Phi^2(HgBa_2Cu0_{4+œ}) = 242.4249 > 0.5\Phi^2(Hg) = 55.9682$,
$\Phi^2(HgBa_2Cu0_{4+œ}) = 242.4249 > \Phi_2(Ba) = 45.6976$,
$\Phi^2(HgBa_2Cu0_{4+œ}) = 242.4249 > 0.5\Phi_2(Cu) = 116.4338$,
$\Phi_2(HgBa_2Cu0_{4+œ}) = 242.4249 < 2\,\Phi_2(O) + 0.5œ\,\Phi^2(O) = 709.8912 + 21.296736$.

$\sum\Phi^2 = 354.9456\,(2+0.5œ) - (55.9682+45.6976+116.4338) =$
$709.8912 + 0.5\,œ\,354.9456 - 218.0996 = 491.7916 + 0.5\,œ\,354.9456$.
$q = 242.4249 / (491.7916 + 0.5\,œ\,354.9456) = 0.44565$, œ=0.12.

From the equation we obtain the interaction parameter (Tc=95) q = 0.445635,
$q = 242.4249 / \sum\Phi^2 = 0.445635$, $\sum\Phi^2 = 543.99878824$.
$543.99878824 - 491.7916 = 52.207188$, æ = 52.207188 / 354.9456●0.5 = 0.294170.

Calculations must be made at T less than Tc for resistance tending to zero.
$Tc=90$, $q^2 - 5.85269q + (191.51842 - 90) / 40.05687=0$, $q^2 - 5.85269q + 2.534357 = 0$,
$q = 2.926345 - 2.471449 = 0.454896$.
The parameter tables for a series of mercury containing mixed copper oxides are calculated. Plasma effects appear when the energy balance condition is met.

References

[1] N.P. Netesova. Plasma model of superconducting crystals //Proc. SPIE 9884, Brussels, Nanophotonics VI, 3R1-3R14 (21 April, 2016).

*Corresponding author: npn@mig.phys.msu.ru

Search for exotic spin-dependent interactions with a liquid-state nuclear spin comagnetometer

T. Wu[*1], **J. W. Blanchard**[1], **D. F. Jackson Kimball**[2], **D. Budker**[1,3]
1. Helmholtz-Institut Mainz, Johannes Gutenberg University, 55128 Mainz, Germany
2. Department of Physics, California State University-East Bay, Hayward, California 94542-3084, USA
3. Department of Physics, University of California at Berkeley, California 94720-7300, USA

Atomic comagnetometers typically consist of overlapping ensembles of at least two different species of atomic spins [1]. It is the ratio of the spin-precession frequency of the different species under the influence of a bias magnetic field that is measured. The ratio is relatively insensitive to the changes in magnetic field but retains sensitivity to Zeeman-like nonmagnetic spin interactions. Therefore, atomic comagnetometers are widely used in fundamental physics experiments and searches for anomalous spin-dependent interactions [2].

However, in fundamental physics experiments using comagnetometers based on overlapping ensembles of different species, one of the systematic effects reducing accuracy is due to uncontrolled magnetic field gradients [3]. Here we describe a comagnetometer based on the nuclear spins within an ensemble of identical molecules [4]. In this single-species comagnetometer, different nuclear spins are probed within the same molecule. By taking advantage of the techniques of ultralow-field nuclear magnetic resonance and sensitive atomic magnetometry [5], the J-coupling (indirect spin-spin coupling) spectrum of a liquid-state ensemble of acetonitrile-2-^{13}C molecule can be measured with sub-mHz precision in an ultralow-field with a single scan. Under the influence of a bias field, the J-coupling resonance lines at different frequencies split into separate peaks (show in Fig. 1). The frequency separation between the split peaks for each J-coupling resonance lines has distinct linear coefficients with respect to the magnetic field. Measurements of these splittings can be employed as a comagnetometer.

We experimentally demonstrate that in the presence of a temperature gradient, such a comagnetometer is insensitive to first-order magnetic field gradients. Our single-species comagnetometer is shown to be capable of measuring the hypothetical spin-dependent gravitational energy of nuclei at the 10^{-17} eV level, comparable to the most stringent existing constraints. Combined with techniques for enhancing the signal such as parahydrogen-induced polarization [6], this method of comagnetometry offers the potential to improve constraints on spin-gravity coupling of nucleons by several orders of magnitude.

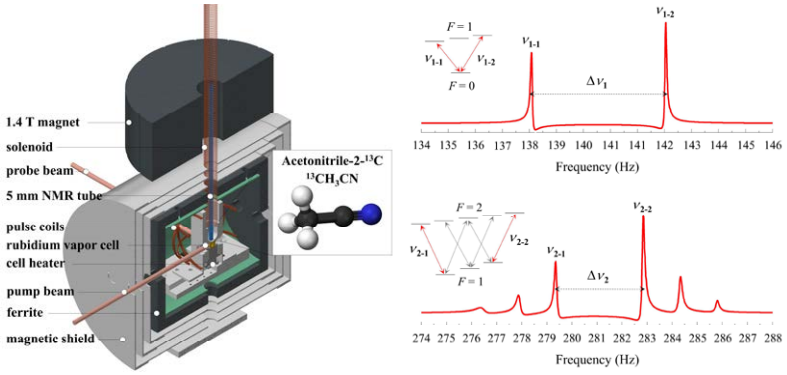

Fig. 1: Schematics of the liquid-state nuclear spin comagnetometer (left) and the experimentally measured J-coupling spectrum of acetonitrile-2-^{13}C in a 80 nT bias field (right). The related transitions used for comagnetometry are shown with solid red arrows.

References

[1] M. E. Limes, D. Sheng, and M. V. Romalis, Phys. Rev. Lett. 120, 033401 (2018).
[2] M. S. Safronova, D. Budker, D. DeMille, D. F. Jackson Kimball, A. Derevianko, and C. W. Clark, arxiv:1710.01833 (2017).
[3] D. F. Jackson Kimball, J. Dudley, Y. Li, D. Patel, and J. Valdez, Phys. Rev. D 96, 075004 (2017).
[4] T. Wu, J. W. Blanchard, D. F. Jackson Kimball, M. Jiang, and D. Budker, arxiv:1804.02096 (2018).
[5] M. P. Ledbetter, S. Pustelny, D. Budker, M. V. Romalis, J. W. Blanchard, and A. Pines, Phys. Rev. Lett. 108, 243001 (2012).
[6] T. Theis, P. Ganssle, G. Kervern, S. Knappe, J. Kitching, M. P. Ledbetter, D. Budker, and A. Pines, Nat. Phys. 7, 571 (2011).

*Corresponding author: teng@uni-mainz.de

Possibilities of investigations of the temporal variation of the constant α in atomic holmium

D. Stefańska*, **B. Furmann, P. Głowacki**
Division of Quantum Engineering and Metrology, Institute of Materials Research and Quantum Engineering, Faculty of Technical Physics, Poznan University of Technology, Piotrowo 3, 60-965 Poznań, Poland

Temporal variations of the fine structure constant α, which constitutes a certain measure of the strength of electromagnetic interactions, are predicted by most of the contemporary unification theories. Investigations can be afforded under laboratory conditions and currently count among the most essential problems in the field of quantum metrology. The measurement consists in determination of the influence of the possible α variation on the frequencies of selected transitions between the electronic levels in atoms or ions.

One of the most promising methods involves the transitions between possibly long-lived levels belonging to considerably different electronic configurations (and thus reacting differently to the α changes), but closely separated in the energy scale [1]. Because of the dense structure of their electronic levels, elements from the lanthanides group seem particularly suitable for this purpose. A particularly favorable pair of degenerate levels of opposite parities was found in the dysprosium atom - this atomic system has been successfully studied for over a decade [2]. Other favorable level pairs in various lanthanides elements were also proposed, among others also two pairs in the holmium atom [3].

Recently we further developed the concept of the use of the suitable level pairs in the holmium atom [3] for the measurement of the temporal variation of the constant α [4]. The experimental schemes, similar to the scheme applied for the dysprosium atom [2], were proposed. Initially these were based on the known electronic levels (Fig. 1a - the first level pair), but in the course of investigations performed in this work also new electronic levels were found, with possible application in alternative versions of the experiment. The lifetimes of the levels belonging to the proposed pairs (hitherto unknown) were estimated and found acceptable, and the absolute frequencies of the transitions between the hyperfine structure sublevels were approximately evaluated (Fig. 1b).

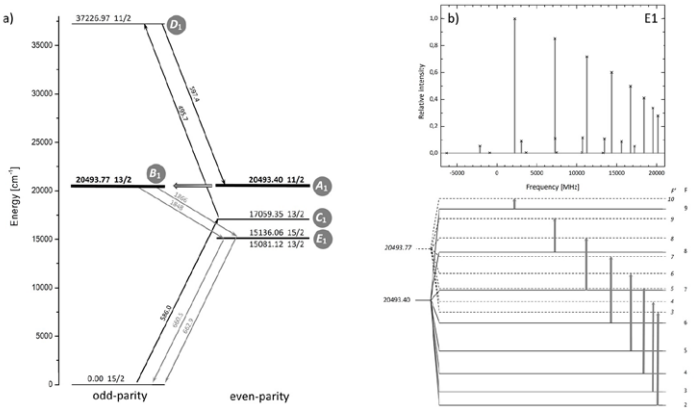

Fig. 1: Proposal of the application of the level pair: $A_1 = 20493.40\ \mathrm{cm}^{-1} \rightarrow B_1 = 20493.77\ \mathrm{cm}^{-1}$ of the holmium atom in the measurement of the temporal variation of the fine structure constant α: a) exemplary experimental scheme, b) simulation of the hyperfine structure of the transition $A_1 \rightarrow B_1$

Spectroscopic investigations, performed by laser induced fluorescence (LIF) in a hollow cathode discharge lamp, concerned mainly the optical transitions directly involved in the planned experimental schemes. The final verification of the schemes is planned in the future on an atomic beam.

The work was supported by Poznan University of Technology under the Project 06/65/DSPB/5183.

References

[1] V.A. Dzuba, V.V. Flambaum, and J.K. Webb, Physical Review A **59**, 230-237 (1999).
[2] A. Cingöz, *et al.*, Physical Review Letters **98**, 040 801 (4pp) (2007).
[3] V.A. Dzuba and V.V. Flambaum, Physical Review A **77**, 012 515 (6pp) (2008).
[4] D. Stefańska, B. Furmann, P. Głowacki, Journal of Quantitative Spectroscopy and Radiative Transfer **213**, 159-168 (2018).

*Corresponding author: danuta.stefanska@put.poznan.pl

B – 21

Software development for alexandrite laser - seeded - diode laser: rotational spectroscopy of the $A^1 0_u^+(5^1P_1) \leftarrow X^1 0_g^+(5^1S_0)$ transition in Cd_2

K. Puczka*, **T. Urbańczyk†**, **J. Koperski**
Smoluchowski Institute of Physics, Jagiellonian University ul. Łojasiewicza 11, 30 - 348 Krakow, Poland

Molecular rotational energy structure is an important source of information for spectroscopists. To resolve rotational structure, a narrowband, well controlled laser source, such as for instance a pulsed alexandrite laser is needed. Parameters of the alexandrite laser depend strongly on its seeding system, in this case a tuneable diode laser. Developing software for the seeding diode laser allows for changing and controlling its parameters such as wavelength, power of the beam or tuning time. The seeding diode laser software is combined with other parts of the software devoted to the detection of molecular LIF excitation spectra. The most important aspect of the software are measurements of the smallest current step available which coresponds to the smallest change in generated wavelenght. The software is written in `C#` programming language with full graphical interface. To test the stability and precision of the seeding laser, measurement of absorption spectrum and saturation spectroscopy in rubidium were performed. The long-term goal is to resolve rotational structure in the $A^1 0_u^+(5^1P_1) \leftarrow X^1 0_g^+(5^1S_0)$ transition in Cd_2 vdW dimer.

This work is supported by the National Science Centre Poland under grant number UMO-2015/17/B/ST4/04016.

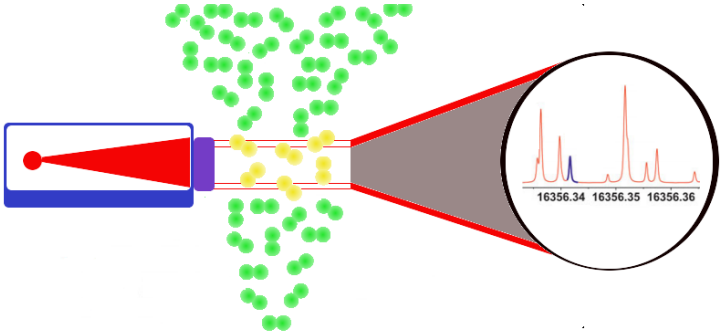

Fig. 1: The idea of an experiment devoted to spectral resolution of rotational structure in the $A^1 0_u^+(5^1P_1) \leftarrow X^1 0_g^+(5^1S_0)$ transition in Cd_2 [1].

References

[1] T. Urbańczyk, M. Strojecki, J. Koperski, *Mol. Phys* 2018, in print.

*Corresponding author: Krystian.slawomir.puczka@gmail.com
†Corresponding author: tomek.urbanczyk@uj.edu.pl

Fine-and hyperfine structure calculation of the odd-parity configuration system of the Ho I

M. Elantkowska[*1], **S. Wilman**[†1], **J. Ruczkowski**[2], **A. Sikorski**[2]

1. Institute of Materials Research and Quantum Engineering, Faculty of Technical Physics, Poznan University of Technology, Piotrowo 3, Poznan 60-965, Poland

2. Institute of Control, Robotics and Information Engineering, Faculty of Electrical Engineering, Poznan University of Technology, Piotrowo 3A, Poznan 60-965, Poland

On the basis of new experimental results concerning the fine (*fs*) and hyperfine structure (*hfs*) [1], [2], [3] as well as on available literature data, a parametric study of the atomic structure for the odd-parity configurations of atomic holmium was performed. A multi-configuration fit of 11 configurations ($4f^{11}6s^2$, $4f^{11}5d6s$, $4f^{11}6s6d$, $4f^{11}6s7s$, $4f^{11}6s8s$, $4f^{11}6p^2$, $4f^{11}5d^2$, $4f^{10}6s^26p$, $4f^{10}6s^27p$, $4f^{10}5d^26p$, $4f^{10}5d6s6p$) in the complete set of $4f^N$-core states was carried out. The present paper is the application of our many-body parametrization method allowing the analysis of a complex electronic system composed of a configuration of up to four open shells, presented in general terms in the first work of the series under the common title *Construction of the energy matrix for complex atoms* [4]. The contributions from the second-order perturbation theory originating from electrostatically correlated spin-orbit interactions [5] in the fine structure, as well as electrostatically correlated hyperfine interactions (core polarization effects) in the hyperfine structure [6], were considered.

The calculations of the enormous fine- and hyperfine structure matrices required high-performance computing (HPC), concerning both CPU (Central Processing Unit) speed and memory allocation. For the purpose of the huge matrix diagonalization in the case of terbium atom, the methods utilizing the personal computer clusters and, alternatively, the Microsoft Azure cloud computing, have been proposed by us in the papers [7], [8].

Within this work for the hyperfine structure angular coefficients calculation HPC software and infrastructure have been used. The independence of states allowed factoring out of sequential component computations. Subsequently, an OpenMP loop calculated the angular coefficients on a Intel Xeon node hosting 28 CPUs. In consequence the total 112 CPUs have been used simultaneously, as calculations for four largest *J* submatrices have been performed on individual nodes.

In the current version the fine structure fitting relied on Intel MKL heavily parallel and vectorized diagonalization routine. However, in our future work the fitting is going to be delegated to GPU devices. The HPC utilization resulted in a significant performance boost. The computing infrastructure has been provided by Poznan Supercomputing Center (www.man.poznan.pl) and Microsoft Azure.

For unknown electronic levels predicted values of the level energies and hfs constants are given, which can facilitate further experimental investigations.

The research within this work was financially supported by Poznan University of Technology under the Project 06/65/DSPB/5183.

References

[1] D. Stefanska, B. Furmann, J. Quantum Spectrosc. Radiat. Transf. **260**, 286-295 (2018).
[2] D. Stefanska, B. Furmann, P. Glowacki, J. Quantum Spectrosc. Radiat. Transf. **213**, 159-168 (2018).
[3] B. Furmann *et al.*, to be published.
[4] M. Elantkowska, J. Ruczkowski, J. Dembczynski, Eur. Phys. J. Plus **130**, 14 (2015).
[5] M. Elantkowska, J. Ruczkowski, J. Dembczynski, Eur. Phys. J. Plus **131**, 47 (2016).
[6] M. Elantkowska, J. Ruczkowski, J. Dembczynski, Eur. Phys. J. Plus **131**, 429 (2016).
[7] M. Elantkowska, A. Sikorski, J. Ruczkowski, J. Dembczynski, Eur. Phys. J. Plus **132**, 134 (2017)
[8] M. Elantkowska, J. Ruczkowski, A. Sikorski, J. Dembczynski, Eur. Phys. J. Plus **132**, 455 (2017)

[*]Corresponding author: magdalena.elantkowska@put.poznan.pl
[†]Corresponding author: sebastian.b.wilman@doctorate.put.poznan.pl

A first principle electronic structure calculation on astrochemically important molecular cation ArH^+

V. Terashkevich[*1], **E. Pazyuk**[†1], **A. Stolyarov**[1]
1. Department of Chemistry, Lomonosov Moscow State University, GSP-1, Leninskie Gory 1/3, 119991, Moscow, Russia

An increase of scientific interest towards physicochemical properties of different isotopologues of molecular cation ArH^+ is mostly inspired by the signals of $^{36}ArH^+$ and $^{38}ArH^+$ isotopologues being recently discovered in the Crab Nebula spectral signature [1], formed as a result of a supernova outbreak of SN 1054 in 1054. The elemental composition of the filament of the Crab Nebula is similar to the composition of the planetary nebula and interstellar gas and is a mixture of hydrogen with other light atoms, such as helium, argon, oxygen, neon, sulfur. The most common argon isotope in the universe is the ^{36}Ar, which is formed as a result of the stellar nucleosynthesis accompanied by supernova outburst. At the same time, the most abundant isotope on earth is the ^{40}Ar. As a result, the data obtained during scientific study is predominantly dedicated to $^{40}ArH^+$ cation, while an obvious lack of such information for molecular cations $^{36}ArH^+$ and $^{38}ArH^+$ can be seen [2]. Obtaining the correct information about the spectral lines of the isotopes of the molecular ion ArH^+ is of great importance, since it is assumed that this ion can correspond to unidentified lines in the spectra of other objects, in particular, the molecular cloud Sgr B2. Quantitative study of isotope switch influence on structure and dynamic properties of the ArH^+ cation isotopologues in a wide range of vibrational and rotational excitation is essential for unambiguous assignment of the spectral lines and a level-by-level description of the radiative cooling in extremely tenuous interstellar medium (ISM).

In the present work we computed a Born-Oppenheimer potential and adiabatic correction in a wide range of internuclear distances for the ground state of the ArH^+ molecular ion. Electronic energies were calculated using non-empirical quantum chemistry methods of various levels of accuracy (CCSD(T), CCSD(T)-F12, MR-AQCC, MR-ACPF) and the XZaPa-NR basic sets. The resulting energies were corrected for the basis set superposition error (BSSE) and extrapolated to the complete basis set (CBS), in the framework of alternative extrapolation schemes. The scalar-relativistic effect was estimated according to Douglas-Kroll approximation and Cowan-Griffin perturbation approach. The reliability of the present *ab initio* adiabatic potential is accessed through a comparison with preceding theoretical and empirical counterparts **[3], [4]**.

The permanent dipole moment and static polarizability in the ground state have been calculated using the finite electric field method. The obtained information on structural properties was used to evaluate the probability of rotational and vibrational-rotat ional transitions of different isotopologues of the ArH^+ cation.

ACKNOWLEDGMENTS
The work was supported by the RFBR Grant Nos. 18-03-00726/18

References

[1] Barlow M. J., Swinyard B. M., Owen P.J., et al. *Detection of a noble gas molecular ion, $^{36}ArH^+$, in the Crab Nebula*, Science. 2013. V. 342 (6164). P. 1343-1345.
[2] Bizzocchi L., Dore L., Esposti C. et al. *First laboratory measurement of the j= 1-0 transitions of $^{36}ArH^+$ and $^{38}ArH^+$: new, improved rest frequencies for astronomical searches*, Astrophysical J. Lett. 2016. V. 820. L26.
[3] Coxon J., Hajigeorgiou P. *Accurate internuclear potential energy functions for the ground electronic states of NeH^+ and ArH^+*, J. Mol. Spec. 2016. V. 330. P. 63-71.
[4] Alekseyev A., Liebermann H.-P., Buenker R. *Theoretical study of the ArH^+ photodissociation*, Phys. Chem. Chem. Phys. 2007. V. 9, P. 5088–5095.

[*]Corresponding author: terversik@yandex.ru
[†]Corresponding author: pazyuk@phys.chem.msu.ru

B – 24

Diode laser direct optical pumping of a cw dye laser operated in red spectral region

D. Stefańska*, M. Suski, K. Nita, M.Chojnacki, B. Furmann
Division of Quantum Engineering and Metrology, Institute of Materials Research and Quantum Engineering, Faculty of Technical Physics, Poznan University of Technology, Piotrowo 3, 60-965 Poznań, Poland

Continuous-wave tunable single-mode dye lasers have been applied for decades as a standard source of exciting radiation in frequency-resolved spectroscopic studies. Although in some parts of the visible spectrum they have commonly been replaced by the more compact and energy-efficient diode lasers, the readily obtained wavelength tunability over tens of nanometers makes dye lasers still competitive in certain applications. However, the high cost of the commonly used pump radiation sources (gas lasers or frequency-doubled Nd-doped DPSS lasers) makes such systems relatively expensive.

Recently we demonstrated cw tunable single-mode operation of a dye laser operated in blue-green spectral region under optical pumping by an economy-class 4 W power diode laser at $\lambda = 445$ nm [1]. That laser system proved to be a useful tool in high-resolution laser spectroscopic experiments performed in our laboratory, and constituted an inspiration for attempts of achieving diode laser pumping of laser dyes also in other spectral regions. Because of the specific requirements of the spectroscopic investigations currently performed, we first focused on the red region.

The optimum laser dye operated in this region, which was expected to be suited for diode laser pumping in blue, was DCM. This is known to be an efficient dye in cw operation [2], [3] and its absorption curve is peaked around 470 nm [4] (the latter was also confirmed by absorption measurements performed for a high-viscosity solution suitable for a dye-jet cw laser).

The cw laser generation of DCM under optical pumping by the blue diode laser mentioned was achieved. Preliminary investigations of the dye laser output power in variable output coupling scheme were performed, which allowed rough estimation of the relative gain and resonator internal loss, as well as the desired output coupling mirror transmission. Optimization of the resonator configuration, dye concentration and the diode laser pump beam focusing system are in progress. Laser generation parameters to be achieved are expected not to be inferior to those obtained in blue-green region.

The work was supported by Poznan University of Technology under the Project 06/65/DSPB/5183.

References

[1] D. Stefańska, M. Suski, B. Furmann, Laser Physics Letters **14**, 045701 (7pp) (2017).
[2] P.R. Hammond, Optics Communications **29**, 331-333 (1979).
[3] T.F. Johnston, R.H. Brady, and W. Proffitt, Applied Optics **21**, 2307-2316 (1982).
[4] U. Brackmann, *Lambdachrome Laser Dyes*, 3rd ed., Lambda Physik AG (2000), and the references therein.

*Corresponding author: danuta.stefanska@put.poznan.pl

Precision description of the atomic structure. Example of the even configuration system of La I

J. Dembczyński*[1], M. Elantkowska[2], J. Ruczkowski[1]

1. Institute of Control, Robotics and Information Engineering, Faculty of Electrical Engineering, Poznań University of Technology, Piotrowo 3A, 60-965 Poznań, Poland

2. Institute of Materials Research and Quantum Engineering, Faculty of Technical Physics, Poznan University of Technology, Piotrowo 3, 60-965 Poznań, Poland

We developed the method, which allows to analyze a complex electronic systems composed of the configurations of up to four open shells, taking into account all electromagnetic interactions expected in an atom, in accordance with the second-order perturbation theory [1],[2]. Within this theory, all possible combinations following the excitation of one or two electrons from closed shells to particular open shells were considered. The appropriate formulae and computer codes have been developed for many years by our research group. The application of this method to the even configurations system $(5d + 6s)^3$ of lanthanum atom in 2010 [1]. For all the levels, the comparison of experimental and calculated energy values, g_J factors and hfs constants was presented. Also, for the levels $5d^3\ ^2D$ $J = 3/2$, $J = 5/2$, the missing attributes were predicted. The experimental studies carried out in subsequent years confirmed the predicted energy value and hyperfine structure constants. Satisfactory results obtained in this work were only possible due to the very precise wave functions obtained from the semi-empirical multi-configuration fine structure analysis, taking into account the first- and second-order effects of perturbation theory.

Recently, the discovery of previously unknown energy levels of lanthanum atom were performed with Doppler-limited laser spectroscopy with optogalvanic or laser-induced fluorescence detection [3],[4],[5],[6],[7],[8].

Currently the La level list contains ca. 430 even La I levels, all of them with known hyperfine constants A (sometimes also B constants are known). 167 odd La levels are known, but few of them may not really exist. It provides an excellent test confirming the correctness of our method and the complex formulae derived, which in the case of consideration, e.g. configurations with three open shells, require recoupling of five or more angular momenta and strict observance of the electron permutation rules, in particular for interconfiguration matrix elements.

For the current study we considered the expended system of 190 even configurations. The energy matrix for the above-mentioned systems was constructed with 2638 independent parameters. Finally, 63 radial integrals were used as adjustable parameters. Other parameters are fixed on zero or the values from theoretical Hartree–Fock calculations.

The hyperfine structure constants were calculated using the fine structure eigenvectors and adjusting radial integrals in a least-squares procedure which compare the calculated constants with the experimental values. Moreover, the values of energy for the levels up to now unidentified and hyperfine structure constants were predicted.

The research within this work was financially supported by Poznan University of Technology under the Project 04/45/DSPB/0184

References

[1] J. Dembczyński, M. Elantkowska, B. Furmann, J. Ruczkowski, and D. Stefańska, J Phys B: At Mol Opt Phys **43**, 06500 (2010)
[2] M. Elantkowska, J. Ruczkowski, and J. Dembczyński, Eur Phys J Plus **130**, 14 (2015)
[3] F. Güzelçimen, I. Siddiqui, G. Başar, S. Kröger, and L. Windholz, J Phys B: At Mol Opt Phys **45**, 135005 (2012)
[4] F. Güzelçimen *et al.*, Astrophys J Suppl Ser **208**, 18 (2013)
[5] I. Siddiqui, S. Khan, B. Gamper, J. Dembczyński, and L. Windholz, J Phys B: At Mol Opt Phys **46**, 065002 (2013)
[6] B. Gamper, P. Głowacki, I. Siddiqui, J. Dembczyński, and L. Windholz, J Phys B: At Mol Opt Phys **47**, 165001 (2014)
[7] Gü. Başar *et al.*, J Quant Spectrosc Radiat Transf **187** 505 (2017)
[8] Ł.M.Sobolewski, T. Binder, C. Güney, B. Gamper, J. Kwela and L. Windholz, J Quant Spectrosc Radiat Transf **200** 108 (2017)

*Corresponding author: jerzy.dembczynski@put.poznan.pl

Comparison of the computer simulation and the experimental spectral line shapes for two N I multiplets

A. Bartecka*, **A. Bacławski, W. Olchawa**
1. Institute of Physics, University of Opole, ul. Oleska 48, 45-052 Opole, Poland

The computer simulation method (CMS) [1] dedicated to the non-hydrogen lines, which energy levels are influenced only by the quadratic Stark effect, is tested in this work. Proposed method extents the range of applicability of computer simulation, which are mainly used for hydrogen, hydrogen-like and helium lines.

In order to calculate spectral line shapes by using CMS, the Schrödinger equation should be solved many times for various plasma conditions. The emitter-plasma interaction potential is given by:

$$V(t) = -\vec{d}\cdot\vec{F}(t), \tag{1}$$

where $\vec{F}(t)$ means the electric field and $\vec{d}$ – the dipol operator of the emiter. The Strang symmetrical splitting formula was applied to solve the Schrödinger equation of evolution, leading to unitary time evolution:

$$\begin{aligned} U(t+\Delta t,t) \cong & \exp(id_xF_x\Delta t/2\hbar)\exp(id_yF_y\Delta t/2\hbar)\exp(id_zF_z\Delta t/2\hbar)\times \\ & \exp(-iH_0\Delta t/\hbar)\exp(id_zF_z\Delta t/2\hbar)\exp(id_yF_y\Delta t/2\hbar)\exp(id_xF_x\Delta t/2\hbar). \end{aligned} \tag{2}$$

This simulation method is proposed in [2].

The results of the computer simulation and measurements concernig the electron impact width w_e, the electron impact shift d_e and the ionic asymmetry parameter A of the spectral lines N I $3p^2S^o - 3d^2P$ and $(^1D)3s^2D - (^1D)3p^2P^o$ are compared.

Line shape measureements were performed using a wall-stabilized arc, operated at atmospheric pressure. The radiation of the plasma, emitted from homogeneous plasma layers in end-on direction, was measured using a grating-spectrometer with a two-dimensional CCD detector. Experimental value of Stark broadening parameters have been obtained from the best fit procedures applying the $j(x)$ profiles [3], convoluted with the corresponding Doppler and apparatus profiles. In the fittig procedure the relation between w_e and A: $Aw_e^{(3/4)}/N_e = const$ was used. This procedure of the asymmetry parameter determination is described in [4]. In Fig. 1 the comparison of the simulated profile with the experimental one for the N I line $(^1D)3s^2D_{3/2} - (^1D)3p^2P^o_{1/2}$ is shown, as an example.

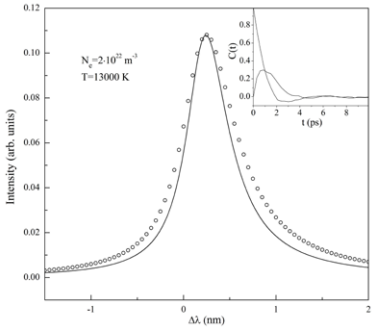

Fig. 1: The simulated profile (solid line) of the spectral line N I $(^1D)3s^2D_{3/2} - (^1D)3p^2P^o_{1/2}$ is presented and compared with experimental result (circles). As can be seen, the experimental profile is more asymmetric and more broadened than simulated one. Real and imaginary parts of the autocorrelation function are shown in the inset.

This work has been carried out within the framework of the EUROfusion Consortium and has received funding from the Euratom research and training programme 2014-2018 under grant agreement No 633053. The views and opinions expressed herein do not necessarily reflect those of the European Commission.

References

[1] J. Seidel, and R. Stamm, J. Quant. Spectr. Rad. Transf.**27**, 499 (1982).
[2] W. Olchawa, A.Bartecka, and A. Bacławski, IOP Conf. Series: Journal of Physics: Conf. Series **810**, 012044 (2017).
[3] H. R. Griem, *Spectral line broadening by plasmas*, Academic Press, New York 1974.
[4] A. Bartecka, W. Olchawa, A. Bacławski, and J. Musielok, Eur. Phys. J. ST **222**, 2381 (2013).

*Corresponding author: bartecka@uni.opole.pl

Light narrowing with spin-exchange optical pumping in a paraffin coated cell

Wei Xiao[1], **Wenhao Li**[1], **Xiang Peng**[*1], **Jingbiao Chen**[1], **Hong Guo**[†1],
1. State Key Laboratory of Advanced Optical Communication Systems and Networks, School of Electronics Engineering and Computer Science, and Center for Quantum Information Technology, Peking University, Beijing 100871, China

The spin-exchange (SE) collisions between alkali atoms are typically the domaint cause of spin relaxation for alkali-metal atomic magnetometry. To suppress the SE relaxation, one of the methods is light narrowing, which was first discovered by Bhaskar et al [1]. In 1999, a significant linewidth narrowing was obtained by utilizing gas cell with $\sim$ 10 atm pressure [2] and lately was investigated by Han et al [3] in pareffin coated cells. However, due to the depolarization caused by radiation trapping, the light narrowing was not observed in paraffin coated ^{87}Rb vapor cells.

In order to eliminate radiation trapping, the spin-exchange optical pumping (SEOP) method was adopted with a paraffin coated K-Cs hybrid cell in our experiment. The difference between SEOP and direct pumping method is that SEOP can polarize the target atoms without inducing spontaneous radiation from the exited atoms in optical pumping process. When we use the minor alkali species (K) to polarize the domaint alkali species (Cs) via SEOP, the radiation trapping can be partly suppressed. As a result, we observed noticeable light narrowing effects by pumping K and probing Cs in our experiment.

The schematic of the experiment is depicted in Fig.1 (a). A 770 nm Distributed Bragg Reflector (DBR) laser is used as pump light and a 852 nm DBR laser is used as probe light. The probe light is kept at 3 μW and detuned away from D1 line F=4. A cylindrical glass cell of 35 mm diameter containing the K-Cs hybrid atomic vapor is placed inside a seven-layer set of magnetic shields. Three sets of coils inside the shield generate magnetic fields needed for RF magnetic field B_{rf} ($\approx$ 0.2 nT) and leading field B_0 ($\approx$ 540 nT). The vapor cell was housed in a boron-nitride oven that was heated with quad-twisted copper wires carrying alternative current at 100 kHz.

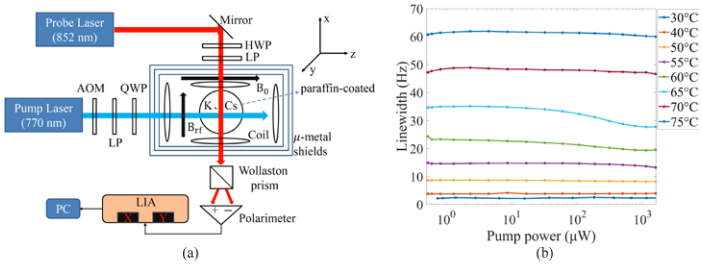

Fig. 1: (a) Schematic of the experiment setup. LP, linear polarizer; HWP, half-wave plate; QWP, quarter-wave plate; LIA, lock-in amplifier; AOM, acousto-optic modulator; PC, personal computer. (b) Pump power dependence of the magnetic resonance for Cs. During the measurements, the pump light is tuned near the center of the K D1 resonance to maximize the resonance amplitude and the probe light is also tuned to the frequency where the resonance amplitude is maximized.

As shown in Fig.1 (a), a continuous pump beam was used to polarize the K atoms along $\hat{z}$ direction, and Cs is polarized along the same direction via spin exchange collisions with K. The Helmholtz coils produce a constant leading field B_0 parallel to the pump light and a small rotating RF field B_{rf} perpendicular to the leading field to exite the Zeeman resonance. The probe light propagates along the $\hat{x}$ direction.

We can see from the Fig.1 (b), the linewidth (FWHW) of the Cs resonance decreases by 10%$\sim$20% with the pump power in each temperature. With the increase of the temperature, the polarization of Cs would be lower due to stronger radiation trapping and the SE relaxation gradually becomes a domaint factor of spin relaxation. Therefore there is no obvious reduction of linewidth in high temperature ($\sim$ 70°C) for low polarization caused by radiation trapping of K. Meanwhile in low temperature ($\sim$ 30°C), the SE relaxation is too low to distinguish the light narrowing from the noise. The most obvious reduction of linewidth (from 35 Hz to 27 Hz) measured is in 65°C.

References

[1] Bhaskar N D, Camparo J, Happer W, et al, Phys. Rev. A, **23**(6), 3048 (1981)
[2] S. Appelt, A. Ben-Amar Baranga, A. R. Young, and W. Happer, Phys. Rev. A, **59**(3), 2078 (1999).
[3] Han R, Balabas M, Hovde C, et al, AIP Advances, **7**(12), 125224 (2017).

[*]Corresponding author: xiangpeng@pku.edu.cn
[†]Corresponding author: hongguo@pku.edu.cn

Three-photon coherent population trapping for high resolution spectroscopy

C. Chatou[*1], **M. Collombon**[1], **M. Marchenay**[1], **G. Hagel**[1], **J. Pedregrosa-Gutierrez**[1], **M. Houssin**[1], **C. Champenois**[1], **M. Knoop**[1]

1. Aix Marseille Université, CNRS, PIIM UMR 7345, 13397, Marseille, France

An ion cloud, represented here by a four level atomic system $|S_{1/2}\rangle, |P_{1/2}\rangle, |D_{3/2}\rangle$ and $|D_{5/2}\rangle$,is trapped in a radio-frequency(RF) trap and detected by the collection of spontaneous emission photons from the $|P_{1/2}\rangle$ to $|S_{1/2}\rangle$ transition.

The lambda (Λ) configuration with lasers at 866nm and 397nm allows for a two photon dark state to take place (because $|S_{1/2}\rangle$ and $|D_{3/2}\rangle$ are a stable and a metastable level). If the $|S_{1/2}\rangle$ is coupled to the $|D_{5/2}\rangle$ state (also a metastable level) a three photon dark state is expected[1]. After computation we can show that the condition for this state to be decoupled from the rest of the system is :

$$\Delta R + \Delta C - \Delta B + \frac{\Omega_C^2}{4\Delta C} = 0 \tag{1}$$

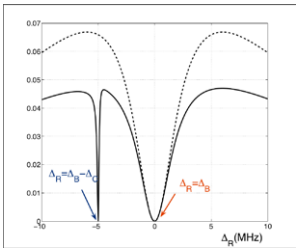

Fig. 1: Theorical spectrum of the spontaneous emission vs. the repumping laser detuning, it shows at -5 MHz the 3 photon dark state (here the $\frac{\Omega_C^2}{4\Delta C}$ term is neglected) and at 0 MHz the two photon dark state. The dashed line is the spectrum without 729nm laser.

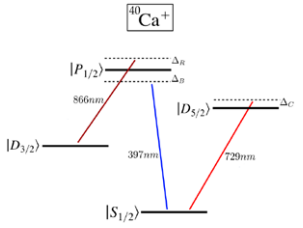

Fig. 2: Energy levels and wavelengths involved in the three-photon process.

To achieve a 3-photon coherent population trapping experimentally[2], one has to reduce the relative phase fluctuations of the three lasers for the dark state to be stable. In order to do so, two lasers are phase-locked to a frequency comb which is itself locked to the 729nm laser. This 729nm ultra-stable Ti:Sa laser was designed and built within the laboratory and has a frequency stability better than 5×10^{-14} at one second and a linewidth of a few Hz.

When the detuning condition (see Eq.1) between the three involved lasers is fulfilled we can access a measurement of the frequency transition between $|D_{3/2}>$ and$|D_{5/2}>$ (a magnetic dipole transition) and obtain a terahertz frequency standard[3]. Indeed the transition linewidth of the three photon dark line is narrower than the one of the two photon dark resonance and allows a higher resolution for spectroscopic measurements. Futhermore three laser wavevectors allow to tune the contribution of first order Doppler effect using their geometric configuration.

At present, experimental resolutions of less than 1 kHz have already been obtained in the interrogation of a large ion cloud, and the protocol has not yet reached its final resolution. Recent progress will be reported at the conference.

References

[1] C. Champenois, G. Morigi, J. Eschner "Quantum coherence and population trapping in three-photon processes", *Phys. Rev. A* 74 053404 (2006).

[2] M. Collombon and *et al.*, in preparation.

[3] C. Champenois, G. Hagel, M. Houssin, M. Knoop, C. Zumsteng, and F. Vedel, "Terahertz frequency standard based on three-photon coherent population trapping", *Phys. Rev. Lett.*, vol.99,no. 1,p. 013001,2007.

*Corresponding author: cyril.chatou@univ-amu.fr

Dipole-Dipole Interaction Strength and Dipole Blockade Radius using Förster Resonances in Rb Atoms

T. Kirova*[1], M. Auzins†[2], I. I. Beterov[3], A. Cinins[1], Y.-H. Chen[4], I. A. Yu[4]
1. Institute of Atomic Physics and Spectroscopy, University of Latvia, LV-1586 Riga, Latvia
2. Laser Centre, University of Latvia, LV-1002, Riga, Latvia
3. Rzhanov Institute of Semiconductor Physics SB RAS and Novosibirsk State University, Quantum Center, 630090 Novosibirsk, Russia
4. Department of Physics, National Tsing Hua University, Hsinchu, Taiwan

In the phenomenon of dipole blockade [1], the dipole-dipole (DD) interaction between Rydberg atoms causes shifting of their energy levels, making the applied laser excitations off-resonant. Thus, only a single atom can be excited within the "blockade sphere" [2] with radius R_b, while simultaneous excitation of two/multiple Rydberg atoms will be suppressed. Our aim is to find the best experimental parameters necessary to achieve $R_b \approx 50\mu m$, which will be later measured experimentally. We are especially interested in the resonant $1/R^{-3}$ type DD interaction, which happens at shorter distances, when the magnitude of the interaction becomes comparable to the energy gaps between atomic levels. For different Förster resonances in a $^{87}Rb -^{87} Rb$ pair the interactions can be remarkably strong, e.g. the $58d_{3/2}+58d_{3/2}\rightarrow 60p_{1/2}+56f_{5/2}$ transition [3] leads to $R_b = 10\mu m$, while the $81s_{1/2}+84s_{1/2}\rightarrow 81p_{1/2}+83p_{1/2}$ transition [4] allows for $R_b = 22\mu m$ to be achieved for the experimentally accessible excitation laser Rabi frequency of $6MHz$.
With our purpose in mind, we calculate the magnitude of the C_6 coefficients for specific Förster transitions in ^{87}Rb of the form $n_a d_{3/2}+n_b d_{3/2}\rightarrow n_\alpha l_\alpha j_\alpha + n_\beta l_\beta j_\beta$. In this case the two atoms are initially in the $d_{3/2}$ states, while the l and j numbers of the final states can take different values. The principal quantum numbers n_a and n_b of the initial states can differ by $\pm 1, \pm 2, \pm 3$, etc., while those of the final states can be the same or different.
A large C_6 coefficient is associated with a minimum in the absolute value of the Förster defect δ_k, which we plot as a function of the principle quantum number n_a for the transititons descibed above. We found that in all cases under study, the "δ_k vs n_a" curves show diverging behavior and no minimum of the absolute value of δ_k is observed. For completeness, we studied the same transitions, but when the two atoms are initially in the $d_{5/2}$ states. All curves exhibit similar behaviour to their $d_{3/2}$ counterparts and if plotted together with them, show very small difference.

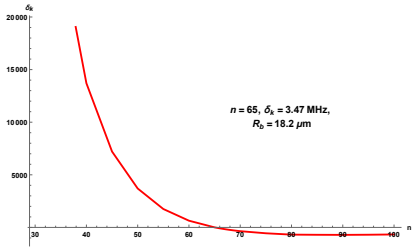

Fig. 1: Förster defect vs principal quantum number when atoms are initially in the $p_{1/2}$ states, where $n_b = n_a + 20$ and $n_\beta = n_\alpha + 19$.

An interesting case when the initial principal quantum numbers of the two atoms differ by a signifficant amount, is studied experimentally in [5], e.g. $60p+80p\rightarrow 59d+78d$. Here, we extended the study of Förster defect vs principal quantum number for transitions $n_a p_{1/2,3/2}+n_b p_{1/2,3/2}\rightarrow n_\alpha l_\alpha j_\alpha + n_\beta l_\beta j_\beta$. The obtained results indicate that all curves are crossing the "$\delta_k = 0$" line in the vicinity of $n_a = 60$. However, for the transition $np_{1/2}+(n+20)p_{1/2}\rightarrow(n-1)d_{3/2}+(n+18)d_{3/2}$, shown in Fig. 1, this minimum occurs at $n_a = 65$, corresponding to $\delta_k = 3.47MHz$, $C_6 = -219000GHz\mu m^6$, and giving a blockade radius of $R_b = 18.21\mu m$.
This work was supported by the Trilateral Grant of the Latvian, Lithuanian, and Taiwanese Research Councils *Quantum and Nonlinear Optics with Rydberg-State Atoms* (2016-2018) FP-20578-ZF-N-100.

References

[1] A. Gaetan *et al.*, Nature,**5**, 115 (2009).
[2] D. Tong *et al.*, Phys. Rev. Lett, **93**, 063001 (2004).
[3] T. Wallker and M. Saffman, Phys. Rev. A, **77**, 032723 (2008).
[4] I. I. Beterov and M. Saffman, Phys. Rev. A, **92**, 042710 (2015).
[5] I. I. Beterov *et al.*, Phys. Rev .A, **97**, 032701 (2018).

*Corresponding author: teo@lu.lv
†Corresponding author: marcis.auzins@lu.lv

B – 30

Nuclear spin polarization of the NV centers ^{14}N nucleus in diamond studies using the method of ODMR

Marcis Auzinsh[1], Andris Berzins[1], Dmitry Budker[2,3], Laima Busaite[*1], Ruvin Ferber[1], Florian Gahbauer[1], Reinis Lazda[†1], Arne Wickenbrock[2], Huijie Zheng[‡2]

1. Laser Centre, University of Latvia
2. Helmholtz Institute Mainz, Johannes Gutenberg University
3. Department of Physics, University of California at Berkeley, USA

In this study the energy levels of the NV centers in diamond were investigated using the method of ODMR spectroscopy [1] near the electronic GSLAC at an axial magnetic field around 102.4 mT in diamond samples with low (1 ppm) and high (200 ppm) nitrogen concentration on the ground state $m_s = 0 \longrightarrow m_s = \pm 1$ transitions to study the hyperfine level structure of NV-center ensembles in the vicinity of the GSLAC [2]. Hyperfine level structure and the transition strengths from the theoretical model (see Eq. 1) were obtained. A parameter-optimization procedure to fit the experimentally measured curves with the results of a theoretical calculation was used. This fitting procedure yielded information about the degree of nuclear polarization of the ^{14}N spin in the vicinity of the GSLAC, a decrease has been observed (see Fig. 1).

The Hamiltonian for the NV center including the hyperfine interaction with ^{14}N (nuclear spin $I = 1$ which interacts with the NV electron spin) in an external magnetic field **B** along the z-axis (NV axis) can be written as [3]

$$\hat{H} = D\hat{S}_z^2 + \gamma_e \mathbf{B}\cdot\hat{\mathbf{S}} + \hat{\mathbf{S}}\cdot\hat{A}\cdot\hat{\mathbf{I}} + Q\hat{I}_z^2 - \gamma_n \mathbf{B}\cdot\hat{\mathbf{I}}, \tag{1}$$

where $D = 2870$ MHz is the zero-field splitting of the ground-state components with spin magnetic quantum numbers $m_S = 0$ and $m_S = \pm 1$, γ_e is the electron gyromagnetic ratio. The matrix $\hat{A}$ is a diagonal hyperfine-interaction tensor between the electron spin **S** and the nuclear spin **I**. The quadrupole interaction parameter Q, and the strengths of the nuclear spin interaction with the external magnetic field is determined by the gyromagnetic ratio of ^{14}N nucleus γ_n.

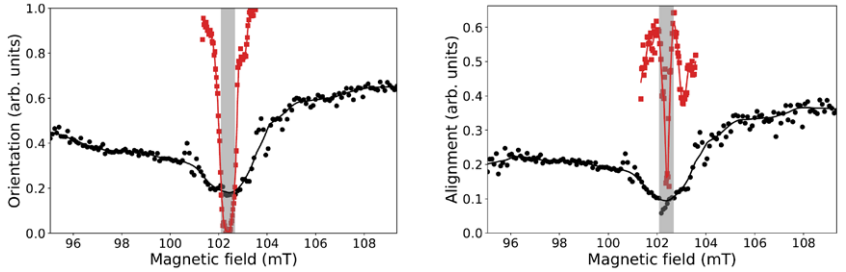

Fig. 1: Nuclear ^{14}N spin orientation (left) and alignment (right) obtained for the ground state $m_S = 0 \longrightarrow m_S = +1$ transition from the fitted ODMR transition peak amplitudes. The red squares correspond to the 1 ppm sample and the black dots to the 200 ppm sample. The gray, shaded region corresponds to the magnetic field range in which the theoretical model does not reproduce the measurements well.

Acknowledgements

The Riga group gratefully acknowledges the financial support from the M-ERA.NET project "Metrology at the Nanoscale with Diamonds" (MyND) and from the Laserlab-Europe Project (EU-H2020 654148), and from the Base/Performance Funding Project Nr. AAP2016/B013, ZD2010/AZ27. A. Berzins acknowledges support from the PostDoc Latvia Project Nr. 1.1.1.2/VIAA/1/16/024 "Two-way research of thin-films and NV centres in diamond crystal". The Mainz group acknowledges support by the German Federal Ministry of Education and Research (BMBF) within the Quantumtechnologien program (FKZ 13N14439) and the DFG through the DIP program (FO 703/2-1). H. Zheng acknowledges support from the GRK Symmetry Breaking (DFG/GRK 1581) program.

References

[1] M. Negyedi, J. Palotás, B. Gyüre, S. Dzsaber, S. Kollarics, P. Rohringer, T. Pichler and F. Simon, Rev. Sci. Instrum. **88**, 013902 (2017).
[2] M. Auzinsh, A. Berzins, D. Budker, L. Busaite, R. Ferber, F. Gahbauer, R. Lazda, A. Wickenbrock and H. Zheng, submitted to arXiv.org, https://arxiv.org/abs/1805.01251v1, submitted to be published in Phys. Rev. B (2018).
[3] J. D. A. Wood, D. A. Broadway, L. T. Hall, A. Stacey, D. A. Simpson, J.-P. Tetienne and L. C. L. Hollenberg, Phys. Rev. B **94**, 155402 (2016).

*Corresponding author: laima.busaite@lu.lv
†Corresponding author: reinis.lazda@lu.lv
‡Corresponding author: zheng@uni-mainz.de

Optical dipole mirror for cold atoms based on Surface Plasmon Polaritons

A. Sierant[*1], **R. Panaś**[1], **J. Fiutowski**[2], **T. Kawalec**[1]
1. Atomic Optics Department, Jagiellonian University, Łojasiewicza 11, 30-348 Kraków, Poland
2. Mads Clausen Institute, NanoSyd, University of Southern Denmark, Alsion 2, 6400 Sonderborg, Denmark

Surface plasmon polaritons (SPPs) are electromagnetic excitations resulting from collective oscillations of the electron gas in a metallic diffraction grating coupled with an electromagnetic wave. The SPPs resonance together with the calculated distribution of the electromagnetic field effective intensity above two gold grooves is shown in the inset of Fig. 1. To measure the effective intensity of the SPPs in the diffraction grating system we have implemented it in an optical dipole mirror for cold rubidium atoms (^{87}Rb isotope) [1]. Such a mirror uses a repulsive dipole force associated with a high intensity gradient of the SPPs to reflect atoms falling under the gravity force, as can be seen in Fig. 2 [1],[2]. Atomic mirror is then a desireable tool for atom control and manipulation and can be used for a construction of a surface trap in the future. We have also directly monitored the thermal effects inherently linked to the light absorption accompanying SPPs excitation.

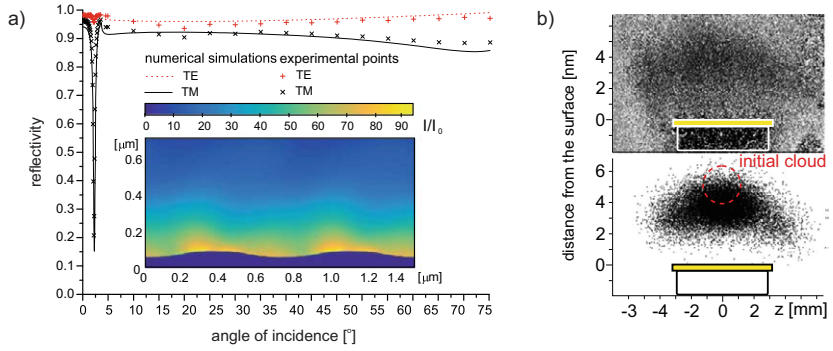

Fig. 1: a) Reflectivity versus angle of incidence for two linear polarizations (TM and TE) of a 785 nm excitation laser beam – calculations and measurements. The inset shows calculated relative field intensity distributions for the preferred angle of incidence. b) Measured (top) and calculated (bottom) distribution of 10^5 atoms, 17 ms after the reflection off the disc. The outline of the disc and its mounting platform as well as the size of the initial cloud are also shown.

References

[1] T. Kawalec et al., *Surface Plasmon Polaritons Probed with Cold Atoms*, Plasmonics, **13**, 639, (2018)
[2] T. Kawalec et al., *Optical dipole mirror for cold atoms based on a metallic diffraction grating*, Opt. Lett. **39**, 2932 (2014)

*Corresponding author: aleksandra.plawecka@doctoral.uj.edu.pl

Testing the parity symmetry in chiral molecules using vibrational spectroscopy

M. Manceau*[1], L. Lecordier[1], M. Pierens[1], A. Cournol[1], D.B.A Tran[1], R. Santagata[1], B. Argence[1], A. Shelkovnikov[1], O. Lopez[1], C. Daussy[1], C. Chardonnet[1], M. Abgrall[2], Y. Le Coq[2], R. Le Targat[2], W. K. Lee[2], D. Xu[2], P-E Pottie[2], R. J. Hendricks[3], T. E. Wall[4], J. Bieniewska[4], B. E. Sauer[4], M. R. Tarbutt[4], A. Amy-Klein[1], S. K. Tokunaga[1], B. Darquié[1].

1. Laboratoire de Physique des Lasers, Université Paris 13, 93 430 Villetaneuse, France
2. LNE-SYRTE, Observatoire de Paris, PSL Research University, CNRS, Sorbonne Universités, UPMC Univ. Paris 06, Paris, France
3. National Physical Laboratory, NPL, Teddington, United Kingdom
4. Centre for Cold Matter, Imperial College London, London, United Kingdom

Unlike the other fundamental interactions, the weak interaction is known to violate the parity symmetry, i.e the symmetry under spatial inversion. It was experimentally demonstrated using nuclear and atomic systems and in high energy physics. However, despite being theoretically predicted, parity-violation (PV) was never measured in molecules. In particular for a chiral molecule, i.e. a molecule non-superimposable to its mirror image, it is expected to lead to energy differences between the left- and right-handed enantiomers, and in turn to frequency differences in their rovibrational spectra potentially measurable using precise mid-infrared spectroscopy. Those PV frequency shifts are however predicted to be extremely small, in the mHz to Hz range [1] depending on the species considered for vibrational transitions at ~ 30 THz. Measuring this allows several fundamental questions to be addressed, from the limit of the standard model in the low-energy regime to the still unexplained origin of biomolecular homochirality, while it can also serve as a benchmark in relativistic quantum chemistry calculations.

Attempting a measurement of PV in chiral molecules starts with the choice of the molecular species to be probed. As the PV effects scale with the fifth power of the nuclear charge Z, large molecules with heavy atoms are considered [1],[2]. Chiral species with a rhenium atom are currently under study. The transitions of interest for measuring PV are vibrational transitions of modes involving the heavy atom, typically in the mid-infrared (MIR) region of the electromagnetic spectrum ($\sim 10\ \mu$m). We are constructing a Ramsey interferometry experiment which comprises three parts: the preparation of molecules in cold, slow and intense beams, an interrogation zone using an ultra-stable and tuneable MIR laser system and finally a part for the detection of internal molecular state populations. First, the molecules will be prepared in high flux, low velocity buffer-gas-cooled beams, one of the latest molecular beam technology. After exiting the cryogenic buffer gas cell, the molecular beam will be probed by a Ramsey interferometer based on frequency stabilized quantum cascade lasers (QCLs) calibrated against primary standards. QCLs offer broad and continuous tuning and cover the entire mid-infrared thus providing considerable flexibility on the chosen rovibrational transitions that can be studied. Finally, after the MIR Ramsey interrogation, the population needs to be measured. We are currently investigating new measurement procedures in the microwave domain to enhance the detection sensitivity compared to direct detection schemes in the MIR region and to enable enantiomer specific measurements [3].

In this context, I will report our latest results on buffer-gas-cooling in the gas phase of complex polyatomic molecules solid at room temperature such as methyltrioxorhenium [4],[5] (MTO, closely related to chiral rhenium complexes for which the parity-violating energy differences between enantiomers is measurable [2]) and trioxane. I will present precise Doppler-broadened and sub-Doppler spectroscopic measurements of the cooled molecules around 10 μm. I will also present ultra-high resolution spectroscopic measurements using a QCL stabilized at the sub-Hz level, via an optical frequency comb, on an ultra-stable near infrared reference signal provided by the French metrology institute (LNE-SYRTE) [6]. This allows rovibrational frequencies to be determined at record uncertainties, with traceability to primary frequency standards.

References

[1] S . K. Tokunaga, et al. , Mol. Phys. **111**, (2013).
[2] N Saleh, et al., Chirality **30**, (2018).
[3] S . Eibenberger, et al. , Physical review letters, **118(12)**, (2017)
[4] S . K. Tokunaga, et al., New Journal of Physics, **19(5)**, (2017).
[5] P . Asselin, et al., Phys. Chem. Chem. Phys. **19**, (2017).
[6] B . Argence, et al., Nature Photonics **9.7** (2015).

*Corresponding author: mathieu.manceau@univ-paris13.fr

Modeling of Current Processes in a System of Surface Electrons Within a Narrow Channel

V. Syvokon[1], I. Sharapova[*1]
1. B.Verkin Institute for Low Temperature Physics and Engineering of NAS of Ukraine, 47 Nauky Ave., 61103 Kharkiv, Ukraine

Since the discovery of electron crystals (EC) above liquid helium in 1979, they have been studied extensively both experimentally and theoretically, but there are still some problems that have not yet been fully solved. In particular, there is no unique understanding of which physical processes determine the dependence of the conductivity of the crystal on electric field in the plane of the electron layer (nonlinear conductivity). According to one point of view, the observed nonlinear behavior is related to loss of spatial ordering in the electronic system (melting or dynamic melting of the crystal), which, in turn, leads to changes in and the disappearance of the deformation (strain induced) relief of the crystal. Another point of view is based on the assumption that the experimentally observed dependence of the conductivity of the crystal on the driving field is caused by features of the electron-ripplon interaction that develops when the crystal moves as a whole at a sufficiently high velocity along the surface of the liquid. In addition, there are problems with the interpretation of experimental data on nonlinear transport in EC. The conductivity of the electron system above liquid helium is usually determined by a capacitive method in cells with different geometries. An exciting electrode produces a driver field so that a current develops in the electron layer which produces a change in the charge on a receiver electrode and, thereby, a current in the input circuits of a measurement instrument. In a capacitive measurement method, the driver field is generally nonuniform and the measured current is an integral characteristic of all the processes associated with the drift of charges in the electron layer. In order to determine the conductivity of the electron layer using the relationship between the measured current and the exciting voltage, it is necessary to supplement the measurement model for the cell (an equivalent circuit of lumped components, a model based on long line analysis, etc.) with some assumptions regarding the properties of the electron layer itself, e.g., to assume that the conductivity of the layer is independent of the driver voltage and that the dimensions of the layer are fixed for all experimental conditions. Evidently, the first condition is not satisfied during studies of nonlinear properties, so that analyzing the output current for a nonuniform driver field and displaying the result as an averaged characteristic of the electron layer (conductivity, electron mobility) involve some uncertainty and will be apparatus dependent.

Results of experimental studies of electron transport in quasi-one dimensional channels with a linear time dependence for the exciting voltage have been published [1]. This experiment has yielded some interesting data: in particular, spikes (bursts) in the current in the channel that depend on the experimental conditions (temperature, external fields) have been observed with a linear variation in the voltage. A physical picture of the processes determining the currents in the channel is constructed using the concepts of slippage of electrons from the deformation relief of the liquid and Bragg-Cherenkov emission of ripplons. Also the explanation proposed in [1] for the observed features of the current in the channel requires an implicit assumption that the electron crystal moves in the channel at a rather high velocity and that its structure is not significantly disrupted at that time.

We have modeled current processes in a system of surface electrons above liquid helium located in a narrow channel [2]. The molecular dynamic method was used in the model calculations. A current was excited in the system by linearly varying the voltage on an exciting electrode in a way similar to that used in experiments [1]. The calculated results are qualitatively consistent with experimental data. It has been found that when the voltage on the exciting electrode is varied, the electrons in the channel undergo a significant realignment of their spatial configuration and do not retain their initial configuration as they move. The realignment of the configuration is accompanied by motion of the total charge in the channel, i.e. by a current. When the exciting voltage is high enough, some of the electrons leave the channel. This leads to a discontinuous change in the field in the channel and, thereby, to spikes in the time dependence of the current in the channel. A comparison of the model results with existing experimental data indicates that the experimentally observed effects are caused exclusively by electron-electron interactions and the influence of external fields, but have nothing to do with electron-ripplon interactions. The role of electron-ripplon interactions in these experiments seems to reduce merely to a renormalization of the effective electron mass.

References

[1] D. Rees, N. Beysengulov, J.-J. Lin, and K. Kono, Phys. Rev. Lett. **116**, 206801 (2016).
[2] V. Syvokon, I. Sharapova, Low Temp. Phys. **43**, 1044 (2017).

[*]Corresponding author: sharapova@ilt.kharkov.ua

Effect of Berry phase on the core of Ly-α line in an external rotating electric field

M. Słowiński[1], **R. Ciuryło**[*1], **J. Szudy**[1], **W. E. Baylis**[†2]
1. Institute of Physics, Faculty of Physics, Astronomy and Informatics, Nicolaus Copernicus University in Toruń, Grudziadzka 5, 87-100 Torun, Poland
2. Department of Physics, University of Windsor, Windsor, Ontario N9B 3P4, Canada

Using an impact approximation, we have evaluated the intensity distribution in the core region of the Lyman-α line perturbed by hydrogen atoms and placed in an external cone-rotating electric field. Following Berry [1], as in our recent work [2] dealing with the shape of the far wings of this line, we have taken into account the geometric phase acquired by the quasimolecular wave function due to cyclic evolution related to a slow rotation of electric field. It was found that the intensity distribution $I(\omega)$ in the core region can be described as the sum of Lorentzian profiles $J(\phi_2^{n_2-n_1,m};\omega)$ representing contributions coming from transitions between the sublevels $\phi_2^{n_2-n_1,m}$ corresponding to parabolic quantum numbers n_1, n_2 and the quantum number m of the projection of the angular momentum on the z axis of the resonance state ($n=2$) of hydrogen and its ground state ($n=1$):

$$I(\omega)=\frac{1}{2}\left\{J\left(\phi_2^{-1,0};\omega\right)+J\left(\phi_2^{+1,0};\omega\right)\right\}\cos^2\vartheta+\frac{1}{2}\left\{J\left(\phi_2^{0,-1};\omega\right)+J\left(\phi_2^{0,+1};\omega\right)\right\}\sin^2\vartheta. \qquad (1)$$

Here ϑ is the polar angle that the electric field F makes with respect to the laboratory fixed axis. Two examples of the dependence of $I(\omega)$ on ϑ are shown in Fig. 1. The maxima of Berry's components are located at frequencies linearly dependent on the angular velocity ω_F with which the electric field rotates.

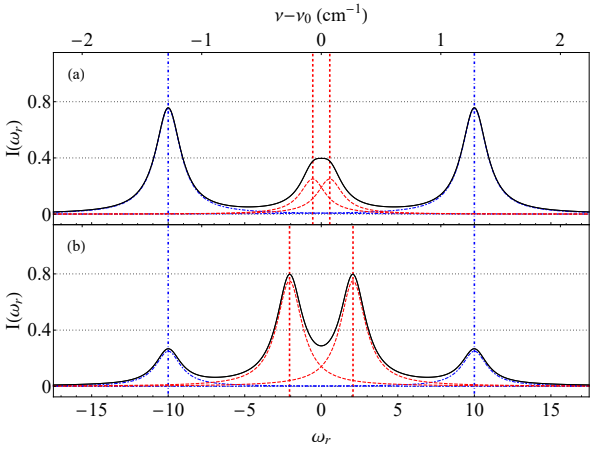

Fig. 1: Intensity distribution in the selfbroadened Lyman-α line at the hydrogen density $N=10^{18}$ cm^{-3} for $F=10^4$ V/cm, $\omega_F=10^{11}$ rad/s, (a) $\vartheta=30^\circ$, (b) $\vartheta=60^\circ$. Red dashed lines represent two Berry components while blue dot-dashed lines represent two Stark componenst of the Lyman-α line. Vertical lines indicate their positions, and $\omega_r=(\nu-\nu_0)/(2\pi\gamma)$, where γ is HWHM linewidth.

References

[1] M. V. Berry, *Quantal Phase Factors Accompanying Adiabatic Changes*, Proc. Roy. Soc. A, 392, 45-57 (1984)
[2] R. Ciuryło, J. Szudy, W. E. Baylis, *Berry phases and profiles of line wings and rainbow satellites induced by optical collisions*, Phys. Rev. A 92, 032503 (2015)

*Corresponding author: rciurylo@fizyka.umk.pl
†Corresponding author: baylis@uwindsor.ca

A Spinor BEC co-magnetometer for phase resolving spin amplification

Pau Gómez Kabelka[*1], **F. Martin** [1], **C. Mazzinghi**[1], **S. Coop**[1], **S. Palacios**[1] **and M.W. Mitchell**[1,2]
1. ICFO—Institut de Ciències Fotòniques, 08860 Castelldefels, Barcelona, Spain.
2. ICREA—Institució Catalana de Recerca i Estudis Avançats, 08015 Barcelona, Spain.

The *co-magnetometer* is a technology developed for rotation sensing [1] and searches for physics beyond the standard model [2], consisting of two different magnetically-sensitive systems operating in the same volume and thus experiencing the same magnetic field. A differential measurement can then reject true magnetic influences (which typically are strong and noisy), while sensitively detecting small signals that differently affect the two components.

Here we report on a ^{87}Rb spinor BEC (SBEC) co-magnetometer, with the two components being the F=1 and F=2 ground state populations, an extension of our recently-reported single-domain magnetic SBEC [3]. The collective spin of each hyperfine manifold is independently detected using Faraday rotation probing [4]. We study spin oscillation and spin amplification in F=2, using the F=1 component as a reference. This novel scheme gives accurate information on both the amplitude and phase of the F=2 SBEC as it rotates in a magnetic field, allowing tomographic study of spontaneous symmetry breaking, spin squeezing, and quantum entropy generation in a magnetically-polarized system.

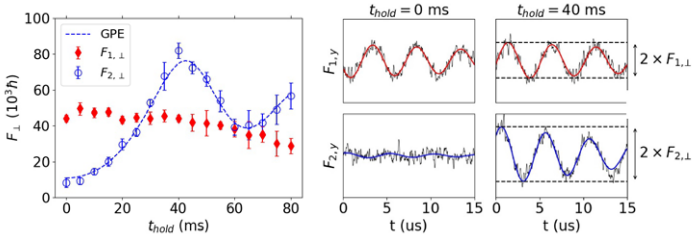

Fig. 1: Temporal evolution of the transverse magnetizations in the F=1 and F=2 manifolds under a magnetic field of $B_z = 283\ mG$. The F=2 component experiences strong spin amplification (left, circles) while the slowly varying F=1 component keeps track of the rotating reference frame (left, diamonds). The combined measurement results in a phase sensitive spin amplifier.
For each hold time, the raw Faraday signals (right) reveal simultaneously the oscillating ($200\,kHz$) spin components along the y-direction ($F_{1,y}$ and $F_{2,y}$). The respective transverse magnetizations ($F_{1,\perp}$ and $F_{2,\perp}$) are given by the observed oscillation amplitudes. Note that the orientation of the rotating reference frame is extracted from the initial phase in the $F_{1,y}$ signal.

References

[1] T. W. Kornack *et al. Nuclear Spin Gyroscope Based on an Atomic Comagnetometer.* PRL **95**: 230801 (2005).
[2] M. Smiciklas *et al. New Test of Local Lorentz Invariance Using a* ^{21}*Ne-Rb-K Comagnetometer.* PRL **107**: 171604 (2011).
[3] S. Palacios *et al. Multi-second magnetic coherence in a single domain spinor BEC.* New Journal of Physics **20.5**: 053008 (2018).
[4] M. Koschorreck *et al. Sub-projection-noise sensitivity in broadband atomic magnetometry.* PRL **104.9**: 093602 (2010).

[*]Corresponding author: pau.gomez@icfo.es

Optically induced Bloch–Siegert shift in magneto–optical resonances

J. Sudyka[*1], **S. Pustelny**[2], **W. Gawlik**[2]
1. Institute of Physical Chemistry, Polish Academy of Sciences, Kasprzaka 44/52 01-224 Warszawa, Poland
2. Marian Smoluchowski Institute of Physics, Jagiellonian University, Łojasiewicza 11, 30-368 Kraków, Poland

Any oscillating electromagnetic field can be decomposed into two counter-rotating waves. If the field of certain frequency interacts with a two-level system, one of the field components drives resonantly the transition between the two states, while the other perturbs the system nonresonantly. Perturbation by this counter-rotating component is often neglected in theoretical considerations, as it is only perturbing the system weakly (rotating-wave approximation). However, the nonresonant component may, in fact, affect the system, and shift the observed resonance [1]. This shift is called the Bloch-Siegert effect (BSE) and is seen in many different resonance schemes, for example in experiments with nuclear magnetic resonances [2]. It can also be observed in magneto–optical experiments [3], where two different cases of BSE may be distinguished:

1. the classical BSE, where an oscillating radio-frequency magnetic field couples magnetic sublevels directly and is responsible for the shift [4],
2. the optically-induced BSE, where an oscillating light field couples magnetic sublevels via excited state (Raman coupling) and generates the shift.

In this contribution we will focus on the latter, more complex situation. We investigated magneto–optical resonances in rubidium vapor generated by both rotating (rotating polarization) and oscillating (amplitude modulated) optical fields. These two schemes enable direct comparison of the variant with a resonance component only and the variant where off-resonance component is leading to the shift in resonance-frequency value respectively. Our results show dependence of the effect on different physical parameters, like optical frequency detuning or light power (see Fig. 1). Experimental results appeared consistent with our numerical model based on Liouville equations for the density matrix of the atomic system.

Besides the fundamental aspects, such as analysis of the rotating wave approximation limits, contrast between classical and optical BSE, etc., this investigation may have important consequences for precise metrology, by reducing systematic errors of optical magnetometers [5]. Moreover, our approach for relatively simple alkali-metal vapors might be extended to more complicated systems, that can be exploited in quantum information processing [6], [7].

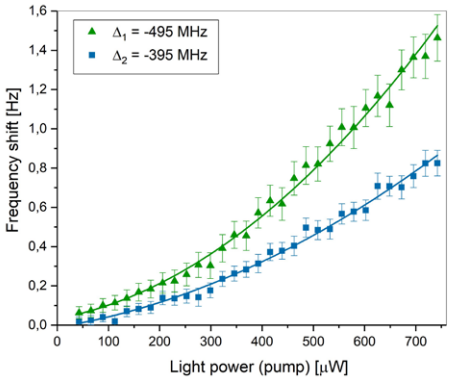

Fig. 1: Dependence of BSE on light power for two different optical transition detunings Δ_1 and Δ_2. Resonance frequency associated with atomic state evolution in static magnetic field $f_r \approx 29$ Hz.

References

[1] F. Bloch, and A. Siegert, Phys. Rev. **57**, 522 (1940).
[2] M. Mehring, P. Hoefer, and A. Grupp, Phys. Rev. A **33**, 3523 (1986).
[3] D. Budker *et al.*, Rev. Mod. Phys. **74**, 1153 (2002).
[4] J. Sudyka, S. Pustelny, and W. Gawlik, arXiv:1709.07194 (2017).
[5] S. Pustelny *et al.*, J. Appl. Phys. **103**, 023405 (2008).
[6] I. Pietikäinen *et al.*, Phys. Rev. B **96**, 020501(R) (2017).
[7] J. Scheuer *et al.*, New J. Phys. **16**, 093022 (2014).

*Corresponding author: jsudyka@ichf.edu.pl

Highly-Efficient Quantum Memory for Polarization Qubits in a Spatially-Multiplexed Cold Atomic Ensemble

M. Cao*[1], P. Vernaz-Gris[1], K. Huang[1], A. S. Sheremet[1], and J. Laurat[1]
1. Laboratoire Kastler Brossel, Sorbonne Université, CNRS, ENS-Université PSL, Collège de France, 4 place Jussieu, 75005 Paris, France

Quantum memory for flying optical qubits is a key enabler for a wide range of applications in quantum information science and technology, such as long-distance optical communication and all-optical quantum computation [1]. In this context, our group focuses on the demonstration of such interfaces based on large cold atom ensembles. In recent years, we demonstrated for instance the implementation of a quantum memory for quantum bits encoded in the orbital angular momentum (OAM) degree of freedom, which provides an essential capability for future networks with multimode capability [2]. We also realized multiple-degree-of-freedom memory, which can find applications in classical data processing but also in quantum network scenarios where states structured in phase and polarization have been shown to provide promising attributes [3].

In all these realizations, a critical figure of merit is the overall storage-and-retrieval efficiency. Theoretically, the retrieval efficiency can be improved with the increase of the optical depth (OD). Efficient optical memory has been demonstrated with large OD, however, high efficiency qubit storage had not been demonstrated. Here, we demonstrate a faithful quantum memory for polarization qubits with a storage-and-retrieval efficiency close to 70% [4]. Our implementation is based on electromagnetically-induced transparency (EIT) in a single spatially-multiplexed ensemble of cold cesium atoms featuring a large optical depth. The reported efficiency approaches the maximal performance achievable on the D2 line transition used here, as shown by a comprehensive model that includes all the involved atomic transitions. Relative to previous works, this advance has been possible by combining a high OD medium, efficient spatial multiplexing and low-noise operation.

More specifically, to obtain an ensemble with large optical depth, our experiment is based on an elongated 2D magneto-optical trap (MOT) of cesium atoms. Thanks to the large OD achieved here, we could investigate the scaling behaviour of the storage-and-retrieval efficiency. The maximal efficiency achieved here reaches $69 \pm 1\%$. This represents a record on the cesium D2 line and, more importantly, the highest achievable value in this configuration. We have demonstrated a highly-efficient memory for optical qubits by successfully operating a large OD elongated atomic ensemble in a dual-rail configuration. This combination enables the reversible mapping of arbitrary polarization states not only with fidelities well above the classical benchmark but also with an overall storage-and-retrieval efficiency close to 70%. This value represents the highest efficiency to date for the storage and readout of optical qubits in any physical platforms and is more than double of the previously reported values. It also outperforms the important 50% threshold required to beat the no-cloning limit without post-selection.

Besides the aforementioned network architecture scalability and potential loss-tolerant schemes, the achieved efficiency opens the way to first tests of advanced quantum networking tasks where the storage node efficiency plays a critical role, such as in certification protocols or unforgeable quantum money. Moreover, the designed platform is directly compatible with recent works based on spatially structured photons and multiple-degree-of-freedom storage and can now yield to very efficient realizations to boost high-capacity network channels.

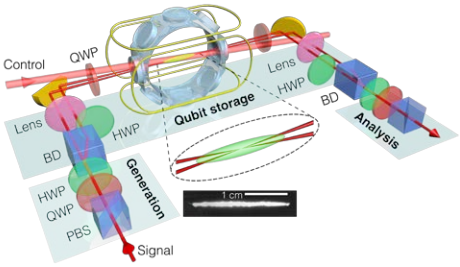

Fig. 1: Highly-efficient quantum memory for polarization qubits in a spatially-multiplexed cold atomic ensemble.

References

[1] K. Heshami, D. G. England, P. C. Humphreys, P. J. Bustard, V. M. Acosta, J. Nunn, and B. J. Sussman, J. Mod. Opt. **23**, 2005 (2016).
[2] A. Nicolas, L. Veissier, L. Giner, E. Giacobino, D. Maxein, and J. Laurat, Nat. Photon. **8**, 234 (2014).
[3] V. Parigi, V. D′Ambrosio, C. Arnold, L. Marrucci, F. Sciarrino, and J. Laurat, Nat. Comm. **6**, 7706 (2015).
[4] P.Vernaz-Gris, K. Huang, M. Cao, A. S. Sheremet, and J. Laurat, Nat. Comm. **9**, 363 (2018).

*Corresponding author: mingtao.cao@lkb.upmc.fr

A broadband magnetic rf spectrum analyzer based on atomic magnetometry

T. Scholtes[*1], **V. Lebedev**[1], **V. Dolgovskiy**[1], **Z. Grujić**[1], **A. Weis**[1]
1. Department of Physics, University of Fribourg, Chemin du Musée 3, Fribourg, CH-1700, Switzerland

Atomic magnetometers have proven to be highly sensitive devices for detecting weak oscillating magnetic fields (rf-magnetometry) [1]. In conventional magnetic resonance based magnetometry one is interested in the magnitude B_0 of a static field $\vec{B}_0$. The measurement proceeds by measuring the frequency $\omega_{\rm rf}$ of a weak oscillating magnetic field of amplitude $B_{\rm rf}$ for which the signal (light power/polarization) amplitude is maximized. The corresponding resonance occurs when $\omega_{\rm rf}$ is equal to the Larmor frequency $\omega_L = \gamma_F B_0$ of the field of interest (for Cs, $\gamma_F/2\pi \approx$3.5 Hz/nT). Optimal magnetometer conditions are achieved when the Rabi frequency $\gamma_F B_{\rm rf}$ is on the order of the magnetic resonance linewidth γ_2. Under such conditions one can achieve signal/noise density ratios (SNDR) exceeding $10^5\sqrt{\rm Hz}$. This implies a detection limit of $\gamma_2/({\rm SNDR}\,\gamma_F)$ for $B_{\rm rf}$ in a 1 Hz bandwidth. For a resonance linewidth of 3.5 Hz (in Cs), a SNDR of 10^5 thus translates into a detection limit $\delta B_{\rm rf}$ of $\approx 10^{-5}$nT=10 fT.

In a homogeneous static magnetic field B_0, an rf-magnetometer is sensitive only to fields oscillating at $\gamma_F B_0$. Here we present an approach that allows the simultaneous (spectrally-resolved) detection of rf magnetic fields over a broad frequency range. The method is based on recording fluorescence emitted by cesium atoms (immobilized in Ar buffer gas) that are exposed to a homogeneous linear magnetic field gradient and that are resonantly excited on a hyperfine component of the (Cs) D_1 transition. As in MRI, the field gradient implies a spatial encoding of the atomic Larmor frequencies over the vapor cell volume (i.e., along the laser beam direction) that can be read out by spatially-resolved fluorescence recording using a CCD camera [2],[3].

Increasing the linear gradient field over the field of interest (the cell length) results in a larger frequency span, but will limit the number of atoms per frequency slice, leading to a decrease in sensitivity. This trade-off between magnetometric sensitivity and dynamic frequency range has to be balanced according to the demands of specific applications. For a given gradient, the frequency resolution of the device is determined by the magnetic resonance linewidth γ_2, the atomic diffusion length during the spin coherence lifetime $1/\gamma_2$, the solid angle of the optical imaging, and the CCD's resolution and quantum efficiency.

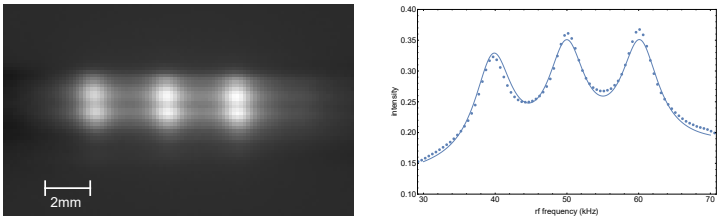

Fig. 1: Left: Fluorescence pattern emitted from optically pumped Cs vapor excited by a tri-chromatic (40, 50, 60 kHz) rf field with $B_{\rm rf}^{\rm rms} = 55\,$nT amplitude each. The magnetic field varies in a linear manner from 8.3 μT (left) to 20.2 μT (right) along the (horizontal) laser beam direction. The central horizontal dark line is a shadow cast by a wire intersecting the laser beam before the vapor cell, used for focussing of the CCD camera. Right: Intensity profile after vertical binning, together with a Lorentzian fit.

Figure 1 shows a proof-of-principle result for the detection and spectral analysis of a multi-component rf signal. We will present preliminary results of a systematic variation of the system parameters (laser power, gradient strength,rf field amplitude) and will discuss estimations on the frequency resolution and sensitivity of the device. A gas handling system that will allow *in situ* buffer gas control in view of optimizing buffer gas composition and pressure is under construction.

We acknowledge financial support by grant No. 200021 172686 of the Swiss National Science Foundation.

References

[1] I. M. Savukov *et al.*, Phys. Rev. Lett. **95**, 063004 (2005).
[2] I. Fescenko, A. Weis, J. Phys. D: Appl. Phys. **47**, 235001 (2014).
[3] V. Dolgovskiy *et al.*, Appl. Phys. Lett. **109**, 023505 (2016).

*Corresponding author: theo.scholtes@unifr.ch

Modeling atom diffraction beyond the weakly-diffracting limit

B. T. Beswick[*1] **I. G. Hughes**[†1], **S. A. Gardiner**[‡1]
1. Joint Quantum Centre (JQC) Durham–Newcastle, Department of Physics, Durham University, Durham DH1 3LE, United Kingdom

Precision measurement of lattice depths is important in many areas of interest in atomic physics, most notably in quantum simulation, atom interferometry and for accurate calculation of transition dipole matrix elements. In such experiments, lattice depths are often measured by exposing an ultracold atomic gas to a series of off-resonant laser-standing-wave pulses, and fitting theoretical predictions for the fraction of atoms found in each of the allowed momentum states by time of flight measurement after some number of pulses N (See Fig. 1 (a)). However, for the case of 'weak' lattice depths ($\sim 0.01 E_R$ for any atom, where $E_R = \hbar^2 k_L^2 / 2M$), the precision on such measurements can be hampered by signal to noise issues. Recently, the work of Herold et al. [1] has suggested that this complication can be mitigated by alternating each standing-wave pulse with a free-evolution stage, both with duration equal to half the Talbot time, $T_T/2 = 2\pi M/\hbar K^2$, where K is twice the laser wavenumber k_L, and M is the atomic mass [2].

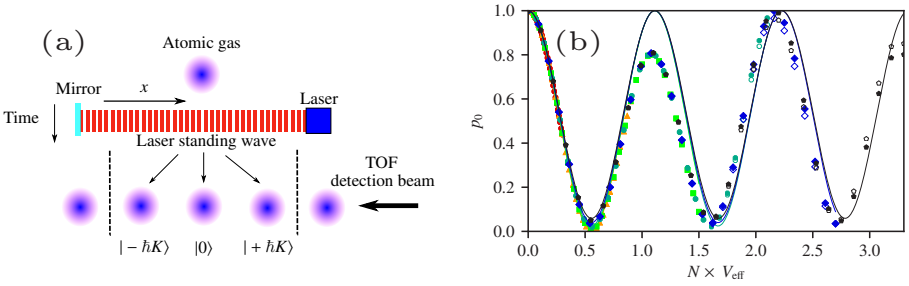

Fig. 1: (a) Schematic of a standing-wave-pulse atom-diffraction setup. An ultracold atomic gas is subjected to some number of lattice pulses N, before a time of flight beam measures the atomic population in each of the allowed momentum states. The gas is diffracted into an (in principle infinite) discrete ladder of momentum states $|n\hbar K\rangle$, $n \in \mathbb{Z}$, where K is twice the laser wavenumber k_L. The dashed lines enclose the three relevant momentum states in the weakly-diffracting case, where the lattice depth is sufficiently small ($\sim 0.01 E_R$). (b) Plot of population in the $|0\hbar K\rangle$ momentum state, p_0, versus the number of pulses N (30 in total for each curve), as calculated analytically using a three state basis (solid lines), and numerically using a five state basis (solid markers), and a 2048 state basis (hollow markers). Each coloured curve corresponds to a specific value of the effective lattice depth V_{eff}, by which the bottom axis has been scaled to reveal an approximate universality. Beyond $NV_{\text{eff}} \sim 0.7$ the three state model ceases to agree, though for values of NV_{eff} up to ~ 1.7 the five state model (in principle analytically solveable) is clearly sufficient.

The modeling approach taken in [1] is valid for a weak lattice which is pulsed a small number of times, corresponding to the 'weakly-diffracting limit'. We present a full analytic model for the time evolution of the atomic populations of the $|0\hbar K\rangle$ and $|\pm\hbar K\rangle$ states, which is sufficient for a 'weak' lattice, as well as numerical simulations incorporating higher momentum states at both strong ($>0.1 E_R$) and weak lattice depths, both of which are compared for typical experimental values in Fig. 1 (b). We also explore the role of finite-temperature effects in such experiments. Finally we use the same techniques to explore the case where either the standing wave is left continuously on, or the free evolution stage is transformed away by employing a 'walking wave' technique [3]. We conclude that, especially for a finite-temperature gas, we should expect this modified approach to provide a more precise measurement of lattice depths both in and out of the weakly-diffracting limit [4].

References

[1] C. D. Herold, V. D. Vaidya, X. Li, S. L. Rolston, J. V. Porto, M. S. Safronova Phys. Rev. Lett. **109**, 243003 (2012)
[2] Y. Zhai, C. H. Carson, V. A. Henderson, P. F. Griffin, E. Riis, A. S. Arnold, Optica **5**, 80 (2018)
[3] M. Saunders, P. L. Halkyard, S. A. Gardiner, K. J. Challis, Phys. Rev. A **79**, 023423 (2009)
[4] B.T. Beswick, I. G. Hughes, S. A. Gardiner, in preparation.

*Corresponding author: b.t.beswick@durham.ac.uk
†Corresponding author: i.g.hughes@durham.ac.uk
‡Corresponding author: s.a.gardiner@durham.ac.uk

X-ray emission from highly charged xenon ions in the EBIT plasma

D. Sobota[*1], **D. Banaś**[1], **Ł. Jabłoński**[1], **P. Jagodziński**[2], **A. Kubala-Kukuś**[1], **I. Stabrawa**[1], **K. Szary**[1], **M. Pajek**[1]

1. Institute of Physics, Jan Kochanowski University, Kielce, Poland
2. Department of Mathematics and Physics, University of Technology, Kielce, Poland

In electron beam ion trap (EBIT) the highly charged ions (HCI) are produced by successive electron impact ionization of neutral atoms/ions in high-density electron beam compressed by strong magnetic field. The equilibrium charge state distribution of ions in the EBIT plasma is achieved as a result of various atomic processes, mainly the electron impact ionization/excitation (EII/E) and radiative (RR) and dielectronic recombination (DR). The x-rays emitted from the EBIT carry thus information on the structure and relaxation of HCI and the dynamics of involved atomic processes.

In this paper we report on the measurements of x-rays of highly charged xenon ions, Xe^{q+}, emitted from the EBIT trap of Kielce EBIS facility [1][2]. The X-ray spectra were measured for electron beam energies 3.3-9.0 keV in order to investigate different atomic processes leading to X-ray emission. The measurements were performed using X-ray Si drift detector (SDD) having energy resolution of 120 eV for 5 keV photons.

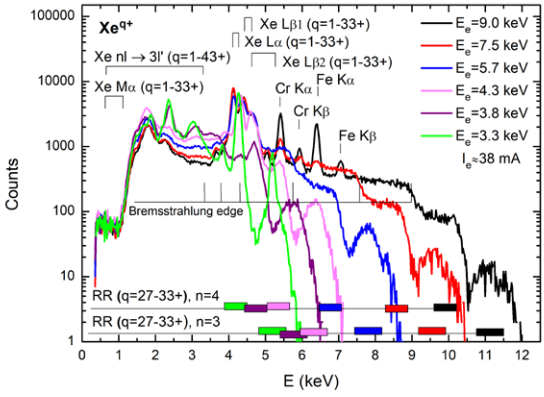

Fig. 1: Measured X-ray spectrum from highly charged xenon ions trapped in the EBIT for different electron beam energies $E_e = 3.3 - 9$ keV and fixed electron beam current of $I_e = 38$ mA. Contributions of electron impact ionization and excitation (EII/E) and RR and DR recombination processes can be identified in the figure.

The measured spectrum (Fig. 1) clearly shows the M- and L-X-ray lines from highly charged Xe^{q+} ions, with $q \sim 40$, being ionized/excited by electron impact, as well as X-ray structure corresponding to RR into n=3 and n=4 states in Xe. The widths of the measured X-ray lines carry information on the distribution of Xe^{q+} charge states in the EBIT plasma. The spectrum shows also a contribution of Cr and Fe fluorescence X-ray lines excited by scattered electrons in the EBIT and the end-point of the X-ray bremsstrahlung varying with the energy of the electrons. The measured X-rays were found to be dependent, despite of the electron impact energy, on the electron beam current and Xe pressure in the trap. This reflects a complex balance of different atomic processes taking place to establish the charge state equilibrium in the EBIT plasma. More detailed discussion of the measured X-ray spectra will be presented in order to understand a contribution of different charge states of Xe ions to the studied emission of X-rays.

Acknowledgements
The financial support of the EU within the Polish Innovative Economy Operational Program (Contact No. WNP-POIG.02.02.00-26-023/08) is acknowledged.

References

[1] G. Zschornack et al., Rev. Sci. Instrum. **79**, 02A703 (2008)
[2] D. Banaś et al., J. Instrum. **5**, C09005 (2010)

*Corresponding author: d.sobota@ujk.edu.pl

Two-electron resonances in strongly anisotropic quantum dots

Arkadiusz Kuroś[*1]
1. Faculty of Physics, Astronomy and Applied Computer Science, Jagiellonian University, ul. prof. S. Łojasiewicza 11, 30-348 Kraków

Recently, it has become possible to fabricate few-particle quantum systems, the geometry of which and the parameters, such as the number of constituents and the interaction between them can be experimentally controlled by applying appropriately designed electromagnetic fields. Semiconductor quantum dots realize simple models of quantum theory being effectively described as Schrödinger systems of few Coulombically interacting electrons in an external potential which models their geometry. This gave an impetus for theoretical studies on simple two-body systems subjected to external potentials and stability properties in dependence on varying parameters.

Here, we consider highly anisotropic two-electron quantum dots that can be realized in semiconductor quantum wires or carbon nanotubes [1], and are well described as quasi-one-dimensional systems with an effective interaction modified by the lateral confinement [2]. With the longitudinal attractive Gaussian potential, the system supports both bound and resonant states [3]. The energies and widths of autoionizing resonances will be determined using complex-coordinate rotation method, which requires non-Hermitian quantum mechanical approach. We perform a detailed analysis of the effect of the lateral and longitudinal confinement parameters on the properties of quantum dots, paying particular attention to the values in the vicinity of the stability limit.

References

[1] J. Salfi, *et al.*, Semicond. Sci. Technol. **25**, 024007 (2010).
[2] S. Bednarek, B. Szafran, T. Chwiej, J. Adamowski, Phys. Rev. **B 68**, 045328 (2003)
[3] Y. Sajeev, N. Moiseyev, Phys. Rev. **B 78**, 075316 (2008).

*Corresponding author: arkadiusz.kuros@uj.edu.pl

Laser cooling of $^9Be^+$ ions in a cryogenic linear Paul trap for sympathatic cooling of highly charged ions

L. Spieß*[1], L. Schmöger[1,2] J. Stark†[1], J. Nauta[1], J.-H. Oelmann[1], S. Kühn[1], T. Leopold[2], S. King[2], P. Micke[1,2], P. O. Schmidt[2], J. R. Crespo López-Urrutia‡[1]

1. Max-Planck-Institut für Kernphysik, Saupfercheckweg 1, 69117 Heidelberg, Germany

2. Physikalisch-Technische Bundesanstalt, Bundesallee 100, 38116 Braunschweig, Germany

High precision spectroscopy of ultra-narrow forbidden optical transitions in highly charged ions (HCIs) is of particular interest for metrology [1],[2] and measuring a possible variation of the fine-structure constant [2],[3]. For this, HCIs need to be trapped and cooled. Unfortunately, there are no suitable optical transitions for laser cooling and therefore other methods need to be applied. At CryPTEx [4],[5], HCIs are produced at MK temperature in an electron beam ion trap and are then transported to a cryogenic Paul trap. There, they are brought into the mK regime through sympathetic cooling using a second laser-cooled ion species [6]. Since $^9Be^+$ can be co-trapped with various HCIs inside a linear Paul trap, they are the ideal candidate for this. Production and cooling of $^9Be^+$ is carried out using two CW lasers: a 235 nm laser for resonance enhanced two-photon ionization based on [7] and 313 nm laser for Doppler-cooling described in [8].

For a sufficiently low temperature, the $^9Be^+$ ions form an ordered structure called a Coulomb crystal, where minimally about 2 mK are reached. Injected HCIs lose energy by Coulomb interaction with the continuously cooled $^9Be^+$ ions. For co-crystallized Ar^{13+}, the temperature was estimated to be approximately 10 mK [6].

References

[1] V. I. Yudi, et al., Phys. Rev. Lett. **113**, 233003 (2014).
[2] V. A. Dzuba et al., Phys. Rev. A **86**, 054502 (2012).
[3] J. C. Berengut et al., Phys. Rev. Lett. **106**, 210802 (2011)
[4] M. Schwarz et al., Rev. Sci. Instrum. **83**, 083115 (2012)
[5] L. Schmöger et al., Rev. Sci. Instrum. **86**, 103111 (2015)
[6] L. Schmöger et al., Science **347**, 6227 (2015)
[7] H.-Y. Lo et al., Appl. Phys. B **114**, 17 (2013)
[8] A. C. Wilson et al., Appl. Phys. B **105**, 741 (2011)

*Corresponding author: lukas.spiess@mpi-hd.mpg.de
†Corresponding author: jstark@mpi-hd.mpg.de
‡Corresponding author: crespojr@mpi-hd.mpg.de

Towards an XUV frequency comb for precision spectroscopy of trapped highly charged ions

J.-H. Oelmann[*1], **J. Nauta**[†1], **A. Ackermann**[1], **L. Spieß**[1], **J. Stark**[1], **P. Micke**[1,2], **S. Kühn**[1], **J. R. Crespo López-Urrutia**[1], **T. Pfeifer**[1]

1. Max-Planck-Institut für Kernphysik, Saupfercheckweg 1, 69117 Heidelberg, Germany
2. Physikalisch-Technische Bundesanstalt, Bundesallee 100, 38116 Braunschweig, Germany

Highly charged ions (HCI) are atomic systems with a few tightly bound electrons. They offer many advantages over neutral and singly charged ions for probing fundamental physics and recently, they have been proposed as candidates for novel frequency standards [1]. Many optical transitions of HCI are located in the extreme ultraviolet (XUV). To study these transitions with high precision, a coherent ultra-narrow light source in this spectral region is required. For these reasons, we are developing an XUV frequency comb. High-harmonic generation (HHG) is used to transfer the coherence and stability of a near infrared frequency comb to the far ultraviolet [2-4]. Reaching intensity levels ($\sim 10^{14}\,\mathrm{W/cm^2}$) necessary for HHG, while operating at high repetition rates to achieve adequate comb-line spacing, is challenging. Therefore, the comb laser pulses are first amplified in a chirped-pulse fiber amplification setup and then resonantly overlapped in an astigmatism-compensated femtosecond enhancement cavity. To achieve high stability and low-noise performance, the cavity is placed on a rigid titanium structure with vibrational decoupling from the vacuum pumps. High-harmonics are generated in a target gas in the tight focus of the cavity. In other experiments, mirror degradation due to hydrocarbon aggregation is observed, which limits continuous operation time of XUV combs [4, 5]. To avoid this, we operate the cavity under ultra-high vacuum conditions. A differential pump setup will enable a high pressures of the HHG target gas without impairing the vacuum in the chamber, as shown in Fig. 1.

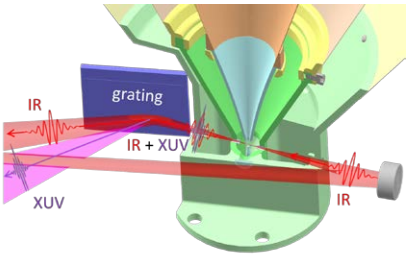

Fig. 1: Overview of the femtosecond enhancement cavity focus region. High-harmonics are generated in a gas jet in the cavity focus. The collinearly propagating XUV pulses are coupled out by a grating etched into a flat cavity mirror. A differential pump setup around the gas jet prevents gas from entering the main vacuum chamber to maintain ultra-high vacuum conditions.

The generated XUV light will be coupled out of the cavity by minus-first order diffraction of a small-period grating etched into a high-reflective cavity mirror directly behind the gas target [6]. Then, the light can be guided to trapped and sympathetically cooled HCI in a superconductive cryogenic linear Paul trap (CryPTEx II experiment at MPIK, based on [7]). By driving narrow transitions with individual comb lines, high-precision XUV spectroscopy of HCI will become possible for the first time [8].

References

[1] M.S. Safronova, V.A. Dzuba, V.V. Flambaum, U.I. Safronova, S.G. Porsev, and M.G. Kozlov, Phys. Rev. Lett. **113**, 030801 (2014).
[2] C. Gohle, T. Udem, M. Herrmann, J. Rauschenberger, R. Holzwarth, H.A. Schuessler, F. Krausz, and T.W. Hänsch, Nature **436**, 234 (2005).
[3] A. Cingöz, D.C. Yost, T.K. Allison, A. Ruehl, M.E. Fermann, I. Hartl, and J. Ye, Nature **482**, 68 (2012).
[4] C. Benko, T.K. Allison, A. Cingöz, L. Hua, F. Labaye, D.C. Yost, and J. Ye, Nat. Photon **8**, 530 (2014).
[5] A.K. Mills, T.J. Hammond, M.H.C. Lam, and D.J. Jones, Mol. Opt. Phys. **54**, 142001 (2012).
[6] D.C. Yost, T.R. Schibli, and J. Ye, Opt. Lett. **33**, 1099 (2008).
[7] L. Schmöger, O.O. Versolato, M. Schwarz, M. Kohnen, A. Windberger, B. Piest, S. Feuchtenbeiner, J. Pedregosa-Gutierrez, T. Leopold, P. Micke, A.K. Hansen, T.M. Baumann, M. Dewsen, J. Ullrich, P.O. Schmidt, and J.R. Crespo López-Urrutia, Science **347**, 1233 (2015).
[8] J. Nauta, A. Borodin, H.B. Ledwa, J. Stark, M. Schwarz, L. Schmöger, P. Micke, J.R. Crespo López-Urrutia, and Thomas Pfeifer, Nucl. Instrum. Meth. B **408**, 285 (2017).

[*]Corresponding author: oelmann@mpi-hd.mpg.de
[†]Corresponding author: nauta@mpi-hd.mpg.de

Angular momentum alignment-to-orientation conversion in ^{85}Rb ground-state

M. Auzinsh[*1], **R. Ferber**[1], **A. Mozers**[†1], **L. Kalvans**[1]
1. Laser Centre, University of Latvia, Rainis Boulevard 19, LV-1586 Riga, Latvia

We present results from a theoretical investigation of ground-state angular momentum alignment-to-orientation conversion (AOC) by observing laser-induced fluorescence (LIF) signals of rubidium atoms at D_1 excitation. The AOC is created by combined action of linearly polarized exciting laser radiation and an external magnetic field. This can be detected by observing circularly polarized light as circularity is direct evidence of angular momentum orientation. The excitation and observation geometry for creating and observing AOC stands as follows: the magnetic field **B** defines the quantization axis and the exciting linearly polarized laser radiation **E** forms an angle of $\pi/4$ with respect to the magnetic field **B**, observation direction is in the direction perpendicular to both **E** and **B**. In the previous work [1], where the same excitation and observation geometry was used, the AOC phenomenon was studied in the excited state where due to the nonlinear Zeeman effect of the excited state magnetic sublevel crossings occurred thus allowing for linearly polarized light to create coherence among sublevels that differ in value by 1 ($\Delta m_F = 1$). In contrast, there is no magnetic sublevel crossings in the ground state and one would not expect to observe AOC. But due to the nonlinear dependencies of the energies of ground-state magnetic sublevels, the angular momentum alignment, created by linearly polarized light, can be partially converted to orientation. The ground-state AOC occurs at relatively high magnetic field values around 2000 gauss, because of relatively large hyperfine splitting in the ground-state — 3.0 GHz for ^{85}Rb.

The theoretical model is based on the optical Bloch equations and takes into account all nearby transitions, the coherence properties of the exciting laser radiation, and the mixing of magnetic sublevels in an external magnetic field and also includes averaging over the Doppler profile [2]. We used the theoretical model to calculate two opposite circularly polarized light components (σ^+ and σ^-) of LIF signal dependencies on hyperfine transition, Rabi frequency of the atom-light interaction and laser linewidth. The results show that peculiar curves suggest about 1% of circularity at around 1500 gauss (Fig.1.). In near future the theoretical curves will be compered with experimentally obtained ones.

We gratefully acknowledge the financial support from the Base/Performance Funding Project No. AAP2016/B013, ZD2010/AZ27. A. Mozers acknowledges support from ERAF PostDoc Latvia project No. 1.1.1.2/16/117 "Experimental and theoretical signals of ground-state angular momentum alignment-to-otientation conversion by the influence of laser radiation and external magnetic field in atomic alkali metal vapour".

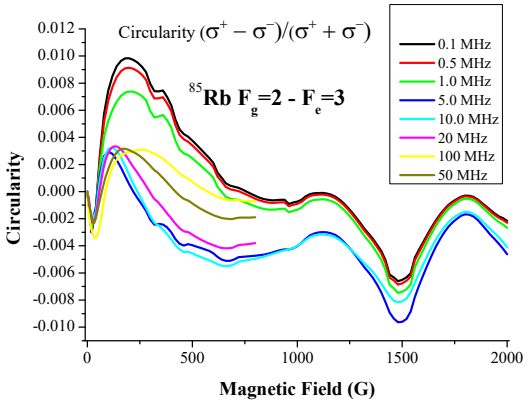

Fig. 1: Calculated circularity of LIF signal dependency on magnetic field for the $F_g = 2 \longrightarrow F_e = 3$ transition of the D_1 line of ^{85}Rb. Various colors denote different Rabi frequencies characterizing atom-light interaction.

References

[1] M. Auzinsh, A. Berzins, R. Ferber, F. Gahbauer, L. Kalvans, A. Mozers, and A. Spiss, Phys. Rev. A **91**, 053418 (2015).
[2] M. Auzinsh, R. Ferber, F. Gahbauer, A. Jarmola, and L. Kalvans, Phys. Rev. A **79**, 053404 (2009).

[*]Corresponding author: marcis.auzins@lu.lv
[†]Corresponding author: arturs.mozers@lu.lv

B – 45

Orientational Dependence of Sensitivity in Double Resonance Atomic Magnetometers

V. Dolgovskiy[*1], **T. Scholtes**[1], **V. Lebedev**[1], **Z. Grujić**[1], **A. Weis**[1]
1. Department of Physics, University of Fribourg, Chemin du Musée 3, Fribourg, CH-1700, Switzerland

Optically pumped atomic magnetometers (OPMs) compete with SQUID magnetometers in their performance reaching intrinsic magnetometric sensitivities in sub-fT/$\sqrt{\text{Hz}}$ range. A detailed overview of the theory and implementations of OPMs based on magnetic resonance is given in Ref. [1]. The core element of such OPMs is an atomic vapor in which spin polarization is created by pumping with resonant polarized or unpolarized light. The magnetization associated with the spin polarization precesses around the static magnetic field $\vec{B}_0$. In double resonance magnetometers a weak magnetic field $\vec{B}_{\text{rf}}(t)$ (or rather the co-rotating component of that field) resonantly drives the precession at the frequency ω_{rf}. As a consequence, the intensity (polarization) of the transmitted light becomes modulated at ω_{rf}. The amplitude, R, and phase, φ, of that modulation are extracted by phase-sensitive detection with a lock-in amplifier. While the resonance frequency is determined by the field modulus $B_0 = |\vec{B}_0|$, both the amplitude and phase of the oscillatory signals depend in a characteristic way on the field orientation $\hat{B}_0$, parametrized by θ and ϕ (Fig. 1, left).

In the past, we have studied the dependencies of the lock-in signals (R and φ) on field orientation $\hat{B}_0$ in **spin-orientated** Cs vapor produced by pumping with circularly-polarized light (CPL) [2]. Here we report on related experiments in **spin-aligned** Cs atoms produced by linearly-polarized light (LPL) pumping. We have studied two distinct configurations with $\hat{B}_{\text{rf}}$ being either parallel or perpendicular to the light polarization ε. In both configurations magnetic resonance spectra were recorded for ∼3'000 discrete field orientations covering the full 4π solid angle. Alignment-based magnetometers also feature signals modulated at $2\omega_{\text{rf}}$, yielding signals $R_{2\omega}(\theta,\phi)$ and $\varphi_{2\omega}(\theta,\phi)$.

The data analysis shows excellent agreement with our algebraic model predictions for all studied signals (two rf field configurations, viz., $\hat{B}_{\text{rf}} \parallel \hat{\varepsilon}$ and $\hat{B}_{\text{rf}} \perp \hat{\varepsilon}$, two demodulation frequencies, viz., ω_{rf} and $2\omega_{\text{rf}}$, two signals, viz., R and φ). Figure 1 shows the comparison for two of the eight studied cases. All results will be presented on the poster.

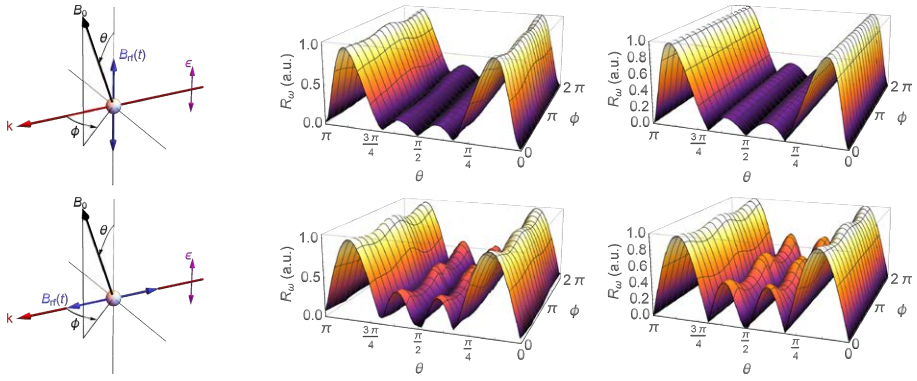

Fig. 1: Anticipated (center) and experimentally recorded (right) angular dependences of the amplitudes R_ω (∝inverse magnetometric sensitivities) of double resonance signals in spin-aligned Cs vapor after demodulation at the frequency ω_{rf}. Two distinct configurations with $\vec{B}_{\text{rf}}$ either parallel (top) or perpendicular (bottom) to the light polarization ε are shown. The parametrization of the experimental geometries in terms of the spherical angles θ, ϕ is illustrated on the left.

References

[1] A. Weis, G. Bison, and Z. Grujić, *Magnetic Resonance Based Atomic Magnetometers*. In *High Sensitivity Magnetometers*, ed. by A. Grosz, M.J. Haji-Sheikh, S.C. Mukhopadhyay, Springer, Berlin 2017.
[2] S. Colombo, V. Dolgovskiy, T. Scholtes, Z. Grujić, V. Lebedev, and A. Weis, Appl. Phys. B **123**, 35 (2017).

*Corresponding author: vladimir.dolgovskiy@unifr.ch

B – 46

Quantitative Comparison of Optical Pumping in Uncoated and Paraffin-Coated Cells

Y. Shi[*1,2,3], **T. Scholtes**[1], **Z. D. Grujić**[1], **V. Dolgovskiy**[1], **V. Lebedev**[1], **A. Weis**[1]
1. Department of Physics, University of Fribourg, Chemin du Musée 3, Fribourg, CH-1700, Switzerland
2. Institute of Electronics, Chinese Academy of Sciences, Beijing 100190, China
3. University of Chinese Academy of Sciences, Beijing 100049, China

We have measured the dependence of the resonant absorption coefficients $\kappa_0^{F_g\to F_e}$ on incident laser power $P_{\rm in}$ when performing optical pumping with unpolarized (UPL, a novelty!), linearly-polarized (LPL), and circularly-polarized (CPL) laser light. Experiments were done on the four $F_g\to F_e$ hyperfine components of the Cs D_1 transition in an uncoated and in a paraffin-coated vapour cell at room temperature. The main difference of the two types of cells is that spin relaxation in the uncoated cell is **isotropic**, since it is limited by the finite transit time of atoms through the laser beam, while in the paraffin-coated cell it is highly **anisotropic**, since it is limited by F- and m_F-dependent spin exchange collisions. In the case of isotropic relaxation we have derived analytical expressions for $\kappa_0\,(x = P_{\rm in}/P_{\rm sat})$ that are of the form [1]

$$\frac{\kappa_0^{F_g\overset{\rm POL}{\longrightarrow}F_e}(x)}{\kappa_{\rm tot}^{\rm unpol.}} = \mathscr{D}\,\frac{\sum_{n=0}^{n_{\rm max}}\mathscr{E}_n\,x^n}{\sum_{m=0}^{m_{\rm max}}\mathscr{F}_m\,x^m}\,, \tag{1}$$

where the (integer) coefficients $\mathscr{D}$, $\mathscr{E}_n$, $\mathscr{F}_m$, $n_{\rm max}\le 6$, $m_{\rm max}\le 7$ depend on the hyperfine transition and on the light polarization POL. Figure 1 shows that the experimental results are very well represented by the model predictions, fitted with only 2 parameters, viz., the pumping saturation parameter $P_{\rm sat}$ (common to all transitions) and the resonant optical density $\kappa_{\rm tot}^{\rm unpol.}$L of the unpolarized medium. These parameters can be expressed in terms of the vapour temperature T and the 4-σ laser beam diameter, whose fitted values agree well with experimental values. Note that the 4→3 and 3→4 transitions have the same power dependence for pumping with CPL and LPL.

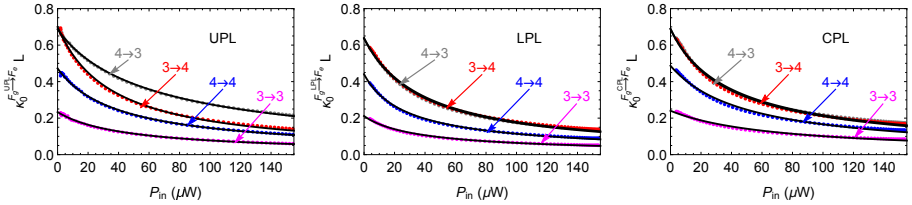

Fig. 1: Dependence of the resonant optical density κ_0L (L=sample thickness) on pumping power for the 4 Cs D_1 transitions with UPL, LPL, and CPL pumping in an **uncoated** cell that features **isotropic spin relaxation**.

Anisotropic relaxation can no longer be handled analytically and we have modeled the $\kappa_0(x)$ dependencies using numerical methods described in detail in Ref. [2]. In this case fitting the data with the model function requires an additional parameter, viz., the ratio $\gamma_{\rm se}/\gamma_1$ of the spin-exchange relaxation rate and the isotropic relaxation rate. The fits of the experimental data shown in Fig. 2 yield $\gamma_{\rm se}/(2\pi)$=3.6(4) Hz [2].

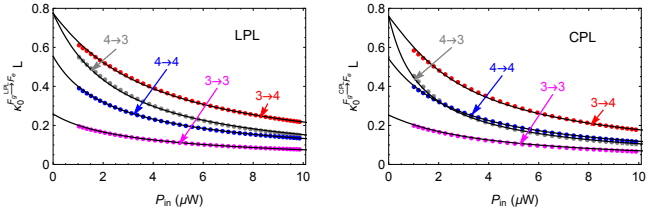

Fig. 2: Dependence of the resonant optical density κ_0L on pumping power for the 4 Cs D_1 transitions with LPL and CPL pumping in a **paraffin-coated** cell that features **anisotropic spin relaxation**.

References

[1] Y. Shi, and A. Weis, Eur. Phys. J. D **72**, 73(2018).
[2] Y. Shi, T. Scholtes, Z.D. Grujić, V. Dolgovskiy, V. Lebedev, and A. Weis, Phys. Rev. A **97**, 013419(2018).

*Corresponding author: yongqi.shi@unifr.ch

High-resolution laser spectroscopy of magnesium Rydberg states in a supersonic beam

M. Génévriez[*1], **D. Wehrli**[†1], **J. A. Agner**[1], **F. Merkt**[1]
1. Laboratory for Physical Chemistry, ETH Zurich, Vladimir-Prelog-Weg 2, CH-8093 Zurich

To study the photoionization and photoelectron spectra of magnesium-containing species we have developed a pulsed laser-ablation source of magnesium atoms based on the design of Ref. [1]. The ablated species are entrained in a carrier gas to form a pulsed supersonic beam which is characterized by time-of-flight mass spectrometry. We present an experimental investigation of the Rydberg states of Mg and Mg^+. These Rydberg states are excited via resonant multiphoton, multi-color excitation using up to four dye lasers and are detected by pulsed field ionization or by monitoring the autoionization signal.

In a first step, we have recorded the spectrum of *s* and *d* Rydberg states of Mg and, for the first time, the *f* Rydberg spectrum of Mg^+. An improved determination of the ionization potential and of the quantum defects of the *f* series of Mg^+ is currently under way.

We shall also present spectra of doubly excited electronic states of Mg obtained using the isolated core excitation (ICE) technique starting from the 3*snd* state [2]. In particular, we investigate the $3pn'l'$, $n' > 20$ autoionizing series, which exhibits the rich structure characteristic of ICE experiments. This study extends the results of the pioneering investigation of Schinn *et al.* by improving the spectral resolution by a factor of more than 20 [2]. At a later stage, we aim at measuring doubly excited states in which one of the Rydberg electrons is excited to a state of principal quantum number $n \gg 100$, a regime largely unexplored so far.

References

[1] D. E. Powers, S. G. Hansen, M. E. Geusic, A. C. Puiu, J. B. Hopkins, T. G. Dietz, M. A. Duncan, P. R. R. Langridge-Smith, and R. E. Smalley, *J. Phys. Chem.*, **1982**, *86*, 2556.
[2] G. W. Schinn, C. J. Dai, T. F. Gallagher, *Phys. Rev. A*, **1991**, *43*, 2316.

*Corresponding author: matthieu.genezvriez@phys.chem.ethz.ch
†Corresponding author: dominik.wehrli@phys.chem.ethz.ch

Long range interactions in time lattices

K. Giergiel[*1], **A. Miroszewski**[2], **K. Sacha**[1,3]

1. Instytut Fizyki imienia Mariana Smoluchowskiego, Uniwersytet Jagielloński, ulica Profesora Stanisława Łojasiewicza 11, PL-30-348 Kraków, Poland

2. National Centre for Nuclear Research, ul.Hoża 69, PL-00-681 Warsaw, Poland

3. Mark Kac Complex Systems Research Center, Uniwersytet Jagielloński, ulica Profesora Stanisława Łojasiewicza 11, PL-30-348 Kraków, Poland

Time crystals are many-body systems which spontaneously self-organize their motion in a periodic way in time by analogy with the formation of crystalline structures in space in solid state physics. Time crystal behavior can be investigated in periodically driven systems if the driving is resonant with unperturbed motion of particles. Wide class of condensed matter problems can be realized in the time domain if single-particle or many-body systems are resonantly driven. It opens up unexplored territory for investigation of condensed matter physics in time and for invention of novel "time devices" because time is our new ally.

In the talk it will be shown how to create time lattices similar to optical (space) lattices. In this new type of systems almost any long range interactions in an effective Bose-Hubbard Hamiltonian can be engineered [1]. This can be achieved in ultra-cold atoms if s-wave scattering length is periodically modulated in time by means of the Feshbach resonance. In Fig.1 an example is presented where the magnitude of the interactions of a particle located at a given site with other particles located at the same or distant sites is nearly the same, but their repulsive or attractive character changes in an oscillatory way. We focus on ultra-cold atoms bouncing on an oscillating atom mirror. Time crystal behavior is such a system still awaits experimental demonstration, but our analysis of the experimental conditions shows that it is easily attainable in current laboratories [2].

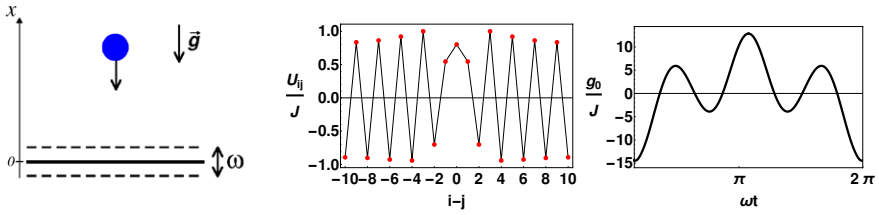

Fig. 1: Example of a system with exotic interactions: ultra-cold atoms bouncing on a harmonically oscillating mirror. The 20:1 resonance condition between the mirror oscillation frequency and the frequency of atom motion is fulfilled and the many-body system is described by the Hamiltonian $\hat{H}_{\rm eff} = -\frac{J}{2}\sum_{\langle i,j\rangle}\hat{a}_i^\dagger\hat{a}_j + \frac{1}{2}\sum_{i,j}U_{ij}\,\hat{a}_i^\dagger\hat{a}_j^\dagger\hat{a}_j\hat{a}_i$,. Middle panel shows the interaction coefficients U_{ij} corresponding to the scattering length $g_0(t)$ that is presented in the right panel — the interactions of a particle located at a given site with other particles located at the same or distant sites is nearly the same, but their repulsive or attractive character changes in an oscillatory way.

References

[1] Giergiel, K., Miroszewski, A. & Sacha, K. 2018, Phys. Rev. Lett., 120, 140401.

[2] KGiergiel K., Kosior A., Hannaford P., Sacha K., preprint https://arxiv.org/abs/1805.05718

*Corresponding author: krzysztof.giergiel+egas@gmail.com

Rydberg-Stark Deceleration of Helium Atoms for Merged-Beam Experiments in Low-Temperature Ion-Molecule Chemistry

M.Žeško[1], V. Zhelyazkova[1], J. A. Agner[1], H. Schmutz[1], F. Merkt*[1]
1. Laboratory of Physical Chemistry, ETH Zürich, Vladimir-Prelog-Weg 2, 8093 Zürich, Switzerland

Ion-molecule reactions at low temperatures (1 – 100 K) play an important role in the synthesis of organic molecules in interstellar gas clouds. We present an experiment designed to study the charge-transfer reactions of the He^+ ion with CO and N_2 which produce C^+ and N^+ ions crucial for a chain of chemical reactions [1].

The study of ion-molecule reactions in the laboratory at temperatures below 10 K is challenging because of the ubiquitous presence of stray electric fields which invariably heat the ions; e.g. a stray electric field of 1 mV/cm heats the ions to ∼12 K. This problem can be circumvented by using a highly excited Rydberg atom instead of the ion. The excited electron serves as a spectator during the reaction because the radius of its orbit is much larger than the interaction distance of the collision complex [2]. Moreover, Rydberg atoms can be accelerated, decelerated or guided along a desired trajectory with inhomogeneous electric fields [3]. This allows the study of the $He^+ + CO/N_2$ reactions by using a Rydberg helium beam merged with a supersonic CO/N_2 beam by deflecting the helium beam with a curved chip-based device (see Fig. 1).

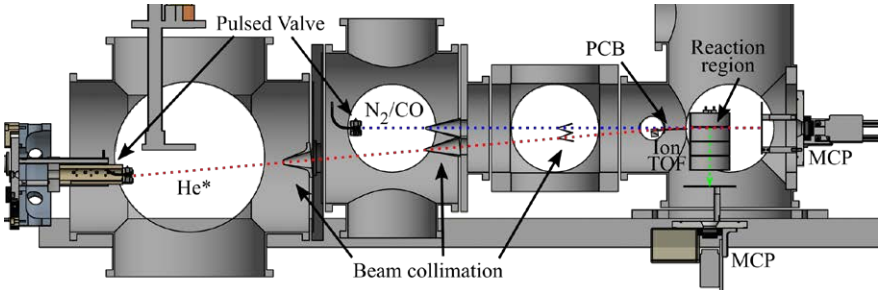

Fig. 1: CAD drawing of the setup designed to study He^+ reactions with CO/N_2 molecules in the ground state.

In this technique, the energy of the $He^+ - CO/N_2$ collision complex only depends on the relative velocities of the two beams. We present the results of experiments in which the velocity of a supersonic beam of Rydberg helium atoms is varied from a starting velocity of 700 m/s (mean velocity of the CO/N_2 beam) to final velocities in the 200 – 1200 m/s range using a chip-based decelerator. The helium atoms are excited with an electric discharge to the metastable $(1s)(2s)\,^3S_1$ state and then photoexcited with UV radiation to a Rydberg state with principal quantum number n between 25 and 32. By scanning the final velocity of the merged Rydberg-atom packet around the mean velocity of the ground-state beam, collisional energies below $k_B \cdot 1$ K can be achieved, as previously demonstrated in the measurement of the temperature dependence of the $H_2^+ + H_2 \rightarrow H_3^+ + H$ reaction rate all the way down to collisional energies of $k_B \cdot 300$ mK [4]. The fact that the chip delivers a spatially compact Rydberg-atom packet also allows us to probe different sections of the pulsed supersonic beam containing the CO/N_2 molecules and so achieve a high energy resolution.

References

[1] D. Smith; *Chem. Rev.* **92**, 1473 – 1485 (1992.)
[2] M. Matsuzawa; *Phys. Rev. A* **82**, 054701 (2010.)
[3] S. D. Hogan; *EPJ Tech. Instrum.* **3**, 2 (2016.)
[4] P. Allmendinger, J. Deiglmayr, K. Höveler, O. Schullian and F. Merkt, *J. Chem. Phys.* **145**(24), 244316 (2016.)

*Corresponding author: merkt@xuv.phys.chem.ethz.ch

Microwave and optical studies of NV^- color centers in diamond implanted by N^+ ion beam at large doses

Andrzej Kruk[1,2], Krystian Sycz[1], Mariusz Mrózek[1], Adam M. Wojciechowski[*1], Paulina Nakonieczna[1], Wojciech Gawlik[†1], Marzena Mitura-Nowak[3], Mateusz Schabikowski[3], Bogusław Rajchel[3], Marta Marszałek[3]

[1] *Institute of Physics, Jagiellonian University, Łojasiewicza 11, 30-348 Kraków, Poland*
[2] *University of Information Technology and Management, Sucharskiego 2, 35-225 Rzeszów, Poland*
[3] *Institute of Nuclear Physics Polish Academy of Sciences, Radzikowskiego 152, PL-31342 Kraków, Poland*

Nitrogen-Vacancy (NV^-) color centers in diamond are widely applied in many fields of physics, biophysics and quantum information [1]. This is due to interesting physical properties of these materials and ability to control them. One of efficient means of such control is implantation of N^+ ions in a diamond crystal matrix. Combining this with a proper choice of diamond substrate may enable creation of samples with specifications tailored to the applications.

In this contribution we present our preliminary results on implantation of N^+ ions with ion beam energy in the range of 10 – 35 keV and doses ranging from 2 x 10^{15} N/cm^2 to 5 x 10^{17} N/cm^2 into single-crystal diamonds (2x2x0.3 mm size, type Ib, (111)-oriented plates supplied by Sumitomo). We are interested in creation of dense NV ensembles, rather than in study of single NVs. The samples were characterized before and after the implantation by fluorescence spectra under illumination with a 532 nm laser light, Raman confocal microscopy, and optically detected magnetic resonance (ODMR) spectroscopy. The characterization was also performed before and after annealing of the implanted samples in air at 750 °C for 150 min. Multiple samples and implantation schemes were analyzed with a focus on sequential implantation at two energies.

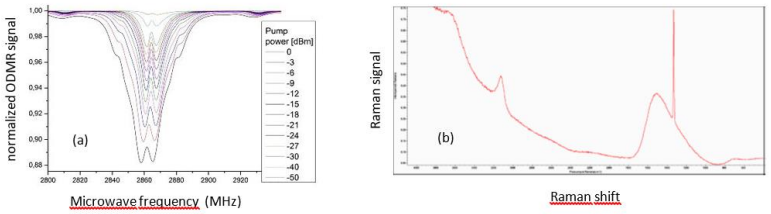

Fig. 1. Spectra of the implanted diamond samples: (a) ODMR spectrum; (b) Raman spectrum.

For all investigated samples we observe substantial increase of the amplitude of the ODMR resonances, reflecting increase of the density of NV centers. A quantitative comparison of various doses and implantation conditions and maps of NV^- spatial distributions will be presented at the conference. We are aiming at characterization of the implantation process and quality of irradiated samples by ODMR mapping. Also, application of the microwave hole-burning method [2] should enable detailed characterization and optimization of the NV diamond samples.

This work was sponsored by the ERA-NET Rus+ (DIABASE) and by Polish National Science Center (grant 2016/21/B/ST7/01430)

References

[1] e.g. M.W. Doherty, N.B. Manson, P. Delaney, F. Jelezko, J. Wrachtrup, L.C.L. Hollenberg, Phys. Rep. **528**, 1-45 (2013) and the references therein

[2] M. Mrozek, A. M. Wojciechowski, D. S. Rudnicki, J. Zachorowski, P. Kehayias, D. Budker and W. Gawlik, Phys. Rev. B **94**, 035204 (2016)

[*]Corresponding author: a.wojciechowski@uj.edu.pl

[†]Corresponding author: gawlik@uj.edu.pl

Spectroscopy of NV^- color centers in nanodiamond powders and suspensions: towards novel diamond-based photonic sensors

Paulina Nakonieczna[1], Krystian Sycz[1], Mariusz Mrózek[1], Andrzej Kruk[2], Adam M. Wojciechowski[*1], Wojciech Gawlik[†1], Mateusz Ficek[3], Maciej Głowacki[3], Robert Bogdanowicz[3]

[1] *Institute of Physics, Jagiellonian University, Łojasiewicza 11, 30-348 Kraków, Poland*

[2] *Faculty of Applied IT, University of Information Technology and Management, Sucharskiego 2, 35-225 Rzeszów, Poland*

[3] *Gdansk University of Technology, Faculty of Electronics, Telecommunication and Informatics, Department of Metrology & Optoelectronics, Narutowicza Str.11/12, 80-233 Gdańsk, Poland*

One of the most intensively studied atom-like solid state systems is the negatively charged nitrogen-vacancy (NV^-) color center in diamond. While most of the studies concentrate on single NVs or their ensembles in single-crystal samples, we focus on nanodiamond (ND; Adámas Nanotechnologies, grain size of 10-1000 nm, [NV^-] ~ 1 ppm) powders and its suspensions. We present the results of our fluorescence imaging and optically detected magnetic resonance (ODMR) studies performed in several experimental arrangements. Our goal is to develop novel sensing approaches by combining nanodiamonds with optical fiber technologies.

We have analyzed ND suspensions' luminescence in both liquid and dried-out state and observed fluorescence increase for irradiated and annealed NDs. Moreover, larger diamond fractions (~40-1000 nm) provide more fluorescence than the finest (~10 nm) ones. The suspensions' ODMR spectra are qualitatively different from those of the single-crystal samples, yet they also can be used for determination of the magnetic field value [1]. Simultaneous application of two microwave fields allows us to perform microwave *hole-burning* spectroscopy (Fig. 1(a)) and, in this way, study the relaxation processes and inhomogeneous broadening in such samples [2, 3].

To facilitate applications of NV sensors we investigate ND-to-glass interfacing methods such as deposition and drying of powder suspensions on glass substrates, sandwiching ND powders between glass slabs or filling fiber capillaries with ND suspensions. We aim at the fabrication of optical fibers with embedded NDs and discuss our initial experiments with optical fiber drawn from the ND-coated preform and tapered fiber tips coated with NDs (Fig. 1 (b)).

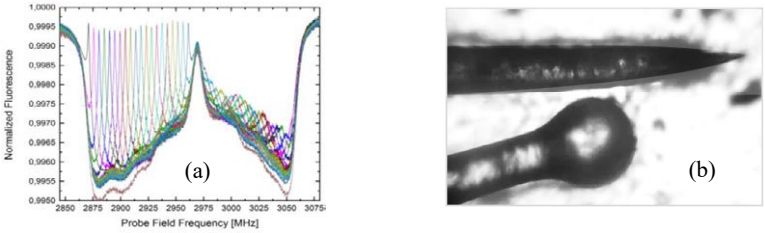

Fig. 1 (a) ODMR spectra (fluorescence intensity vs. frequency of the probe microwave field) of dry layer of NDs (140 nm grain size) in a magnetic field of 30 G. The wide distribution is broadened inhomogeneously by arbitrary orientations of individual NDs, the narrow resonances in the left part reflect holes burned by the pump of various frequencies when the pump and probe interact with the same transition in NVs, the wide dips on the right side are the holes burnt when the pump and probe interact with different transitions. **(b)** Photography of the tapered and ball-shaped optical fiber tips coated with ND powder.

This work was sponsored by the ERA-NET Rus+ (DIABASE) and by Polish National Science Center (grant 2016/21/B/ST7/01430)

References

[1] I.V. Fedotov, L.V. Doronina-Amitonova, D.A. Sidorov-Biryukov, N.A. Safronov, A.O. Levchenko, S.A. Zibrov, S. Blakley, H. Perez, A.V. Akimov A B. Fedotov, P. Hemmer, K. Sakoda, V.L. Velichansky, M.O. Scully, and A.M. Zheltikov, Opt. Lett. **39**, 6755 (2014)

[2] P. Kehayias, M. Mrozek, V. M. Acosta, A. Jarmola, D. S. Rudnicki, R. Folman, W. Gawlik, and D. Budker, Phys. Rev. B **89**, 245202 (2014)

[3] M. Mrozek, A. M. Wojciechowski, D. S. Rudnicki, J. Zachorowski, P. Kehayias, D. Budker and W. Gawlik, Phys. Rev. B **94**, 035204 (2016)

[*]Corresponding author: a.wojciechowski@uj.edu.pl

[†]Corresponding author: gawlik@uj.edu.pl

M-X-ray Emission in Interaction of Slow Highly Charged Xe Ions with Be Surface

Ł. Jabłoński[*1], **D. Banaś**[1], **P. Jagodziński**[2], **A. Kubala-Kukuś**[1], **D. Sobota**[1], **I. Stabrawa**[1], **K. Szary**[1], **M. Pajek**[1]

1. Institute of Physics, Jan Kochanowski University, Kielce, Poland

2. Department of Mathematics and Physics, University of Technology, Kielce, Poland

In interaction of slow highly charged ions (HCI) with matter the "hollow atoms" are formed in ultrafast neutralization of HCI at the surface [1]. The X-rays emitted from hollow atoms carry information about their structure and relaxation. In this work we report on the measurements of X-rays emitted from $\sim$ 8 keV$\times$q Xe^{q+} ions (q=23-40) interacting with Be foil. The ion beams were produced in the Dreebit EBIS-A facility [2]. The X-rays were measured with XFlash silicon drift detector (SDD) having a resolution of about 80 eV in 1-2 keV photon energy range studied.

The M-X-rays measured for different charge states of Xe^{q+} ions were interpreted in terms of electric dipole $nf \rightarrow 3d$ transitions with a small contribution of $nl \rightarrow 4,l-1$ transitions. The energies of these transitions, including their x-ray *satellites* and *hypersatellites*, were calculated using the GRASP code [3]. To model the shape of the spectral lines experimental and natural broadening were taken into acount as well as incomplete charge collection effect (ICC) in the SDD detector was considered. The measured M-X-rays support a picture of radiative X-ray cascade following fast neutralization of HCI at a Be surface. However, we found a strong contribution of the internal dielectronic excitation (IDE) process [4] responsible for creation of additional vacancies in the core of Xe^{q+} ions. In particular, the IDE process is crucial for interpretation of observed M-X-rays for Xe^{26+} ions having no initial vacancies in the M-shell.

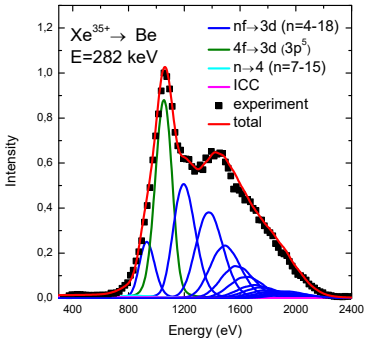

Fig. 1: Measured spectrum of X-rays emitted in interaction of 282 keV Xe^{35+} ions with Be foil compared with the predictions of the GRASP code for indicated X-ray transitions.

The measured M-X-rays can be explained in terms of the radiative deexcitation cascade involving n-states with $n \leq 18$. For estimated critical Rydberg state for resonant neutralization of Xe^{35+} ions at Be surface $n_c \sim 30$ the observed X-rays seems to be insensitive to early, very fast stage of the deexcitation process, which was recently proposed to be explained by the interatomic Coulombic decay (ICD) mechanism [5].

Acknowledgements

The financial support of the EU within the Polish Innovative Economy Operational Program (Contact No. WNP-POIG.02.02.00-26-023/08) is acknowledged.

References

[1] H. Winter and F. Aumayr, J. Phys. B **58**, R39 (1999)
[2] D. Banaś et al., J. Instrum. **5**, C09005 (2010)
[3] P. Jönsson et al., Comp. Phys. Comm. **184**, 21972203 (2013)
[4] R. Schuch et al., Phys. Rev. Lett. **70**, 1073 (1993)
[5] R. A. Wilhelm et al., Phys. Rev. Lett. **119**, 103401 (2017)

*Corresponding author: l.jablonski@ujk.edu.pl

On the Creation and Suppression of Alignment by Optical Pumping with Circularly-Polarized Light

Z.D. Grujić*[1], Y. Shi[1,2,3], T. Scholtes[1], V. Lebedev[1], V. Dolgovskiy[1], A. Weis[1]

1. Physics Department, University of Fribourg, Ch. du Musée 3, 1700 Fribourg, Switzerland
2. University of Chinese Academy of Sciences, Beijing 100049, P.R. China
3. Institute of Electronics, Chinese Academy of Sciences, Beijing 100190, P.R. China

The spin polarization produced in an atomic ground state with angular momentum F by optical pumping is suitably described by atomic multipole moments $m_{k,q}$ with $1 \leq k \leq 2F$ [1]. Electric dipole transitions (usually used to probe the spin polarization) couple only to the vector multipole moments $m_{1,q}$ (orientation) and second-rank tensor moments $m_{2,q}$ (alignment). The scalar multipole moment $m_{0,0}$ describes the total population of the state F. One can show that the absorption coefficient (on a dipole transition) of a spin-polarized atomic medium is fully described by the (real) moments $m_{0,0}$, $m_{1,0}$ $m_{2,0}$, and the (complex) moment $m_{2,2}$, where q refers to a quantization axis along the light's propagation direction $\hat{k}$.

Pumping with linearly-polarized light (LPL) produces only the moment $m_{2,2}$, where the phase of the complex number $m_{2,2}$ is a measure for the orientation of the light polarization in the plane transverse to $\hat{k}$. Pumping with circularly-polarized light (CPL) produces both longitudinal orientation $m_{1,0}$ and longitudinal alignment $m_{2,0}$, the latter term being often neglected in model calculations.

Here we report on a measurement of $m_{2,0}$'s dependence on the power P of a CPL beam (pump beam), and compare the results to previously derived model calculations [2][3]. Those calculations have revealed that of all four hyperfine components of the Cs D_1 transition, the 4→3 transition features a 'bipolar' $m_{2,0}(P)$ dependence, the alignment vanishing for a certain power P^*. The other three transition show a monotonic power dependence without any sign change. This feature may have the following useful application: In high accuracy magnetometry, the alignment contribution may lead to unwanted systematic side effects, so that driving the magnetometer with the 'magic' power P^* may suppress such effects.

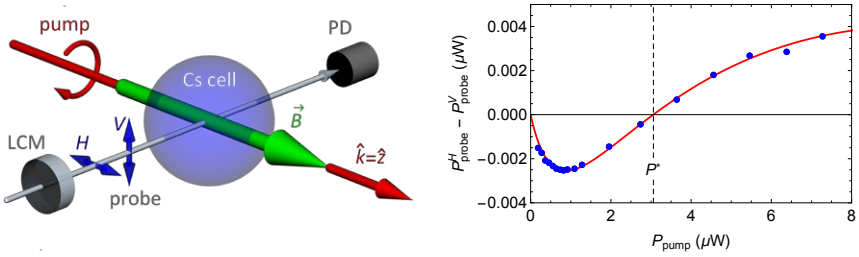

Fig. 1: Left: Experimental setup (LCM: liquid crystal modulator, PD: photodiode). Right: Experimental results and model fit.

In the experiments, a circularly-polarized laser beam, resonant with the 4→3 transition, creates spin-polarized (oriented and aligned) Cs atoms in a paraffin-coated cell. The spin polarization is stabilized by a small magnetic field. A weak H- or V-polarized probe beam traverses the cell at right angles to the pump beam, yielding transmitted power levels P^H_{probe} and P^V_{probe}, respectively (left graph of Fig. 1). One can show that $P^H_{\text{probe}} - P^V_{\text{probe}} \propto m_{2,0}$. In praxis, the H/V modulation is achieved by a liquid crystal modulator (LCM).

The right graph of Fig. 1 shows the experimental results, together with a fit of model calculations, yielding P_{sat} (pumping saturation power) and $\gamma_{\text{se}}/\gamma_1$ (ratio of spin exchange and isotropic spin relaxation rates) that are in agreement with our former measurements [2] of these quantities in the same cell (see also poster by Y. Shi et al.).

References

[1] K. Blum, *Density matrix theory and applications*, 3rd edn. Springer-Verlag, Berlin, Heidelberg, 2012.
[2] Y. Shi, T. Scholtes, Z.D. Grujić, V. Lebedev, V. Dolgovskiy, and A. Weis, Phys. Rev. A **97**, 013419 (2018).
[3] Y. Shi, and A. Weis, Eur. Phys. J. D **72**, 73 (2018).

*Corresponding author: zoran.grujic@unifr.ch

Towards ultracold potassium-cesium mixture.

P. Arciszewski[1], **M. Bocheński**[1], **J. Dobosz**[1], **B. Szczerba**[1], **and M. Semczuk**[*1]
1. Faculty of Physics, University of Warsaw, Pasteura 5, 02-093 Warsaw, Poland

We present progress towards creating a new experimental setup for laser cooling of cesium and potassium atoms. The apparatus will be used to explore ultracold, heteronuclear mixtures in species selective potentials and will enable production of ground state molecules of KCs.

The magneto-optical traps for both species are loaded from the background gas with the help of light induced atomic desorption. A novel laser system is designed for laser cooling of all stable isotopes of potassium (i.e. ^{39}K, ^{40}K and ^{41}K). The switching between isotopes is done without any moving parts, is computer controlled and can be reliably performed in less than 1 ms, limited only by the settling time of the tapered amplifiers used in the setup. Due to seeding of optical amplifiers with either D1- or D2-line light, two stage cooling can be implemented using D1-line gray molesses thanks to the built-in phase coherence between the cooling and repumping beams. Though not implemented here, the laser system can also provide light for a 2D-MOT.

A light sheet beam located 34 cm below the trapping region will enable single atom resolved detection of dilute clouds after long expansion times exceeding 250 ms.

The project is funded by the National Science Centre grant no. 2015/16/S/ST2/00425 and 2016/21/D/ST2/02003, and by the Fundation for Polish Science (Homing Programme).

[*]Corresponding author: msemczuk@fuw.edu.pl

Charge transfer in He^+ (10 keV – 29 keV) - He collisions analyzed by the use of the anticrossing spectroscopy

P. Kaminski[1], R. Drozdowski[1], G. von Oppen[2]

1. Institute of Experimental Physics, University of Gdansk, Wita Stwosza 57, 80-308 Gdansk, Poland
2. Institut für Atomare Physik und Fachdidaktik, Technische, Universität Berlin, Hardenbergstraße 36, D – 10623 Berlin, Germany

In many experimental measurements and theoretical calculations, the charge-transfer and excitation cross-sections were analysed. During ion–atom and atom–atom collisions the electronic clouds of the colliding partners evolve according to the laws of the quantum dynamics. However, the unified theory of the collisions over the entire range of the impact-energy no exist. In particular, interesting are the intermediate energies, where the projectile velocities v_p are of the order of the bound-electron velocities of the targets, that is of the order of the Bohr velocity v_B. In such collisions, some stationary states of the projectiles or the target atoms can be excited coherently. The measured cross–sections (the diagonal elements of the density matrix), give the probability of the excitation or electron capture process, but there is no information about the coherence of the excited states (the off-diagonal elements of the density matrix). The collision mechanism is very complex and cannot be easily analysed, neither theoretically nor experimentally, even for the single electron collision system H_2^+, where the electron moves in two-centre Coulomb potential of two protons. An intuitive insight into the collision process give the Paul–trap model and the quantum saddle dynamics [1-2]. This theoretical approach with the anticrossing spectroscopy measurements were used to analyse excited states of the helium target atoms for the He^+– He collision-system at intermediate energies [3-4]. In this case, an electron moves in a two-centre Coulomb potential of two ionic He^+ cores.

Now we use the same technique - the anticrossing spectroscopy, in order to determine the post – collisional states of the fast He atoms created by an electron capture He^+(10 – 29 keV) – He. The preliminary result (for 26 keV impact energy) was presented in the paper [5]. In this paper we showed, that He atoms excited by electron capture in He^+– He collisions at intermediate energies have large electric dipole moments (*EMD*) after collision. In the present investigations, we analysed the intensity of the triplet line λ ($1s4l^3D \rightarrow 1s2p^3P$) ≈ 447.2 nm emitted by helium atoms formed by electron capture for projectiles velocity 0.3 v_B – 0.6 v_B (10 – 29 keV). The intensity was measured as a function of the axial electric field in the collision volume varied from -30 kV/cm to +30 kV/cm. The obtained anticrossing spectra are highly asymmetric with respect to the direction of the electric field F_z (parallel or antiparallel to the velocity of the projectiles). These results clearly show that the dipole moment of the fast He atoms is parallel to the direction of the projectile beam whereas the dipole moment of the excited He target atoms is antiparallel. The detailed studies of the intensity of the anticrossing peaks show that these peaks have non-Lorentzian profile with oscillation structure. In order to determine the excited states the theoretically calculated anticrossing spectra were fitted to the measured ones. In the calculations, the time-dependent density-matrix theory was used:

$$\frac{d}{dt}\rho(t) = \left(\frac{d}{dt}\rho(t)\right)_{excitation} + \left(\frac{d}{dt}\rho(t)\right)_{evolution} + \left(\frac{d}{dt}\rho(t)\right)_{decay} \qquad (1)$$

The evolution of the system is described by Liouvill equation. The differential equation (1) was solved numerically by the use of the Runge-Kutta method. The Hamiltonian of the helium atoms was calculated as in [3-4]. Obtained results will be discussed at the conference.

References

[1] J.M. Rost, J. S. Briggs, J. Phys. B 24, 4293 (1991).
[2] G. von Oppen, Europhys. Lett, 27, (1994).
[3] E Baszanowska R. Drozdowski, P. Kaminski, G. von Oppen, J. Phys. B: At. Mol. Opt. Phys. 45 115203 (10pp) (2012).
[4] E Baszanowska R. Drozdowski, P. Kaminski, G. von Oppen, J. Phys. B: At. Mol. Opt. Phys. 47 195201 (10pp) (2014).
[5] P. Kaminski, R. Drozdowski, G. von Oppen, Eur. Phys. J. Special Topics 222, 2293-2300 (2013).

Ground state spectroscopy of ultracold dipolar ^{6}Li^{40}K molecules

A. Yang[1], S. Botsi[1], S. Kumar[1], A. Laugharn[1] S. B. Pal[1], M. Lam[1], and K. Dieckmann*[1,2]

1. Centre for Quantum Technologies (CQT), 3 Science Drive 2, 117543 Singapore
2. Department of Physics, National University of Singapore, 2 Science Drive 3, 117542 Singapore

With the creation of dipolar molecules in their ro-vibrational ground state, a long-standing scientific goal has been achieved [1-6]. In the ultracold quantum regime such molecules are a promising tool for the quantum simulation of a large class of many body effects [7] and for quantum information processing [8], ultracold chemistry and mertrological applications. In our experiment, we use bosonic heteronuclear dimers of ^{6}Li and ^{40}K. Their deeply-bound ro-vibronic state possess a large permanent electric dipole moment of 3.6 Debye. This makes them a suitable candidate for investigating the plethora of effects originating from the long-range anisotropic dipole interaction.

Here we describe our two-photon spectroscopy scheme that recently enabled us to experimentally identify and address the diploar ground state of LiK. Our scheme differs from spectroscopic routes previously used for other alkali heteronuclear dimers as only unperturbed singlet molecular spin states are involved and predominantly only one sole hyperfine state is addressed. As an important consequence this establishes an ideal three level system for the transfer by stimulated rapid adiabatic passage (STIRAP) to a single hyperfine component of the ground state.

We start from a sympathetically cooled, quantum-degenerate Fermi-Fermi mixture, and create weakly-bound ^{6}Li-^{40}K molecules via magnetic Feshbach association at 215.6 G in an optical dipole trap. We use the asymptotic bound state model (ABM) [9] to calculate the hyperfine composition of the Feshbach state and identify a spin singlet admixture of up to 52%. We then present data from our one-photon spectroscopic survey of the $B^1\Pi$ and $A^1\Sigma$ electronically excited states of the LiK* asymptote. A variety of new lines have been found and analyzed for the suitability as intermediate states for the transfer. In particular, we were able to address very deeply bound states of the $A^1\Sigma$ potential that offer a large overlap with the ground state at this inner turning point. Navigating a path written by the the available laser wavelengths, power and Franck-Condon overlap, we were first able to locate the $v = 3$ state by two-photon spectroscopy and Autler-Townes spectroscopy. Subsequently, the implementation of a new dye laser setup provided the necessary output power and wavelength tuning range for the discovery of the lower vibrational states $v = 2$ and $v = 1$ and eventually $v = 0$ (see Fig.1). We further present our efforts to coherently populate the ground state vie STIRAP, and to apply a static electric field to investigate the high ground state dipole moment of the ^{6}Li^{40}K molecule.

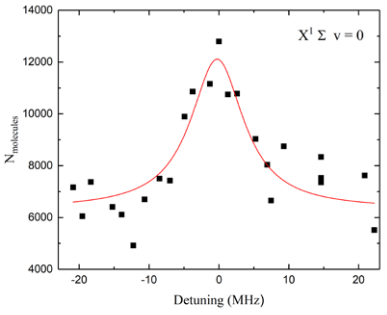

Fig. 1: Two-photon spectroscopy of the absolute electronic and ro-vibronic ground state ($X^1\Sigma, v = 0$) of *LiK*.

References

[1] K . - K. Ni., *et al.*, Science, **322**, 231-235 (2008).
[2] M . Debatin, Ph.D. Thesis (2013). 205301 (2014).
[3] P . K. Molony, *et al.*, Phys. Rev. Lett. **113**, 255301 (2014).
[4] J . W. Park, *et al.*, Phys. Rev. Lett. **114**, 205302 (2015), J. W. Park, *et al.*, New Journ. Phys. **17**, 075016 (2015).
[5] M . Y. Guo, *et al.*, Phys. Rev. Lett. **116**, 205303 (2016).
[6] T .M. Rvachov, *et al.*, Phys. Rev. Lett. **119**, 143001 (2017).
[7] M . A. Baranov, *et al.*, Chem. Rev. **112** (9), pp 5012-5061 (2012).
[8] A . Micheli *et al.*, Nat. Phys. **119**, 143001 (2017).
[9] T . G. Tiecke, *et al.*, Phys. Rev. A, **82**, 042712 (2010).

*Corresponding author: phydk@nus.edu.sg

Wide-field imaging of magnetic fields using nitrogen-vacancy centers in diamond

Adam M. Wojciechowski[*1,2], Louise F. Frellsen[1], James L. Webb[1], Mürsel Karadas[3], Sepehr Ahmadi[1], Haitham El-Ella[1], Axel Thielscher[3,4], Fedor Jelezko[5], Jan Meijer[6], Alexander Huck[†1], and Ulrik L. Andersen[1]

1. Department of Physics, Technical University of Denmark, 2800 Kgs. Lyngby, Denmark
2. Institute of Physics, Jagiellonian University, Lojasiewicza 11, 30-348 Kraków, Poland
3 Department of Electrical Engineering, Technical University of Denmark, 2800 Kgs. Lyngby, Denmark
4. Danish Research Center for Magnetic Resonance, Copenhagen University Hospital Hvidovre, 2650 Hvidovre, Denmark
5. Institute for Quantum Optics and IQST, Ulm University, Albert-Einstein-Allee 11, 89081 Ulm, Germany
6. Felix Bloch Institute of Solid State Physics, Leipzig University, Linnéstraße 5, 04103 Leipzig, Germany

We present our work on wide-field imaging of magnetic field using negatively charged nitrogen-vacancy (NV) centers in diamond, aiming towards studies of biological systems with high spatial and temporal resolution.

At the heart of our microscope is a carefully engineered ultra-pure diamond substrate, with a top micrometer-thin layer grown with >99.99% of ^{12}C isotope and rich in ^{15}NV centers (~0.1-1 ppm). Fluorescence light from the NV layer is collected with a high numerical aperture objective and imaged on a camera. In our setup, we use a high-speed, large-pixel-well-capacity sensor capable of in-pixel lock-in demodulation. This allows us to record small relative changes of the NVs fluorescence level, $\Delta F/F \sim 10^{-4}$, in the optically detected magnetic resonance spectra [1]. Together with the narrow (~600 kHz) resonance linewidths observable in our diamond sample, this results in a sub-microtesla magnetic field sensitivity per single pixel and frame (exposure), while maintaining a video framerate of over 50 fps and image resolution of 300x300 pixels.

We are aiming at magnetic imaging of micro particles such as beads commonly used for biological tagging, with a focus on both static images and particle-flow videos. Additionally, we have carried out electromagnetic modelling of complex neurological systems [2]. The simulation results indicate magnetic signals on micrometer length-scales, from single neurons to a brain tissue. In case of evoked activity in the brain tissue, the numerical results show the generation of magnetic fields with a magnitude of a few nanotesla, with most of the time-information contained within the DC-800 Hz bandwidth. Such signals are expected to be measurable using our current experimental setup. Finally, we demonstrate a technique for making the NV magnetometer immune to the temperature shifts caused by drifts resulting from toggling the laser and microwave fields [3].

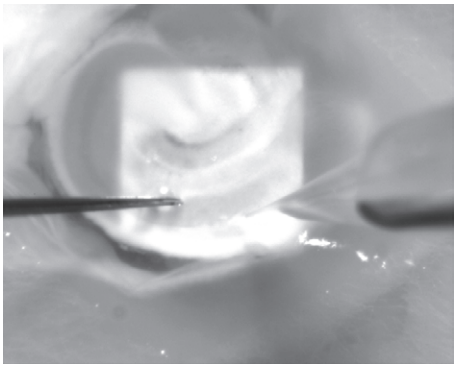

Fig. 1. Hippocampus area of a rat brain slice placed on top of the diamond sensor (central white square) with stereotrode for electric stimulation (left) and pipette electrode (right) for local field potential recording.

References

[1] A.M. Wojciechowski, M. Karadas, A. Huck, C. Osterkamp, S. Jankuhn, J. Meijer, F. Jelezko, and U. L. Andersen, Review of Scientific Instruments **89**, 031501 (2018)
[2] M. Karadas, A.M. Wojciechowski, A. Huck, N.O. Dalby, U.L. Andersen, and A. Thielscher, Scientific Reports **8**, 4503 (2018)
[3] A.M. Wojciechowski, M. Karadas, A. Huck, C. Osterkamp, S. Jankuhn, J. Meijer, F. Jelezko i U. L. Andersen, *submitted to Applied Physics Letters*, arXiv:1802.07224

[*]Corresponding author: a.wojciechowski@uj.edu.pl
[†]Corresponding author: alexander.huck@fysik.dtu.dk

Laser Photodetachment of Negative Ions

D. Lu[*1], J. Welander[1], V. Ideböhn[1], J. Sundberg[1], M. Kristiansson[3], K. Chartakunchand[3], J. Warbinek[2], A. Aleman[1], H. Liang[1], O. Windelius[1], A. M. Martschini[4], J. Lachner[4], S. Rothe[5], D. Hanstorp[†1]

1. Department of Physics, University of Gothenburg, Box 100, 405 30 Gothenburg, Sweden
2. Institut für Physik, Johannes Gutenberg-Universität, Staudingerweg 7, D-55099 Mainz, Germany
3. Department of Physics, Stockholm University, SE-106 91 Stockholm, Sweden
4. Isotope Research and Nuclear Physics, University of Vienna, Währinger Str. 17 1090 Wien, Austria
5. CERN, CH-1211 Geneva 23, Switzerland

Negative ions are loosely bound quantum systems. Their formation and destruction are strongly dependent on the correlated motion of their valence electrons. During the last few years, the interest in negative ions has significantly increased in various branches of physics, ranging from astrophysics, atmospheric and plasma physics to surface physics and accelerator physics [1].

In this work, we report on several recent research activities at the Gothenburg University Negative Ion Laser LAboratory (GUNILLA) [2]. This is a collinear laser-ion beam apparatus where negative ions are neutralized due to photon-induced electron emission in the so-called photodetachment process. Current research interests involve doubly excited states, double detachment processes and fundamental properties of negative ions. Based on a resonance ionization scheme with final state selectivity, investigations of branching ratios to highly excited Rydberg states of the residual atom and the double detachment process where two electrons are simultaneously detached from negative ions can be realized [3-4].

Spectroscopy of excited states of negative ruthenium ions has been studied. The spectroscopic results are needed when lifetime measurements of these excited states will be performed using the Double ElectroStatic Ion Ring ExpEriment (DESIREE) at Stockholm University. Preliminary results show good agreement with previous work done by P. L. Norquist *et al*. [5]. In addition, two transitions from Ru^- (J = 5 and 3 ^{4}F) into Ru (^{5}F) states are resolved. Further data analysis is in progress.

One of the applications of negative ions is to improve the detection limits in Accelerator Mass Spectrometry (AMS) using tandem accelerators [6], which is the most sensitive method for trace element analysis. Recently, detachment threshold behaviour of several heavy elements has been carried out using an OPO laser system. The research aims to investigate the relative detachment cross section as a function of wavelength. This information provides valuable data for suppression of interfering isobars in AMS.

Neutral Particle Detector (NPD) is commonly utilized in photodetachment studies. In the UV range, due to insufficient transparency and intensive photoelectric effect, a traditional Indium Tin Oxide (ITO) based NPD faces enormous difficulties. Investigation of graphene as a substitute through the wavelength range of 225 nm to 472 nm proved at least 80% transparency, and several orders of magnitude smaller signals from secondary laser induced electrons [7]. This will allow neutral particle detection of photodetached negative ions in the UV energy range.

Finally, we attempt to improve the ion yield of the cesium sputtering negative ion source at GUNILLA by applying photon excitation of neutral Cs atoms (6s 7p) in the vicinity of the cathode sputter target since the production yield of negative ions in a charge transfer process is expected to increase when the target Cs atom is excited. The Cs atoms are excited by a focused Ti:Sa laser beam with wavelength of 455.528 nm and 459.317 nm respectively. Simultaneously, a Cs hollow cathode lamp is employed for wavelength calibration [8].

References

[1] M. C. McCarthy, C. A. Gottlieb, H. Gupta, and P. Thaddeus, ApJ **652**, L141-144 (2006).
[2] C. Diehl, K. Wendt, A. O. Lindahl, P. Andersson, and D. Hanstorp, Rev. Sci. Instrum. **82**, 053302 (2011).
[3] A. O. Lindahl, *Two-Electron Excitations in Negative Ions*, Ph.D. Thesis (2011).
[4] J. Rohlén, *Excited States in Negative Ions*, Ph.D. Thesis (2014).
[5] P. L. Norquist, D. R. Beck, R. C. Bilodeau, M. Scheer, R. A. Srawley, and H. K. Haugen, Phys. Rev. A **59**, 1896-1902 (1999).
[6] W. Kutschera, P.Collon, H.Friedmann, R.Golser, P.Hille, A.Priller, W.Rom, P.Steier, S.Tagesen, A.Wallner, E.Wild, and G.Winkler, Nucl. Instr. and Meth. B **123**, 47-50 (1997).
[7] J. Warbinek, *Investigation of the photoelectric effect in graphene and ITO in a neutral particle detector*, Bachelor Thesis (2018).
[8] A. Duckworth, R. S. Adrain, and B. A. Tozer, Optics & Laser Tech. **24**, 39-43 (1992).

[*]Corresponding author: di.lu@physics.gu.se
[†]Corresponding author: Dag.Hanstorp@physics.gu.se

An inverse scattering scattering method based on the density matrix

J. Franz[*1],

1. Department of Theoretical Physics and Quantum Informatics, Faculty of Applied Physics and Mathematics, Gdansk University of Technology, Narutowicza 11/12, 80-233 Gdańsk, Poland

The inverse scattering method should help to extract the interaction potential from the knowledge of the scattering cross sections. However, most approaches to inverse scattering theory are requiring the knowledge of intermediate quantities, for example the phase-shift or amplitude (see e.g. Chapter 20 in book by Newton [1]) or the scattering matrix (see e.g. the formalism by Gelfand, Levitan and Marchenko as described in the book by B. N. Zakhariev and A. A. Suszko [2]). Usually these intermediate quantitaties have to be extracted from the scattering cross sections in a preliminary step, which is not always well defined.

Here we want present a formalism for inverse scattering, that allows the extraction of the interaction potential directly from the knowledge of the differential cross section. Our approach is based on the use Liouville-von Neumann equation for the density matrix (see e.g. Chapter 5 in the book by Tannor [3]). An additional advantages of the formalism is, that it can be extended to take into account the profile of the incoming particle beam. Furthermore the experimental uncertainties can be taken into account and can be translated into uncertainties of the extracted interaction potential.

This work is supported by the grant 2014/15/D/ST2/02358 of the Narodowe Centrum Nauki (National Science Center Poland) and by computer grants from the computer centers WCSS (Wroclawskie Centrum Sieciowo-Superkomputerowe, Politechnika Wroclawska) and TASK (Trójmiejska Akademicka Sieć Komputerowa Gdańsk).

References

[1] R. G. Newton, *Scattering Theory of Waves and Particles*, Dover Publications, Mineola 2013.
[2] B. N. Zakhariev and A. A. Suszko, *Direct and Inverse Problems*, Springer-Verlag, Berlin 1990.
[3] D. J. Tannor, *Introduction to Quantum Mechanics: A time-dependent Perspective*, University Science Books, 2007.

*Corresponding author: janfranz@pg.edu.pl

Metastability Exchange Optical Pumping of ^{3}He in high magnetic field

B. Głowacz*[1], M. Suchanek[3], T. Pałasz†[1], L. Mikowska[1], Z. Olejniczak[2], T. Dohnalik[1]
1. Faculty of Physics, Astronomy and Applied Computer Science, Jagiellonian University, Gołebia 24 31-007 Kraków, Poland
2. Department of Magnetic Resonance Spectroscopy, Institute of Nuclear Physics PAN, Radzikowskiego 152, 31-342 Kraków, Poland
3. Faculty of Chemistry and Physics, University of Agriculture in Krakow, Al. Mickiewicza 21, 31-120, Krakow, Poland

Nuclear hyperpolarization of ^{3}He, which is several orders of magnitude higher than thermal polarization, can be achieved by Spin Exchange Optical Pumping (SEOP) or Metastability Exchange Optical Pumping (MEOP) techniques. The MEOP involves principally two processes: the optical pumping of metastable state (the first excited triplet state of ^{3}He) atoms and the metastability exchange in collisions between metastable and ground state atoms [1]. The SEOP method is described in the accompanying poster. Comparing to the SEOP method, the MEOP allows to obtain a higher polarization, exceeding 80%, in much shorter time. However, the required physical condition, namely low ^{3}He gas pressure (1 mbar), seriously limit potential medical application, where about 1 liter of hyperpolarized helium at 1 bar is needed to obtain MRI images of human lungs. Therefore a novel MEOP regime has been developed, where ^{3}He at the pressure of the order of 100 mbar is polarized in magnetic field exceeding 0.1 T, which is necessary to quench the hyperfine coupling [2],[3],[4].

The presented polarizer with the compatible ventilator is designed to work in high magnetic field and it fits inside the diagnostic tunnel of the most commonly used medical 1.5 T MRI scanner [5],[6].The polarizer works at the ^{3}He pressure of 60 mbar. The 30% polarization of 600 ml of ^{3}He portion is obtained in 40 minutes. The in vivo MRI images of human lungs filled with hyperpolarized ^{3}He were obtained.

References

[1] T. Pałasz, B. Tomanek, Optical hyperpolarization of noble gases for medical imaging. In: *Gas Phase NMR*, (p. 336-363), Royal Society of Chemistry (2016).
[2] M. Abboud et al., EPL 68 (4), 480 (2004).
[3] A. Nikiel et al., Eur. Phys. J. - Special Topics 144,255 (2007).
[4] A. Nikiel-Osuchowska, et al., Eur. Phys. J. D 67 (9), 1 (2013).
[5] T. Dohnalik et al. Eur. Phys. J. Appl. Phy. 54 (2), 20802 (2011).
[6] G. Collier et al., J. of Appl. Phy. 113 (20), 204905 (2013).

Acknowledgments
The Diagnostics Division of the John Paul II Hospital in Krakow and the TransCom International are involved in the project. The contribution of Dr Guilhem Collier (Faculty of Medicine, Dentistry & Health University of Sheffield UK) to the construction of the ^{3}He polarizer is acknowledged.

Financial support
The Polish National Centre for Research and Development, PBS3/A9/35/2015;
National Laboratory for Quantum Technologies, European Regional Development Fund, WND-POIG.020200-00-003/08;
6^{th} Framework Program, a Marie Curie Research and Training Network, PHeLiNet, MRTN-CT-2006-036002;
Polish Ministry of Science and Higher Education, 7150/E-338/M/2017.

*Corresponding author: b.glowacz@uj.edu.pl
†Corresponding author: tadeusz.palasz@uj.edu.pl

Spin Exchange Optical Pumping of ^{129}Xe for Medical Diagnostics

T. Pałasz*[1], L. Mikowska†[1], Z. Olejniczak[2], B. Głowacz[1], T. Dohnalik[1]
1. Faculty of Physics, Astronomy and Applied Computer Science, Jagiellonian University, Gołebia 24 31-007 Kraków, Poland
2. Department of Magnetic Resonance Spectroscopy, Institute of Nuclear Physics PAN, Radzikowskiego 152, 31-342 Kraków, Poland

Magnetic Resonance Imaging (MRI) with hyperpolarized noble gases as contrast agents is an answer to the call for a more precise diagnostic tool of the Chronic Obstructive Pulmonary Disease - the fifth leading cause of death (according to WHO) [1]. Due to sensitivity limitations, the imaging of human lungs is only feasible by using noble gases (^{3}He, ^{83}Kr or ^{129}Xe), that are optically polarized to the level exceeding the thermal polarization by several orders of magnitude. Therefore, the standard medical MRI scanner has to be supplemented by a specialized optical polarizer [2].

We are presenting ^{129}Xe polarizer based on the Spin Exchange Optical Pumping (SEOP) method. The SEOP process consist of two stages: optical pumping of rubidium vapour, and spin transfer between rubidium and xenon atoms via the Fermi Contact Interactions in the presence of buffer gases. Rubidium vapor is optically pumped by the laser beam of 8.5 W power (0.2 nm bandwidth VBG laser diode matrix) [3]. The diameter of the pumping beam (6 cm) is fit to one litre, cylindrically shaped, optical cell filled with rubidium vapour and 1 bar of the gas mixtures (Xe, buffer gases). The proportions of gases in the mixture are controlled by the gas dosing system. The highest polarization of 55% was obtained for the gas mixtures with 3% of ^{129}Xe concentration. The polarization was calibrated with respect to the NMR signal of the thermally polarized water phantom. In order to separate polarized xenon from the buffer gases (^{4}He, N_2) for medical purposes, a cold trap inserted in the NdFeB Halbach magnet producing about 0.6 T is used. The NMR signal and relaxation time of polarized and extracted xenon samples were measured in a home made low field MRI scanner.

References

[1] WHO—Burden of COPD. [online] Available at: http://www.who.int/respiratory/copd/burden/en/ [Accessed 27 May. 2018]
[2] T. Pałasz, B. Tomanek, Optical hyperpolarization of noble gases for medical imaging. In: *Gas Phase NMR*, (p. 336-363), Royal Society of Chemistry (2016).
[3] A. Wojna-Pelczar, *Polarized xenon for medical applications* (Diss.), Jagiellonian University, Kraków (2015)

Financial support
The Polish National Center for Research and Development, PBS3/A9/35/2015;
National Laboratory for Quantum Technologies, European Regional Development Fund, WND- POIG.020200-00-003/08;

*Corresponding author: tadeusz.palasz@uj.edu.pl
†Corresponding author: lutoslawa.mikowska@student.uj.edu.pl

B – 62

Large-scale multiconfiguration Dirac-Hartree-Fock and relativistic configuration interaction calculations of transition data for B-like S XII

Kai Wang[*1,2], **Michel Godefroid**[†3], **Per Jönsson**[4], **Jörgen Ekman**[4], **Chun Yu Zhang**[2], **Ran Si**[5], **Xiao Hui Zhao**[1], **Chong Yang Chen**[2], **Jun Yan**[6,7,8]

1. Hebei Key Lab of Optic-electronic Information and Materials, The College of Physics Science and Technology, Hebei University, Baoding 071002, China

2. Shanghai EBIT Lab, Key Laboratory of Nuclear Physics and Ion-beam Application, Institute of Modern Physics, Department of Nuclear Science and Technology, Fudan University, Shanghai 200433, China

3. Chimie Quantique et Photophysique, CP160/09, Université libre de Bruxelles, Av. F.D. Roosevelt 50, 1050 Brussels, Belgium

4. Department for Materials Science and Applied Mathematics, Malmö University, SE-20506, Malmö, Sweden

5. Department of Computer Science, University of British Columbia, Vancouver, V6T 1Z4, Canada

6. Institute of Applied Physics and Computational Mathematics, Beijing 100088, China

7. Center for Applied Physics and Technology, Peking University, Beijing 100871, China

8. Collaborative Innovation Center of IFSA (CICIFSA), Shanghai Jiao Tong University, Shanghai 200240, China

Due to the lack of accurate atomic data, a large fraction of the lines from ions of astrophysically abundant elements (C, O, F, Ne, Mg, Al, Si, S, Ar, Fe and Ni) are unknown in various EUV wavelength regions of interest [1]. To fill this gap, highly accurate energy and radiative transition data have been estimated for L-shell and M-shell atomic ions of the above elements (see for example [2]). The present work focuses on accurate atomic data of boron-like S XII. Sulfur ($Z = 16$) is indeed one of the most abundant elements in the milky way galaxy and S XII lines are often observed in astronomical objects including the sun. These lines are crucial for the determination of sulfur abundance and for modeling and diagnosing astrophysical plasmas.

Excitation energies and lifetimes for the 213 lowest states of the $n \leq 5$ configurations in B-like S XII are calculated using highly correlated wave functions [3] optimised with the fully relativistic multiconfiguration Dirac–Hartree–Fock method [4]. Multipole transition rates and associated radiative data (line strengths and oscillator strengths) connecting these levels are also reported. The theoretical excitation energies are systematically compared with the NIST Atomic Spectra Database [5], in which misidentifications are pointed out. After eliminating the latter, a mean energy difference with the standard deviation between computed and observed energies of 12 ± 341 cm^{-1} is obtained for the $n \geq 3$ high-lying states. This level of accuracy confirms that elaborate ab initio calculations can assist the identification of new emission lines in the solar and other astrophysical spectra. The present work provides atomic data of high accuracy for an ion of astrophysical interest, the B-like S XII, for which experimental data remain scarce.

References

[1] P. Beiersdorfer and E. Träbert, Astrophys. J. **854**, 114 (2018).
[2] K. Wang *et al.* Astrophys. J. Suppl. Ser. **234**, 40 (2018).
[3] C. Froese Fischer, M. Godefroid, T. Brage, P. Jönsson and G. Gaigalas, J. Phys. B: At. Mol. Opt. Phys. **49**, 182004 (2016).
[4] P. Jönsson, G. Gaigalas, J. Bieroń, C. Froese Fischer and I. Grant, Comput. Phys. Comm. **184**, 2197 (2013).
[5] A. Kramida, Yu. Ralchenko, J. Reader , B. Nowak, and & and NIST ASD Team. 2018, NIST Atomic Spectra Database (ver. 5.5.6), [Online]. Available: https://physics.nist.gov/asd [2018, April 13]. National Institute of Standards and Technology, Gaithersburg, MD.

*Corresponding author: kaiwangcn@qq.com
†Corresponding author: mrgodef@ulb.ac.be

Spin self-rephasing in the system of several atoms

K. Szymański[*1], **K. Pawłowski**[2]
1. Marian Smoluchowski Institute of Physics, Uniwersytet Jagielloński, ul. Łojasiewicza 11, 30-348 Kraków, Poland
2. Center For Theoretical Physics, al. Lotników 32/46, 02-668 Warszawa, Poland

In this work a system consisting of a number of atoms evolving under the influence of external magnetic field is analyzed. Due to the inhomogenities of the external field, the atomic spins undergo dephasing: classically, since each atom feels different field along its trajectory, the spin rotation differs as well and the average spin decays. In a quantum mechanical context this corresponds to entanglement of spin and spatial degrees of freedom; additionally, two other modes of dephasing are possible: formation of internally (spin-spin) entangled state and population transfer to nonsymmetric spin state.

The spin dephasing can be prevented by tuning the interaction between the atoms: such an effect, called spin self-rephasing has been observed experimentally [1] and can increase the coherence time by a large factor.

While such systems have been studied from a semiclassical point of view, a quantum mechanical description does not exist yet. In this work we fill in the gap by providing a numerical simulation of the behavior of the quantum mechanical system of several interacting, indistinguishable particles in the presence of inhomogenous magnetic field and analysis of the spin rephasing and coherence.

A work in progress involving evolution analysis of so-called anticoherent state (Schrödinger's cat, equal superposition of maximal and minimal spin projection states along fixed axis) and squeezed state, which both can not be approximated semiclassically, may lead to interesting results regarding feasibility of quantum metrology schemes. Such states are sensitive to external perturbations, which makes them useful simultaneously lowering their stability.

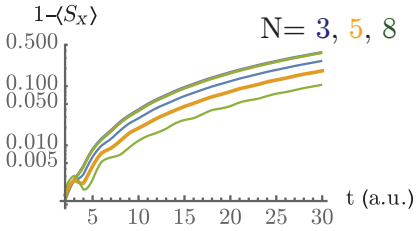

Fig. 1: Envelope of visibility $\langle S_x \rangle$ for different number of particles. The parameters expressed in oscillator units are: temperature $T = 0.1$, interaction strengths $g_{\downarrow\downarrow} = 0.0099, g_{\uparrow\uparrow} = 0.011, g_t = 0.01$, and magnetic field $B(x) = 0.03x^2$. Solid line denotes presence of particle-particle interactions, dashed – interaction-free case. Progressively better (with growing number of particles) coherence protection is visible: already for $N = 8$ the coherence time is increased by factor of 5 (note the logarithmic scale).

References

[1] C. Deutsch et al., Physical Review Letters **105.2**, 020401 (2010)
[2] G. K. Büning et al., Physical Review Letters **106.24**, 240801 (2011)

*Corresponding author: konrad.szymanski@uj.edu.pl

Self-compensating atomic magnetometer for particle physics exploration

M. Padniuk*, **S. Pustelny**
1. Marian Smoluchowski Institute of Physics, Jagiellonian University, Łojasiewicza 11, 30-348 Kraków, Poland.
On behalf of GNOME collaboration

The search for physics beyond the Standard Model is an active topic of nowadays fundamental research. One of the possible directions of this investigation is to search for ultralight particles such as axions and axion-like particles. These particles are theoretically well-motivated candidate for dark matter [1] but they also solves several other problems of today's fundamental physics, including, the strong CP problem [1]. A particular scheme for axion hunts is to search for exotic spin interactions of the particles with ordinary-matter particles.

Axions are considered to be very light particles. Predicted mass of axions is below milli-electron volts, being significantly smaller than the mass of neutrinos [1]. Due to this fact, it is more convenient to treat axions as a classical field rather than independent particles. According to theoretical predictions such a field can produce time-depended effects on atomic energy levels in a form of transients (when topological defects of dark matter is considered) or oscillating shifts of the levels [2,3,4].

The Global Network of Optical Magnetoemters for Exotic physics search (GNOME) is a novel scheme to search for exotic spin couplings [2]. The GNOME forms an atomic-magnetometer network distributed around the Earth, which will be sensitive to global spin-precession perturbations. In general, the network will be sensitive to magnetic coupling, but also other spin couplings, e.g., those produced by axions.

For a network searching for tiny effects such as those induced by the dark matter, it is extremely important to cancel magnetic field and its gradients, as they have many orders of magnitude stronger effect on the spins as any hypothesized exotic couplings. For this purpose, mu-metal and ferrite magnetic shields, combined with sets of compensating coils, are used. While this reduces environmental noise, the technique does not cancel out slow drifts of magnetic fields, e.g., induced by thermal drifts of current sources and ferromagnetic domains at magnetic-shield materials. It limits the magnetometer stability, which is important parameter in long-term measurements.

Using the atomic magnetometer in the so-called self-compensating regime [5] allows one for sufficient suppression of magnetic-field drifts. The self-compensating magnetometer uses a mixture of gases (alkali and noble gases) which through optical pumping and spin-exchange collisions create nuclear magnetisation of the noble gas and both electron and nuclear alkali-metal-atom magnetisation. The noble gas as well as the alkali vapor(s) are contained in a spherical glass cell, occupying the same volume. Under this conditions, the system reveals resonance behaviour, leading to simultaneous rotation of both atomic-ensembles polarisations due to magnetic-field changes. If gyromagnetic ratios of the noble gas and alkali-metal atoms have opposite signs such rotation effectively leads to suppression of magnetic-field sensitivity of alkali atoms as well as, its first-order gradients. On the other hand, this regime does not effect sensitivity to hypothetical exotic spin couplings.

Self-compensating optical magnetometers will be used as second generation sensor for the GNOME. It should improve the sensitivity of the whole network to perturbations induced by exotic spin couplings. First of such magnetometers is currently under development at the Jagiellonian University in Kraków. The heart of the magnetometer is a glass cell filled with a K-Rb-^{3}He-N_2 mixture. The K-Rb atom concentration proportion at liquid mixture placed inside of the cell is 1/9, enabling efficient pumping K by resonant light. The K polarization is transferred to Rb through spin-exchange collisions, and than both polarised Rb and K polarises the ^{3}He nuclei through the same collisions type. Such a process of hybrid optical pumping [6] allows higher magnetisations of ^{3}He and Rb. During the presentation,the current status of the magnetometer construction will be discussed.

References

[1] D. DeMille et al, Science **357** (2017) .
[2] S. Pustelny et al, Ann. Phys. (Berlin) **525**, 659–670, (2013) .
[3] M. Pospelov et al, Phys. Rev. Lett. **110**, 021803 (2013) .
[4] A. Derevianko, Nat. Phys. **10** (2014) .
[5] T. W. Kornack, M.V. Romalis, Phys. Rev. Lett. **89**, 253002 (2002) .
[6] E. Babcock, Phys. Rev. Lett. **91**, 123003 (2003) .

*Corresponding author: michal.padniuk@student.uj.edu.pl

Towards zero- and ultra- low-field nuclear magnetic resonance with atomic magnetometers

P. Put*, **K. Popiołek, S. Pustelny**
1. Marian Smoluchowski Institute of Physics, Jagiellonian University, Łojasiewicza 11, 30-348 Kraków, Poland

Devices using nuclear magnetic resonance (NMR) are routinely used for non-invasive medical imaging as well as chemical analysis [1]. Conventional NMR requires high (>1 T) magnetic field for samples' polarization and magnetization detection. The need for ultra-strong homogenous field is possibly the largest drawback of standard NMR, leading to high cost and low mobility of NMR scanners and spectrometers. This also limits the technique applicability (e.g., inapplicability to people with pacemakers).
In recent years, efforts has been made to perform NMR experiments at ultra-low magnetic fields or even entirely without the field [2]. Aside from solving the problems arising from the high magnetic field, rich chemical information can be extracted under these conditions [3]. Additionally, at zero- and ultra-low fields spin relaxation processes are suppressed, leading to ultra-narrow NMR lines leading to high spectroscopic sensitivity of the technique [4] and high spatial resolution of imaging [5].
In zero- and ultra- low-field (ZULF) NMR experiments, where inductive coils are not applicable, direct detection of samples magnetization takes place through application of the most sensitive magnetic-field sensors: superconducting quantum interference devices (SQUIDs) or atomic magnetometers [6]. Former solution seems especially promising, as atomic magnetometers can operate near room temperature, can be miniaturized and still routinely reach the near-DC field sensitivity better than 10 fT $Hz^{-1/2}$. This last feature guarantees high SNR of measured NMR signals, while the first two open avenue for construction of portable NMR devices.
In our presentation, we describe experimental setup used to perform preliminary NMR experiments at zero and ultra-low magnetic field using high sensitivity atomic magnetometers. An atomic magnetometer, used for the purpose, exploits nonlinear Faraday rotation. Our device can be used in nearly identical experimental configuration to measure quasi-static magnetic field or oscillating magnetic fields tuned to particular frequency. With this respect, the devices can be used for spectroscopy, as well as, imaging. To eliminate environmental noise, which is predominant in the setup, a gradiometer scheme, employing differential signal from two sensors is used. This enables measurement of magnetization of a sample, shuttled pneumatically from a high field region produced by constructed pseudo-Halbach magnet, where samples are polarized, to a volume inside an ultra-low magnetic field, where detection is performed. Thanks to the broad, tunable range of the magnetometer and a remote prepolarization scheme, this experimental arrangement is suitable for simultaneous detection of NMR signals from different nuclei species at low magnetic fields, as well as spatial imaging with information encoded by magnetic field gradients.

References

[1] Levitt, Malcolm H. "Spin dynamics." Jon Wiley and Sons 196 (2001).
[2] Ledbetter, Micah P., Dmitry Budker. "Zero-field nuclear magnetic resonance." Physics Today 66(4) (2013).
[3] Blanchard, John W., and Dmitry Budker. "Zero-to Ultralow-Field NMR." eMagRes (2016).
[4] Emondts, Meike, et al. "Long-lived heteronuclear spin-singlet states in liquids at a zero magnetic field." Physical Review Letters 112.7 (2014): 077601.
[5] Xu, Shoujun, et al. "Submillimeter-resolution magnetic resonance imaging at the Earth's magnetic field with an atomic magnetometer." Physical Review A 78.1 (2008): 013404.
[6] Budker, Dmitry, and Michael Romalis. "Optical magnetometry." Nature Physics 3.4 (2007): 227.

This work was supported by the grant number 2015/19/B/ST2/02129 financed by the Polish National Science Centre.

*Corresponding author: piotr.put@doctoral.uj.edu.pl

Magnetic shielding constant for Dirac one-electron atom in an arbitrary discrete energy eigenstate

Patrycja Stefańska[*1]

1. Atomic Physics Division, Department of Atomic, Molecular and Optical Physics, Faculty of Applied Physics and Mathematics, Gdańsk University of Technology, ul. Narutowicza 11/12, 80-233 Gdańsk, Poland

We provide an application of the Sturmian expansion of the Dirac–Coulomb Green function [1] to obtain closed-form expression for the magnetic dipole shielding constant (σ) of the relativistic hydrogenlike atom in an arbitrary discrete energy eigenstate [2]. The technique utilized in the present work has been succesfully used in calculations of many electromagnetic parameters of Dirac one-electron atom in the ground state (cf. e.g. [3], [4]), and also for the excited hydrogenic quantum states [5]–[8].

In contrast to the final analytical results for the magnetizability [5] and the magnetic-dipole-to- electric-quadrupole cross susceptibility [7] of the relativistic hydrogenlike atom being in *an arbitrary discrete energy eigenstate*, the expression for σ obtained in a such general case was found to be possible to transform it into an *elementary* form with the use of the theory of hypergeometric functions. Magnetic shielding constant for the atom being in the state characterized by the set of quantum numbers $\{n_r, \kappa, \mu\}$, in which n_r denotes the radial quantum number, κ is an integer different from zero (related to the principal quantum number n through $n = n_r + |\kappa|$), μ is the magnetic quantum number, reads as follows:

$$\sigma_{n_r\kappa\mu} = \frac{\alpha^2 Z}{N_{n_r\kappa}^2(4\kappa^2-1)}\left[\kappa^2 - \frac{\eta_{n_r\kappa}^{(+)}}{4} - \frac{\eta_{n_r\kappa}^{(-)}}{4} + \frac{\mu^2}{4\kappa^2-1}\left(\frac{2\kappa+1}{2\kappa-1}\eta_{n_r\kappa}^{(+)} + \frac{2\kappa-1}{2\kappa+1}\eta_{n_r\kappa}^{(-)}\right)\right.$$
$$\left. + \frac{4\kappa^2\mu^2}{4\kappa^2-1}\left(\frac{4\kappa^2-5}{4\kappa^2-1} + \frac{8\kappa[2\kappa(n_r+\gamma_\kappa) - N_{n_r\kappa}](\alpha Z)^2}{\gamma_\kappa(4\gamma_\kappa^2-1)N_{n_r\kappa}^2}\right)\right], \tag{1}$$

where

$$\eta_{n_r\kappa}^{(\pm)} = \frac{N_{n_r\kappa}(2\kappa \pm 1)}{n_r + \gamma_\kappa \pm N_{n_r\kappa}} \tag{2}$$

with

$$N_{n_r\kappa} = \pm\sqrt{n_r^2 + 2n_r\gamma_\kappa + \kappa^2} \tag{3}$$

and

$$\gamma_\kappa = \sqrt{\kappa^2 - (\alpha Z)^2}. \tag{4}$$

For states with zero radial quantum number $n_r = 0$, the formula in Eq. (1) reduces to the one obtained by Moore [9]. In turn, by substituting $\kappa = -1$ into the above mentioned equation, we reconstruct the result provided by Ivanov *et al.* in [10]. For very special case, i.e. the atomic ground state, our general expression for σ is in agreement with the formulas derived earlier by Zapryagaev *et al.* [11], Cheng *et al.* [12], and also by us [13]. Moreover, for states with $n = 2$ we get the same results as Pyper and Zhang [14].

Numerical values of the nuclear magnetic shielding constant for some low-lying energy eigenstates were published recently in [15].

References

[1] R. Szmytkowski, J. Phys. B **30**, 825 (1997); Erratum: J. Phys. B **30**, 2747 (1997).
[2] P. Stefańska, Phys. Rev. A **94**, 012508 (2016).
[3] R. Szmytkowski, P. Stefańska, Phys. Rev. A **85**, 042502 (2012).
[4] R. Szmytkowski, P. Stefańska, Phys. Rev. A **89**, 012501 (2014).
[5] P. Stefańska, Phys. Rev. A **92**, 032504 (2015).
[6] P. Stefańska, At. Data Nucl. Data Tables **108**, 193 (2016).
[7] P. Stefańska, Phys. Rev. A **93**, 022504 (2016).
[8] P. Stefańska, At. Data Nucl. Data Tables **113**, 316 (2017).
[9] E. A. Moore, Mol. Phys. **97**, 375 (1999).
[10] V. G. Ivanov, S. G. Karshenboim, R. N. Lee, Phys. Rev. A **79**, 012512 (2009).
[11] S. A. Zapryagaev, N. L. Manakov, L. P. Rapoport, Yad. Fiz. **19**, 1136 (1974).
[12] L. Cheng, Y. Xiao, W. Liu, J. Chem. Phys. **130**, 144102 (2009).
[13] P. Stefańska, R. Szmytkowski, Int. J. Quantum Chem. **112**, 1363 (2012).
[14] N. C. Pyper, Z. C. Zhang, Mol. Phys. **97**, 391 (1999).
[15] P. Stefańska, At. Data Nucl. Data Tables **120**, 352 (2018).

[*]Corresponding author: patrycja.stefanska@pg.edu.pl

B – 67

Dynamic interference in the multi-photon resonance enhanced ionization of hydrogen atoms by short and intense laser pulses

A.D. Müller[*1], **E. Kutscher**[1], **A.N. Artemyev**[1], **L.S. Cederbaum**[2], **Ph.V.Demekhin**[1]
1. Institut für Physik und CINSaT, Universität Kassel, Heinrich-Plett-Str. 40, 34132 Kassel, Germany
2. Theoretische Chemie, Physikalisch-Chemisches Institut, Universität Heidelberg, Im Neuenheimer Feld 229, 69120 Heidelberg, Germany

The photoionization of hydrogen atoms by intense and short coherent laser pulses is investigated from first principles by a numerical solution of the time-dependent Schrödinger equation. The parameters of the pulse are chosen, such that the photon energies are resonant to the 1s $\rightarrow$ 2p excitation, and that the intensities are high enough to induce corresponding Rabi floppings. To be able to observe the dynamic interference [1], the photoelectron wave packets were propagated on a large spatial grid undisturbed until the end of the pulse.

As one can see in Fig. 1, the computed spectra of the resonance enhanced two-photon ionization (PI) and three-photon above threshold ionization (ATI) exhibit pronounced multi-peak interference patterns, which become more complex with the increase of the intensity. These patterns are due to the so called dynamic interference [1], which has been predicted for the resonance enhanced multiphoton photoionization of hydrogen in Ref. [2]. Here, the pulse couples the 1s ground state and the 2p excited state, which split in energy. Due to the shape of the pulse-envelop, the energy splitting and the respective kinetic energy of emitted electrons change in time. For a Gaussian pulse, two electron wave packets emitted at two different times at the rising and falling edges of the pulse have the same energy. These waves interfere and give rise to the dynamic interference.

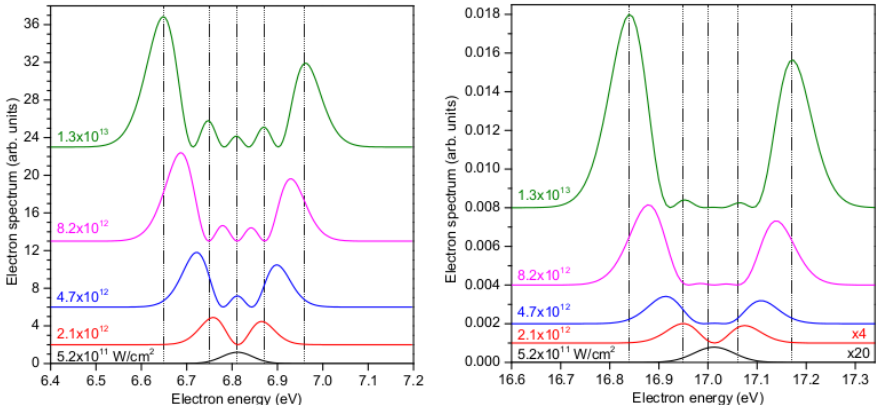

Fig. 1: Spectra of the resonance enhanced multi-photon ionization after the Gaussian-shaped pulses with the carrier frequency of $\omega = 0.375\ a.u.$, duration of $\tau = 30\ fs$ and different peak intensities (indicated on the left of each curve in W/cm) have expired. On the left, the spectra for the resonance enhanced two-photon ionization (PI), and on the right the spectra for the resonance enhanced above threshold ionization (ATI) are depicted. In the latter, the spectra for the two lowest intensities (two lowermost curves) are shown on an enhanced scale, as indicated by the factor $\times$K at the right-hand side of these curves. For the lowest considered intensity (lowermost curves), the PI spectrum exhibits a single peak at the central electron energy $\varepsilon_0 = 2\omega - IP = 0.25\ a.u. = 6.81\ eV$ and the ATI one at $\varepsilon_0 = 3\omega - IP = 0.62\ a.u. = 17.00\ eV$, as expected in a weak-field regime. With the increase of the pulse intensity, the spectra become enriched by multiple peak structures.

To get more insight into the dynamic interference the angular distribution of the photoelectrons with different energies is investigated. Here, the angular distribution for PI is almost independent of the electron energy, while for ATI, a strong dependence can be observed. This dependence is due to the additional interference of the multiple pathways, which lead to the same final continuum states εp. This effect can be utilized in experiments, for the verification of the dynamic interference.

References

[1] Ph.V. Demekhin, and L.S. Cederbaum, PRL **108**, 253001 (2012).
[2] Ph.V. Demekhin, and L.S. Cederbaum, Phys. Rev. A **86**, 063412 (2012).

*Corresponding author: anne.d.mueller@uni-kassel.de

Electronic structure of the molecular system HPS^+/HSP^+

S. Ben Yaghlane[1], B.Mehnen[1], and M. Hochlaf[2]

[1] Laboratoire de Spectroscopie Atomique, Moléculaire et Applications – LSAMA. Université de Tunis El Manar, Tunis, Tunisie.
[2]Université Paris-Est, Laboratoire Modélisation et Simulation Multi Echelle, MSME UMR 8208 CNRS, 5bd Descartes, 77454 Marne La-Vallée, France

Astrophysical observations have shown that many molecules containing sulfur (SH, SH+, SN, SO+, SO2 et OCS) were detected in the interstellar medium in significant density in different areas of the electromagnetic spectrum. Nevertheless, the molecular system HPS/HSP is not detected and the reasons for such non-detectability are not yet established. Recently, Ben Yaghlane and al [1] have characterized spectroscopically ground states of HPS^q/HSP^q species (q = -1,0, + 1). Our work completes this study; it is to study the excited electronic states of HPS^+/HSP^+system. One dimension potential cuts were calculated along the elongation as well as along the bending angle.

References:

[1]S. Ben Yaghlane, N.E. Jaidane, C. E. Cotton, J. S. Francisco, M. M. Al Mogren, R. Linguerri et M. Hochlaf. J. Chem. Phys. **140**, 244309 (2014).

Fourier-transform study of the $A\,^1\Sigma_u^+ \sim b\,^3\Pi_u \rightarrow X\,^1\Sigma_g^+$ laser induced fluorescence spectra and deperturbation analysis of the spin-orbit coupled A∼b complex of Cs_2 dimer

V. Krumins [1], A. Kruzins[1], M. Tamanis[1], R. Ferber[1], A. Znotins,*[1], E.A. Pazyuk [2], A.V. Stolyarov [2]
1. Laser Centre, University of Latvia, Rainis blvd. 19, Riga, Latvia, LV-1586
2. Department of Chemistry, Lomonosov Moscow State University, 119991 Moscow, Leninskie gory 1/3, Russia

In Cs_2 molecule the lowest electronically excited $A\,^1\Sigma_u^+$ and $b\,^3\Pi_u$ states are strongly coupled due to pronounced spin-orbit interaction between them, and, hence, may be considered as a single singlet-triplet A∼b complex with complicated energy level structure. There is great interest in accurate description of this complex, since it can serve as a gateway for excitation of higher singlet and triplet states manifold. Also, these fully mixed states are used as intermediate states to transfer weakly bound ultra-cold alkali diatomics to their absolute ground state, e.g. in case of Cs_2 $X\,^1\Sigma_g^+$ (v = 0, J = 0) [1]. Present work is continuation of the previous studies [2,3] in which the A∼b complex of Cs_2 was examined in a low energy region. The purpose of this work is to extend accurate spectroscopic data to higher vibrational levels as well as to apply a global deperturbation analysis to reproduce rovibronic energies and radiative properties of the A∼b complex within the experimental accuracy.

In the experiment caesium dimers were produced in a stainless steel heat-pipe at 300^{o}C. The titanium-sapphire laser (MBR 110, Coherent) and various diode lasers were used for excitation. Fourier transform spectrometer (Bruker IFS125 HR) was used to register laser induced fluorescence (LIF) spectra $A\sim b \rightarrow X\,^1\Sigma_g^+$ with an instrumental resolution of 0.03 cm^{-1}. A rotational analysis of the recorded LIF spectra provided about 4000 new rovibronic term values of the A∼b complex covering J range from 4 to 380 in energy range from 9917 to 13439 cm^{-1}. The experimental data undergone a rigorous 4 x 4 coupled channel deperturbation analysis. The deperturbed Expanded-Morse-Oscillator potentials of the both *A* and *b* coupled states as well as the morphed spin-orbit coupling functions reproduce overall 98% of the experimental term values of the A∼b complex of Cs_2 with a rms uncertainty of 0.01 cm^{-1}. The relative intensity distributions measured in the long $A\sim b \rightarrow X\,^1\Sigma_g^+(v'')$ LIF progressions confirm their theoretical counterparts calculated by the present multi-component (non-adiabatic) wavefunctions of the A∼b complex and *ab initio* spin-allowed A→X transition dipole moment [3].

The Moscow team is grateful for the support from RFBR Grant No. 16-03-00529-a. The support from Base/Performance Funding project no. AAP2016/B013, ZD2010/AZ27 and project 1.1.1.2/VIAA/1/16/068 is gratefully acknowledged by MOLPOL team.

References

[1] J. G. Danzl *et al.,* Nature Physics, **6**, 265, 2010.
[2] Feng Xie *et al.,* The Journal of Chemical Physics, **128**, 204313, 2008.
[3] Jianmei Bai *et al.,* Phys. Rev. A **83**, 032514, 2011.

*Corresponding author: znotins.aigars@gmail.com

Index

Index

Index

Index